Impact of heterogeneity on flow in fluvial-deltaic reservoirs: Implications for the giant ACG field, south Caspian Basin

Kevin Choi

2008

A thesis submitted for the degree of Doctor of Philosophy of the University of London and for the Diploma of Imperial College

Department of Earth Science and Engineering Petroleum Engineering and Rock Mechanics Group

BIBL
LONDON
UNIV.

Abstract

The Azeri, Chirag and Gunashli (ACG) oilfield is located in the offshore Azerbaijan sector of the south Caspian Basin. This dissertation focuses on the Azeri Field which has over 8 billion barrels of oil in place. The major reservoir interval is the Pliocene Pereriv Suite, which is characterized by laterally continuous layers of variable net-to-gross (NTG) deposited in a fluvial-deltaic environment. The Azeri Field is being developed by both down-dip water injection and up-dip gas injection. This dissertation uses high-resolution models, derived from outcrop analogue and subsurface data, in conjunction with experimental design techniques, to rank the impact of different geological heterogeneities on recovery by both displacement mechanisms. Firstly, the impact of reservoir-unit scale heterogeneities on water and gas injection is assessed using a simplified fluid PVT description. At this level, the principal controls on oil recovery are the factors that affect sandbody connectivity and sweep efficiency. Secondly, the impact of reservoir- and genetic-unit scale heterogeneities on gas injection in high NTG intervals is assessed. The genetic-unit scale heterogeneities that control the approach to vertical equilibrium (VE) are found to be the principal controls on recovery. Their impact is large when gravity forces dominate the mobility unstable displacement, but decreases with increasing production rate as viscous forces dominate and the displacement moves out of VE. The presence of laterally extensive shales is also important, because they change the geometry of the reservoir layering and yields higher recovery than equivalent homogeneous models. The same rank order of key heterogeneities is obtained for simulations with simplified and a more realistic PVT description. Finally, the results are applied to develop a methodology to identify the upper and lower boundaries on predicted recovery using a simple analytic approach that incorporates some geological heterogeneity.

Acknowledgements

I sincerely acknowledge my supervisors Matthew Jackson, Gary Hampson, Alistair Jones and Tony Reynolds for their guidance, support and patience over the whole research period. They have made this research project an exciting, rewarding and enjoyable adventure.

I would like to acknowledge the UK Engineering and Physical Sciences Research Council (EPSRC) and BP for funding this work. Also I would like to thank the examiners for reviewing this thesis

Moreover I would like to thank Thomas Gundacker and Dave Waldren for giving their time to answer my endless questions when I was in Sunbury. I would like to thank Gill Watson, Bobby Lau, Richard Sech, Matthew Rhodes, Ping Gang Zhang and John Hughes who spent a lot of time to help me improve my writing skills.

Finally I would like to thank my parents for their constant support and tolerance.

Table of Contents

Abstract 3
Acknowledgements 4
List of Figures 10
List of Table 24
Chapter 1 Introduction 26
1.1 Project background 26
1.2 Introduction to the ACG field and the challenges of the project 28
1.3 Aim and objective 32
1.4 Methodology 32
1.5 Outline of this thesis 33
Chapter 2 Literature review 35
2.1 Overview 35
2.2 Geology of the Productive Series and the ACG field 36
2.2.1 Regional geological setting and petroleum system 36
2.2.2 Reservoir geology 41
2.3. Fluvial-Deltaic reservoirs 43
2.3.1 Classification of deltas and deltaic reservoirs 44
2.3.2 Previous work on fluvial-deltaic reservoirs 48
2.3.3 Outcrop Analogues 50
2.4. Impact of sedimentological/geological heterogeneity on flow 57
2.4.1 Impact of fluid type and production mechanism 60
2.4.2 On field and reservoir-unit scale heterogeneity 62
2.4.3 On genetic-unit and smaller scale heterogeneity 67
2.5. Modelling of flow in heterogeneous reservoirs 69
2.5.1 Object based modelling 69
2.5.2 Sensitivity analysis techniques 71
2.5.3 Top-Down reservoir modelling scheme 73
2.6. Summary 74
Chapter 3 Preliminary displacement study 76
3.1. Overview 76
3.2. Aims 77
3.3. Introduction of reservoir properties 77
3.4. Displacement under Buckley-Leverett flow conditions 82
3.5. Displacement under segregated flow conditions 83
3.6. Results 86
3.6.1. Buckley-Leverett flow analysis 86

3.6.2. Segregated flow analysis....91
3.6.3. Stability analysis....92
3.7 Discussion of the Buckley-Leverett flow and segregated flow analysis....97
3.7.1. Comparison of the Buckley-Leverett flow model and the segregated flow model analysis....97
3.7.2. Comparison of water-oil displacement against gas-oil displacement 98
3.7.3. Comparison of the different Pereriv Suite model....99
3.7.4. Comparison of the different dip angle....99
3.7.5. Limitation of analytical solutions on gravity assisted displacement 100
3.8. Conclusion....102
Chapter 4 Screening study of reservoir-unit scale heterogeneities....103
4.1. Introduction....103
4.2. Aims....104
4.3. Reservoir-unit scale heterogeneities in fluvial-deltaic....104
reservoirs....104
4.3.1. Channel orientation....105
4.3.2. Channel sinuosity....106
4.3.3. Channel stacking....107
4.3.4. Channel dimensions....107
4.3.5. Interlayer connectivity....108
4.3.6. Internal variation of NTG within Pereriv C....108
4.4. Reservoir model construction....110
4.5. Fluid flow simulation....111
4.6. Screening study design....112
4.6.1. First screening study: Analysis of Pereriv B, C and D....113
4.6.2. Second screening study: Analysis of Pereriv B, C and D (models with net sand in Pereriv C)....114
4.6.3. Third screening study: Analysis of Pereriv B and C layers in isolation 115
4.6.4. Impact of uncertainty....116
4.7. Results....117
4.7.1. First screening study: Analysis of Pereriv B, C and D....117
4.7.2. Second screening study: Analysis of Pereriv B, C and D (models with net sand in Pereriv C)....123
4.7.3. Third screening study: Analysis of Pereriv B and C layers in isolation 128
4.7.3.1. High NTG layer: Pereriv B....128
4.7.3.2. Low NTG layer: Pereriv C....134

4.8. Discussion 142
4.8.1. Impact of NTG variation in Pereriv C 142
4.8.2. Impact of interlayer connectivity 143
4.8.3. Impact of heterogeneities within low NTG layers 144
4.8.4. Impact of heterogeneities within high NTG layers 144
4.8.5. Impact of different displacement schemes 145
4.8.6. Wider application to ACG reservoir 147
4.9. Conclusion 148
Chapter 5 Combined screening study of genetic-unit and reservoir-unit scale heterogeneities 151
5.1. Overview 151
5.2. Aims 154
5.3. Combination of genetic-unit scale and reservoir-unit scale heterogeneities in a fluvial deltaic reservoir 154
5.3.1. Reservoir-unit scale heterogeneity factors 155
5.3.1.1. Channel orientation 156
5.3.1.2. Channel stacking 157
5.3.1.3. Channel dimensions 157
5.3.2. Extensive shale within high NTG layers 158
5.3.3. Upward-fining trends within channel-fill sandbody 158
5.3.4. Ratio of vertical and horizontal permeability within channel-fill sandbodies (Kv:Kh) 159
5.3.5. Mud-clast lags at channel bases 160
5.4. Screening study design 161
5.5. Reservoir model construction 162
5.6. The design of the displacement simulations. 166
5.6.1. Gas-oil displacement in a high NTG layer with simplified fluid PVT description 167
5.6.2. Gas-oil displacement in a high NTG layer with realistic fluid PVT description 167
5.6.3. Study of a range of production rates on both simplified and realistic fluid PVT description 170
5.6.4. Well control scheme with realistic fluid PVT description 170
5.7. Results and Discussion 172
5.7.1. Gas-oil displacement in a high NTG layer with simplified fluid PVT description 172
5.7.2. Gas-oil displacement in a high NTG layer with realistic fluid PVT description 175

5.7.3. Discussion of gas oil displacement in a high NTG layer with different fluid PVT description 180
5.7.3.1 Impact of the sand Kv:Kh ratio 180
5.7.3.2. Impact of the different fluid PVT description 181
5.7.4. Impact of production rate 187
5.7.5. Discussion of the impact of production rate 191
5.7.6. Impact of well control scheme 192
5.7.7. Discussion of the impact of the well control scheme 196
5.8. General discussion 202
5.9. Conclusions 205
Chapter 6 Rapid estimation of oil recovery 207
6.1 Overview 207
6.2 Aims 208
6.3 The challenge of recovery prediction 209
6.4 Shale description and influence in high NTG sandstone reservoirs 213
6.5 Methodology and design of experiment 214
6.6 2D model construction and flow simulation 217
6.7 Results 219
6.7.1 On recovery at gas breakthrough in a reservoir model with NTG less than 100% 219
6.7.2 Oil recovery at gas breakthrough in 100% NTG reservoir model 223
6.8 Discussion 224
6.8.1 Impact of shale continuity on recovery 224
6.8.1.1 System with discontinuous shales 224
6.8.1.2 System with continuous shales 228
6.8.2. The problem of defining Kv:Kh ratio 232
6.8.3. Limitations of the study 233
6.8.3.1 Impact of small scale geological features 233
6.8.3.2 On 2D net-to-gross 233
6.8.3.3 Reliability of the streamline simulator 234
6.8.3.4 On grid refinement 235
6.8.3.5 On single-phase Kv:Kh correlation and gravity drainage after gas invasion 236
6.9 Conclusion 238
Chapter 7 Conclusion and recommendation 240
7.1 Overview 240
7.2 Conclusions 241
7.2.1 Preliminary displacement study 241

7.2.2 Screening study of reservoir-unit scale heterogeneities.....241
7.2.3 Screening study of combined genetic-unit and reservoir-unit scale heterogeneities 242
7.2.4 Methodology for the rapid estimation of oil recovery 244
7.3 Recommendations.....245
References.....247
Appendix 1 Supplementary notes for preliminary displacement study 258
Appendix 2 Test of the reliability of the grid cell resolution.....263
Appendix 3 Test of the reliability of the number of realizations 267
Appendix 4 Test of the variation of reservoir model size.....269
A4.1 Results of the gas-oil displacement simulation in a high NTG layer with simplified fluids description; subset model 271
A4.2 Discussion on the impact of variation in reservoir model size 273
Appendix 5 Test of the different gas-oil displacement relative permeability data .274
A5.1 Results of gas-oil displacement simulation in a high NTG layer sector model with simplified fluid description and re-viewed relative permeability data.....276
A5.2 Discussion on the impact of variation in relative permeability 279
Appendix 6 Test of the reliability of the streamline simulation.....283

List of Figures

FIGURE 1.1. (A, TOP) MAP OF THE WESTERN SOUTH CASPIAN BASIN HIGHLIGHTING OIL FIELDS, INCLUDING THE ACG FIELD, AND THE LOCATION OF OUTCROP ANALOGS ON THE APSHERON PENINSULA (Y = YASAMAL VALLEY, B = BALAKHANY QUARRY, K = KIRMAKY VALLEY). (B, BOTTOM) PALEOGEOGRAPHIC MAP OF THE SOUTH CASPIAN BASIN DURING DEPOSITION OF THE PRODUCTIVE SERIES. NOTE THAT THE PALEO-VOLGA DELTA UNDERWENT MULTIPLE EPISODES OF ADVANCE AND RETREAT ACROSS THE AREA OF THE ACG FIELD DURING DEPOSITION OF THE PRODUCTIVE SERIES.....29

FIGURE 1.2. MAP OF THE ACG FIELD HIGHLIGHTING THE AZERI, CHIRAG AND GUNASHLI ACCUMULATIONS. SIMPLIFIED CROSS-SECTIONS AND PLAN-VIEW MAPS ARE SHOWN FOR THE NORTH AND SOUTH FLANKS OF THE AZERI RESERVOIR. THE MODELS PRESENTED IN THIS THESIS ARE CONSTRUCTED FOR THESE RESERVOIR-PRODUCTION SYMMETRY ELEMENTS. 31

FIGURE 2.1. STRATIGRAPHY OF THE PRODUCTIVE SERIES IN ASPHERON PENINSULA, AZERBAIJAN.....38

FIGURE 2.2. PLAN VIEW OF THE SOUTH CASPIAN BASIN INCLUDING OIL/GAS FIELDS. THE ACG FIELD ARE A COMBINATION OF AZERI-CHIRAG AND GUNASHLI RESERVOIRS. THE AZERI RESERVOIR IS LOCATED AT THE SOUTH-EAST SECTION OF THE ACG STRUCTURE. OUTCROP ANALOGUES ARE LOCATED ON THE APSHERON PENINSULA. BALAKHANY QUARRY CONTAIN OUTCROP ANALOGUES FOR HIGH NTG INTERVALS IN THE PRODUCTIVE SERIES: PERERIV B,D. THE YASAMAL VALLEY CONTAIN OUTCROP ANALOGUES FOR LOW NTG INTERVALS: PERERIV A,C,E.....38

FIGURE 2.3. PROCESS-BASED CLASSIFICATION FOR THREEFOLD DIVISION OF DELTAS. MODIFIED FROM THE ORIGINAL FIGURE OF GALLOWAY 1975. THERE ARE 9 EXAMPLES THAT REPRESENT DIFFERENT TYPE OF DELTA: 0. VOLGA DELTA; 1. MISSSISSIPPI DELTA; 2. MAHAKAM DELTA; 3. NIGER DELTA; 4. MEKONG DELTA; 5. FLY DELTA; 6. SAO FRANCISCO DELTA; 7. EBRO DELTA; 8. COPPER DELTA.....45

FIGURE 2.4. (A, TOP) SATELLITE IMAGE OF THE MODERN VOLGA DELTA. THE DELTA IS DIVIDED INTO THREE PARTS (1) DELTA PLAIN, THE LARGE UPSTREAM REGION OF THE DELTA SYSTEM DOMINATED BY SUBAERIAL FLUVIAL CHANNELS; (2) DELTA FRONT, THE DOWNSTREAM REGION OF THE DELTA, IS A ZONE OF INTERACTION BETWEEN FLUVIAL AND BASINAL PROCESS; (3) PRODELTA, AT THE OUTER LIMIT OF THE SUBAQUEOUS DELTA. IN DIFFERENT PARTS OF THE DELTA, SANDBODIES HAVE DIFFERENT GEOMETRIES AND ARCHITECTURES. ON

THE DELTA PLAIN, THE CONNECTIVITY OF BRANCHING CHANNEL SANDBODIES IS CONTROLLED BY THEIR DISTRIBUTION, WIDTH, THICKNESS AND SINUOSITY, WHILST THE DELTA FRONT CONTAINS MOUTH-BAR SANDBODIES (HTTP://MAPS.GOOGLE.COM/). (B, BOTTOM) SATELLITE IMAGE OF THE MODERN MISSISSIPPI DELTA. COMPARED WITH THE MODERN VOLGA DELTA, THE MISSISSIPPI DELTA HAS A SMALL NUMBER OF DISTRIBUTARY CHANNELS AND THE DELTA FRONT IS COMPOSED OF WIDELY SEPARATED MOUTH BARS. THE DIFFERENT FACIES ARCHITECTURE BETWEEN THESE TWO FLUVIAL-DOMINATED DELTAS IS MAINLY BECAUSE OF THE RAPID LAKE LEVEL CHANGE, GENTLE OFFSHORE GRADIENT AND HOMOPYCNAL INFLOW OF THE VOLGA DELTA. (HTTP://MAPS.GOOGLE.COM/). 47

FIGURE 2.5. (A, TOP) CONCEPTUAL DIAGRAM OF HIGH NTG RESERVOIR ARCHITECTURE IN PERERIV B AND D LAYERS. FIGURE BASED ON OUTCROPS LOCATED AT BALAKHANY QUARRY. THE SANDBODY CIRCLED SHOWS AN EXAMPLE OF THE INTERNAL COMPLEXITY OF EACH SANDBODY (REYNOLDS AND RILEY 2003). (B, BOTTOM) CONCEPTUAL DIAGRAMS OF LOW NTG RESERVOIR ARCHITECTURE IN PERERIV A, C AND E LAYERS. FIGURE BASED ON OUTCROPS LOCATED AT YASAMAL VALLEY (REYNOLDS AND RILEY 2003). 55

FIGURE 2.6. WEBER'S 1986 HIERARCHICAL OF RESERVOIR HETEROGENEITY AT DIFFERENT LENGTH SCALES; EXAMPLE FROM A FLUVIAL RESERVOIR. 60

FIGURE 2.7. HIERARCHY OF HETEROGENEITY IN THE FLUVIAL-DOMINATED DELTAIC PERERIV SUITE RESERVOIR OF THE ACG FIELD. THE HIERARCHY IS MODIFIED FROM WEBER'S 1986 SCHEME. SUB-METRE SCALE (CORE-UNIT AND PORE SCALE) ARE NOT INCLUDED. 63

FIGURE 2.8. THE THREE DIFFERENT GENERIC RESERVOIR ARCHITECTURES IDENTIFIED BY WEBER AND VAN GEUNS 1990. THE FIGURE DEMONSTRATES THAT DIFFERENT GEOLOGICAL FEATURES CAN BE FOUND IN VARIOUS TYPES OF RESERVOIR WHICH HAVE VARIOUS SANDBODY CONNECTIVITIES. 64

FIGURE 3.1. GEOMETRY OF THE SECTOR RESERVOIR MODEL FOR THE ANALYTICAL STUDY. THE DISTANCE BETWEEN PRODUCTION WELLS WAS CHOSEN TO BE THE WIDTH (W) FOR THE ANALYTICAL STUDY WHICH IS 750M. THE LENGTH (L) IS 1900M FOR THE NORTH FLANK MODELS AND 478M FOR THE SOUTH FLANK MODELS. THE THICKNESS (H) OF THE MODEL DEPENDS ON WHICH LAYER OF THE PERERIV SUITE IS BEING STUDIED. 79

FIGURE 3.2. GAS-OIL (A, TOP) AND WATER-OIL (B, BOTTOM) RELATIVE PERMEABILITY CURVES IN THE PERERIV SUITE RESERVOIR OF THE AZERI FIELD. 81

FIGURE 3.3. DIFFERENT STAGES OF A DISPLACEMENT'S STABILITY UNDER SEGREGATED FLOW CONDITIONS. 83

FIGURE 3.4. FRACTIONAL FLOW CURVES OF GAS (A, TOP) AND WATER (B, BOTTOM). DETERMINATION OF GAS (A, TOP) AND WATER (B, BOTTOM) SATURATION AT THE SHOCK FRONT BY APPLYING WELGE'S GRAPHICAL TECHNIQUE AND ASSUMING OIL DISPLACEMENT FROM A SYSTEM WITH UNIFORM INITIAL CONNATE WATER SATURATION (S_{WC}: 0.112) AND ZERO INITIAL GAS SATURATION (S_{GC}: 0). A TANGENT IS DRAWN TO THE FRACTIONAL FLOW CURVE FROM THE INITIAL GAS/WATER SATURATION. THE TANGENT POINT INDICATES THE SATURATION OF THE SHOCK FRONT. THE INTERCEPT OF THE TANGENT AT F=1 INDICATES THE AVERAGE SATURATION BEHIND THE FRONT AT BREAKTHROUGH TIME AT THE PRODUCTION WELL.....87

FIGURE 3.5. THE ESTIMATION OF THE DIMENSIONLESS CUMULATIVE OIL RECOVERY PROFILE (PORE VOLUME) AND GAS CUT (A, TOP) AND WATER CUT (B, BOTTOM) PROFILE FOR THE ENSEMBLES FROM THE NORTH AND SOUTH FLANK OF THE AZERI FIELD. 89

FIGURE 3.6. SUMMARY OF THE BREAKTHROUGH TIME (A, TOP) AND CUMULATIVE OIL RECOVERY AT BREAKTHROUGH (B, BOTTOM) IN EACH ENSEMBLE UNDER GAS AND WATER INJECTION. THE RESULTS ARE ESTIMATED BY BUCKLEY-LEVERETT FLOW AND SEGREGATED FLOW MODEL. 90

FIGURE 3.7. THE ESTIMATION OF THE DIMENSIONLESS CUMULATIVE OIL RECOVERY PROFILE (PORE VOLUME) (A, TOP) AND GAS CUT (B, BOTTOM) PROFILE FOR THE ENSEMBLES UNDER DIFFERENT STABILITY ASSUMPTIONS. THE FIGURES COVERED THE CASE WHEN THE NORTH FLANK HAS DIFFERENT DIP ANGLES THAT EQUIVALENT TO APPLY A RANGE OF DIFFERENT DIETZ'S CRITICAL RATE FOR THE DISPLACEMENT. FOR THE RANGE OF DIP ANGLES FROM 45^{O}, 35^{O} TO 25^{O} THE CURRENT THE PRODUCTION RATE IS EQUIVALENT TO C. 72%, 89% AND 121% DIETZ'S CRITICAL RATE.....95

FIGURE 3.8. SUMMARY OF THE BREAKTHROUGH TIME (A, TOP) AND CUMULATIVE OIL RECOVERY AT BREAKTHROUGH (B, BOTTOM) IN EACH ENSEMBLE UNDER GAS INJECTION. THE RESULTS ESTIMATED USING A SEGREGATED FLOW MODEL. THE CURRENT OFFTAKE RATE APPLIES TO RESERVOIR MODELS THAT HAVE A DIP ANGLE EQUAL TO 45^{O} , 35^{O} AND 25^{O} RESPECTIVELY; THAT IS EQUIVALENT TO 72%, 89% AND 121% DIETZ'S CRITICAL RATE THAT IS APPLIED TO THE MODEL. 96

FIGURE 4.1. 3D IMAGES OF NORTH-FLANK STATIC RESERVOIR MODELS THAT WERE USED TO CONDUCT THE 1^{ST}, 2^{ND} AND 3^{RD} SCREENING STUDIES. THE MODELS DEMONSTRATE THE DIFFERENT SETTINGS OF RESERVOIR-UNIT SCALE HETEROGENEITIES THAT WERE EXAMINED. FOR EXAMPLE, A MODEL WITH SINUOUS CHANNELS OBLIQUE TO THE TECTONIC DIP (WITH 49^{O} OFFSET) **(A)** IS COMPARED WITH A CASE WHERE STRAIGHT CHANNELS ARE ALIGNED

PARALLEL TO THE TECTONIC DIP **(B)**. THE BLUE ARROW SHOWS THE OVERALL CHANNEL ORIENTATION. A MODEL WITH SEVERAL MULTISTOREY LARGE CHANNEL-FILL SANDBODIES **(C)** IS COMPARED WITH A MODEL CONTAINING MANY SMALL, SINGLE-STOREY CHANNEL-FILL SANDBODIES **(D)**. FIGURES **A-D** WERE CAPTURED FROM LOW NTG MODELS (PERERIV C). FIGURES **E** AND **F** DEMONSTRATE LATERAL VARIATIONS IN NTG WITHIN THE PERERIV C LAYER WHEN THE STATIC MODELS INCLUDE PERERIV B, C AND D LAYERS. THE GREEN DOTTED LINES DEMONSTRATE BOUNDARIES BETWEEN EACH SUB-PERERIV LAYER, WHICH WERE SET EITHER TO ALLOW NO CONNECTIVITY BETWEEN PERERIV B, C AND D LAYERS **(E)** OR TO ALLOW SANDBODY CONNECTIVITY ACROSS THE LAYER BOUNDARIES **(F)**. 109

FIGURE 4.2. RECOVERY FACTOR, CUMULATIVE GAS OIL PRODUCTION RATIO (GOR) AND CUMULATIVE WATER CUT FROM GAS INJECTION (A,C) AND WATER INJECTION (B,D) AS A FUNCTION OF TIME FOR EACH OF THE 16 SIMULATION EXPERIMENTS RUN IN THE FIRST SENSITIVITY ANALYSIS ON THE PERERIV B, C AND D LAYERS. ANALYSIS OF THESE CURVES YIELDED THE RESPONSES SHOWN IN FIGURES 4.3..... 119

FIGURE 4.3. RESULTS OF 1ST SCREENING STUDY, AVERAGE PERCENTAGE CHANGE IN (A, TOP) OIL RECOVERED AFTER 20 YEARS, AND (B, BOTTOM) OIL RECOVERED AT BREAKTHROUGH OF GAS (NORTH FLANK) AND WATER (SOUTH FLANK), OBSERVED WHEN EACH FACTOR IN THE SENSITIVITY ANALYSIS IS VARIED FROM SETTING 1 TO SETTING 2 (TABLE 4.1). PERERIV B, C AND D LAYERS ARE INCLUDED IN THE MODELS. IF THE BAR LIES TO THE RIGHT THEN THE CHANGE IS POSITIVE. FOR EXAMPLE, MODELLING PERERIV C WITH 45% NTG (SETTING 2) INCREASES CUMULATIVE OIL RECOVERY BY C. 14% COMPARED WITH MODELLING IT WITH ZERO NTG (SETTING 1). THE DASHED LINES DENOTE THE AVERAGE PERCENTAGE CHANGE OBSERVED FROM DIFFERENT STOCHASTIC REALIZATIONS. IF THE IMPACT OF VARYING A FACTOR IS AT OR BELOW THE LEVEL OF STOCHASTIC UNCERTAINTY THEN MODELLING DECISIONS ARE UNIMPORTANT FOR THE CHOSEN RANGE OF PARAMETERS. 120

FIGURE 4.4. RESULT OF 1ST SCREENING STUDY, AVERAGE PERCENTAGE CHANGE IN OIL RECOVERY FACTOR AFTER 20 YEARS, OBSERVED WHEN EACH FACTOR IN THE SENSITIVITY ANALYSIS IS VARIED FROM SETTING 1 TO SETTING 2 (TABLE 4.1). PERERIV B, C AND D LAYERS ARE INCLUDED IN THE MODELS. IF THE BAR LIES TO THE RIGHT THEN THE CHANGE IS POSITIVE. RECOVERY FACTOR WAS DEFINED AS THE CUMULATIVE OIL RECOVERED OVER THE STOIIP OF THE MODEL. AS POOR CONNECTIVITY OF SANDBODIES IN THE LOW NTG LAYER (PERERIV C), THEREFORE THE OVERALL RECOVERY FACTOR REDUCED IF

MORE NET SAND WAS INTRODUCED INTO THIS LAYER. 122
FIGURE 4.5. RECOVERY FACTOR, CUMULATIVE GAS OIL PRODUCTION RATIO (GOR) AND CUMULATIVE WATER CUT FROM GAS INJECTION (A,C) AND WATER INJECTION (B,D) AS A FUNCTION OF TIME FOR EACH OF THE 16 SIMULATION EXPERIMENTS RUN IN THE SECOND SENSITIVITY ANALYSIS ON THE PERERIV B, C AND D LAYERS. ANALYSIS OF THESE CURVES YIELDED THE RESPONSES SHOWN IN FIGURES 4.6..... 126
FIGURE 4.6. RESULT OF 2ND SCREENING STUDY, AVERAGE PERCENTAGE CHANGE IN OIL RECOVERED AND TOTAL GAS (NORTH FLANK) AND WATER (SOUTH FLANK) PRODUCED AFTER 20 YEARS IN (A, TOP) NORTH FLANK MODELS, AND (B, BOTTOM) SOUTH FLANK MODELS, OBSERVED WHEN EACH FACTOR IN THE SENSITIVITY ANALYSIS IS VARIED FROM SETTING 1 TO SETTING 2 (TABLE 4.1). PERERIV B, C AND D LAYERS ARE INCLUDED IN THE MODELS; PERERIV C IS MODELLED WITH A FIXED NTG OF 45%. 127
FIGURE 4.7. RECOVERY FACTOR, CUMULATIVE GAS OIL PRODUCTION RATIO (GOR) AND CUMULATIVE WATER CUT FROM GAS INJECTION (A,C) AND WATER INJECTION (B,D) AS A FUNCTION OF TIME FOR EACH OF THE 8 SIMULATION EXPERIMENTS RUN IN THE THIRD SENSITIVITY ANALYSIS ON THE PERERIV B LAYERS. ANALYSIS OF THESE CURVES YIELDED THE RESPONSES SHOWN IN FIGURES 4.8. 131
FIGURE 4.8. RESULTS OF 3RD SCREENING STUDY (PERERIV B), AVERAGE PERCENTAGE CHANGE IN OIL RECOVERED AND TOTAL GAS (NORTH FLANK) AND WATER (SOUTH FLANK) PRODUCED AFTER 20 YEARS IN (A, TOP) NORTH FLANK MODELS, AND (B, BOTTOM) SOUTH FLANK MODELS OF PERERIV B ONLY, OBSERVED WHEN EACH FACTOR IN THE SENSITIVITY ANALYSIS IS VARIED FROM SETTING 1 TO SETTING 2 (TABLE 4.1). 132
FIGURE 4.9. PLAN VIEWS OF (LEFT COLUMN) SHALE DISTRIBUTION; (CENTER COLUMN) THICKNESS-AVERAGED PERMEABILITY; AND (RIGHT COLUMN) THICKNESS-AVERAGED MOBILE OIL SATURATION AFTER 5 YEARS OF WATER INJECTION IN (TOP ROW) SOUTH-FLANK MODEL OF PERERIV B WITH CHANNEL BELTS PARALLEL TO THE TECTONIC DIP AND (BOTTOM ROW) SOUTH-FLANK MODEL OF PERERIV B WITH CHANNEL BELTS OBLIQUE TO THE TECTONIC DIP (WITH A 49° OFFSET TO THE EAST). THE TWO PRODUCERS AND ONE INJECTOR ARE ALSO LABELED. THE MODEL WITH CHANNEL BELTS OBLIQUE TO THE TECTONIC DIP EXHIBITS A WIDER RANGE OF THICKNESS-AVERAGED PERMEABILITY (BOTTOM CENTER). THUS, FOR THIS MODEL, SWEEP EFFICIENCY IS SUBTLY DECREASED BECAUSE OF A WIDER RANGE OF FLOW PATH LENGTHS. EARLIER BREAKTHROUGH OCCURS IN THE MODEL (BOTTOM

RIGHT) AS A RESULT OF THIS SUBTLE DECREASE IN AREAL SWEEP EFFICIENCY. 133

FIGURE 4.10. RECOVERY FACTOR, CUMULATIVE GAS OIL PRODUCTION RATIO (GOR) AND CUMULATIVE WATER CUT FROM GAS INJECTION (A,C) AND WATER INJECTION (B,D) AS A FUNCTION OF TIME FOR EACH OF THE 8 SIMULATION EXPERIMENTS RUN IN THE THIRD SENSITIVITY ANALYSIS ON THE PERERIV C LAYERS. ANALYSIS OF THESE CURVES YIELDED THE RESPONSES SHOWN IN FIGURES 4.11. 137

FIGURE 4.11. RESULTS OF 3RD SCREENING STUDY (PERERIV C), AVERAGE PERCENTAGE CHANGE IN OIL RECOVERED AND TOTAL GAS (NORTH FLANK) AND WATER (SOUTH FLANK) PRODUCED AFTER 20 YEARS IN (A, TOP) NORTH FLANK MODELS, AND (B, BOTTOM) SOUTH FLANK MODELS OF PERERIV C ONLY, OBSERVED WHEN EACH FACTOR IN THE SENSITIVITY ANALYSIS IS VARIED FROM SETTING 1 TO SETTING 2 (TABLE 4.1). 138

FIGURE 4.12. RESULTS OF 3RD SCREENING STUDY (PERERIV C), AVERAGE PERCENTAGE CHANGE IN CONNECTED FRACTION OF CHANNEL-FILL SANDSTONES BETWEEN INJECTION AND PRODUCTION WELLS, AND OIL RECOVERED AFTER 20 YEARS OF TRACER INJECTION, IN (**A, TOP**) NORTH FLANK MODELS, AND (**B, BOTTOM**) SOUTH FLANK MODELS OF PERERIV C ONLY, OBSERVED WHEN EACH FACTOR IN THE SENSITIVITY ANALYSIS IS VARIED FROM SETTING 1 TO SETTING 2 (TABLE 2). 140

FIGURE 4.13. PLAN VIEW OF THICKNESS-AVERAGED OIL SATURATION AFTER 5 YEARS OF TRACER INJECTION IN (LEFT) NORTH-FLANK MODEL OF PERERIV C WITH MULTISTOREY, CHANNEL-BELT SANDBODIES AND (RIGHT) NORTH-FLANK MODEL OF PERERIV C WITH INDIVIDUAL, SINGLE-STOREY CHANNEL-FILL SANDBODIES. THE TWO PRODUCERS AND ONE INJECTOR ARE LABELED. WHERE THE FIGURES SHOW THICKNESS AVERAGED MOBILE OIL SATURATION LESS THAN 1 INDICATED THAT ONE OR MORE LAYERS AT THAT LOCATION IS OCCUPIED BY THE INJECTED FLUID. THIS PLOT COULD ENABLE IDENTIFICATION OF INDIVIDUAL FLOW PATHS WITHIN THE MODEL (E.G. A FLOW PATH OF INJECTED FLUID MOVING TOWARDS THE PRODUCER WAS IDENTIFIED BY A WHITE CIRCLE). FLOW PATHS IN THE SINGLE-STOREY MODEL (RIGHT) WERE MORE TORTUOUS, RESULTING IN POORER AREAL SWEEP OF THE OIL. THEREFORE, EARLIER BREAKTHROUGH RESULTS FROM MODELLING SINGLE-STOREY CHANNEL-FILL CHANNEL SANDBODIES. HENCE, THE CUMULATIVE OIL RECOVERED IS LOWER FOR SUCH A MODELLING SETTING. ON AVERAGE WHEN SINGLE-STOREY CHANNEL-FILL SANDBODIES WERE MODELLED, OIL RECOVERY WAS C. 19% LOWER THAN IN WHEN MULTISTOREY

CHANNEL-FILL SANDBODIES WERE MODELLED. 142
FIGURE 4.14. IMPACT OF DIFFERENT HETEROGENEITIES ON FLOW WITHIN PERERIV B, C AND D IN **(A, LEFT)** THE NORTH FLANK AND **(B, RIGHT)** THE SOUTH FLANK. ABSOLUTE PERCENTAGE CHANGE IN OIL RECOVERED AFTER 20 YEARS WAS PLOTTED AS DISTANCE FROM THE CENTER OF THE CHART FOR EACH HETEROGENEITY, TO ENABLE COMPARISON BETWEEN THE PREVIOUS SIMULATIONS OF TRACER FLOW, GAS INJECTION, AND WATER INJECTION. THE AREA AROUND THE CENTER OF EACH CHART REPRESENTS THE AVERAGE PERCENTAGE CHANGE OBSERVED FROM DIFFERENT STOCHASTIC REALIZATIONS. THE TRACER SIMULATIONS CAPTURED THE RANKING ORDER ABOVE STOCHASTIC UNCERTAINTY FOR BOTH GAS-OIL AND WATER-OIL DISPLACEMENTS, SUGGESTING THAT GRAVITY SEGREGATION, AND RELATIVE PERMEABILITY EFFECTS, WERE SMALL. 147
FIGURE 5.1. THE SETTING OF THE SUBSET RESERVOIR MODELS MIMICS THE DISPLACEMENT MECHANISM IN THE SYMMETRY ELEMENT MODEL..... 165
FIGURE 5.2 (A-E). AZERI RESERVOIR FLUIDS DESCRIPTION AT DIFFERENT RESERVOIR PRESSURE. (2A) OIL FORMATION FACTOR; THE RESERVOIR BUBBLE POINT PRESSURE IS APPROXIMATELY 302 BARA (2B) GAS FORMATION FACTOR; (2C) OIL VISCOSITY (2D) GAS VISCOSITY (2E) GAS COMPRESSIBILITY MEASURED IN THE AZERI RESERVOIR. THE FLUIDS SAMPLE TESTS WERE DONE AT C. 342K. 169
FIGURE 5.3. THE SETTING OF THE SUBSET RESERVOIR MODEL TO MIMIC DISPLACEMENT MECHANISM CLOSE TO THE PRODUCTION WELL IN ORDER TO STUDY THE INFLUENCE OF WELL CONTROL ON THE SCREENING STUDY..... 171
FIGURE 5.4. RECOVERY FACTOR (A) AND CUMULATIVE GAS OIL PRODUCTION RATIO (GOR) (B) AS A FUNCTION OF TIME FOR EACH OF THE 16 SIMULATION EXPERIMENTS RUN IN THE FOURTH SENSITIVITY ANALYSIS ON THE PERERIV B LAYERS BASED ON SIMPLIFIED FLUID PVT DESCRIPTION. ANALYSIS OF THESE CURVES YIELDED THE RESPONSES SHOWN IN FIGURES 5.5. 174
FIGURE 5.5. AVERAGE PERCENTAGE CHANGE IN RECOVERY FACTOR IN SUBSET MODELS WITH SIMPLIFIED FLUID PVT DESCRIPTION AFTER 10 YEARS IN NORTH FLANK SUBSET MODELS OF PERERIV B, OBSERVED WHEN EACH FACTOR IN THE SENSITIVITY ANALYSIS IS VARIED FROM SETTING 1 TO SETTING 2 (TABLE 5.1). IF THE BAR LIES TO THE RIGHT THEN THE CHANGE IS POSITIVE. FOR EXAMPLE, MODELLING THE CHANNEL SAND KV:KH RATIO EQUAL TO 1 (SETTING 2) INCREASED RECOVERY FACTOR BY C. 14.3% COMPARED WITH MODELLING IT EQUAL TO 0.1 (SETTING 1). THE DASHED LINES DENOTE THE AVERAGE PERCENTAGE CHANGE OBSERVED FROM DIFFERENT STOCHASTIC REALIZATIONS. IF THE IMPACT OF VARYING A FACTOR IS AT OR BELOW THE

LEVEL OF STOCHASTIC UNCERTAINTY THEN MODELLING DECISIONS ARE UNIMPORTANT FOR THE CHOSEN RANGE OF PARAMETERS. 175
FIGURE 5.6. RECOVERY FACTOR (A) AND CUMULATIVE GAS OIL PRODUCTION RATIO (GOR) (B) AS A FUNCTION OF TIME FOR EACH OF THE 16 SIMULATION EXPERIMENTS RUN IN THE FOURTH SENSITIVITY ANALYSIS ON THE PERERIV B LAYERS BASED ON REALISTIC FLUID PVT DESCRIPTION. ANALYSIS OF THESE CURVES YIELDED THE RESPONSES SHOWN IN FIGURES 5.7. 177
FIGURE 5.7. AVERAGE PERCENTAGE CHANGE IN RECOVERY FACTOR AND TOTAL GAS PRODUCED IN SUBSET MODELS WITH REALISTIC FLUID PVT DESCRIPTION AFTER 10 YEARS IN NORTH FLANK SUBSET MODELS OF PERERIV B, OBSERVED WHEN EACH FACTOR IN THE SENSITIVITY ANALYSIS IS VARIED FROM SETTING 1 TO SETTING 2 (TABLE 5.1). THE REALISTIC FLUID PVT DESCRIPTION (FIGURE 5.2) IS APPLIED. 178
FIGURE 5.8. ABSOLUTE PERCENTAGE CHANGE IN RECOVERY FACTOR AT THE END OF PRODUCTION PERIOD IS PLOTTED AS DISTANCE FROM THE CENTRE OF THE CHART FOR EACH HETEROGENEITY, TO ENABLE COMPARISON BETWEEN SIMULATIONS WITH SIMPLIFIED AND REALISTIC FLUID PVT DESCRIPTION..... 179
FIGURE 5.9. CROSS SECTION VIEW OF GAS SATURATION AFTER 3 YEARS OF PRODUCTION IN PERERIV B. AN EXTENSIVE SHALE WAS PRESENT IN THE MIDDLE OF THE MODEL AND REALISTIC FLUID PVT DESCRIPTION (A) AND SIMPLIFIED FLUID PVT DESCRIPTION WERE APPLIED (B). COMPARED WITH THE CASE WHERE NO EXTENSIVE SHALE WAS PRESENT, AND REALISTIC FLUID PVT DESCRIPTION (C) AND SIMPLIFIED FLUID PVT DESCRIPTION WERE APPLIED (D). THE PRODUCERS AND INJECTOR WERE LABELED. THE PLOTS SHOWED THAT THE GAS SATURATION IS HIGHER IN THE INVADED ZONE IN THE MODELS CONTAINING THE EXTENSIVE SHALE (A,B) THAN IN THE MODELS LACKING THE EXTENSIVE SHALE (C,D). WITH THE EXTENSIVE SHALE PRESENT, THE GAS SATURATION WAS SUBTLY HIGHER IN THE INVADED ZONE. THIS EFFECT IS MORE OBVIOUS WHEN REALISTIC FLUID PVT DESCRIPTION WAS APPLIED. 185
FIGURE 5.10. AVERAGE RESERVOIR PRESSURE AT DATUM CHANGES AS A FUNCTION OF TIME FOR EACH OF THE 16 SIMULATION EXPERIMENTS RUN WITH THE REALISTIC FLUID PVT DESCRIPTION. THE RESERVOIR DATUM PRESSURE DROPPED BELOW BUBBLE POINT DURING THE PRODUCTION PERIOD. THEREFORE GAS WAS EVOLVED OUT OF SOLUTION. 186
FIGURE 5.11. CONCEPTUAL CROSS-SECTION VIEWS OF RESERVOIRS WITH DIFFERENT LAYERING GEOMETRY. GAS INJECTION FROM THE TOP (UP-DIP POSITION) AND A PRODUCTION WELL IS LOCATED AT THE BOTTOM OF THE MODEL. THE MODEL WITH A THINNER EFFECTIVE FLOW PATH (HIGHER DIP

ANGLE GROUP N_θ, 11B, RIGHT) YIELDED HIGHER BREAKTHROUGH AT OIL RECOVERY (BOR)..... 186

FIGURE 5.12 (A-D). AVERAGE PERCENTAGE CHANGE IN RECOVERY FACTOR (A, C) AND TOTAL GAS PRODUCED (B, D) AFTER 10 YEARS OF PRODUCTION. A RANGE OF PRODUCTION RATES WERE APPLIED WITH THE SIMPLIFIED FLUID PVT (A, B) AND REALISTIC FLUID PVT PROPERTIES (C, D). THE POINTS PLOTTED SHOWED THE RESPONSE WHEN EACH FACTOR IN THE SENSITIVITY ANALYSIS IS VARIED FROM SETTING 1 TO SETTING 2 (TABLE 5.1). 190

FIGURE 5.13. RECOVERY FACTOR (A) AND CUMULATIVE GAS OIL PRODUCTION RATIO (GOR) (B) AS A FUNCTION OF TIME FOR EACH OF THE 16 SIMULATION EXPERIMENTS RUN IN THE FOURTH SENSITIVITY ANALYSIS ON THE PERERIV B LAYERS BASED ON REALISTIC FLUID PVT DESCRIPTION; WELL CONTROL SCHEME WAS APPLIED. THE RESULTS WERE GENERATED UNDER C.93.3% OF DIETZ'S CRITICAL RATE. ANALYSIS OF THESE CURVES YIELDED THE RESPONSES SHOWN IN FIGURES 5.14..... 194

FIGURE 5.14 (A-B). AVERAGE PERCENTAGE CHANGE IN RECOVERY FACTOR (A, TOP) AND TOTAL GAS PRODUCED (B, BOTTOM) AFTER 10 YEARS OF PRODUCTION IN NORTH FLANK SUBSET MODELS OF PERERIV B. A RANGE OF PRODUCTION RATES WERE APPLIED WITH THE REALISTIC FLUID PVT DESCRIPTION AND WELL CONTROL SCHEME. THE POINTS PLOTTED SHOW THE RESPONSE WHEN EACH FACTOR IN THE SENSITIVITY ANALYSIS WAS VARIED FROM SETTING 1 TO SETTING 2 (TABLE 5.1). 195

FIGURE 5.15. AVERAGE GOR (A, TOP) AND RECOVERY FACTOR (B, BOTTOM) AS A FUNCTION OF PRODUCTION RATE WHEN DIFFERENT WELL CONTROL SCHEME WAS APPLIED. THE CUMULATIVE RECOVERY FACTOR WAS FOUND TO BE C. 10% HIGHER THAN THE CASE WHEN WELL CONTROL SCHEME WAS APPLIED. HOWEVER THE CUMULATIVE GOR WAS FOUND TO BE MUCH LOWER WHEN THE WELL CONTROL SCHEME WAS APPLIED, AND THE HIGHEST CUMULATIVE GOR IS FOUND WHEN C.116.7% DIETZ'S CRITICAL RATE WAS USED. BOTH SIMULATIONS WERE CONDUCTED UNDER REALISTIC FLUID PVT DESCRIPTION. 198

FIGURE 5.16. PLAN VIEW OF THICKNESS-AVERAGED PERMEABILITY (A) ; AND THICKNESS-AVERAGED MOBILE GAS SATURATION PLOT OF YEAR 1 (B) , YEAR 2 (C) , YEAR 3 (D) AND YEAR 5 (E-I) OF GAS INJECTION IN A NORTH-FLANK SECTOR MODEL OF PERERIV B UNDER REALISTIC FLUID PVT DESCRIPTIONS WITH A WELL CONTROL SCHEME APPLIED. THE WHITE DOTTED LINE REPRESENTS THE INLET FACE OF GAS INJECTION AND THE LOCATION OF A PRODUCER WELL IS ALSO LABELED. THE 5^{TH} YEAR OF INJECTION WAS FOCUSED IN ORDER TO

DEMONSTRATE THE INFLUENCE OF WELL CONTROL. A CROSS-SECTION VIEW OF GAS SATURATION WAS ALSO PLOTTED FOR FIGURE E-I. IN THE 5TH YEAR OF INJECTION, THE PRODUCER WAS SHUT DURING THE 1ST (E) , 5TH (G) AND THE 9TH (I) MONTH AND RE-OPENED DURING THE 3RD (F) AND THE 7TH (H) MONTH. THE OPENING AND SHUTTING-IN OF THE PRODUCER WAS BASED ON THE WELL'S GOR CONSTRAIN. THERE WAS A SUBTLE VARIATION OF GAS SATURATION BETWEEN THE SHUT-IN AND OPEN PERIODS; WHILE THE PRODUCER WAS CLOSED, LOWER GAS SATURATION WAS FOUND NEAR THE PRODUCER AND HIGHER GAS SATURATION WAS FOUND AT A HIGHER POSITION (BLACK CIRCLE). THE RESULTS DEMONSTRATED THAT GAS MOVED TO A HIGHER POSITION DURING THE SHUT-IN PERIOD. THE FIGURES DEMONSTRATED AN EXAMPLE OF THE VARIATION OF GAS SATURATION IN ONE OF THE HIGH NTG SECTOR MODELS UNDER 93.3% DIETZ'S CRITICAL RATE. 202

FIGURE 6.1. EXAMPLE OF SCHEME A MODEL (EXPLICITLY MODELLED SHALES) IN A RESERVOIR OF 90%NTG; (A, LEFT) LEFT SHOWS THE CASE WHERE THE SHALE: RESERVOIR LENGTH RATIO EQUAL TO 0.01. (B, RIGHT) RIGHT SHOWS THE CASE WHERE THE SHALE: RESERVOIR LENGTH RATIO EQUAL TO 0.8. 215

FIGURE 6.2. EXTENSIVE SHALES DIVIDE THE RESERVOIR INTO A NUMBER OF THIN LAYERS. 216

FIGURE 6.3. VARIATION OF EFFECTIVE FLOW PATH THICKNESS AGAINST PERCENTAGE CHANGE OF NTG. IF THE FRACTION OF EFFECTIVE FLOW PATH: RESERVOIR THICKNESS RATIO IS 1 THAT MEANS THE RESERVOIR THICKNESS IS EQUAL TO THE EFFECTIVE FLOW PATH THICKNESS. 217

FIGURE 6.4. CUMULATIVE OIL RECOVERY AT BREAKTHROUGH (CORB) UNDER 46.7% DIETZ'S CRITICAL RATE IN VARIOUS SAND/SHALE 2D HETEROGENEOUS MODELS WITH DIFFERENT MODELLING SCHEMES. THREE SETS OF NUMERICAL SIMULATIONS WERE CONDUCTED TO REPRESENT RESERVOIRS CONTAINING SHALES OF DIFFERENT CONTINUITY. THE CORB VALUES OF 100% NTG RESERVOIR MODEL WITH KV:KH EQUAL TO 1 AND 0 WERE ALSO ESTIMATED. 220

FIGURE 6.5. BEGG AND KING (1985) CORRELATION OF THE KV:KH RATIO WITH NTG ASSUMING DIFFER AT SHALE LENGTH AND DENSITY. THE FIGURE DEMONSTRATED TWO EXAMPLES WITH DIFFERENT RATIOS OF THE SHALE LENGTH: (1) SHALE: RESERVOIR LENGTH RATIO EQUAL TO 0.1 WHICH WAS PLOTTED IN A LOG SCALE (A, TOP, PLOTTED IN LOG SCALE); AND (2) SHALE: RESERVOIR LENGTH RATIO EQUAL TO 0.01 (B, BOTTOM). INCREASING THE NUMBER OF SHALES PRESENT CAUSED THE KV:KH TO REDUCE. MOREOVER, IN MODELS HAVING THE SAME SHALE DENSITY (NTG) THE LARGER NUMBER OF SHALES PER UNIT RESERVOIR THICKNESS AND LONGER SHALES RESULTED IN

LOWER KV:KH RATIOS. 222
FIGURE 6.6. CORB AS A FUNCTION OF KV:KH RATIO OF THE HOMOGENEOUS MODELS. REALISTIC FLUIDS DESCRIPTION AND SIX PRODUCTION RATES WERE USED (23.3%, 46.7%, 70.0%, 93.3%, 116.7% AND 186.7% OF THE DIETZ'S CRITICAL RATE WERE APPLIED). IT WAS OBSERVED THAT IF THE OFFTAKE RATE WAS HIGHER THAN DIETZ'S CRITICAL RATE (186.7%) THE CORB WAS EQUAL TO THE CASE WHEN DISPLACEMENT WITH OFFTAKE RATE AT 46.7% OF THE DIETZ'S CRITICAL RATE IN SANDBODY WITH KV:KH EQUAL TO 0. THE RESULT DEMONSTRATED THAT RECOVERY WAS THE SAME FOR ANY REASON THAT PREVENTS VE E.G. VISCOUS DOMINATED DISPLACEMENT OR NO VERTICAL CROSS FLOW.....227
FIGURE 6.7. EXAMPLE OF ANALYTICAL ESTIMATION OF SEGREGATED DISPLACEMENT OF OIL BY WATER (DAKE 1978). IT ASSUMES THAT MOVABLE OIL IN THE WATER-INVADED ZONE WAS DISPLACED. SIMPLE TRIGONOMETRY SHOWS THAT RECOVERY CAN BE ESTIMATED BY: OIL RECOVERY EQUAL TO $(1-\frac{(h-y_e)^2}{2hL\tan\beta})$. Y_E IS THE WATER LEVEL HEIGHT AT DIFFERENT STAGES OF DISPLACEMENT AFTER BREAKTHROUGH WHICH CORRESPONDS TO THE FRACTION OF WATER PRODUCTION. THEREFORE AT BREAKTHROUGH Y_E IS EQUAL TO 0. THE EQUATION WAS QUOTED FROM DAKE 1978.....229
FIGURE 6.8. ANALYTICAL ESTIMATION OF CORB UNDER SEGREGATED FLOW MODEL WITH DIFFERENT EFFECTIVE FLOW PATH THICKNESS UNDER VARIOUS PRODUCTION RATES. THE FIGURE DEMONSTRATE THAT FOR GRAVITY DOMINATED DISPLACEMENTS, THE RECOVERY INCREASES WITH A REDUCTION OF THE RESERVOIR THICKNESS.....229
FIGURE 6.9. (A-C) IMPACT ON THE DISPLACEMENT FRONT WHEN A RESERVOIR WAS SUB-DIVIDED INTO EIGHT THIN LAYERS. WHEN RESERVOIR HAD NO EXTENSIVE IMPERMEABLE SHALE THE GLOBAL KV:KH OF THE RESERVOIR IS EQUAL TO 1 (A, LEFT). GAS INJECTED AT POINT B COULD FREELY TRAVEL TO POINT A OR C. WHEREAS, IN A CASE WHEN LATERALLY EXTENSIVE IMPERMEABLE SHALES WERE PRESENT (B, MIDDLE) GAS INJECTED AT POINT X CANNOT TRAVEL TO POINT W OR Y, THUS THE GLOBAL RESERVOIR KV:KH WAS ZERO. HOWEVER, THE DISPLACEMENT IN THE RESERVOIR WAS CLOSER TO A 'PISTON' LIKE MOBILITY STABLE DISPLACEMENT (C, RIGHT) INSTEAD OF A BUCKLEY-LEVERETT FLOW DISPLACEMENT WHICH WAS OUT OF VERTICAL EQUILIBRIUM, WHEN KV:KH WAS CONSIDERED TO BE ZERO OR BUCKLEY-LEVERETT FLOW.....230
FIGURE 6.10. ESTIMATION OF CUMULATIVE OIL RECOVERY AT BREAKTHROUGH UNDER 46.7% DIETZ'S CRITICAL RATE IN MODELS WITH EXTENSIVE SHALES

AND VARYING NTG. 231
FIGURE 6.11. ESTIMATION OF CUMULATIVE OIL RECOVERY AT BREAKTHROUGH UNDER 46.7% DIETZ'S CRITICAL RATE IN VARIOUS ANALYTICAL MODELS. ANALYTICAL ESTIMATION OF THE GRAVITY FORCE DOMINATED DISPLACEMENT RECOVERY. 235
FIGURE A2.1 (A-B). SHOWS THE COMPARISON OF THE OIL RECOVERY PROFILE (A, TOP) WITH THE GAS PRODUCTION PROFILE (B, BOTTOM) IN NORTH FLANK PERERIV C MODELS WITH VARIED GRID CELL THICKNESS. THE RESULTS SHOW THAT THE RESULT CONVERGED WHEN THE GRID CELL IS 0.5M. 264
FIGURE A2.2. SHOWS THE IMPACT OF DIFFERENT HETEROGENEITIES ON FLOW IN PERERIV C IN THE NORTH FLANK. ABSOLUTE PERCENTAGE CHANGE IN TOTAL OIL RECOVERY AFTER 20 YEARS IS PLOTTED, IN ORDER TO COMPARE THE CURRENT GRID CELL THICKNESS (1M) AND THE GRID REFINEMENT STUDIES (GRID CELL THICKNESS EQUAL TO 0.5M). REFINING THE GRID DOES NOT CHANGE THE RELATIVE IMPACT OF THE DIFFERENT HETEROGENEITIES, SUGGESTING THE GRID'S RESOLUTION APPLIED IN THIS RESEARCH ARE ROBUST. 266
FIGURE A3. SHOWS THE ABSOLUTE PERCENTAGE CHANGE OF RESERVOIR UNIT SCALE HETEROGENEITY FACTORS AND STOCHASTIC NOISE IN TOTAL OIL RECOVERY AT NORTH FLANK PERERIV B (HIGH NTG LAYER). SINGLE PHASE TRACER SIMULATION WAS APPLIED TO CONDUCT THE TEST. UP TO 15 REALIZATIONS WERE APPLIED TO CONDUCT THE TEST; IT IS OBSERVED THAT THE VARIATION OF THE MAGNITUDE OF THE RESPONSES CONVERGE WHEN 13 REALIZATIONS WERE APPLIED. HOWEVER THE SCREENING PROCESS CAN ALWAYS IDENTIFY THE MOST SIGNIFICANT FACTORS TO THE OBJECTIVE MEASURE WHEN MORE THAN 3 REALIZATIONS WERE APPLIED. 268
FIGURE A4.1 (A-B). AVERAGE PERCENTAGE CHANGE IN RECOVERY FACTOR FROM RESERVOIR MODELS WITH DIFFERENT VOLUME, OBSERVED WHEN EACH FACTOR IN THE SENSITIVITY ANALYSIS IS VARIED FROM SETTING 1 TO SETTING 2 (TABLE 5.1). RESULT FOR SYMMETRIC ELEMENT MODEL IS SHOWED IN (A, TOP) AND SUBSET RESERVOIR MODELS IN (B, BOTTOM). IF THE BAR LIES TO THE RIGHT THEN THE CHANGE IS POSITIVE. 272
FIGURE A4.2. ABSOLUTE PERCENTAGE CHANGES IN OIL RECOVERY FACTOR AT THE END OF PRODUCTION ARE PLOTTED AS DISTANCE FROM THE CENTRE OF THE CHART FOR EACH HETEROGENEITY, TO ENABLE COMPARISON BETWEEN THE TWO DIFFERENT RESERVOIR MODEL SIZES. THE REDUCED MODEL SIZE DOES NOT CHANGE THE RELATIVE IMPACT OF THE DIFFERENT HETEROGENEITIES, SUGGESTING THAT THE SUBSET RESERVOIR MODELS REPRESENT THE

SYMMETRIC ELEMENT MODEL SETTING.....273
FIGURE A5.1. REPRESENTATION OF THE ORIGINAL AND REVIEWED OIL-GAS RELATIVE PERMEABILITY MEASURED IN AZERI RESERVOIR.....275
FIGURE A5.2 (A-B). AVERAGE PERCENTAGE CHANGE IN RECOVERY FACTOR AND TOTAL GAS PRODUCED AFTER 20 YEARS IN NORTH FLANK SYMMETRIC ELEMENT MODELS OF PERERIV B, OBSERVED WHEN EACH FACTOR IN THE SENSITIVITY ANALYSIS IS VARIED FROM SETTING 1 TO SETTING 2 (TABLE 5A). THE ORIGINAL RELATIVE PERMEABILITY DATA ARE APPLIED IN (A, TOP) AND REVIEWED RELATIVE PERMEABILITY DATA ARE APPLIED IN (B, BOTTOM).....277
FIGURE A5.3. ABSOLUTE PERCENTAGE CHANGE IN RECOVERY FACTOR AFTER 20 YEARS IS PLOTTED AS DISTANCE FROM THE CENTRE OF THE CHART FOR EACH HETEROGENEITY FACTOR, TO ENABLE COMPARISON BETWEEN THE TWO DIFFERENT GAS-OIL RELATIVE PERMEABILITY CURVES. THE AREA AROUND THE CENTRE OF EACH CHART REPRESENTS THE ABSOLUTE PERCENTAGE CHANGE OBSERVED FROM DIFFERENT STOCHASTIC REALIZATIONS. THE REVIEWED RELATIVE PERMEABILITY DATA INCLUDED A MUCH LARGER MAGNITUDE OF RESPONSE FOR THE MOST SIGNIFICANT HETEROGENEITY FACTOR, SUGGESTING THAT RELATIVE PERMEABILITY HAS A LARGE IMPACT ON THE DISPLACEMENT.....278
FIGURE A5.4. FRACTION FLOW CURVES AND SHOCK FRONT MOBILITY RATIO FOR DIFFERENT RELATIVE PERMEABILITY DATA (FIGURE A5.1). THE FRACTIONAL FLOW CURVES INCLUDE GRAVITY. A TANGENT IS DRAWN TO THE FRACTIONAL FLOW CURVE FROM THE INITIAL WATER SATURATION. THE TANGENT POINT INDICATES THE SATURATION AT BREAKTHROUGH. THE INTERCEPT OF THE TANGENT AT F=1 INDICATED THE AVERAGE SATURATION BEHIND THE FRONT UP TO THE BREAKTHROUGH TIME AT THE PRODUCTION WELL.....280
FIGURE A5.5 (A-D). VERTICAL CROSS SECTION VIEW THROUGH THE MIDDLE OF A SUBSET MODEL OF GAS SATURATION AFTER 1 YEAR OF DISPLACEMENT WITH THE ORIGINAL RELATIVE PERMEABILITY CURVES AND THE KV:KH OF THE CHANNEL SAND EQUAL TO 1 **(A, TOP LEFT)** AND 0.1 **(B, TOP RIGHT)**. COMPARE WITH THE CASE WHERE REVIEWED RELATIVE PERMEABILITY DATA ARE APPLIED WITH THE KV:KH OF THE CHANNEL SAND EQUAL TO 1 **(C, BOTTOM LEFT)** AND 0.1 **(D, BOTTOM RIGHT)**. THE PRODUCERS AND INJECTOR ARE LABELED. THE PLOTS SHOW THAT THE GAS SATURATION IS HIGHER IN THE INVADED ZONE IN MODELS WITH SAND KV:KH RATIO EQUAL TO 1 (LEFT) THAN 0.1 (RIGHT). THE EFFECT IS MORE PRONOUNCED WHEN THE REVIEWED RELATIVE PERMEABILITY DATA IS APPLIED.....282
FIGURE. A6.1 COMPARISON OF THE 3DSL AND ECLIPSE ESTIMATION ON OIL

RECOVERY PROFILE AND THE WATER PRODUCTION PROFILE UNDER WATER-OIL DISPLACEMENT IN A 2D SOUTH FLANK HOMOGENEOUS MODEL. THE RESULT SHOWS THE ESTIMATION BY 3DSL AND E-CLIPSE ON WATER OIL DISPLACEMENT IS ALMOST IDENTICAL.....284

FIGURE. A6.2 COMPARISON OF THE 3DSL AND ECLIPSE ESTIMATION ON OIL RECOVERY PROFILE AND THE GAS PRODUCTION PROFILE UNDER GAS-OIL DISPLACEMENT IN A 2D NORTH FLANK HOMOGENEOUS MODEL. THE TOTAL OIL RECOVERY AND THE TOTAL GAS PRODUCTION ARE MATCHED BETWEEN 3DSL AND ECLIPSE'S ESTIMATION. COMPARING THE TWO SIMULATIONS, IN GENERAL, THE STREAMLINE SIMULATION (3DSL) ESTIMATED AN EARLIER GAS BREAKTHROUGH TIME. THE GRAPH ALSO SHOWS THAT THE RESULTS CONVERGED WHEN 100 DAYS TIMESTEPS (WHICH WERE APPLIED TO ALL THE GAS FLOODING SIMULATIONS IN THE RESEARCH) APPLIES ON THE STREAMLINE SIMULATION.....285

List of Table

TABLE 3.1. TABLE OF CRITICAL RESERVOIR PROPERTIES OBTAINED FROM AZERI FOR ANALYTICAL CALCULATION..... 79
TABLE 3.2. TABLE OF NOMENCLATURE OF THE KEY PARAMETERS IN THE STABILITY CALCULATION..... 84
TABLE 3.3. CRITICAL WELL RATES..... 93
TABLE 3.4. END POINT MOBILITY RATIO AND DIMENSIONLESS GRAVITY NUMBER..... 93
TABLE. 4.1. FACTORS (HETEROGENEITIES) INVESTIGATED IN THE SENSITIVITY ANALYSIS. THE IMPACT OF THESE SIX FACTORS IS INVESTIGATED BY OBSERVING THE PERCENTAGE CHANGE IN AVERAGE RESPONSE WHEN EACH FACTOR IS VARIED FROM SETTING 1 TO SETTING 2. 105
TABLE. 4.2. INFORMATION ON RESERVOIR MODEL SETTING FOR 1ST SCREENING STUDY. SAME GRID BLOCK SIZE IS APPLIED TO ALL 3 SCREENING STUDY. 111
TABLE. 4.3. EXPERIMENTAL DESIGN MATRIX FOR 1ST SENSITIVITY SCREENING STUDY. THE PARAMETER ROW DENOTES THE HETEROGENEITY FACTOR; 1: CHANNEL ORIENTATION; 2: CHANNEL SINUOSITY; 3: CHANNEL STACKING; 4: CHANNEL DIMENSIONS; 5: INTER-LAYER CONNECTIVITY; 6: LATERAL VARIATION OF NTG WITHIN PERERIV C..... 114
TABLE. 4.4. EXPERIMENTAL DESIGN MATRIX FOR 2ND SENSITIVITY SCREENING STUDY. PARAMETER DENOTES THE HETEROGENEITY FACTOR; 1: CHANNEL ORIENTATION; 2: CHANNEL SINUOSITY; 3: CHANNEL STACKING; 4: CHANNEL DIMENSIONS; 5: INTER-LAYER CONNECTIVITY. 115
TABLE. 4.5. EXPERIMENTAL DESIGN MATRIX FOR 3RD SENSITIVITY SCREENING STUDY. PARAMETER DENOTES THE HETEROGENEITY FACTOR; 1: CHANNEL ORIENTATION; 2: CHANNEL SINUOSITY; 3: CHANNEL STACKING; 4: CHANNEL DIMENSIONS. 116
TABLE 5.1. FACTORS (HETEROGENEITIES) INVESTIGATED IN THE SENSITIVITY ANALYSIS. THE IMPACT OF THESE SEVEN FACTORS IS INVESTIGATED BY OBSERVING THE PERCENTAGE CHANGE IN AVERAGE RESPONSE WHEN EACH FACTOR IS VARIED FROM SETTING 1 TO SETTING 2. 155
TABLE 5.2. EXPERIMENTAL DESIGN MATRIX FOR 4^{TH} SENSITIVITY SCREENING STUDY. PARAMETER DENOTES THE HETEROGENEITY FACTOR; 1: CHANNEL ORIENTATION; 2: CHANNEL STACKING; 3: CHANNEL DIMENSIONS; 4: EXTENSIVE SHALES; 5: UPWARD FINING TREND; 6: KV:KH RATIO; 7: MUD-CLAST LAGS 162
TABLE 5. 3. TABLE OF NOMENCLATURE. 164
TABLE 5.4. INFORMATION ON SUBSET RESERVOIR MODEL SETTING. 165

TABLE 5.5. SUMMARY OF SCREENING STUDIES UNDER VARIOUS CONDITIONS.....167
TABLE 6.1. TABLE OF NOMENCLATURE. 211
TABLE. 6.2. INFORMATION ON RESERVOIR MODEL SETUP FOR THE NUMERICAL SIMULATIONS PRESENTED IN THIS CHAPTER. 218
TABLE. A1 THE SUMMARY OF PARAMETERS THAT ARE USED IN THE EQUATIONS THAT ARE LISTED ABOVE. 258

Chapter 1
Introduction

1.1 Project background

In order to maximize profit from finite reserves, optimising hydrocarbon recovery is one of the main interests of the energy industry. Hydrocarbon reservoirs generally have complex systems, so to maximize recovery efficiency a good understanding of the reservoir is required. Reservoirs are generally heterogeneous in different aspects. The fluid properties within a reservoir change with local physical conditions, especially pressure and temperature, at a given time. Hydrocarbon reservoirs contain geological heterogeneities on many different length scales, from the pore scale to the scale of basin depositional system. Previously, many workers used a variety of ways to define different length scale for geological features within a reservoir (e.g. Kortekaas 1985; Weber 1986; Allen 1983; Barthel 1991; Weber and van Geuns 1990; Jones et al. 1992; Hartkamp-Bakker 1993; Jones et al. 1994; Jones et al. 1995; Kjønsvik et al. 1995; Jackson and Muggeridge 2000; Cubillos et al. 2005 and Hunedi et al. 2005).

Geological heterogeneities at different length scale have various ways to influence reservoir performance. Faults or boundaries between genetic sand bodies (e.g. long extensive shales) control sand connectivity and sweep efficiency, if the sand bodies are disconnected they cause moveable oil to be by-passed. This is normally the cause of poor recovery at reservoir-unit scale (c.10-100m) (Weber 1986; Hartkamp-Bakker 1993 and Larue and Hovadik 2006). At the genetic-unit scale (c.1-10m), geological

features such as permeability zonation within sand bodies (e.g. upward fining trend of grain size within channel fill sand body) or baffles within genetic sand bodies affect both vertical and areal sweep efficiency (Jones et al. 1994 and Jones et al. 1995). At the bed-form scale (c. 1-0.1m) geological features such as crossbedding and lamination control the variation of lithology, porosity, and permeability (between foreset and bottomset within cross-bed set). Previous studies have demonstrated that these factors cause the variation of capillary pressure and control the by-pass oil in a rock volume during displacement (Hartkamp-Bakker 1993). At the pore scale (c. <0.1m), the variability of pore structure and mineralogy control the wettability and relative permeability; these factors controls the residual oil saturation. Therefore the variety of pore structure determines the amount of maximum recovery from a reservoir for a given displacement scheme.

In general, geological heterogeneities are related to the porosity and permeability of a reservoir. These features determine how fluids flow through the reservoir towards production wells. However, not all geological heterogeneities have a significant influence on recovery. So the key question is to find out which geological features are important to reservoir performance. To answer this, one needs to identify the key geological features that must be captured for a particular scale of reservoir model in order to conduct a study on reservoir performance. The answer will provide important guidelines for data collection, reservoir management and strategies for field development.

The geological features present in the reservoir are mainly governed by the depositional environment. This thesis investigates the impact of depositional heterogeneities on oil recovery in a fluvial dominated deltaic reservoir developed by

both water and gas injection. Fluvial deltaic reservoirs generally have numerous types and length scales of geological heterogeneities. All of these levels of heterogeneities have a potential effect on the displacement. Many important oil and gas fields in the world are interpreted to have been deposited in a fluvial deltaic deposition environment, such as Prudhoe Bay (Begg et al. 1992; Hand et al. 1994), Lake Maracaibo in Venezuela (Ambrose et al. 1997) and the Mahakam Delta Indonesia (including examples such as Serang field; Waryan et al. 2001 and Attaka field; Vo et al. 2001 are exhibits both fluvial and tidal influences). Fluvial deltaic reservoirs are normally complex belonging to the jigsaw-type reservoirs in the scheme of Weber and van Geuns (1990) and many are characterized by difficulties in maintaining reservoir pressure, poor displacement efficiency and early breakthrough.

1.2 Introduction to the ACG field and the challenges of the project

The ACG petroleum system contains three accumulations: Azeri, Chirag and deep water Gunashli. The ACG field development project is one of the largest current hydrocarbon projects (US$20 billion aggregate) in the world, and is thus important to Azerbaijan. BP has obtained a 30 year exploration license for the ACG development which will expire in 2025. BP plans to bring the total production in ACG to 1 million barrels of oil per day by 2008. This thesis focuses on the Azeri accumulation in the south east of the ACG structure, which contains an estimated 8 billion barrels of oil in place. The ACG field is a large, steeply dipping reservoir which is located in the south Caspian basin offshore Azerbaijan sector (Figure 1.1 A,B).

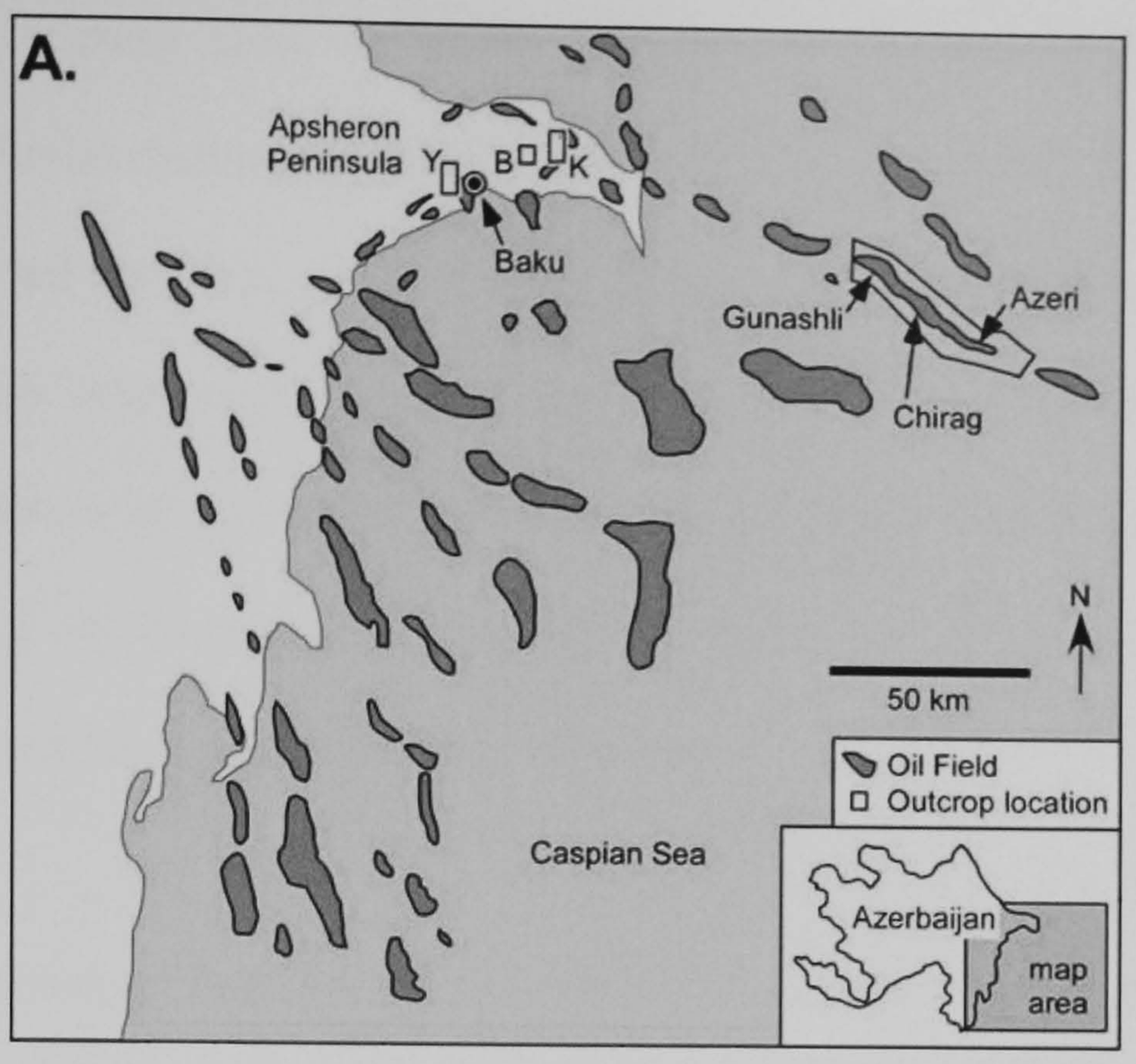


Figure 1.1.A

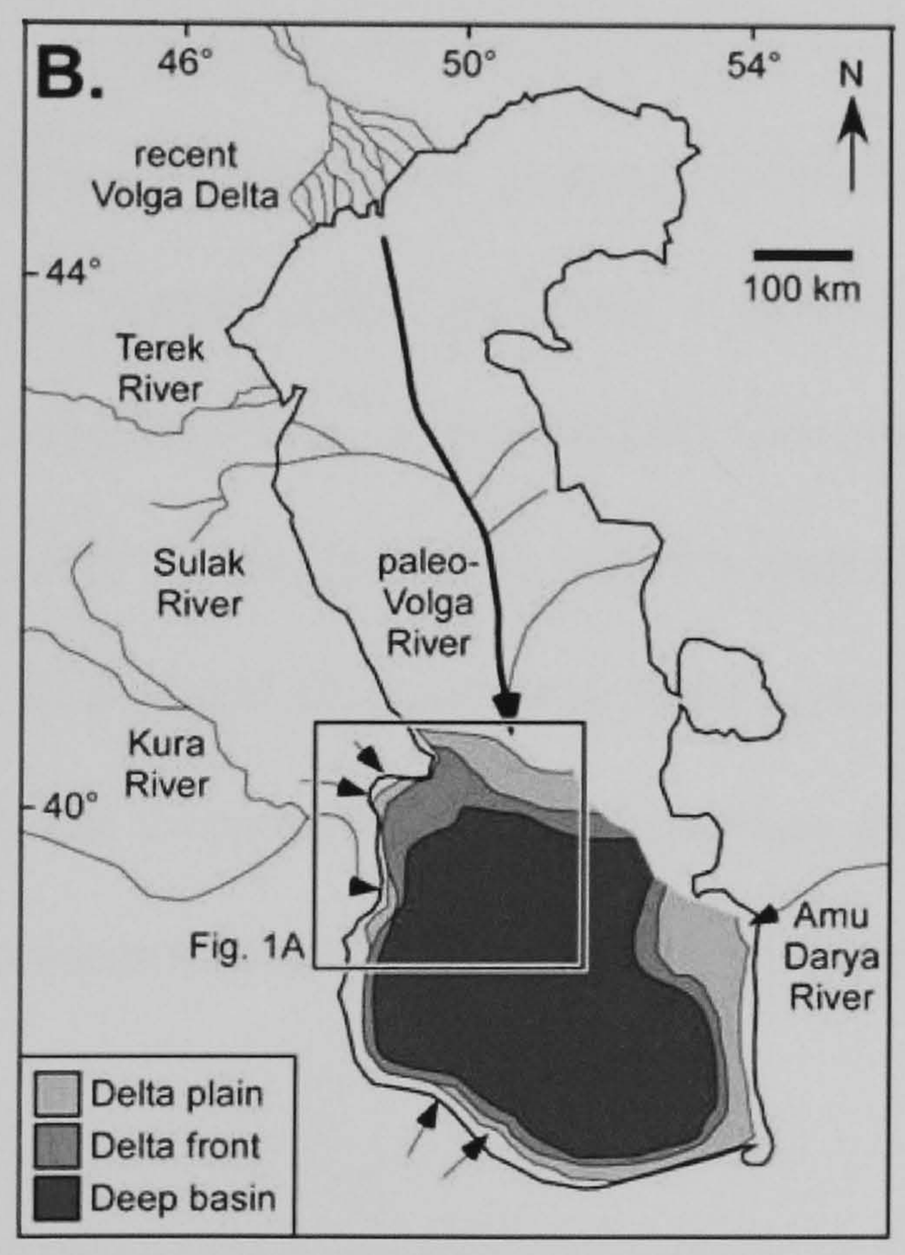


Figure 1.1B

Figure 1.1. **(A, top)** Map of the western South Caspian Basin highlighting oil fields, including the ACG field, and the location of outcrop analogs on the Apsheron Peninsula (Y = Yasamal Valley, B = Balakhany Quarry, K = Kirmaky Valley). **(B, bottom)** Paleogeographic map of the South Caspian Basin during deposition of the Productive Series. Note that the paleo-Volga Delta underwent multiple episodes of advance and retreat across the area of the ACG field during deposition of the Productive Series

The major oil bearing zone of Azeri reservoir is the Pereriv Suite which is interpreted as a fluvial dominated deltaic depositional environment. The Pereriv Suite is vertically divided into five layers with different net to gross (NTG) (more detail about the reservoir stratigraphy is presented in Chapter 2). The reservoir comprises channel sand bodies with variable connectivity and mud/shale sheets forming internal barriers to flow of oil. These sedimentary heterogeneities make the internal structure of the reservoir complex and challenging to model.

The Azeri structure is being developed using two production schemes: down-dip water injection on the south flank (tectonic dip of c.5 ^{o}-30^{o} depending upon location) and up-dip gas injection on the more steeply dipping (c.25 ^{o}-45 ^{o} depending upon location) north flank (Figure 1.2). The initial analytical prediction suggested that the proposed production rate would result on both water and gas displacement mechanisms are stable if the reservoir is geologically homogeneous. However, in reality it is difficult to predict the displacement stability because of the nature of the geological heterogeneity. If unstable displacement occurs, gas or water tongues will develop which will reduce the sweep efficiency and increase gas or water production (depending on the displacement mechanism) thus reducing oil recovery.

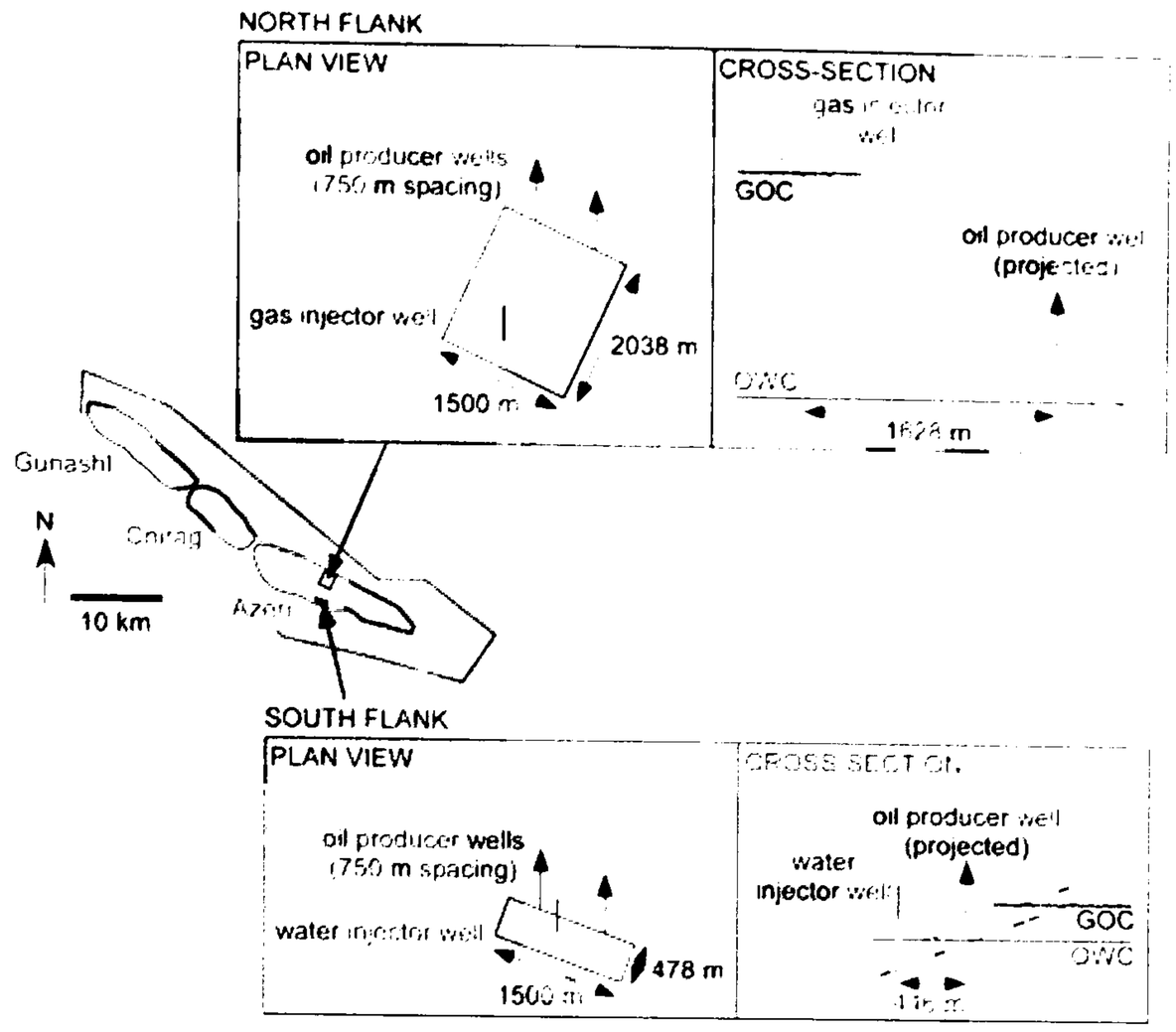


Figure 1.2. Map of the ACG field highlighting the Azeri, Chirag and Gunashli accumulations. Simplified cross-sections and plan-view maps are shown for the north and south flanks of the Azeri reservoir. The models presented in this thesis are constructed for these reservoir-production symmetry elements.

An additional complexity is that the reservoir pressure was found to be at the bubble point pressure of the oil phase; any pressure reduction therefore leads to gas escaping from solution. So if the reservoir pressure maintenance fails, significant volumes of gas will potentially be produced even under water displacement mechanism or when the gas displacement is predicted to be stable. This adds to the challenge of predicting, monitoring and managing each displacement. The optimum development of the Azeri field therefore requires a sound understanding of the impact of geological heterogeneity on displacement by both water and gas injection.

1.3 Aim and objective

The aim of this project is to investigate the impact of reservoir heterogeneity on oil recovery behavior in fluvial deltaic reservoirs, with specific reference to the Azeri field offshore Azerbaijan.

The following are the objectives of the project:

1. Identify the key geological and petrophysical heterogeneities in the ACG field and quantify their impact on flow during water and gas injection.

2. Identify how the heterogeneities should best be captured in a reservoir model.

1.4 Methodology

There are different methods to obtain sub-surface information, e.g. well-log, core, seismic and production data of the field, however, all these methods have their own limitations. In this research outcrop analogues are used to obtain detailed geological information for the reservoir. By using outcrop analogue, the geological features can be measured directly in detail. In Chapter 2, more details on the advantages of using outcrop analogue and the limitations of the other sub-surface measurement methods are discussed. As there are a large amount of information and the complexity of the reservoir environment, 'top-down' approach and experimental design method are adopted, in order to conduct the investigation in a more efficiency approach, a more detailed description of these methods are shown in Chapter 2.

1.5 Outline of this thesis

This investigation begins with an overview of the south Caspian regional geology and reviews previous studies on the fluvial deltaic environment in the first part of Chapter 2. Given that there are significant geological heterogeneities present in the reservoir at different length scale, in the second part of Chapter 2, a number of previous approaches to study the impact of heterogeneities on displacement are reviewed. In order to conduct the investigation in an efficient way, a 'top-down' approach (Williams et al. 2004) is adopted. This method begins with the simplest model and progressively increases the level of complexity toward smaller scale heterogeneities. By using this approach, one can filter out the issues that are negligible at the early stage of the research.

This investigation starts with an analytical study of fluid (water or gas) displacement in a homogeneous environment. This preliminary calculation is described at Chapter 3, in order to understand the reservoir performance (i.e. breakthrough time, cumulative oil recovery and flow stability for both gas and water injection). The objective of Chapter 3 is to study the displacement behaviour when the impact of geological heterogeneities is omitted and flow conditions are simplified. The analytical study applies the classical theories (Buckley and Leverett 1942; Dietz 1952) to estimate displacement behaviour under simplified conditions.

Then the investigation moves on to study the impact of geological heterogeneities. The research begins with a study of the impact of heterogeneities at reservoir-unit scale with simplified fluid properties in Chapter 4. This investigation progressively

moves toward the smaller scale study. In Chapter 5 investigations of the impact of the combination of reservoir-unit scale and genetic-unit scale heterogeneities on recovery are presented. At the end of Chapter 5, both simplified fluid properties and realistic Azeri properties are applied and investigated. Finally, in Chapter 6, an investigation to develop an approach to rapidly estimate the range of possible oil recoveries by gravity stable displacement through a heterogeneous system which is simplified into shale with various length and continuity in a sand background is conducted.

In order to have a sound understanding of a reservoir, it is necessary to understand the geology of the depositional environment for the reservoir. There is a vast literature on the geology of fluvial deltaic environments. For the purpose of studying the impact of heterogeneity on reservoir performance from a production point of view, the key literature is reviewed in the next chapter.

Chapter 2
Literature review

2.1 Overview

This research studies the impact of heterogeneities on production from a fluvial-dominated deltaic reservoir in the Southern Caspian Basin. The Pereriv Suite reservoir of the Azeri-Chirag-Gunashli (ACG) Field is selected for this investigation. This chapter begins with a review of some earlier studies on the geological setting of the Southern Caspian Basin and the petroleum system of the region, in order to place in context the geology and stratigraphy of the reservoir interval (Productive Series). Many previous studies have identified the Productive Series as the deposits of a fluvial-dominated deltaic system. Establishing this specific type of deltaic depositional environment is the first step taken to characterise this reservoir. In the second part of this chapter, a number of previous studies are reviewed in order to understand the definition and classification of the different types of deltaic reservoirs. To characterise a reservoir, it is necessary to collect information from all available sources. An evaluation of the advantages and disadvantages of different methodologies for obtaining information about the reservoir is conducted, in order to choose the ideal method for characterising the ACG reservoir.

The main objective of this investigation is to identify those heterogeneities that have the most significant influence on the behaviour of a fluvial-deltaic reservoir, and explain the reasons why these factors have such a large influence under a particular displacement mechanism. It is recognised that there is a large range of geological

features within the Productive Series reservoirs. Each of the heterogeneities has a different influence on reservoir performance. In the third part of this chapter, a number of previous studies on the impact of heterogeneities on reservoir performance are reviewed. These previous approaches provide some instruction for conducting this investigation.

In the final part of this chapter, various methods of studying the sensitivity of reservoir models to geological heterogeneity are evaluated. The most suitable scheme is then selected and applied in this investigation.

2.2 Geology of the Productive Series and the ACG field

It is essential to understand reservoir geological architecture for effective reservoir modelling. Reservoir model construction is based on the interpretation of reservoir geology. Without such information it is not possible to build a representative model to capture the reservoir behaviour for monitoring, forecasting and eventually improving the reservoir performance.

2.2.1 Regional geological setting and petroleum system

The Caspian Sea is enclosed between Asia and Europe. The region is surrounded by Russia, Azerbaijan, Iran, Turkmenistan and Kazahstan. The Caspian Sea is the world's largest lake. It is recognised as one of the world's richest hydrocarbon-bearing regions and has a long history of oil production. For example the oldest oil field in Azerbaijan, Kirmaku, has a record of production since 1834

(Buryakovsky 2003). ACG is one of the offshore hydrocarbon fields located within the region called the Apsheron Threshold in the Southern Caspian Basin. About 90% of all identified hydrocarbon reserves in the South Caspian basin are located here (Buryakovsky 2003).

Production from the Azeri reservoir which is focus of this research project is relatively new, as it started as recently as 2004.

In the southern Caspian region, the major hydrocarbon-bearing interval is the Productive Series which was formed in the late Miocene to early Pliocene during a dramatic fall in lake level (Reynolds et al. 1998; Morton et al. 2003; Buryakovsky 2003; Hinds et al. 2004). Reynolds et al. (1998) and Abreu and Nummedal (2007) describe the sequence stratigraphic context of the Productive Series. The Kalin Suite at the base of the Productive Series is overlain by Kirmaky Suite and Pereriv Suite. From the Kirmaky Suite to the Pereriv Suite, there is a progressive increase in grain size and an associated change in depositional environment from delta front (Kirmaky Suite) to fluvial (Pereriv Suite). This succession therefore demonstrates a long-term progradation of the palaeo-Volga delta. Above the Pereriv Suite, there is an upward decrease in sand content and a reversion to delta front facies through the Balakhany Suite, which indicates the retreat of the palaeo-Volga delta in response to a long term base-level rise. Figure 2.1 shows the stratigraphy of the Productive Series. A key effect of the latest Miocene lake level fall was to restrict sedimentation to the South Caspian, which lies south of the Apsheron Peninsula region (Figure 2.2). Sediment was mainly supplied from the north by the paleo-Volga river system (Overeem et al. 2003; Morton et al. 2003, Hinds et al. 2004; Kroonenberg et al. 1997 and Kr[illegible]berg 2004).

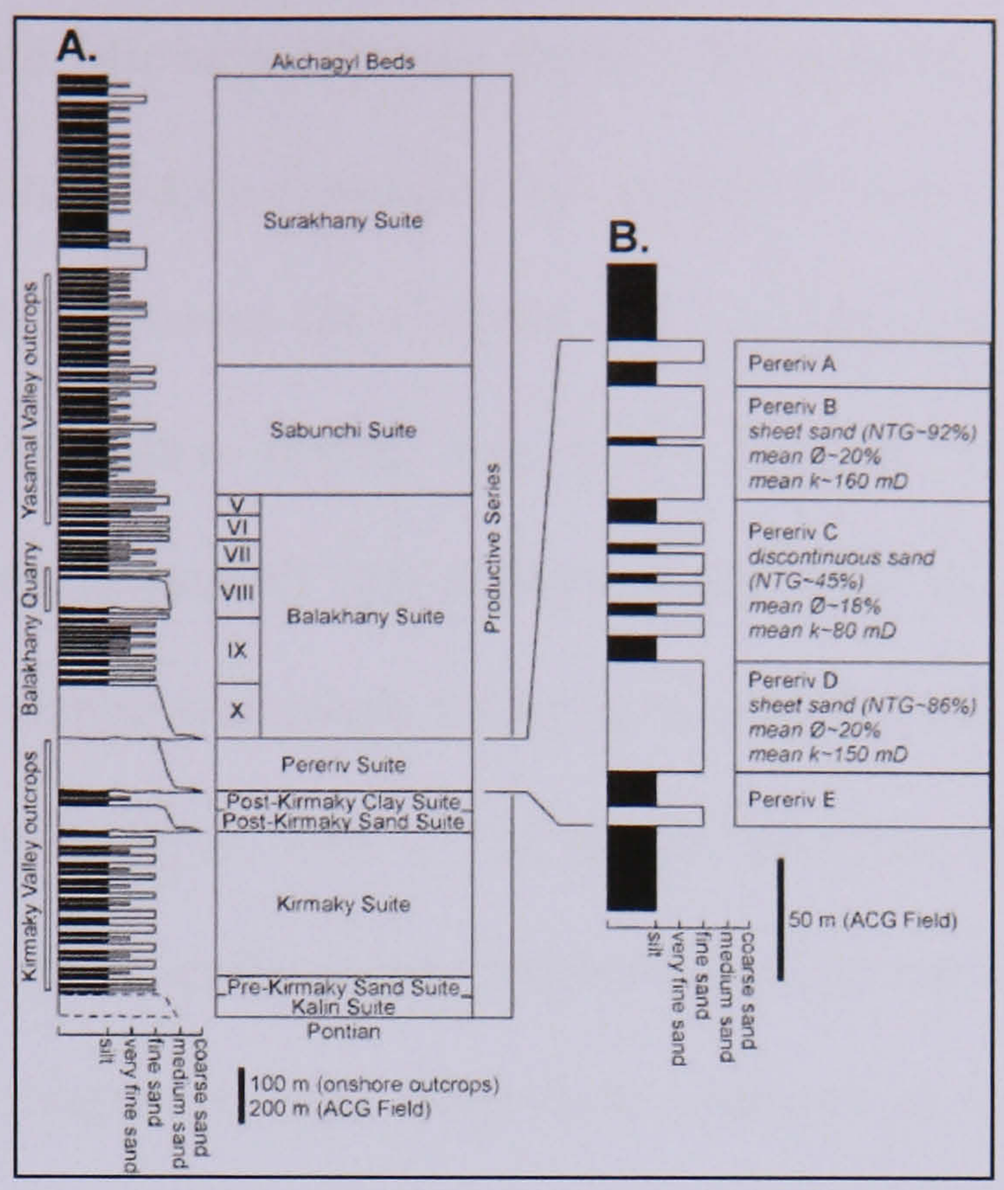


Figure 2.1. Stratigraphy of the Productive Series in Aspheron Peninsula, Azerbaijan.

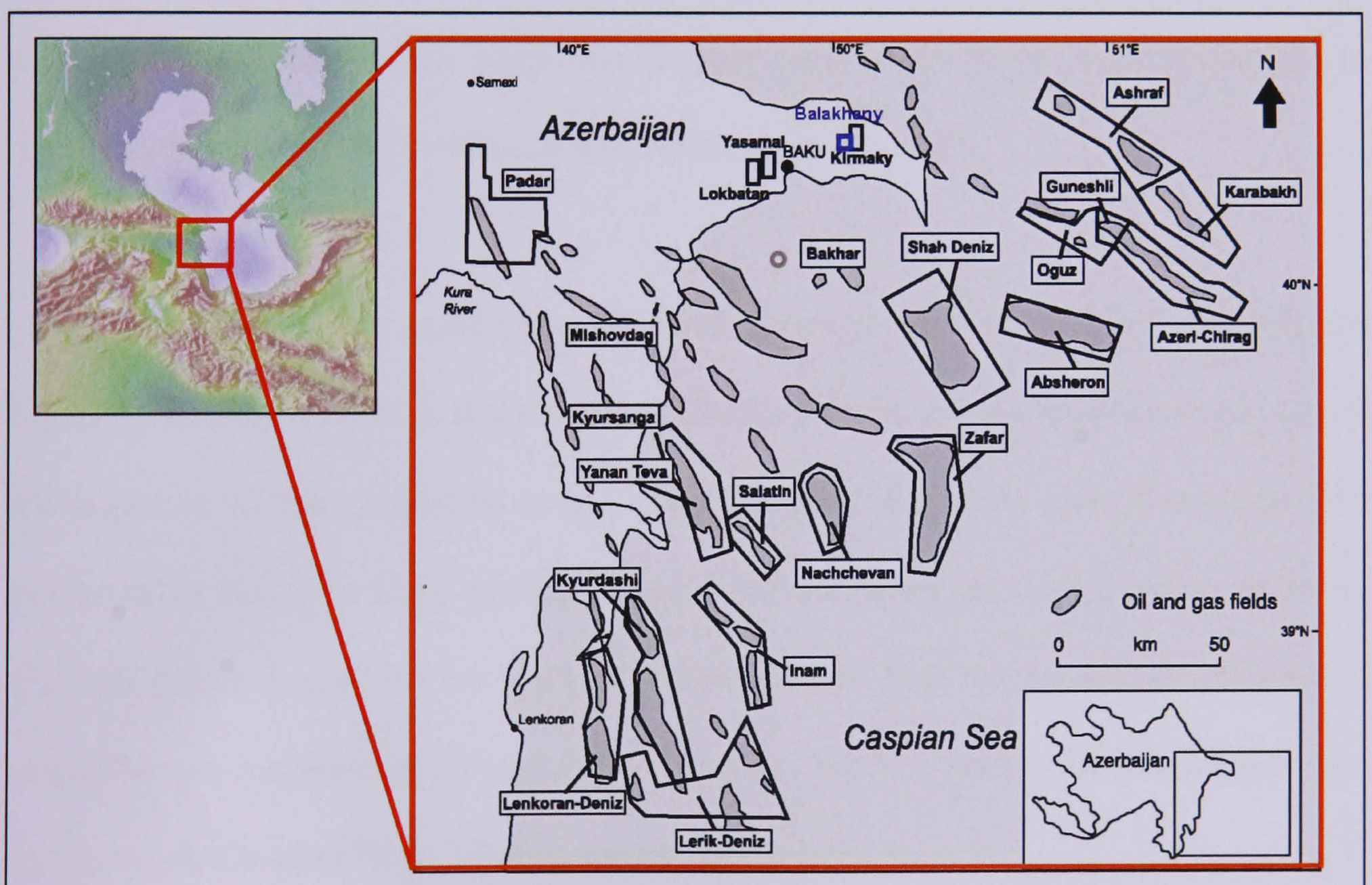


Figure 2.2. Plan view of the South Caspian Basin including oil/gas fields. The ACG field are a combination of Azeri-Chirag and Gunashli reservoirs. The Azeri reservoir is located at the south-east section of the ACG structure. Outcrop analogues are located on the Apsheron Peninsula. Balakhany Quarry contain outcrop analogues for high NTG intervals in the Productive Series: Pereriv B,D. The Yasamal Valley contain outcrop analogues for low NTG intervals: Pereriv A,C,E.

During much of the late Miocene-Pliocene period, the paleo-Caspian Sea was a large inland lake with sedimentation controlled by changes of lake level (Reynolds et al. 1998, Hinds et al. 2004). Because the Caspian Sea is a lake and contains a lower volume of water than the open ocean, the water level is more sensitive to climatically-forced changes in rainfall that control water input to the Caspian Sea. Therefore the lake level change was much more rapid than the sea level changes in the open ocean (Kroonenberg et al. 1997). The deltaic stratigraphy in this basin is therefore different to that of an open ocean. Sedimentation in the Productive Series was controlled by high-frequency, high-magnitude changes in lake level, which caused rapid shifts in the location of the paleo-Volga delta and associated shoreline (Reynolds et al. 1998 and Hinds et al. 2004). The South Caspian Basin underwent extremely rapid subsidence, such that roughly half of the 20km thick basin fill has accumulated in the last 5.5 million years (Morton et al. 2003).

Paleogene to Neogene argillaceous rocks are widespread in the South Caspian Basin. Previous studies recognise that these argillaceous rocks are the major component of the cap-rock of the reservoirs in the South Caspian Basin, because they have low permeability thus providing good sealing properties. There are no thick shale sections to act as regional seals for the hydrocarbon reservoirs, however local seals are present, and these are responsible for trapping oil and gas reserves in the Azerbaijan portions of the South Caspian Basin (Buryakovsky 2003).

In the South Caspian region, four different types of hydrocarbon traps have been identified: (1) anticlinal non-faulted traps, (2) anticlinal faulted traps, (3) stratigraphic traps, and (4) lithological traps. The oil and gas accumulations in the Productive

Series are restricted to anticlinal traps. Accumulations in the Upper Productive Series (including Azeri and Guneshli) occur in faulted anticlinal traps (Buryakovsky 2003).

The Productive Series was introduced previously as the major reservoir interval of the South Caspian region. Previous studies suggested that the paleo-Volga river system supplied sediment from the Russian Plain to the Productive Series (e.g.: Reynolds et al. 1998; Kroonenberg et al. 1997; Kroonenberg 2004; Kroonenberg et al. 2005; Hinds et al. 2004). Caspian sea level changes were more dynamic than those of the world ocean. Consequently, delta regression and transgression were much more rapid. As mentioned before, because the Caspian Sea was an inland lake, with only minimal wave and tidal action (Kroonenberg et al. 2005), as the deposits of the palaeo-Volga delta have undergone no marine reworking. Moreover, the onshore and offshore gradients of this basin are extremely shallow (c.5cm/km; Kroonenberg et al., 1997), which promoted rapid lateral changes in delta position as it regressed and trangressed.

The Productive Series is highly layered because of the rapid lake level changes. The series consists of a large number of vertical intervals that are sub-divided into a number of sedimentary sequences (Suites) corresponding to major progradational-retrogradational cycles. These sequences are sub-divided by extensive flooding surfaces marked by distinct changes in lithological character. The highly layered strata comprise the Kalin (Kala) Suite, Pre-Kirmaky Sand Suite, Kirmaky Suite, Post-Kirmaky Sand Suite, Post-Kirmaky Clay Suite, Pereriv Suite, Balakhany Suite, Sabunchi Suite and Surakhany Suite (Figure 2.1 Reynolds et al. 1998; Buryakovsky 2003). The Balakhany and Pereriv Suites are the major

litho-stratigraphic sections that contain hydrocarbon-bearing sandstones within the ACG field.

The Pereriv Suite is up to 110m thick and forms the most important producing interval in the ACG field. From outcrop exposures, it is identified that the Pereriv Suite contains characteristics that can be interpreted as a fluvial or distributary channel system (Reynolds et al. 1998). In the next section further details of the geological features of the Pereriv Suite within ACG will be discussed.

2.2.2 Reservoir geology

In order to understand the geology of the ACG field, this investigation reviewed nearby developed fields with similar reservoirs and previous studies on outcrop analogues of the Productive Series.

The Bahar Field has one of the nearby Productive Series reservoirs in the south Caspian Basin (Figure 2.2). The Bahar structure was discovered in c.1956; production started during 1970. Previous studies investigated the influence of geological heterogeneity on reservoir performance (Narimanov et al. 1998; Abdullaev et al. 1998). The Bahar Field is divided into eight fault blocks. Reservoir stratigraphic intervals are separated by shale beds and have different fluids and petrophysical properties (Buryakovsky 2003). The main reservoir intervals of the Bahar Field are the Balakhany X and Pereriv Suite of the Productive Series, as in the ACG field. Water injection was applied in the Bahar Field, 20 years after the start of its primary produ Analysis of reservoir and production data has demonstrated that mud

stone sheets and faults within the Productive Series have influenced fluid flow (Narimanov et al. 1998; Abdullaev et al. 1998). The wide variation in channel-fill sandbody orientation is also recognised as one of the most important geological heterogeneities that influences reservoir performance. Similar heterogeneities can also be found in the ACG field.

Reynolds et al. (1998); Reynolds et al. (2003); Reynolds and Riley (2003) presented a detailed investigation of the outcrop analogues of the Productive Series. The Pereriv Suite outcrops demonstrate the characteristics of a fluvial or distributary channel system. These fluvial facies form a high quality reservoir sandstone because they lack low permeability units that would act as flow barriers and they display few internal heterogeneities. Three other facies types within the Productive Series outcrops were identified: delta plain, proximal delta front and distal delta front. Thus four possible reservoir architecture models were predicted for the Productive Series and it was thought that each of them would lead to different reservoir performance. Although the outcrops differ slightly from the subsurface expression of the Perereiv Suite, these four facies types and reservoir architectures can be identified in the ACG reservoir.

The Pereriv Suite is sub-divided into five intervals according to vertical variations in net-to-gross (NTG). Extensive shales form boundaries of these sub-Pereriv Suite intervals (Reynolds et al. 2003; Reynolds and Riley 2003). The layers are labelled Pereriv A at the top to Pereriv E at the base. The major oil reserves are contained in Pereriv B and D due to their high NTG and high net permeability. Reynolds et al. (2003); Reynolds and Riley (2003) attributed the differences between each sub-layer within the Pereriv Suite to rapid variations in lake level during reservoir deposition. The different facies architecture of each layer reflects varrations in depositional

environment. The low NTG intervals (Pereriv A, C and E and Balakhany X) are considered to represent delta front depositional environments whereas the high NTG intervals (Pereriv B and D) are likely to be the result of a combination of fluvial or delta plain domination. Reservoir objects such as distributary channels and flooding-surface shales are found in each sub-Pereriv layer. However, because the paleo-Volga delta lacked marine influence, heterogeneities resulting from wave or tidal re-working are absent. Compared with other fluvial-deltaic systems like the Mississippi Delta, the Pereriv Suite also lacks evidence of objects like crevasse splays, lobes and levees. Mouth bars are found in the Productive Series outcrops, but not in the subsurface ACG field dataset.

The geological features found from the ACG sub-surface core data, the relevant outcrop analogues and the nearby field examples are all indicators that the Pereriv Suite reservoir of the ACG field is a fluvial-dominated deltaic reservoir. This interpretation provides a framework for reservoir engineers and production geologists to characterise the ACG field. Such a framework provides guidelines for the distribution and type of possible geological heterogeneity within the reservoir. It is necessary to understand the properties of the fluvial-deltaic environment in order to construct an approprate reservoir model.

2.3. Fluvial-Deltaic reservoirs

Knowing the characteristics of different parts of a fluvial-deltaic reservoir is useful when identifying which geological heterogeneities are present. Firstly, it is necessary to understand what a deltaic reservoir is, and the classification of the different type of delta. Moreover, it is important to know the different parts of the delta environment.

2.3.1 Classification of deltas and deltaic reservoirs

Galloway (1975) defined a delta as a partially subaerial, continuous sediment deposit around the point where a river enters a standing body of water. Two main sedimentological processes occur in the deltas: (1). sediments are carried and deposited by fluvial channels, (2). sediments are then reworked by marine or lacustrine processes (Galloway 1975; Bhattacharya 2006). Galloway (1975) recognised that there are various sources of energy that are supplied by marine currents (e.g. oceanic and wind-generated currents, density currents, gravitational potential, tidal currents and wave surge). However, the major sources of marine energy that influence the sediment distribution within deltas are tidal currents and the wave surge (Galloway 1975). On this basis three major types of delta systems were identified by Galloway (1975): fluvial-, tide- and wave-dominated deltas (Figure 2.3). These three deltaic depositional systems have different characteristics and are widely used in geology research. For example, fluvial-dominated deltaic systems normally have elongated plan-view geometries, whereas wave-dominated deltas have an arcuate shape. The different characteristics of deltaic depositional systems are summarised in Table 2.1.

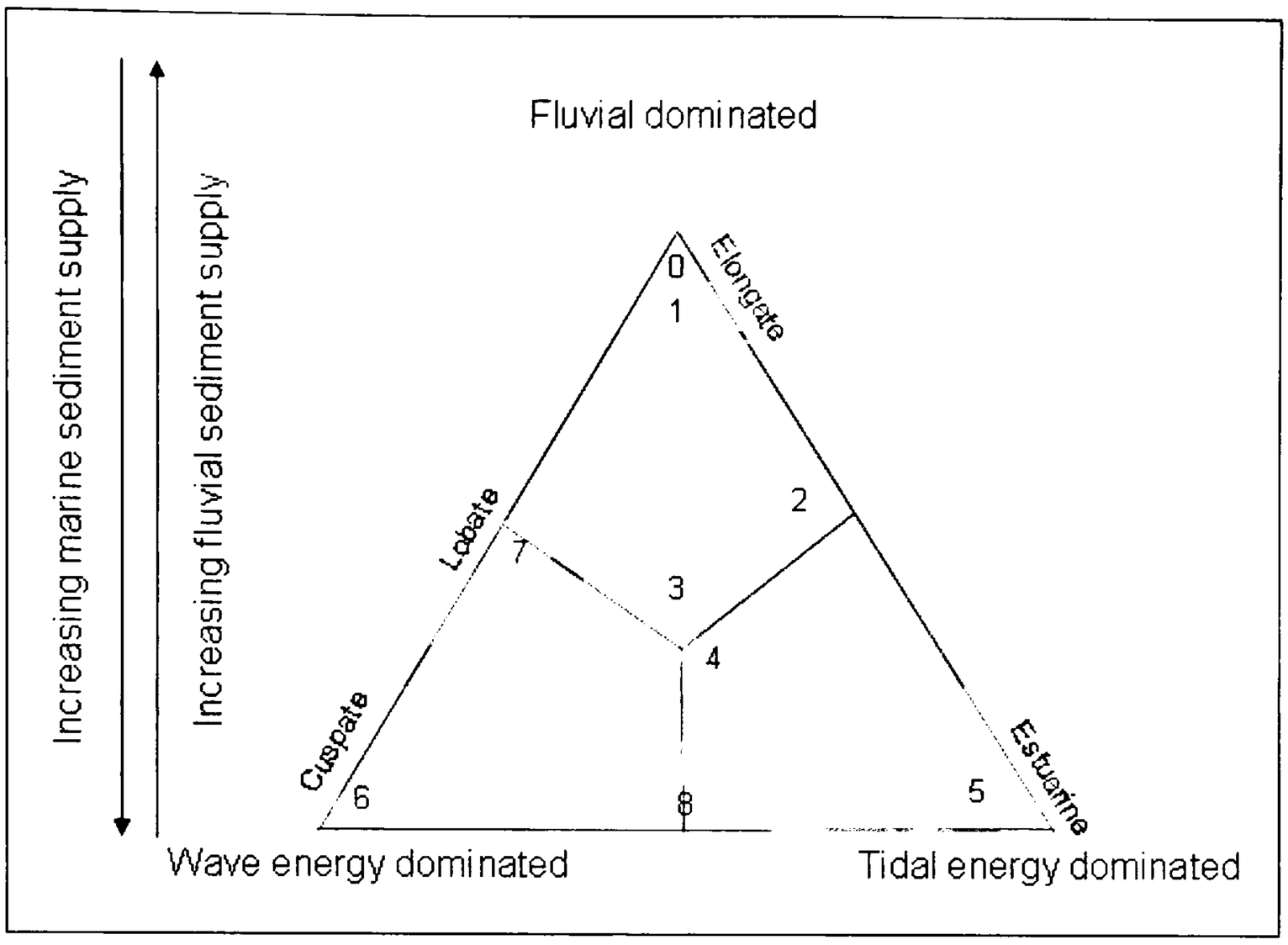


Figure 2.3. Process-based classification for threefold division of deltas. Modified from the original figure of Galloway 1975. There are 9 examples that represent different type of delta: 0. Volga Delta; 1. Misssissippi Delta; 2. Mahakam Delta; 3. Niger Delta; 4. Mekong Delta; 5. Fly Delta; 6. Sao Francisco Delta; 7. Ebro Delta; 8. Copper Delta.

	Fluvial-dominated	Wave-dominated	Tide-dominated
Geometry	Elongate to lobate	Arcuate	Estuarine to irregular
Channel type	Straight to sinuous distributaries	Meandering distributaries	Flaring straight to sinuous distributaries
Bulk composition	Muddy to mixed	Sandy	Variable
Framework facies	Distrinutary mouth bar and channel fill sands, delta margin sand sheet	Coastal barrier and beach ridge sands	Estuary fill and tidal sand ridges
Framework orientation	Parallels depositional slope	Parallels depositional strike	Parallels depositional slope

Table 2.1. Summary of characteristics of various delta systems (Galloway 1975).

The offshore gradient of the modern and paleo-Volga delta was gentle and no marine reworking took place (Overeem et al. 2003; Kroonenberg 2004). The paleo-Volga delta has been identified as a fluvial-dominated deltaic system (Reynolds et al. 1998; Overeem et al. 2003).

Morphologically, deltas can be divided into three parts: (1) delta plain; (2) delta front and (3) prodelta. Sand-body architecture varies between each component part of a fluvial-deltaic system. It is thought that Pereriv B and D were deposited in distributary channel, delta plain and fluvial environments whereas Pereriv A, C and E were deposited in delta front environments. A fluvial-dominated delta plain is unaffected by basinal processes so it is similar to other fluvial systems. They consist of a series of variably connected channelised sandbodies which exhibit predominately unidirectional flow internally.

Compared with fluvial systems, the distributary channels more frequently switch position because shorter and steeper courses are created as the delta progrades into the basin. The lower reaches of the distributary channels are influenced by basinal processes even in low-energy basins. Moreover, it is rare to find multiple distributary channel systems in fluvial-dominated delta plains. In inter-distributary areas, geological features like levees, various types of crevasse lobes and crevasse channels are often found (Reading and Collinsons 1996).

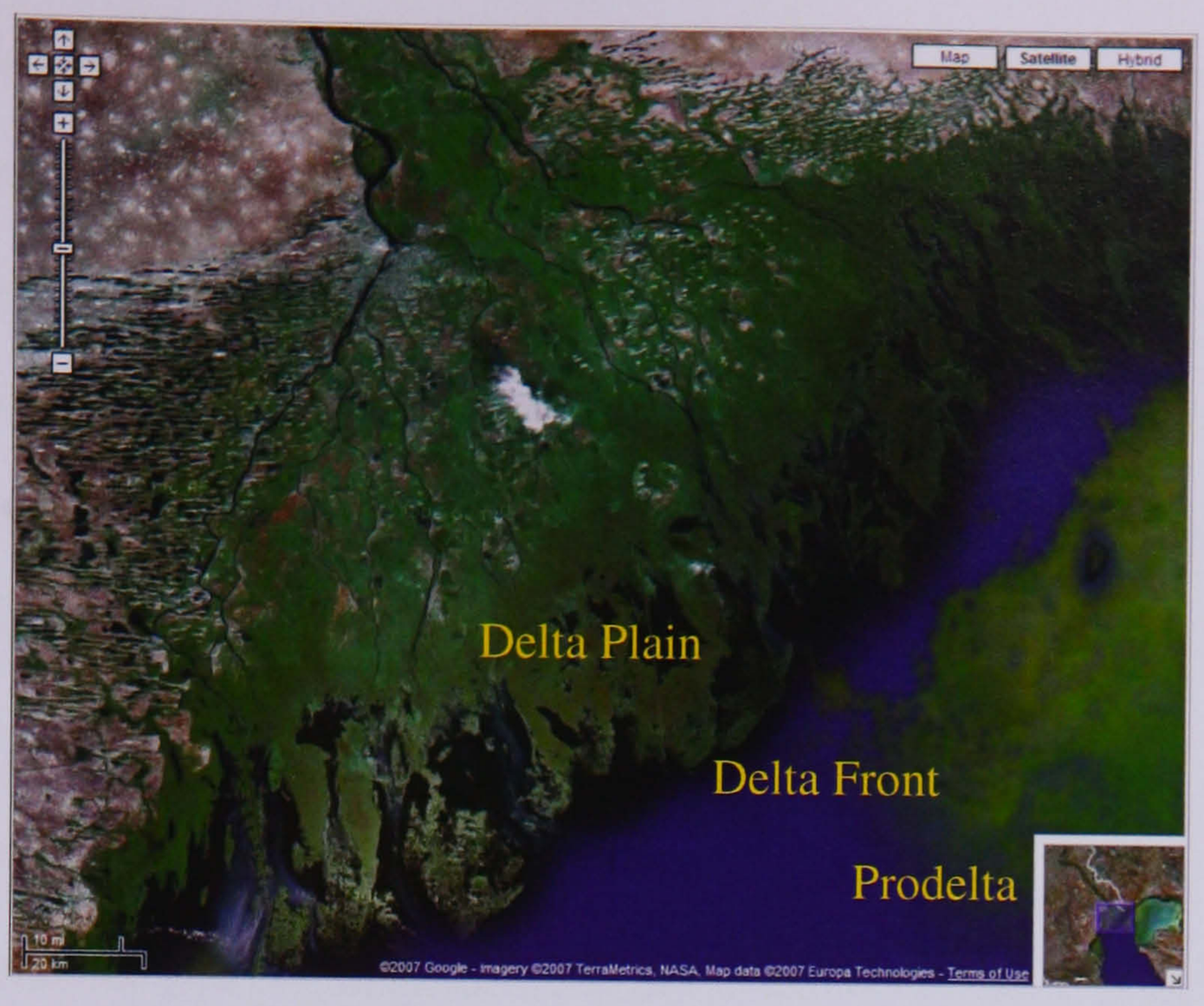


Figure 2.4A

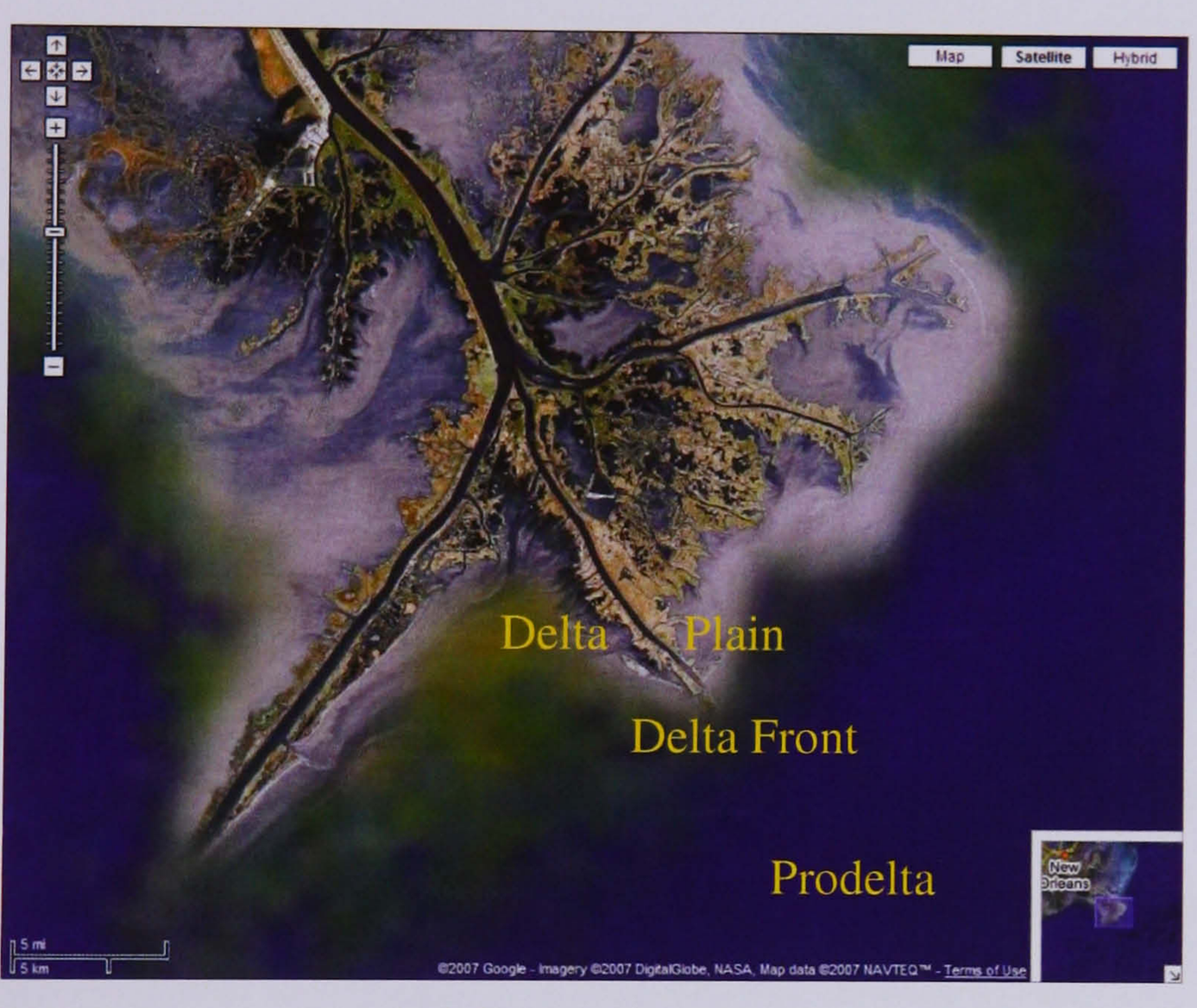


Figure 2.4B

Figure 2.4. (A, top) Satellite image of the modern Volga Delta. The delta is divided into three parts (1) delta plain, the large upstream region of the delta system dominated by subaerial fluvial channels; (2) delta front, the downstream region of the delta, is a zone of interaction between fluvial and basinal process; (3) prodelta, at the outer limit of the subaqueous delta. In different parts of the delta, sandbodies have different geometries and architectures. On the delta plain, the connectivity of branching channel sandbodies is controlled by their distribution, width, thickness and sinuosity, whilst the delta front contains mouth-bar sandbodies (http://maps.google.com/). **(B, bottom)** Satellite image of the modern Mississippi Delta. Compared with the modern Volga Delta, the Mississippi Delta has a small number of distributary channels and the delta front is composed of widely separated mouth bars. The different facies architecture between these two fluvial-dominated deltas is mainly because of the rapid lake level change, gentle offshore gradient and homopycnal inflow of the Volga Delta. (http://maps.google.com/).

The Mississippi Delta is often quoted as an example that represents fluvial-dominated delta systems. However the facies architecture is different between the Volga Delta and the Mississippi Delta, as the Volga delta experienced rapid lake-level changes with gentle offshore gradients (c. 5cm/km; Kroonenberg et al. 1997) and homopycnal inflow. Figure 2.4 demonstrates a plan view of the Mississippi Delta and Volga Delta. The Mississippi Delta has a relatively low number of terminal distributary channels and bifurcation. In contrast, the Volga delta has a much higher number of terminal distributary channels (modern Volga delta has c. 800 terminal distributary channels; Olariu and Bhattacharya 2006) and because of the coalescence of multiple terminal distributary channels and mouth bars the facies architecture is different from that of the 'bird-foot' shaped Mississippi Delta.

2.3.2 Previous work on fluvial-deltaic reservoirs

Tyler et al., (1991) estimated that deltas host 30% of all the world's oil, coal and gas deposits (Bhattacharya 2006). Some of the largest oil and gas field in the world are hosted in fluvial-deltaic reservoirs; water injection or miscible gas injection have been applied in some of these fields: the Yanchang Oil Field (Ordos Basin; North China); Lake Maracaibo Field (Venezuela); Granny Creek Field (Appalachian Basin; USA); Sanga-Sanga Block (Indonesia); Prudhoe Bay Field (Alaska); Mahakam Delta Fields (Indonesia); (Haldorsen et al. 1987; Begg et al. 1994; Hohn 1997; Ambrose et al. 1997; Knapp and Yang 1999; Luo 2002; Nikijuluw et al. 2005). Due to the complex nature of fluvial-deltaic geology, most of the published examples have experienced difficulties in maintaining reservoir pressure, experienced oil by-pass and early water breakthrough and/or yielding poor recovery at the end of field life. The

main challenge of producing from fluvial-deltaic reservoirs is to avoid bypassing of hydrocarbons, because there are numerous non-continuous sandbodies of variable connectivity and stacking arrangement (Dyer et al. 2000); in order to develop this sort of field one needs a large number of wells for high recovery. Various groups of researchers have conducted geological modelling and flow simulations on fluvial-deltaic reservoirs in order to better understand, monitor and manage them.

Some early modelling of deltaic reservoirs was less concerned with geological descriptions, but focussed instead on stochastically distributing the rock and petrophysical properties obtained from reservoir core and well log data. In the early 1980s, some studies characterised and modelled fluvial-deltaic reservoirs (e.g. Prudhoe Bay) by stochastically distributing sand and shale within a reservoir model (e.g. Begg et al. 1985; Haldorsen et al. 1987). Because shales act as barriers to flow, the lateral continuity of shale controls vertical permeability and inclined shales may form oil traps (Jackson and Muggeridge 2000). However, by characterising the reservoir in terms of shale-length statistics, one cannot represent the geological environment because geostatistic manipulations do not accurately represent complex object shapes. Hence, certain geological features would not be captured accurately in these models, and misleading predictions of the residual oil distribution could result.

Weber (1986) pointed out that building conceptual models that contain realistic geological features at different length-scales is necessary in order to compare different development schemes. Conceptual models can also help reservoir engineers to understand the typical configuration of heterogeneity and to predict production behaviour. Given that the sub-surface environment is highly uncertain, it is necessary to gather as much information from all data sources as possible to realistically

describe the reservoir architecture. Weber (1986) also pointed out that outcrop analogues can provide a better understanding of the relationship of certain heterogeneity types with depositional environment and tectonic features. Consequently the use of an outcrop analogue is recommended to demonstrated a view of the reservoir architecture. Many previous studies (e.g. Haldorsen et al. 1987; Begg et al. 1994; Abdullaev et al. 1998; Reynolds et al. 1998) have demonstrated that fluvial-deltaic environments have complex architecture. The geological structure significantly influences pressure communication and oil sweep efficiency. Consequently it is necessary to understand the reservoir architecture of a fluvial-deltaic system in order to construct a geological model. Reliable distributions of geological parameters may be difficult to recover from subsurface measurements. It is necessary to borrow such distributions from outcrop analogues or high-quality subsurface analogues.

2.3.3 Outcrop Analogues

The ACG development is in its early stages; production data is limited and well spacing is large. Subsurface data is therefore limited. Well log and core data may show the vertical distribution of selected parameters at a particular location, but because the well density is low, it is not feasible to obtain reliable information about the lateral distribution and continuity of geological heterogeneities, and such information can only be inferred from outcrop analogues or seismic data.

Previous studies indicate that seismic data are useful in order to identify the top and bottom boundaries and the location of faults within a reservoir (Richardson et al.

1987a). In addition, using seismic data may also enable some geological features (e.g. channel orientation and areal distribution) to be resolved (Yao and Chopra 2000). However, it has often been found that the vertical resolution of seismic data is not sufficient to identify many geological features within the reservoir. Richardson et al., 1989 identified that in a deltaic reservoir, individual reservoir units can be thinner than a single seismic reflection. Moreover, because seismic data contain a mixture of signal and noise, it is commonly difficult to distinguish between real features and seismic artifacts (Grammer et al. 2004). Therefore, it is essential to conduct a robust quality control on seismic data (Hesthammer et al. 2001). It is often useful to use high-resolution information from outcrop analogues integrated with well, core and low-resolution seismic data to enhance the interpretation of a reservoir. Schwab et al. (2004), for example, applied such an approach to characterise a carbonate reservoir in western Canada.

Warren and Skiba (1963) published one of the earliest papers that recognised the value of outcrop analogues. They pointed out that core data does not provide a valid macroscopic description of the reservoir. Previous research also indicated that the integration of outcrop data and geostatistical analysis allowed for the construction of a quantitative sedimentological model, which helps to improve the efficiency of outcrop observations as a predictive tool for estimating facies heterogeneity in subsurface reservoirs (Felletti 2003). Outcrop analogues provide insights into understanding the boundaries and internal facies distributions of a reservoir. By using outcrop analogue data, a reservoir engineer can obtain better reservoir characterisation and modelling understanding, because the outcrop data provide a clear view of sandbody geometry and facies distribution (e.g. Ballin et al. 1997; Lerat et al. 2002). Previous work by Grammer et al. 2004), Sullivan et al. 2004 and Schwab

et al. 2004) demonstrated that outcrop analogue data provide constrained information on facies geometry and architecture that can be integrated with well data to characterise the reservoir below seismic resolution. Larue 2004) indicated that the major uncertainties in reservoir architecture are areal variation and sub-seismic thin bed effects. Suro-Perez et al. (1991) demonstrated that production parameters (cumulative oil production, cumulative WOR, breakthrough time) are sensitive to the reservoir geological architecture. Outcrop analogues can provide information about smaller scale heterogeneity, such as permability distributions within channel sandbodies as well as sandbody connectivity at a large scale.

There are many examples that illustrate the use of outcrop analogues to study fluvial-deltaic depositional systems or distributary channel systems. (e.g. Geehan et al. 1986; Matheron et al. 1987; Hand et al. 1994; White and Barton 1997; Knox and Barton 1999; Li and White 2003; Wach et al. 2004). The well exposed, Cretaceous Ferron Sandstone (Utah, USA) is one of the outcrop analogue examples of fluvial-deltaic systems that has been used most frequently. White and Barton (1997); Li and White (2003) used the Ferron Sandstone outcrops to develop a novel grid construction technique that can be constrained by high-resolution outcrop stratigraphic data.

White and Barton (1997) small-scale 2D geological models of the delta plain environment (Picture Flats outcrop) contained more tortuous flow paths and had lower recovery efficiency than comparable models of the delta front environment (I-70 outcrop). They found features like shale barriers and mud-filled channels reduced sweep and recovery. However, the 2D models cannot capture the correct interaction between the reservoir architecture and fluid flow, because a 2D model

presumes the geological feature to be uniform in the third dimension. Li and White, (2003) conducted a flow simulation on a 3D geological model of the Ferron sandstone. They mapped the variogram of the dimensions and orientations of shale throughout a 3D volume using nearby cliff exposures. Their 3D modelling demonstrated that heterogeneity reduced the breakthrough time. However, the volume of the 3D model (150m x 110m x 12m) was not large enough to capture larger, reservoir-scale heterogeneities such as channel sandbody architecture. White and Barton (1997) conducted tracer simulations of flow, which did not investigate the interaction between multi-phase flow and the effect of gravity. Moreover, neither study of the Ferron Sandstone made clear what are the key factors influencing water/gas flooding oil recovery.

The depositional environment of the Ferron Sandstone is different from that of the Pereriv Suite within the ACG field, because the Ferron Sandstone contains evidence of marine influence. For example, the Ferron sandstone contains barrier, lagoonal, estuarine and coal deposits, some of which have not been found in the ACG reservoir. The Pereriv Suite reservoir in the ACG field is evidently a highly fluvial-dominated type of delta (Kroonenberg et al. 1997; Anna 2003). Moreover, the paleo-Volga delta was connected to an inland lake and the rapid lake level changes caused the highly layered properties of the ACG stratigraphy. The internal architecture therefore is different between the two fluvial-deltaic systems.

The outcrop analogues used in this research project consist of Pereriv Suite and Balakhany Suite strata exposed on the Apsheron Peninsula c.100km north-west of the ACG field; the lower interval of the Productive Series in Kirmaky Valley and the upper interval in Balakhany Quarry and Yasamal Valley (Figure 2.5). Two outcrops

have been selected as specific analogues for the ACG reservoir, based on the similar depositional environments interpreted for both outcrops to those of the ACG reservoir (Reynolds et al. 2003; Reynolds and Riley 2003). These outcrops are described in Reynolds et al. (1998, 2003); Reynolds and Riley (2003) and Hinds et al. (2004). This research study adopted the analysis of Reynolds et al. 2003; Reynolds and Riley (2003), which compared the outcrop and subsurface sedimentology to select appropriate analogues based on lithofacies composition, grain size and NTG in different layers.

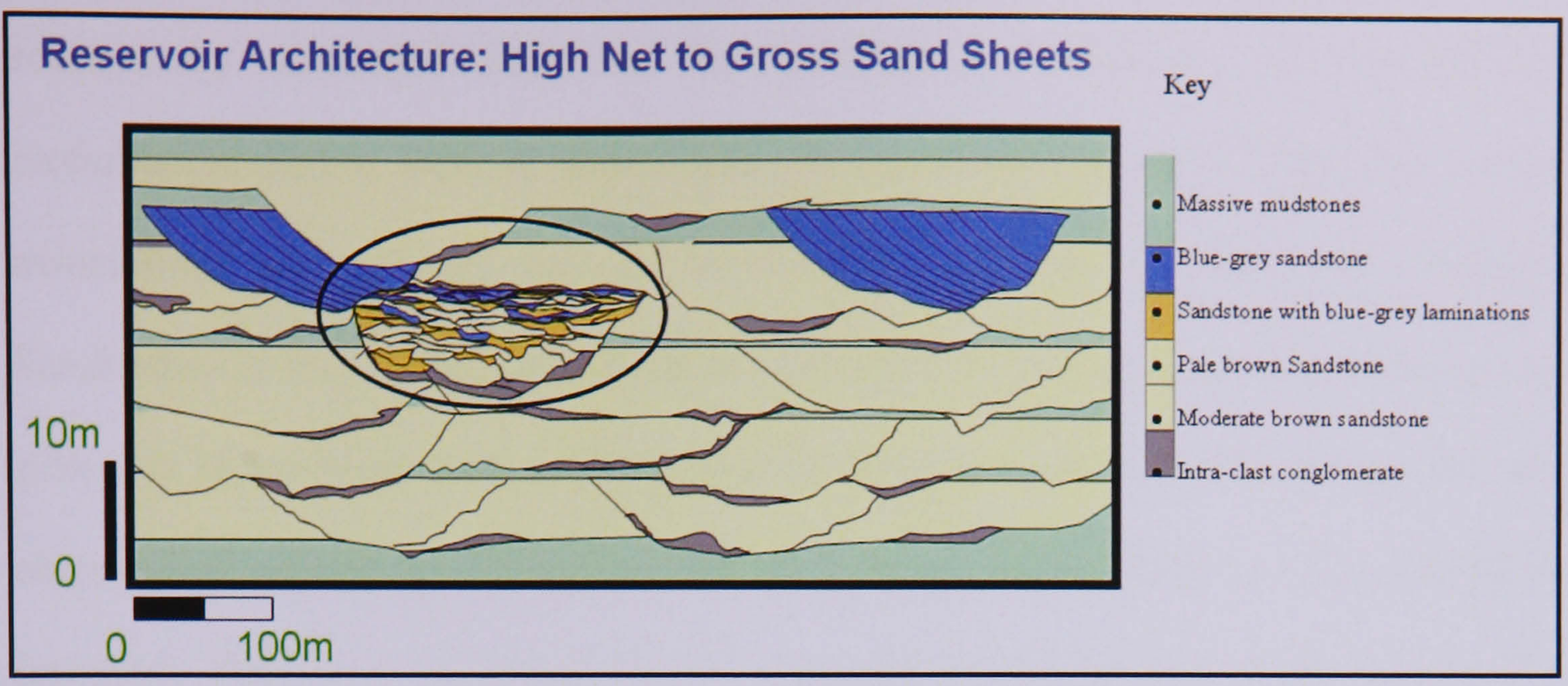


Figure 2.5A

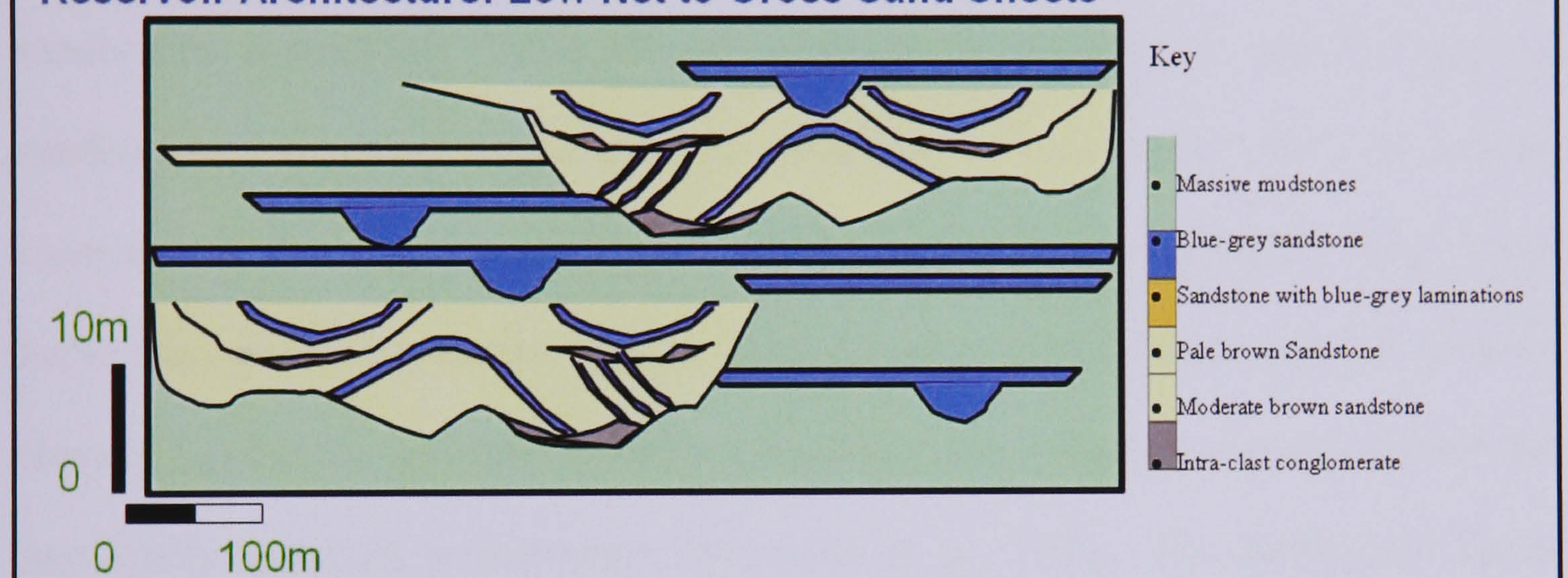


Figure 2.5B

Figure 2.5. **(A, top)** Conceptual diagram of high NTG reservoir architecture in Pereriv B and D layers. Figure based on outcrops located at Balakhany Quarry. The sandbody circled shows an example of the internal complexity of each sandbody (Reynolds and Riley 2003). **(B, bottom)** Conceptual diagrams of low NTG reservoir architecture in Pereriv A, C and E layers. Figure based on outcrops located at Yasamal Valley (Reynolds and Riley 2003).

The Balakhany Quarry is an outcrop analogue for high NTG intervals of the Pereriv Suite (Pereriv B and D) and the Yasamal Valley outcrop is analogous to the low NTG Balakhany Suite and Pereriv A,C and E intervals (Reynolds and Riley 2003). Reynolds et al. (1998) outlined four facies associations present in both outcrop and subsurface data that encompass a range of paleoenvironments within fluvial-dominated deltas, namely: (1) fluvial, (2) delta plain, (3) proximal delta front and (4) distal delta front. In each facies association, there is an abundance of

sedimentary structures deposited by unidirectional currents, an absence of bioturbation, and a lack of wave- and tide-generated structures. The four facies associations are arranged into an architecture controlled by lake-level changes. Sandbodies in the fluvial, delta-plain and proximal delta-front facies associations are generally sharp-based with a fining-upward trend in grain size. The sandbodies are observed at outcrop to define channels of varying width, which are interpreted to represent deposition in either fluvial channels or fluvial-dominated distributary channels. The fluvial facies association contains the coarsest grain size, with channel sandbodies comprising coarse-grained sandstone at their bases and fine-grained sandbodies comprising coarse-grained sandstone at their bases and fine-grained sandstone at their tops, suggesting relatively high porosity and permeability. This facies association also contains only a small degree of internal heterogeneity, because channel sandbodies are densely stacked together, and is thus considered to have the best likely reservoir performance (Reynolds et al. 1998). The delta-plain facies association also contains multi-storey channel sandbodies of upward-fining or uniform grain size trend, but the likely reservoir performance of this facies association is dominated by the occurrence of laterally extensive flood plain shales that can act as barriers to vertical flow. Proximal delta front and distal delta front facies associations are characterised by fine-grained sandstones and interbedded siltstones, which causes strongly layering within reservoir. These facies associations are expected to have poor reservoir characteristics (Reynolds et al. 1998; Hinds et al. 2004)

The ACG reservoir contains a number of geological features at different length scales which can also be identified from the outcrops, such as channel sandbodies of variable geometry (channel width and thickness) and variable distribution

(single-storey channels and multi-storey channel belts), and mudstone layers of variable lateral extent.

Weber (1986) highlighted that geological heterogeneities cannot be neglected and that simple averaging procedures cannot lead to reliable results. However it is very time consuming to study all known heterogeneities; thus it is not feasible to input all possible geological features within a reservoir model. The question is which types of heterogeneity have a major influence on reservoir performance?

2.4. Impact of sedimentological/geological heterogeneity on flow

Many studies have demonstrated that ignorance of geological heterogeneity will lead to inaccurate prediction of reservoir performance (e.g. Weber 1986; Suro-Perez et al. 1991; Damsleth et al. 1991; Jones et al. 1994, Jones et al. 1995; Kjønsvik et al. 1995; Jackson and Muggeridge 2000; Larue and Friedmann 2005; Larue and Hovadik 2006).

Weber (1986) indicated that although many cases in history have demonstrated the role that geological heterogeneity plays on recovery, it is still very difficult to derive general conclusions and principles about what part these geological features would play in a new field. This is because the geological heterogeneities can react differently depending on other reservoir environment parameters, like mobility ratio, PVT properties, displacement mechanism, reservoir dip, aquifer strength, oil column and well spacing. Therefore, a reservoir heterogeneity study is required for each

individual reservoir development project. Lasseter (1986) indicates that the challenge of reservoir modelling is the need to describe reservoir geology realistically and also to make sure the model behaves accurately and efficiently. In addition, Weber (1986) also demonstrated that geological heterogeneities at different length scales influence fluid flow in different ways. For example, on a small scale where capillary forces play a major role, heterogeneity can cause oil entrapment (e.g. inclined shales that caused bypassed oil in Jackson and Muggeridge 2000), whereas, on a large scale the viscous and gravity forces become more significant. Large scale geological heterogeneities like barriers, faults or contrasts in permeability cause the problem of bypassed oil. Ottesen et al. (2005) examined the influence of varying the properties of faults on recovery. In their work, the fault density and transmissibility are the two most significant factors that influence the recovery factor of a reservoir. Li and Lake (1995) studied immiscible displacements through a heterogeneous system at different length scales. They found that, local and global heterogeneities cause fingering and dispersive flows, while zonal heterogeneity causes channelling. From the results of these studies, it is clear that heterogeneities at all length scales are potentially important for reservoir performance. Therefore, to accurately model and simulate a reservoir, it is necessary to build models that include all the geological features. However, not all the heterogeneities necessarily have a significant impact on recovery, and because of the limitations of computational power and time it is not feasible to model and simulate all the heterogeneities across the various different length scales. Reservoir heterogeneity is hierarchical in nature. The geometries and mutual relationships of component facies have a wide range of scales. Identifying the influence of heterogeneity factors at each individual length scale could be a better approach to understanding reservoir performance than including all possible parameters in a single model.

Previous research suggested different schemes for defining the hierarchy of geological heterogeneities by their length scale (e.g. Miall 1985; Weber 1986; Haldorsen 1986; Miall 1988; Van de Graaff and Ealey 1989; Jones et al. 1992). The different schemes were largely dictated by the nature of the successions studied. There is no universal guideline for how to divide the lengthscale intervals in order to capture the various heterogeneities in a reservoir model. How boundaries between different lengthscales are drawn depends on the depositional environment of the reservoir. Therefore, for a particular reservoir it is necessary to assess at what scale the reservoir is to be modelled in order to know which geological heterogeneities needs to be captured explicitly. Various lengthscales of heterogeneity are identified, from the basin scale (100's m and larger) down to the pore scale (10-100's nm) (Weber 1986; Van de Graaff et al. 1989). Figure 2.6 demonstrates the hierarchy of reservoir heterogeneity suggested by Weber (1986). Within the ACG reservoir, major structural heterogeneities are only recognized at a scale that is larger than the sector models that were used to study the displacement between injector and producer wells. This research is mainly focused on heterogeneities at the reservoir-unit and genetic-unit scales.

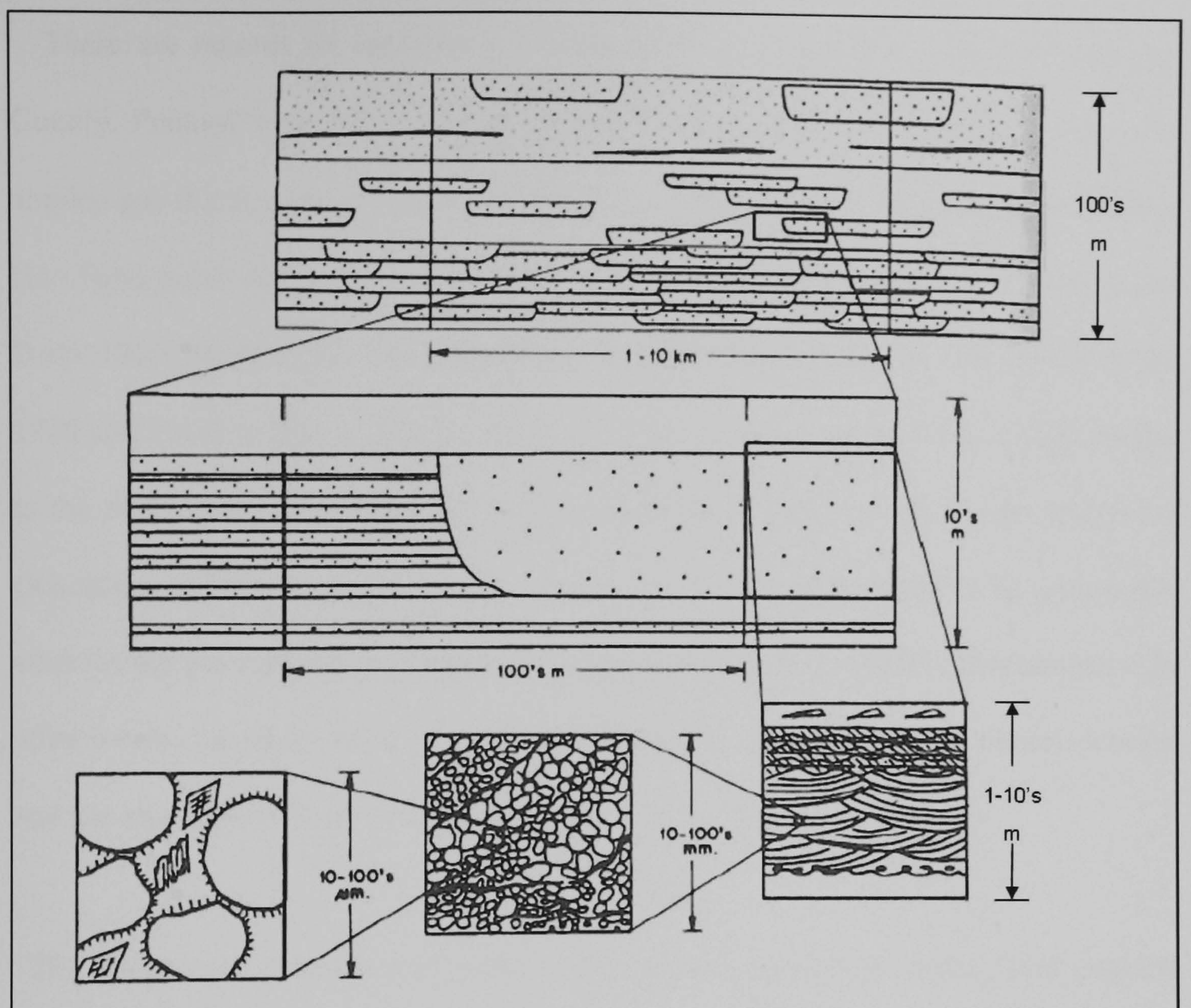


Figure 2.6. Weber's 1986 hierarchical of reservoir heterogeneity at different length scales; example from a fluvial reservoir.

2.4.1 Impact of fluid type and production mechanism

It is recognised that geological heterogeneities can behave differently under various flow mechanisms (e.g. displacement fluids of varying mobility ratio; Weber 1986). In the ACG reservoir, both water and gas injections are applied in order to enhance oil recovery. There are plenty of field examples for using water flooding to enhance oil recovery, but only relatively few using gas injection.

There are records of applying gas injection to increase oil recovery in Venango County, Pennsylvania USA as early as 1890. Some large oil field operations also applied gas injection (e.g. Jones Sand Pool in Arkansas, USA; Mile Six Pool in Peru; Frio Sand reservoir in south Texas, USA; Brent Field in the North Sea; Broekers and Dorp, 1986; Burns et al., 2002; Hawkins Woodbine Field in Texas, USA; King et al., 1970 and Prudhoe Bay in Alaska, USA.) is a gas injection project that is very similar to the ACG development project, because both fields have fluvial-deltaic reservoirs. One major difference is that the gas injection in ACG is considered to be immiscible whereas the gas injected in Prudhoe Bay was classified as a miscible displacement. In other words, the phase behaviour effects between the injected gas and the resident oil and gas phases have been treated negligible in ACG (miscible pressure).

The reason that gas injection projects are not as common as water flood projects may be because sufficient gas is not always available for re-injection. Also, gas has a much lower viscosity than oil, and therefore unstable displacement normally occurs (gas override) unless the reservoir and displacement conditions can fulfil Dietz's condition for stable displacement (Dietz 1952; Dake 1978; see Chapter 3). Indeed, the main differences between gas-oil and water-oil displacements, is that gas-oil displacement has a much higher mobility ratio between the two fluids. Because of these differences, by using different production mechanisms, the same reservoir can give a completely different performance. (e.g. Ringrose et al. 1993). According to Dietz's theory, a displacement can be stabilised by buoyancy forces, and therefore gas-oil displacement is more sensitive to heterogeneities that influence vertical cross flow, whereas these factors may not be so important for mobility stable water-oil displacement.

The ACG reservoir has a highly layered structure. Also the Azeri reservoir has a steep tectonic dip (up to 45°), which makes it unique in comparison with all other previous examples of gas injection. With such a steep dip, it is easier to achieve stable gas-oil displacement according to Dietz's theory. However Dietz's theory only applies to homogeneous models. The previous sections have already acknowledged that there are many heterogeneities present at different length scales in the ACG reservoir.

2.4.2 On field and reservoir-unit scale heterogeneity

In this investigation, the length scale of reservoir-unit scale features is defined as between 100m and 10km, and the length scale of genetic-unit scale features is between 1m and 100m (similar to Weber 1986; Van de Graaff and Ealey 1989; Jones et al. 1992; Figure 2.7). Van de Graaff and Ealey (1989), Barthel (1991), Suro-Perez et al. (1991) and Larue and Friedmann (2005) suggest that production parameters (cumulative oil production/water-oil ratio, breakthrough time) are sensitive to the geological architecture. Some previous studies have recognised that the most important stratigraphic parameters for oil recovery are sandbody continuity and interconnectedness (Van de Graaff and Ealey 1989). Sandbody connectivity is important for reservoir performance because it sets a boundary for possible flow paths. At the reservoir-unit scale, Weber and van Geuns (1990) suggest a scheme to simplify reservoir descriptions by introducing a connectivity spectrum for reservoir-unit scale sandbody architecture. They suggest that the reservoir architecture can be divided into three different types: layer-cake (highest connectivity), jigsaw-puzzle and labyrinth (lowest connectivity). Figure 2.8 demonstrates the different sandbody connectivities in reservoir with various generic sandbody architectures.

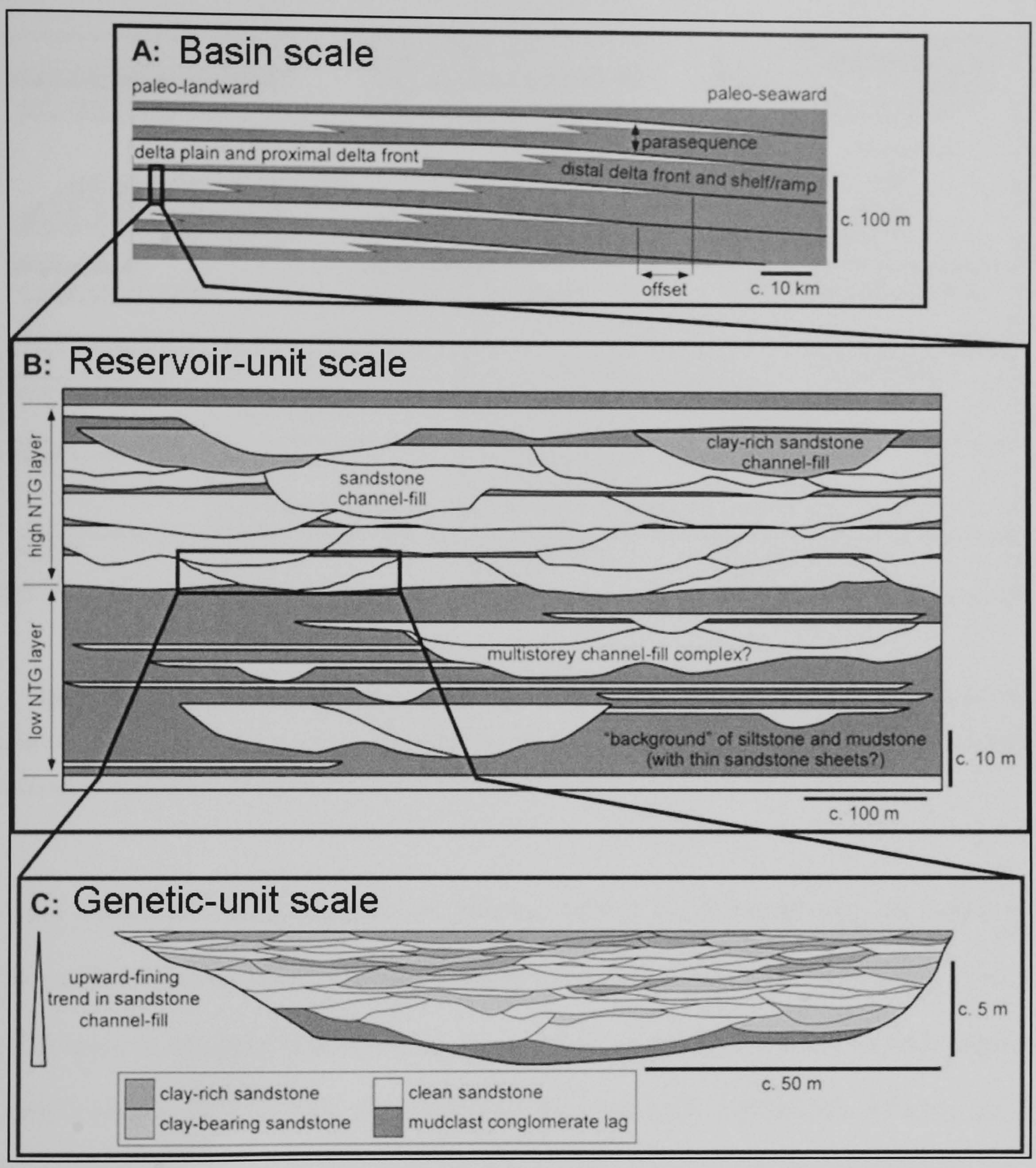
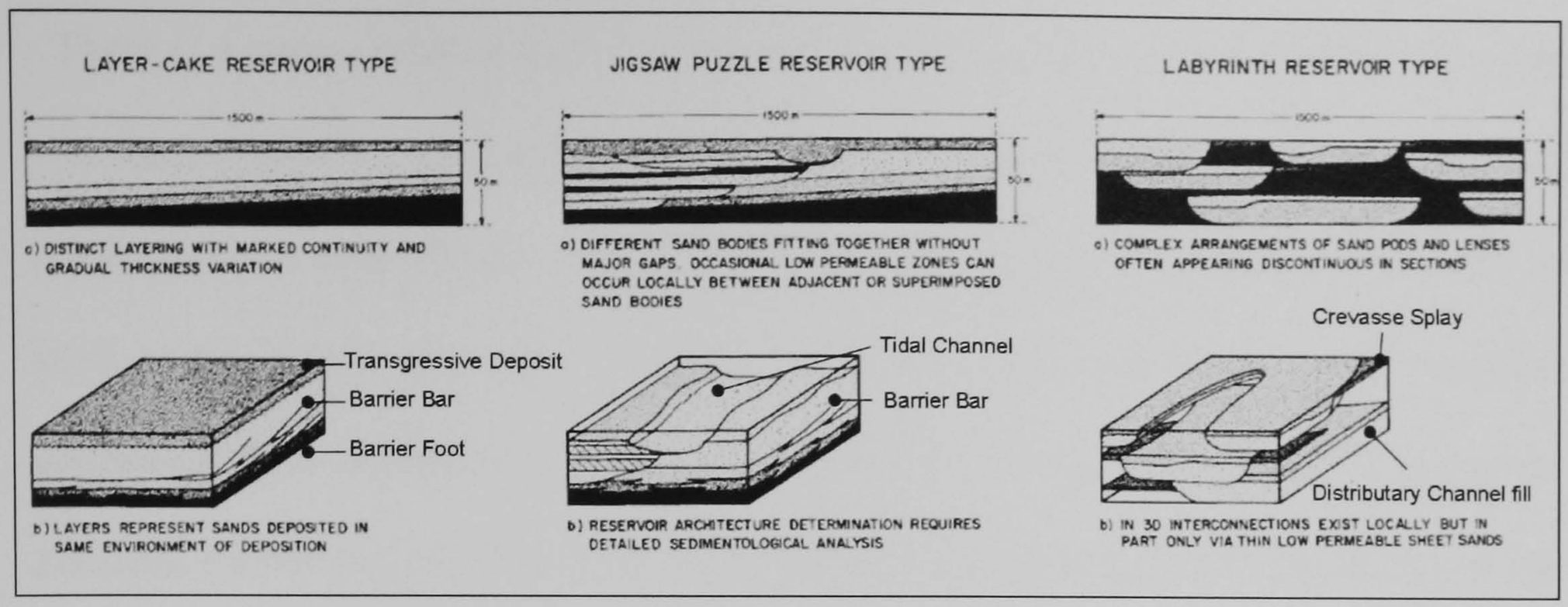


Figure 2.7. Hierarchy of heterogeneity in the fluvial-dominated deltaic Pereriv Suite reservoir of the ACG field. The hierarchy is modified from Weber's 1986 scheme. Sub-metre scale (core-unit and pore scale) are not included.



	Terrestrial	Coastal	Tide-dominated
Layer cake	Sheet flood deposits Lacustrine sheet sand Aeolian dunes	Barrier bars Chenier deposits Trangressive sands	Shallow marine sheet sands Offshore bars Outer-fan turbidites
Jigsaw puzzle	Braided river deposits Point bars Mixed lacustrine/fluvial Mixed aeolian/wadi	Combined facies complexes e.g. barrier bar plus tidal channel-fill channel-fill/mouth bar combinations with high NTG	Storm sand lenses Mid-fan turbidites
Labyrinth * NTG = net/gross ratio	Fluvioglacial deposits with low NTG Low-sinuosity channel-fills	Low-sinuosity distributary channel-fills	Upper fan turbidites Slumps Storm deposits with low NTG

Figure 2.8. The three different generic reservoir architectures identified by Weber and Van Geuns 1990. The figure demonstrates that different geological features can be found in various types of reservoir which have various sandbody connectivities.

The sweep efficiency depends on different factors for different types of reservoir. For a layer-cake reservoir, which contains laterally extensive sandbodies, the sweep efficiency is strongly dependent on permeability ordering of layers, gravity effects and mobility. A labyrinth reservoir has discontinuous sandbodies existing in a complex spatial arrangement, and the sweep efficiency is controlled by the reservoir architecture and the position of the wells. The jigsaw-puzzle reservoir is in between these two types and all of its description parameters are potentially important. This scheme provides a starting point for identifying key geological features. By using Weber and van Geuns (1990) classification scheme, the high NTG Pereriv B and D layer in the ACG reservoir would be classified as layer-cake system and the low NTG Pereriv A, C and E layers Azeri as complex, labyrinth systems.

There is a strong relationship between NTG and connectivity. King (1990); Hovadik and Larue (2007) demonstrated that there is a threshold value of NTG at which connectivity is established. Once the NTG in a 3D system drops below c.30-35% the sand connectivity decreases rapidly, assuming that sandbodies are randomly distributed. The threshold is much higher in a 2D system (c.55-60% NTG). Larue and Hovadik (2006) demonstrated that for a system with the same NTG, the reservoir unit geometry also contributes to connectivity. They demonstrated that parallel channel sandbodies of low sinuosity in a 3D reservoir system tend to behave as a quasi-2D system, because channels do not intersect within stratigraphic layers. Therefore, the sandbody connectivity of such systems is much lower than that of systems with the same NTG but different stratigraphic architecture. These studies (King 1990; Larue and Hovadik 2006; Hovadik and Larue 2007) provide some insight into what researchers need to be aware of when studying reservoir connectivity. However, the studies focus on the static structure of reservoirs, and provide limited insight into how displacement would be influenced in systems of different connectivity.

Barthel (1991) investigation on the impact of fluvial reservoir architecture on recovery demonstrated that channel density, distribution and permeability contrasts between channels have an important influence on displacement efficiency. However, their work did not demonstrate the interaction between the geological features and different production mechanisms, nor did it explain how the geology influences oil recovery. A recent study of waterflood application in conceptual channelized reservoirs (Larue and Friedmann, 2005) demonstrated, using a number of different reservoir models with similar connectivity but different reservoir architecture, that the recovery efficiency was very similar in each case. Sandbody connectivity has a bigger influence on recovery efficiency than the different reservoir architecture, and

therefore the focus should be on studying the parameters that control sandbody connectivity. Up to this point, it is clear that, at reservoir-unit scale, it is necessary to identify the geological heterogeneity that has the largest influence on connectivity and displacement efficiency in order to characterise recovery efficiency.

There have been many previous sensitivity studies on geological heterogeneities (e.g. Jones et al. 1994,1995; Kjønsvik et al. 1995; Jackson and Muggeridge 2000). Jones et al. (1994) studied two high NTG fluvial reservoir examples with a water flooding recovery scheme, and showed that when the reservoir NTG was higher than 75%, the fluvial reservoir behaved like a homogeneous reservoir (i.e. layer-cake structure). Their study showed that the permeability contrast between sandbodies is important. However, it did not address the complex interaction between displacement and the characteristics of a fluvial reservoir (i.e. channel sandbody dimensions and distribution, or the upward-fining character of fluvial sandbodies). The study characterised the reservoir by distributing sand and shale rather than constructing an object-based model to characterise the depositional environment.

Studies of low NTG fluvial reservoirs (Jones et al. 1995) and shallow-marine reservoirs (Kjønsvik et al. 1995) have shown that sub-seismic-scale sedimentary heterogeneity has an impact on waterflooding performance. These studies ranked the influence of heterogeneities in the different depositional environments on sand connectivity and cumulative oil recovery at different recovery stages. They provided a basis for understanding the key geological heterogeneities and the sensitivity of the reservoir performance to them. Jones et al. (1995) demonstrated that the number of channel sandbodies within a channel belt and the channel width and thickness affects the waterflood performance in a low NTG fluvial reservoir. The work of Jones et al.

(1995) and Kjønsvik et al. (1995) helps one to reduce the uncertainties who studying these two types of reservoirs. However, no similar investigation has been conducted on fluvial-deltaic reservoirs; studies of sensitivity analysis on the interaction between geological heterogeneities and immiscible gas- flooding recovery schemes is also limited.

At the reservoir-unit scale, the features that control sandbody connectivity have a major impact on the entire reservoir recovery efficiency. For channelised reservoir systems, features such as channel width and thickness, sinuosity and stacking patterns are all potentially important for reservoir performance. Geological features within each genetic sandbody contribute to displacement efficiency. For example, vertical permeability variations within channel sandbodies and discontinuous shale barriers occur within reservoirs, and numerous studies have demonstrated that these features have a significant impact on displacement. (e.g. Weber 1982; Haldorsen and Lake 1982; Haldorsen and Chang 1986; Hartkamp-Bakker 1993; Ciammetti et al. 1995; Jackson and Muggeridge 2000). Therefore it is necessary to identify which genetic-unit scale heterogeneities would influence reservoir performance.

2.4.3 On genetic-unit and smaller scale heterogeneity

In this study, the length scale of genetic-unit scale heterogeneities is defined as 10s -100s of meters (Weber et al. 1986; Figure 2.6 and 2.7). Features within architectural elements like channels and bars are considered to belong to the genetic-unit scale. It is considered that mud-clast lags at channel bases, the vertical permeability variation within a sandbody, the ratio of the vertical and horizontal permeability within sand

facies (Kv:Kh), and shale bodies of various geometries (both extensive or discontinuous) belong to this scale.

Jones et al. (1995) (in fluvial reservoirs) and Kjønsvik et al. (1995) (in shallow-marine reservoirs) have compared the influence of geological heterogeneities at different length scales. Although their research demonstrated that the most dominant heterogeneities are the large-scale geological factors, they also suggested that smaller scale heterogeneities cannot be neglected. Jackson and Muggeridge (2000) suggested that small-scale heterogeneities are even more important than large-scale heterogeneities within the tidal environment. This research found that permeability contrasts due to this heterogeneity within larger scale objects were greater than the permeability contrast between objects. Another study on tidal reservoirs by Brandsater et al. (2001) used single phase tracer simulations to study reservoir performance. Their research found that the Kv:Kh ratio at facies scale has an important effect on the production profile. Their work was mainly based on single phase tracer simulation and did not take gravity and capillary effects into account.

Many reservoir models characterise genetic-unit scale feature by using grid based modelling schemes and assigning the petrophysical parameters (i.e. different rock properties) stochastically to grid cells, with constraints provided by well data. However, by only using this type of grid-based modelling technique, aspects of reservoir geology can be neglected.

Another way of characterising genetic-unit scale properties is to simplify the reservoir description of geology to reservoir (sand) and non-reservoir facies (shale). In fact many reservoir objects in various depositional environments contain

discontinuous shales which act as barriers to fluid flow. It is traditionally recognised there are two ways to deal with discontinuous shales: (1) to model shales explicitly and (2) to estimate the effective Kv:Kh ratio of a system that contains discontinuous shales (Begg and King 1985; Haldorsen and McDonald 1987). In this study, genetic-unit scale geological features (e.g. upward trends in grain size within sandbodies) will be explicitly included in reservoir models. These features are constrained by sub-surface measurements and outcrop analogue data for the Productive Series.

2.5. Modelling of flow in heterogeneous reservoirs

2.5.1 Object based modelling

Many studies adopt grid-base modelling techniques for reservoir modelling. It is a common practice to characterise and model reservoirs by stochastically distributed petrophysical properties within sand facies. (e.g. Damsleth et al. 1991). Although grid base modelling techniques honour well data, they often neglect reservoir geology. Wang and Shibli 2001) stated that simple grid-based modelling schemes cannot represent complex geological shapes. Many researchers suggest that object-based models would generate a better characterisation of the fluvial or fluvial dominated deltaic reservoir at the large scale (e.g. Deutsch and Wang 1996; Deutsch and Tran 2002; Shmaryan and Deutsch 1999; Chike and Onyekonwu 2005).

Deutsch and Wang (1996) and Deutsch and Tran (2002) used an object-based stochastic modelling approach to model fluvial systems and demonstrated the following advantages:

1. Geologically intuitive and accessible input data control channel sizes and shapes.
2. Explicit control over vertically and areally varying facies proportions.
3. Realistic channel geometries.
4. Realistic non-undulating channel-top surfaces.
5. Integrated porosity and permeability models, in which the main directions of continuity conform to channel geometries.

Object-based modelling has its limitations, because the algorithm may find it difficult to honour well data given that there is a fixed range of the geometry of geological objects present in the reservoir model. Nevertheless, it is considered that object-based modelling would provide the most realistic reservoir descriptions for the fluvial dominated reservoirs and lead to the most reliable results. The object based modelling technique will be adopted for this research project since the advantages of the scheme were demonstrated by a number of previous studies. Also, as there are no specific well data to honour in the models, the limitations of the technique are reduced.

A number of deterministic reservoir models could be constructed based on all possible interpretations, in order to study reservoir performance. This is obviously not feasible given reasonable time and computing constrains. Therefore some statistical approach has to be adopted in order to conduct the investigation in an efficient way.

2.5.2 Sensitivity analysis techniques

Damsleth et al. (1991); Haldorsen and Damsleth (1990) paper stated that it is necessary to generate a number of realisations of reservoir architecture of a model for reservoir modelling purposes, but it is unwise to focus on the least relevant uncertainties. Therefore it is necessary to conduct screening studies. Screening the impact of heterogeneities creates the challenge of dealing with a large number of parameters. Previous research studied the effects of heterogeneities on production in different environments (Jones et al. 1994, 1995 in fluvial reservoirs; Kjønsvik et al. 1995 in shallow-marine reservoirs; Jackson et al. 1999 in tidal environments). In their work, they applied experimental design methods to conduct the sensitivity analysis and to identify the key heterogeneities impacting on reservoir performance.

Experimental design is a way to conduct experiments with the aim of obtaining information efficiently. This statistical technique was developed in the 1920s for agricultural applications, but a more modern application was introduced by Box et al. (1978). The technique was first used in the oil industry in the early 1990s (C.Chu 1990; Chu 1990; Damsleth et al. 1991). Experimental design has subsequently become a popular technique (Friedmann et al., 2001; White and Royer 2003; Manceau et al. 2001; Cheong and Gupta 2003; McLennan and Deutsch 2005; Peake et al. 2005; Salhi et al. 2005)

The experimental design method applied in this research is called fractional factorial design. Chu, (1990) paper is recognised as the first group of studies using fractional factional design to investigate the impact of different heterogeneities on project life

time, recovery and cumulative steam-oil ratios. This technique enables the maximum amount of information to be extracted whilst minimising the number of simulations. The technique calculates the average impact of varying the parameter to the objective function by changing the parameter from one setting to another. Therefore, instead of testing all the possible outcomes from the different parameter settings, this technique can rapidly identify those input parameters that have the most significant influence on the objective value. The result of varying each parameter can be ranked by the magnitude of impact upon a chosen objective measure (Box et al. 1978; Montgomery 2005).

Experimental design has its limitations. The method can only identify which parameter is the most important for a specific measure; it cannot explain the reason behind this result. Therefore, further simulations are typically required. Another problem in using experimental design is that the results change with time for objective measures that involve dynamic behaviour (Peake et al. 2005). For example, the most influential factor on oil recovery after one pore volume of injection may be insignificant when the measurement is taken at another time; the experimental design method is not able to identify the relationship between these various measures. Nevertheless, the experimental method still provides a great advantage by screening the most significant heterogeneities impacting on the objective measure and filtering out any factors that are not important. Fractional factorial design provides great advantages in time efficiency, because if requires few simulations.

2.5.3 Top-Down reservoir modelling scheme

The presence of heterogeneity at different length scales in a reservoir has already been recognised. Heterogeneities at length scales smaller than genetic-unit scale (e.g. cross-bedding, lamination and various pore networks) are often too fine to be captured within reservoir-scale models. To model core-scale heterogeneities requires high grid resolution, which in turn requires a high number of grid cells. This is time consuming and computationally expensive, and therefore is not feasible.

The length scale of core-scale heterogeneity is defined as 0.1cm to 1m (Weber 1986). At this scale, heterogeneities that control permeability include grain size and sorting, cross-bedding, lamination and the continuity of different facies types. There is a limitation on time and computational power to honour all the information at all length-scales, commonly heterogeneities at core-scale are treated by using an upscaling technique to obtain pseudo or effective properties on a larger scale (Haldorsen 1986). The problem of upscaling is that the process causes loss of information on lateral continuity and barrier distributions (Lasseter et al. 1986 Lasseter 1986). Sablok and Aziz 2005) point out the problems of existing upscaling techniques.

1. Total upscaling errors. The technique assumes that flow equations do not change with scale. This is not always true when the flow pattern is modelled at different scales, and the boundary conditions of the volume are subjective.

2. Error due to loss of heterogeneity. Most techniques assume flow in coarse grids is uniform which is not true. For example, when the reservoir includes channel

sandbodies of higher permeability than the background facies, fluids move faster in the channel sandbodies. Such phenomenon would be omitted using standard upscaling techniques.

3. Discretization errors. The multiphase pseudoisation technique is still developing and upscaling techniques are not sufficient to generate reliable results when dealing with multiphase displacement within coarse grids.

In order to limit the use up-scaling technique, a 'top-down' reservoir modelling scheme has been adopted in this research. The scheme's philosophy is to start the investigation with the simplest possible model (i.e. consider only large-scale heterogeneity) and add details later if required, based on uncertainty analysis. A top-down modelling scheme has the advantage of reducing research time because it obviates the need to study issues which are not critical (Williams et al. 2004).

2.6. Summary

From a combination of outcrop and subsurface data, and in the context of the South Caspian Basin geology, the Pereriv Suite reservoir of the ACG field was deposited by a fluvial-dominated delta system that is controlled by rapid lake-level changes. Fluvial and deltaic reservoirs have complex heterogeneities, such as channelised sandstones with variable connectivity and mudstone barriers of variable extent. The heterogeneities may have a great impact on reservoir performance. Therefore it is necessary to conduct an investigation of the impact of heterogeneities on the performance of the ACG reservoir.

There have been previous studies that have characterised geological heterogeneity in fluvial-deltaic reservoirs. However, the architecture of these reservoirs is different to that of the ACG field, which has a steep tectonic dip and two different recovery schemes. Different layers of the Azeri reservoir have high and low NTG values. Thus, geological heterogeneities observed in outcrop and sub-surface data will potentially have a large impact on the reservoir performance.

The approach taken in this research is to compare gas and water injection in models that contain heterogeneities at different length scales. Comparison of modelled reservoir performance for immiscible gas and water injection displacements will indicate which heterogeneities are important in the Azeri reservoir. To conduct this investigation a 'top-down' reservoir modelling scheme is applied. By using this 'top-down' approach, the investigation starts from studying the displacement behaviour in the simplest structure of the reservoir and progressively adding complexity and smaller scale features to the investigation. Moreover, in order to honour the reservoir geology and characterise the reservoir realistically, an object-base modelling scheme is applied. Because of the large number of geological features that are involved, it is not feasible to construct reservoir models based on all possible interpretations, therefore an experimental design method is applied in order to obtain efficiently filter out the most significant heterogeneities that influence displacement.

Chapter 3
Preliminary displacement study

3.1. Overview

Following the 'top-down' approach, this chapter starts by analyzing the displacement behaviour in Azeri from a point where all the reservoir properties are uniform. There are some classical analytical methods that allow the estimation of reservoir performance, assuming a simplified reservoir description. These methods provide references by which a reservoir engineer can understand reservoir behaviour based on the given fluid properties and operating conditions (e.g. well spacing or production rate).

Production rate is one of the items that a reservoir engineer can control in order to optimize the performance of a reservoir. The effects of the variation in production rate have been studied in the past (e.g. stability analysis; Dietz 1952 or coning effects; Urbanczky and Wattenbarger 1994). These studies suggested that reservoir performance can be influenced by the production rate. For example, high production rates can lead to the occurrence of coning, and recovery will be reduced because of the early water or gas breakthrough (Ekrann 1992). With mobility unstable displacement schemes, gravity tongue form during the displacement causing early breakthrough of the displacing phase at the production wells. Previous work (e.g. Dietz 1952; Kleppe 2004) demonstrated that such phenomena can be avoided or minimized by gravity force in a segregated displacement. Dietz (1952) suggested that

when a suitable production rate applies, the gravity segregated front moves through the reservoir without changing its shape. That means a gravity 'stable' displacement occurs. The maximum production rate for a gravity stable displacement in a homogeneous reservoir is the so called Dietz's critical rate.

This chapter started by introducing the fluid and rock properties of the Azeri Field. Secondly, both Buckley-Leverett flow and segregated flow models were used to estimate reservoir performance (cumulative oil recovery and breakthrough time). A Dietz stability analysis was conducted to determine the displacement stability for the Azeri Field oil recovery process, assuming segregated flow. Finally reservoir performances under segregated flow models were cross compared.

3.2. Aims

1. Obtain a preliminary understanding of the reservoir performance.
2. Identify the conditions for a stable gas-oil displacement in the north flank of central Azeri and water-oil displacement in the south flank of Azeri.

3.3. Introduction of reservoir properties

The Azeri Field has different dip angles in its north and south flanks and is being developed by down-dip water injection in the south flank, and up-dip immiscible gas injection in the central north flank (Figure 1.1). In the south flank, the dip is between c.5°-30° depending upon location whereas in the north flank the dip is between c.25°-45° depending upon location. As described in Chapter 2, the reservoir interval

was known as the Productive Series. Within the Productive Series. the Pereriv Suite was identified as the major lithostratigraphic section that contains hydrocarbon bearing sandstone. In this chapter, the displacement study was focused on the inter-well region within the Azeri Field (Figure 3.1). Therefore the model width and length was correlated with the well spacing in the north and south flank. For the analytical calculation, the length of each north flank model was 1900m and for each of the south flank models it was 478m (Figure 1.1B). The width of each model was the same as the production well spacing, which was 750m. The Pereriv Suite was sub-divided into five layers (Pereriv A-E) by the vertical variation in NTG and by the presence of potentially extensive shales between each interval (Reynolds et al. 2003; Reynolds and Riley 2003). However, it was not clear whether these shales completely isolate each layer. It was possible to study displacement within the Pereriv Suite through two different approaches:

1. Each Pereriv Suite layer A-E was isolated by shale. Therefore the displacement was examined separately in each layer.
2. The Pereriv Suite acted as a single reservoir with averaged properties.

The thickness of the model therefore depended on whether the Pereriv Suite layers were studied together or in isolation. The dip angle of the north and south flank were assumed to be 35^{o} and 21^{o} respectively. Figure 3.1 summarises the geometry of the analytical model.

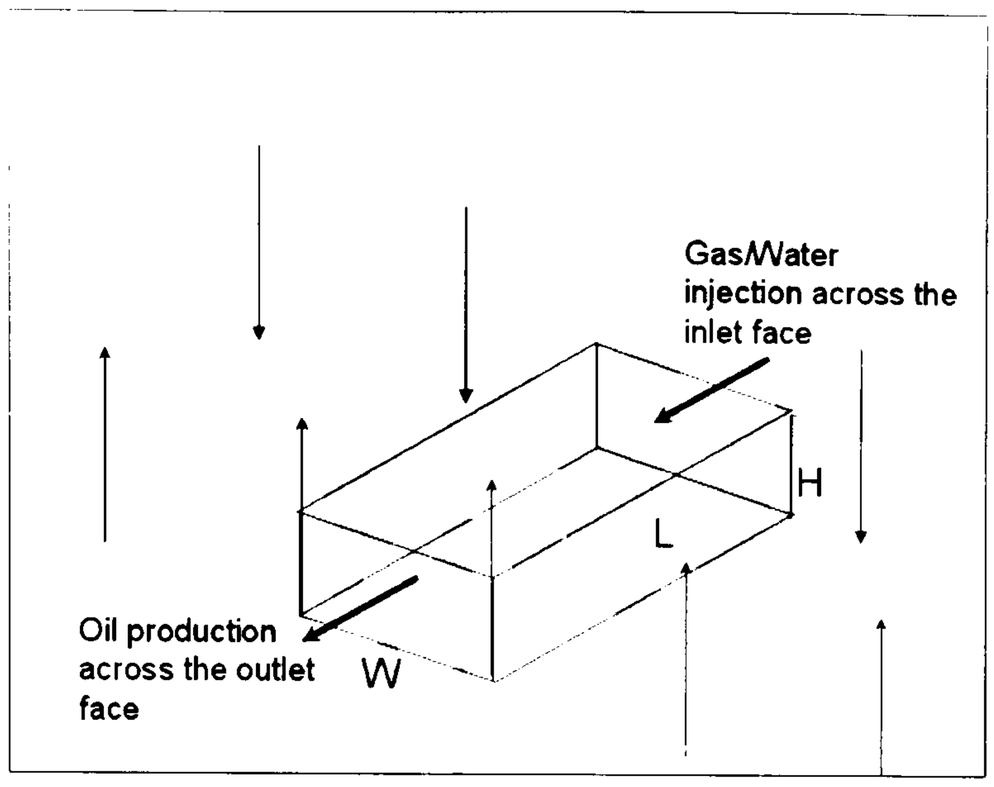


Figure 3.1. Geometry of the sector reservoir model for the analytical study. The distance between production wells was chosen to be the width (W) for the analytical study which is 750m. The length (L) is 1900m for the north flank models and 478m for the south flank models. The thickness (H) of the model depends on which layer of the Pereriv Suite is being studied.

Fluid properties			
	Oil	Water	Gas
Density (kgm^{-3})	738.1	1038	88
Viscosity ($kgm^{-1}s$)	$6.3x10^{-4}$	$45x10^{-4}$	$3.0x10^{-5}$

Reservoir properties						
	Pereriv A	Pereriv B	Pereriv C	Pereriv D	Pereriv E	Total Pereriv Suite
Net-to-Gross (NTG)	50%	92%	45%	86%	50%	73%
Sandbody porosity (ϕ)	20%	20%	20%	20%	20%	20%
Mean porosity of layer (ϕ)	10%	18%	9%	17%	10%	15%
Sandbody permeability; k (mD)	178	178	178	178	178	178
Mean permeability of layer; k (mD)	89	163.76	80.1	153.08	89	129.94
Cross-sectional area (m^2)	$6.4x10^3$	$27.0x10^3$	$19.3x10^3$	$20.8x10^3$	$3.2x10^3$	$76.5x10^3$

Table 3.1. Table of critical reservoir properties obtained from Azeri for analytical calculation.

In order to simplify the problem a single value of sandbody porosity and permeability was used to represent the general Azeri Field rock properties. Therefore the mean value of porosity and permeability of each Pereriv Suite layer was correlated with their NTG. The NTG for the whole Pereriv Suite was obtained by using the arithmetic average according to the NTG and volume of each sub-Pereriv layer. The general rock and fluid properties of ACG are summarised in Table 3.1. Pereriv B and D were considered as the major oil bearing intervals, because of the

high quality of sand and high NTG. However, although Pereriv C had a lower NTG, it could also be considered as part of the reservoir. The relative permeability curves were averaged from rock samples from various locations within the field. Therefore, these relative permeability curves represent the general character of the Azeri Field. The average gas-oil and water-oil relative permeability curves against water/gas saturation data are shown in Figure 3.2.

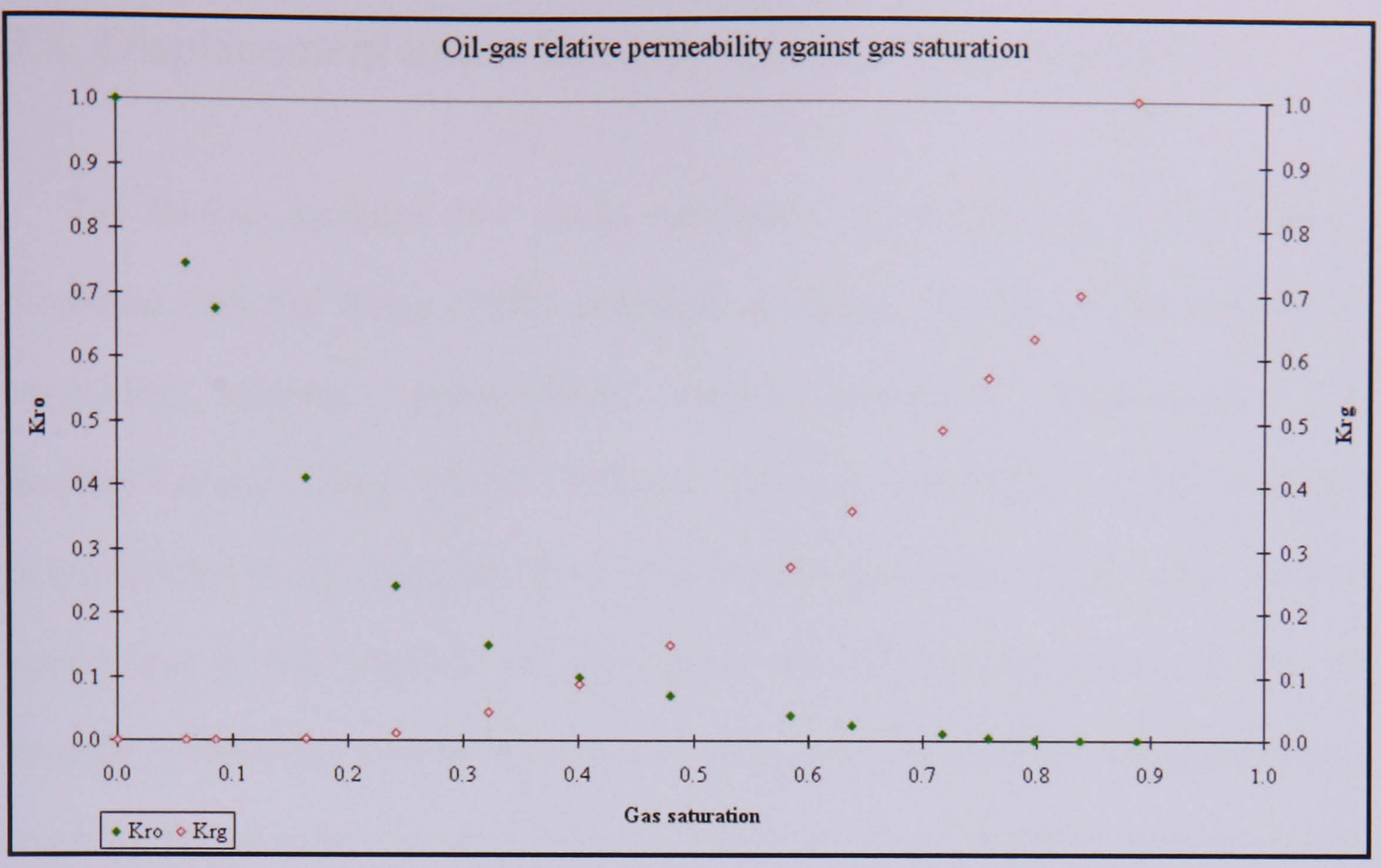


Figure 3.2A

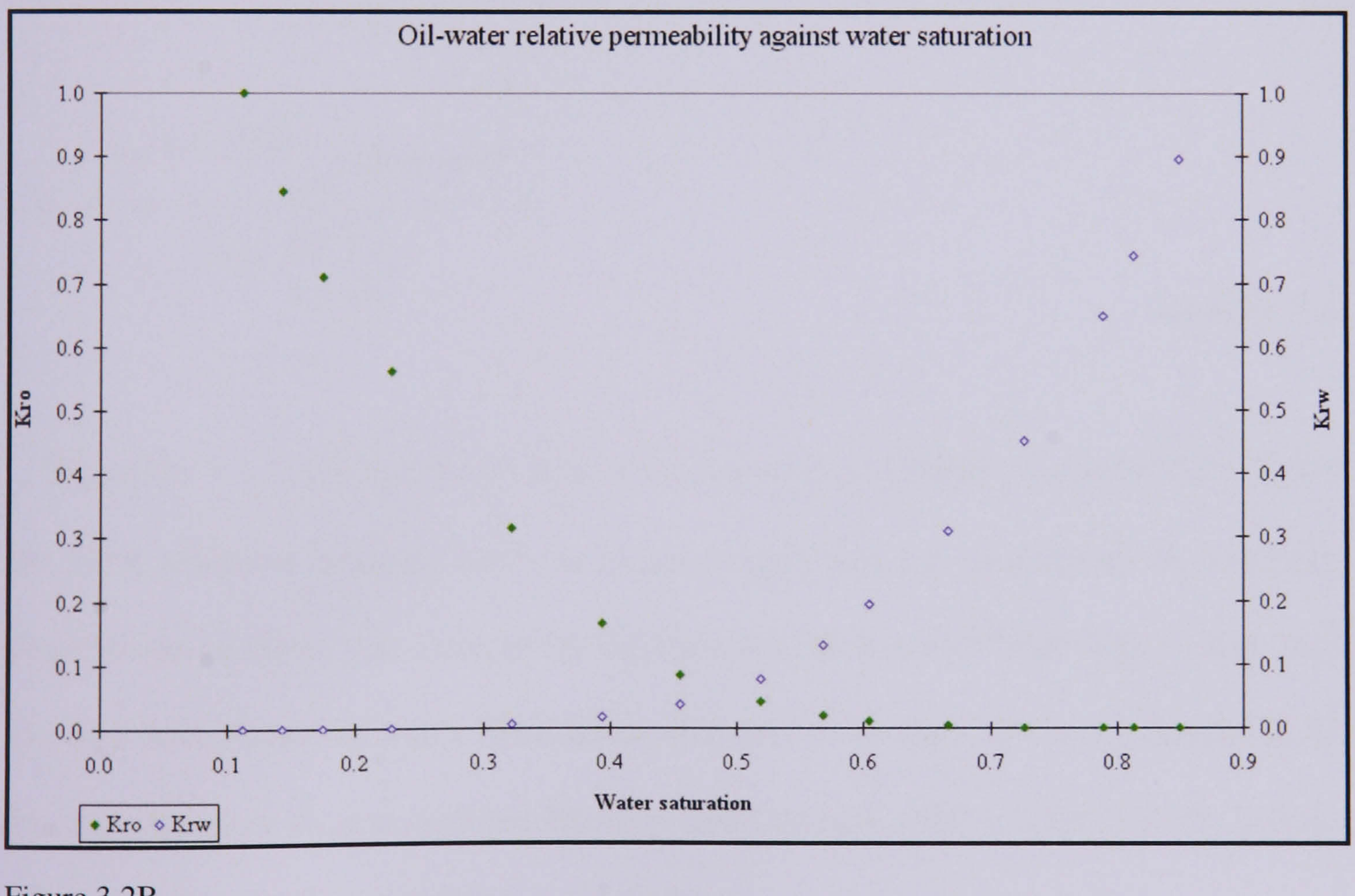


Figure 3.2B

Figure 3.2. Gas-oil **(A, top)** and water-oil **(B, bottom)** relative permeability curves in the Pereriv Suite reservoir of the Azeri Field.

3.4. Displacement under Buckley-Leverett flow conditions

The Buckley-Leverett flow model developed by Buckley and Leverett (1942) combined with the Welge (1952) graphical technique provides a rapid method for estimating reservoir performance; during immiscible displacement. The Buckley-Leverett flow model assumes constant saturation in the direction perpendicular to the principle flow. Buckley-Leverett flow occurs when vertical equilibrium is not achieved and the effects of capillary and gravity forces are negligible. Buckley-Leverett flow can also occur when the capillary transition zone is much thicker than the reservoir thickness and vertical equilibrium is achieved (Dake 1978).

$$f_i = \frac{1 + \left. k_i k_{ro} W H_i \right/ q_i \, (\Delta \rho g \sin\theta)}{(1 + \frac{\mu_f}{k_{rf}} \frac{k_{ro}}{\mu_o})} \qquad \text{equation 3.A}$$

Equation 3.A is the fractional flow equation used in Buckley-Leverett flow model for flow behavior analysis such as breakthrough time or cumulative oil recovery. Gravity can be taken into account for the fractional flow calculation. This is important because both flanks of Azeri Field have relatively steep dips. For more details of the Buckley-Leverett flow model see Buckley and Leverett (1942), Dake (1978), Schulte et al. (1990) and Kleppe (2004).

3.5. Displacement under segregated flow conditions

Another analytical method assumes that displacement occurs under segregated flow conditions. The Dietz (1952) theory assumes that a sharp interface exists between the displacing and displaced fluids, with no capillary transition zone and no mobile oil present in the gas invaded zone. The segregated flow model assumes that vertical equilibrium is achieved in the displacement and because the capillary force is neglected therefore only gravity is responsible for the fluid distribution in the vertical direction (Dake 1978).

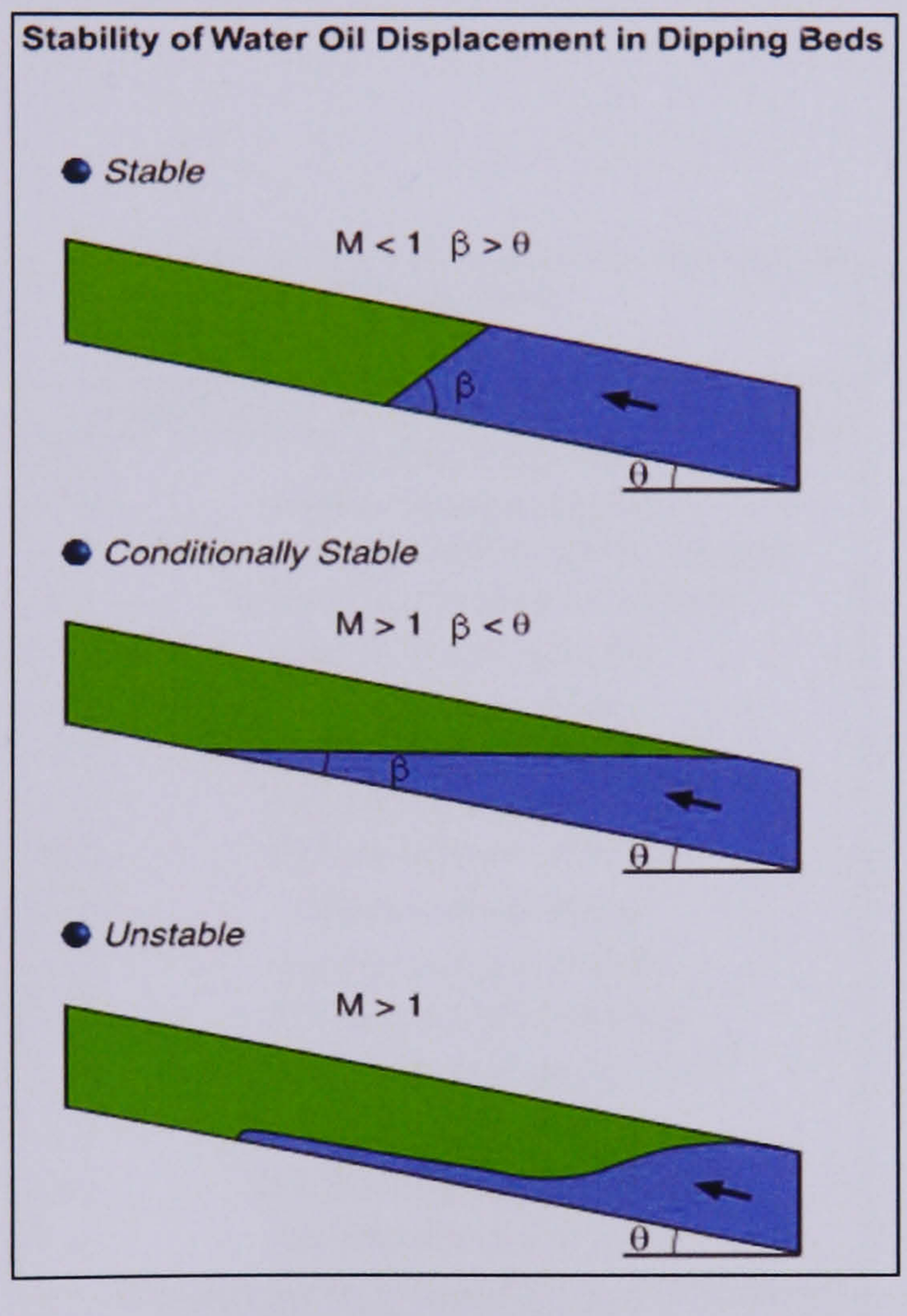


Figure 3.3. Different stages of a displacement's stability under segregated flow conditions.

Segregated flow can be regarded as gravity stable or unstable in a dipping reservoir, depending on the conditions of the displacement mechanism. Figure 3.3 shows the different gravitational stability conditions for segregated flow. The displacement gravitational stability condition depends on the balance between gravity and viscous

force. For the gravity unstable condition the injectant (gas/water) will over-ride (gas) or under-ride (water) the oil zone towards the producer, if its mobility is higher than the mobility of oil. However, if a displacement is gravity stable, such over-riding (gas) or under-riding (water) effect will be prohibited by gravity force. The net result is that the injectant and oil will form an interface with a constant length, thus a stable displacement will occur.

The 'end-point' mobility ratio M and 'dimensionless gravity number' G are used to indicate the displacement stability. There are 3 cases which indicate whether the displacement is stable.

Nomenclature	
L : length; F : force; t : time; m : mass; [=] means 'has units of'	
M	End-point mobility ratio
G	Dimensionless gravity number
θ	Reservoir dipping angle [=] radians or degrees
β	Interface angle [=] radians or degrees
k	Sandbody permeability [=] L^2
A	Cross-sectional area [=] L^2
H	Effective flow path thickness [=] L
L	Effective flow path length [=] L
W	Effective flow path width [=] L
ρ_j	Density of phase j [=] m/L^3
μ_j	Viscosity of phase j [=] $(F\text{-}t/L^2)$
ϕ	Sandbody porosity [=] fraction
λ_{rj}	Relative mobility of phase j [=] $(F\text{-}t/L^2)^{-1}$
q	Volumetric flow rate [=] L^3/t
g	Gravitational acceleration [=] L/t^2
u_T	Displacement velocity [=] L/t
kr'_j	End-point relative permeability of phase j [=] fraction
Subscripts	
f	Displacing fluid phase (e.g. gas or water)
o	Oil phase
g	Gas phase
w	Water phase
or	Residual oil
wc	Connate water

Table 3.2. Table of nomenclature of the key parameters in the stability calculation.

$M<1$; $\beta<\theta$

$M=1$; $\beta=\theta$

M>1 and G>M-1 and $\beta>\theta$

$$M = \frac{k'_{rf} / \mu_f}{k'_{ro} / \mu_o}$$

equation 3.B

$$G = \frac{kk'_{rf}\, A\Delta\rho g \sin\theta}{q\mu_f}$$

equation 3.C

Due to the difference in fluid density, gravity can maintain a flat interface between the two fluids, if the rate is relatively low. Such a condition is recognised as gravity stable ($G>M$-1, $M<1$). However, such a condition can be changed for example, when a higher displacement rate is applied and the fluid interface angle (β) is reduced. When the fluid contact angle becomes parallel to the reservoir dip (β becomes 0), the displacement is described as gravity unstable. Equation 3.C is the Dietz's critical rate, which is the maximum rate that keeps the displacement stabilised by the force of gravity. If the production rate exceeds the critical rate, a gas/water tongue will penetrate into the oil bearing zone, and lead to early breakthrough, which is also understood as a 'gravity unstable' displacement.

$$q_{crit} = \frac{kk'_{rf}\, A\Delta\rho g \sin\theta}{\mu_f (M-1)}$$

equation 3.D

3.6. Results

3.6.1. Buckley-Leverett flow analysis

Displacement behaviour of gas-oil and water-oil was first estimated using the modified Buckley-Leverett method which includes gravity. The total production rate of both north and south flank model was c.9% STOIIP of the whole Pereriv Suite per year, which was approximately the target production rate for the Azeri Field. For each sub-Pereriv Suite layer, their offtake rate was a fraction of the total production rate which was in proportion to their mean permeability and thickness (kH).

Figure 3.4 shows the fractional flow curve for both the gas-oil displacement and water-oil displacement in the Azeri Field. Since the offtake rate was proportional to the kH of each layer, a single fractional flow curve could therefore be used to conduct the Buckley-Leverett flow analysis for all the ensembles. The supplementary notes in Appendix 1 shows the relationship between the fractional flow curves and the mean permeability related production rate in details.

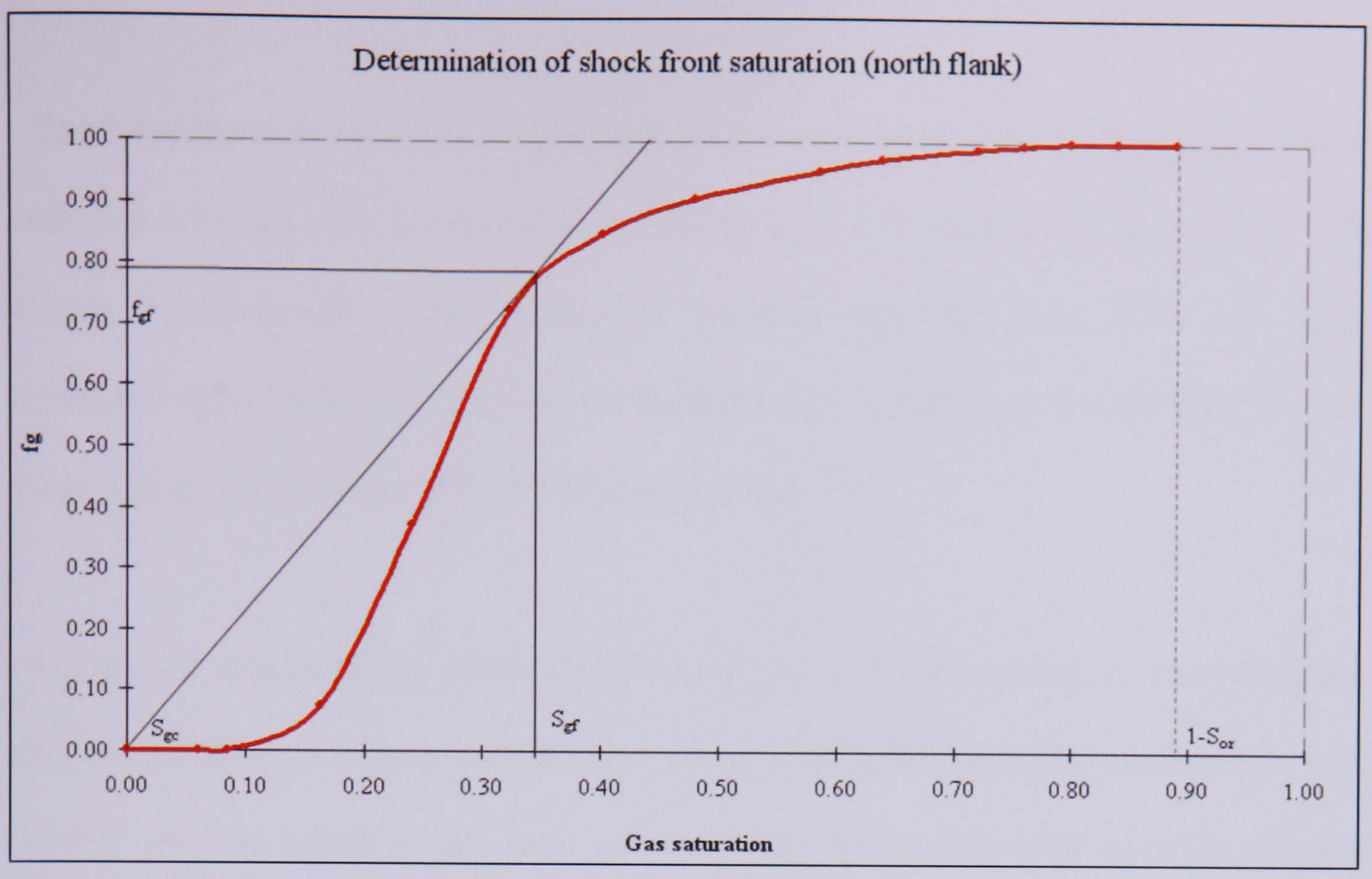


Figure 3.4A

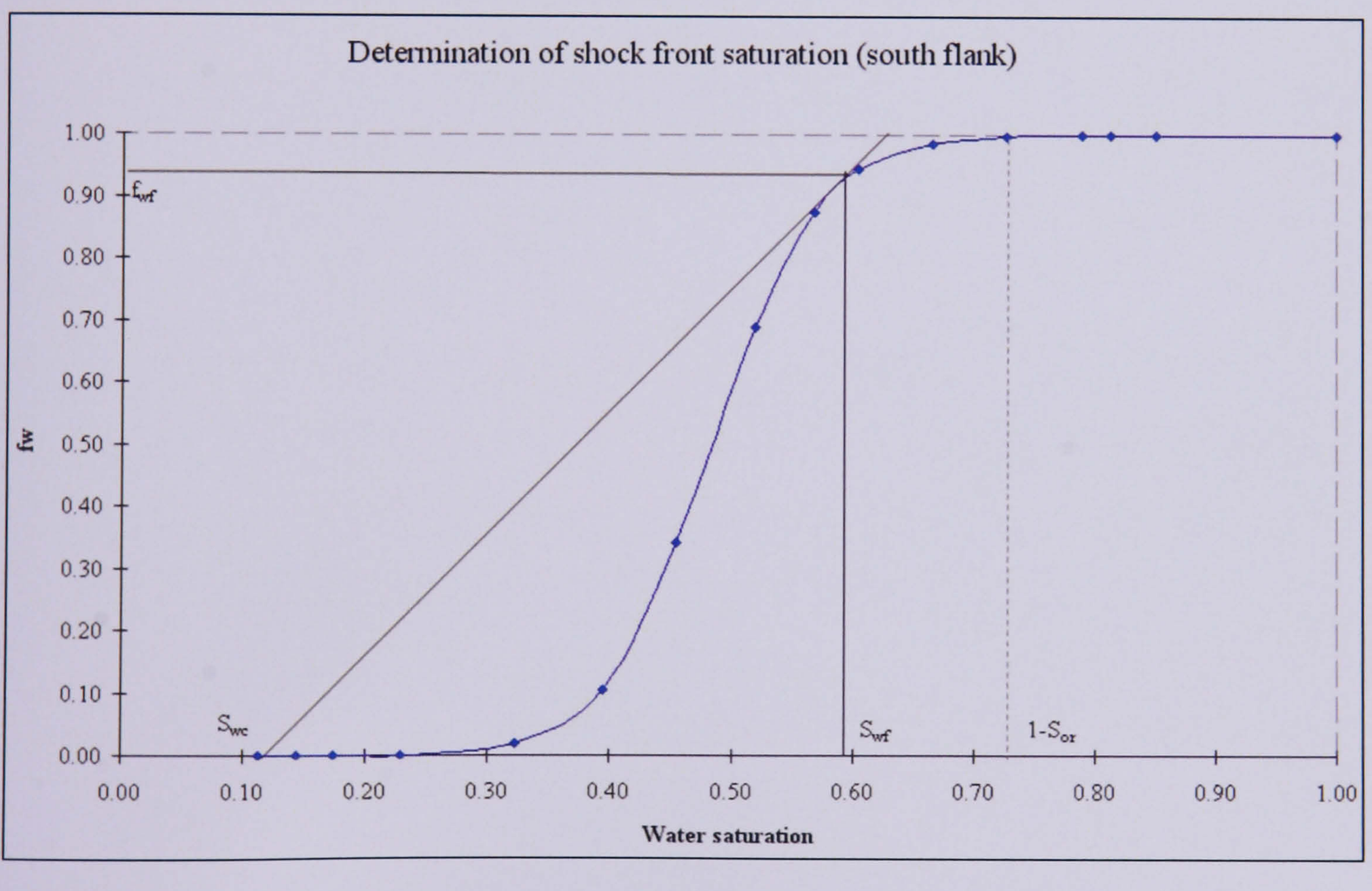


Figure 3.4B

Figure 3.4. Fractional flow curves of gas **(A, top)** and water **(B, bottom)**. Determination of gas **(A, top)** and water **(B, bottom)** saturation at the shock front by applying Welge's graphical technique and assuming oil displacement from a system with uniform initial connate water saturation (S_{wc}: 0.112) and zero initial gas saturation (S_{gc}: 0). A tangent is drawn to the fractional flow curve from the initial gas/water saturation. The tangent point indicates the saturation of the shock front. The intercept of the tangent at f=1 indicates the average saturation behind the front at breakthrough time at the production well.

The breakthrough time and cumulative oil recovery profile for both gas and water injection schemes were estimated using the Buckley-Leverett flow model (Figure 3.5). Under the water-oil displacement, the breakthrough time was 6.54 year. The estimated cumulative oil recovery at breakthrough (CORB) at south flank Pereriv Suite was estimated to be 0.52 PV (Figure 3.5 and 3.6).

On gas-oil displacement, under the Buckley-Leverett flow model, it was estimated that the cumulative oil recovery at breakthrough in all the north flank ensembles was 0.44PV and the breakthrough time was estimated 5.52 years after injection (Figure 3.5).

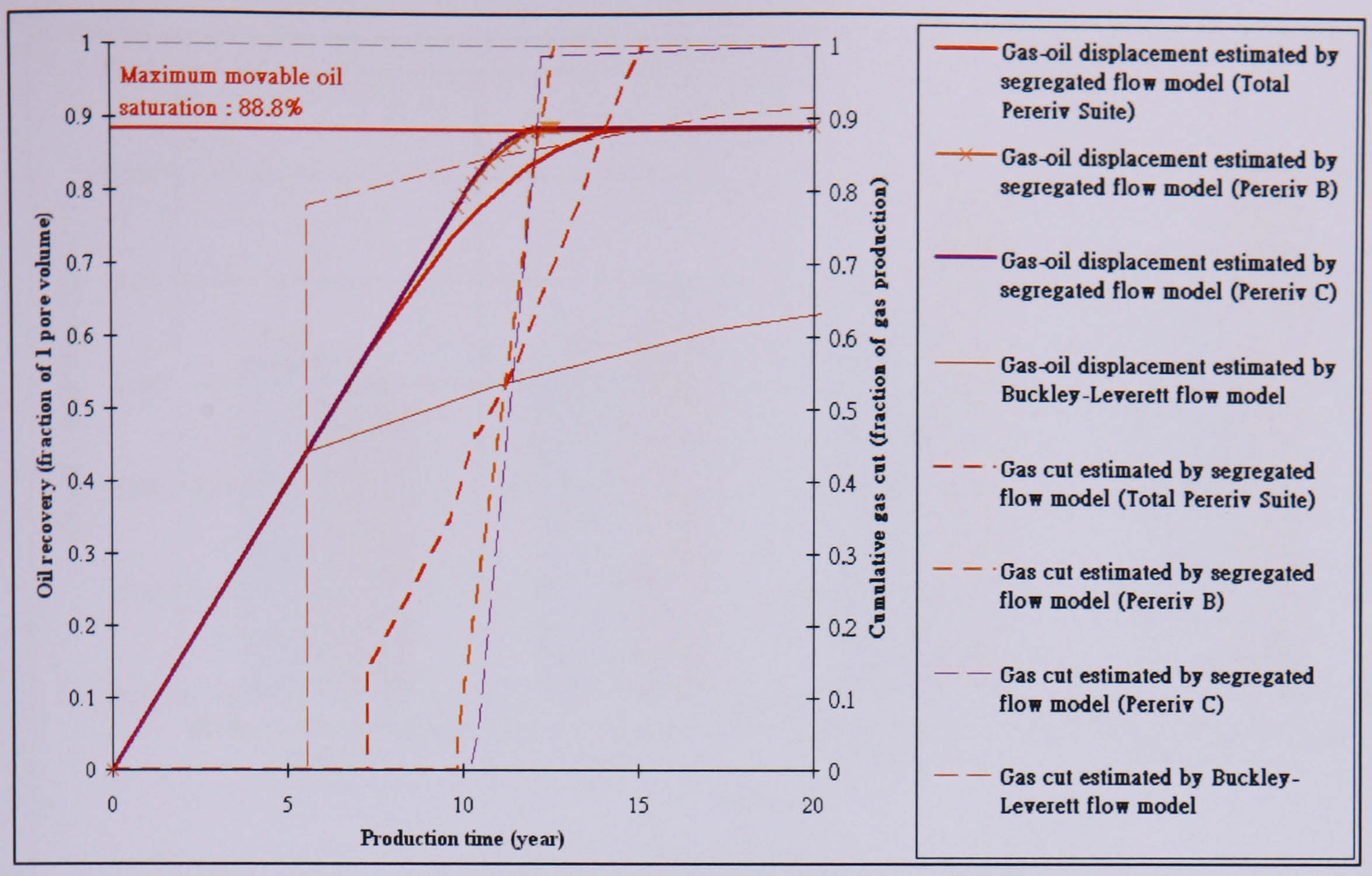


Figure 3.5A

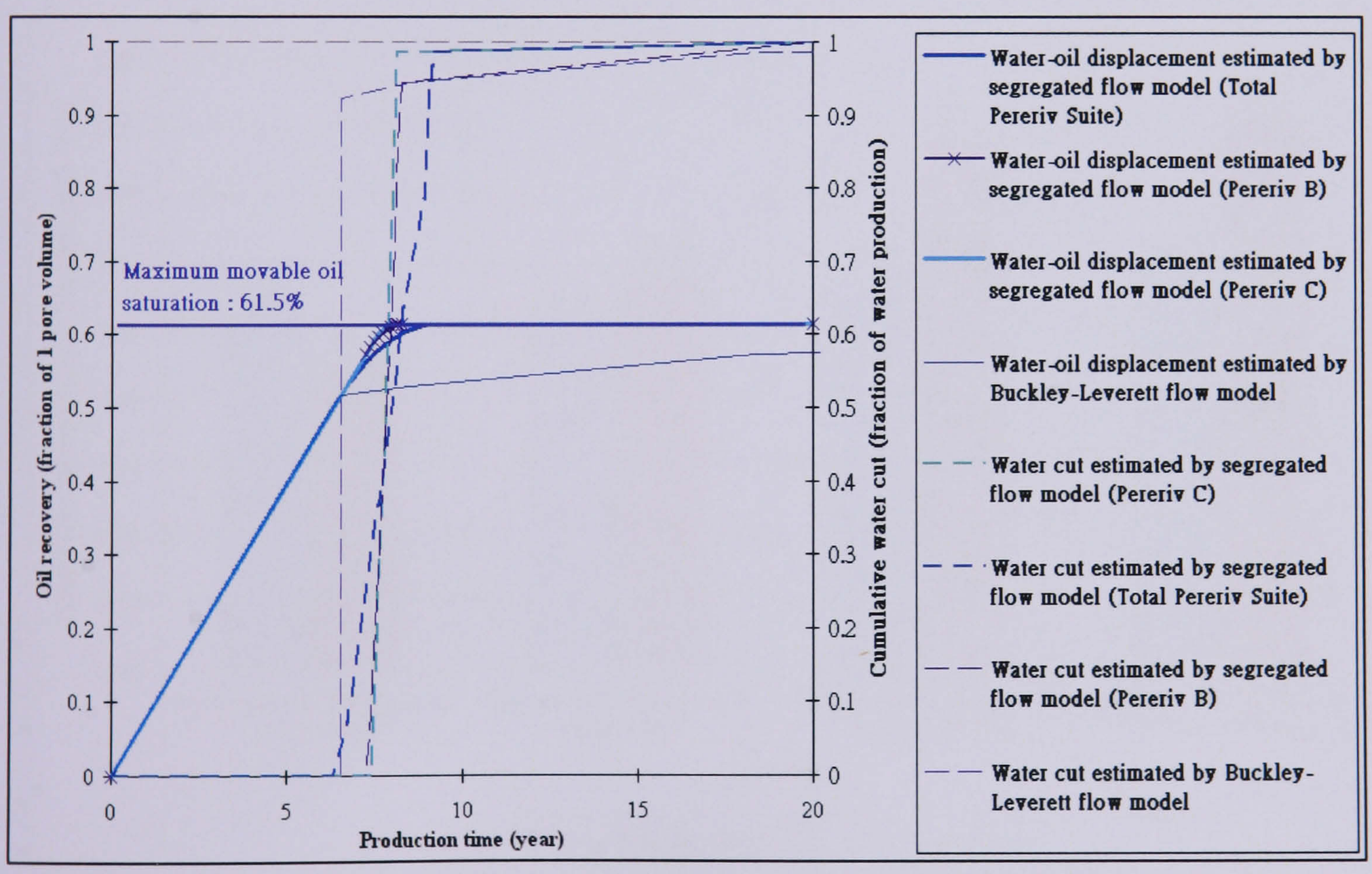


Figure 3.5B

Figure 3.5. The estimation of the dimensionless cumulative oil recovery profile (pore volume) and gas cut (A, top) and water cut (B, bottom) profile for the ensembles from the north and south flank of the Azeri Field.

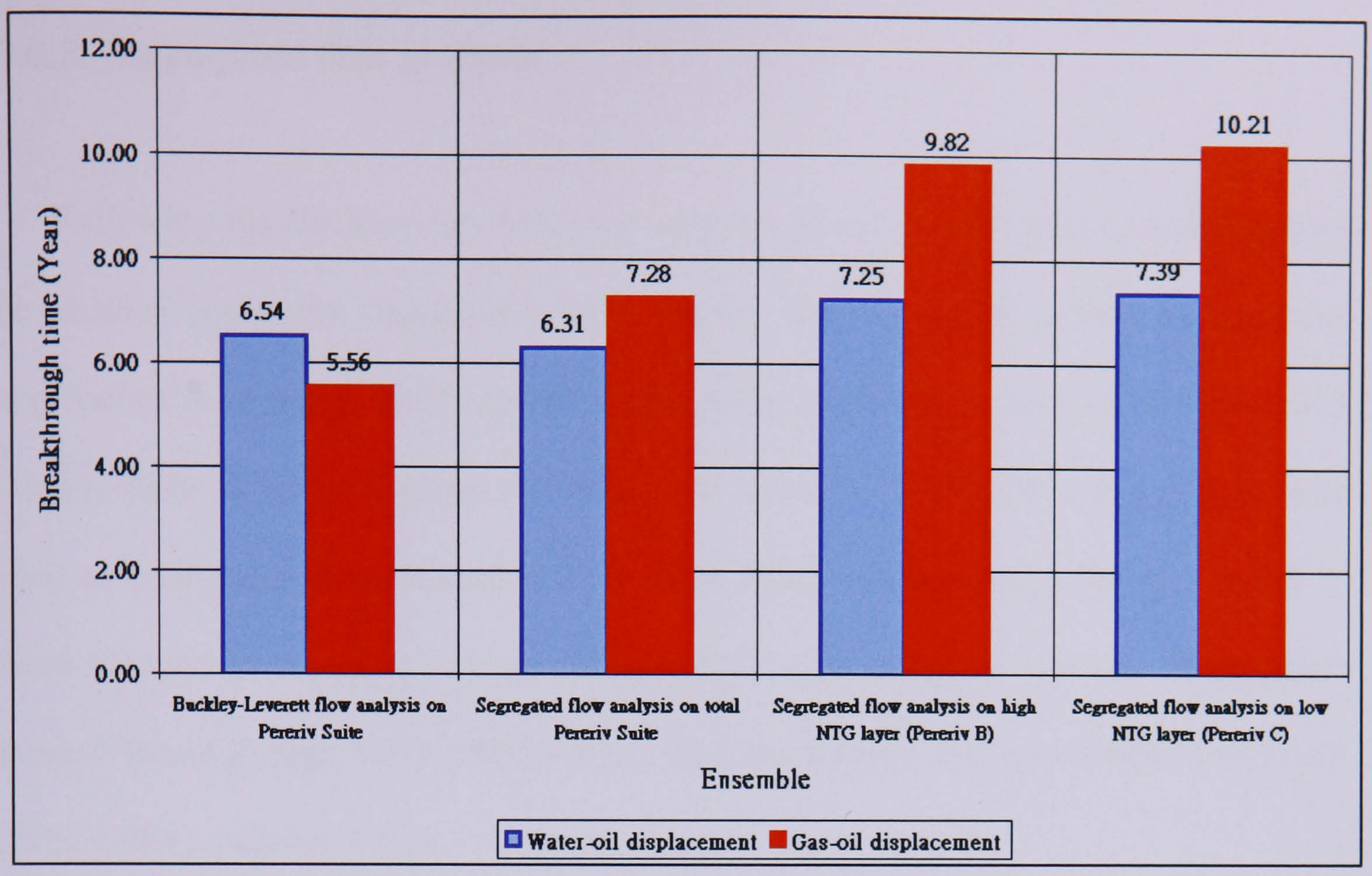


Figure 3.6A

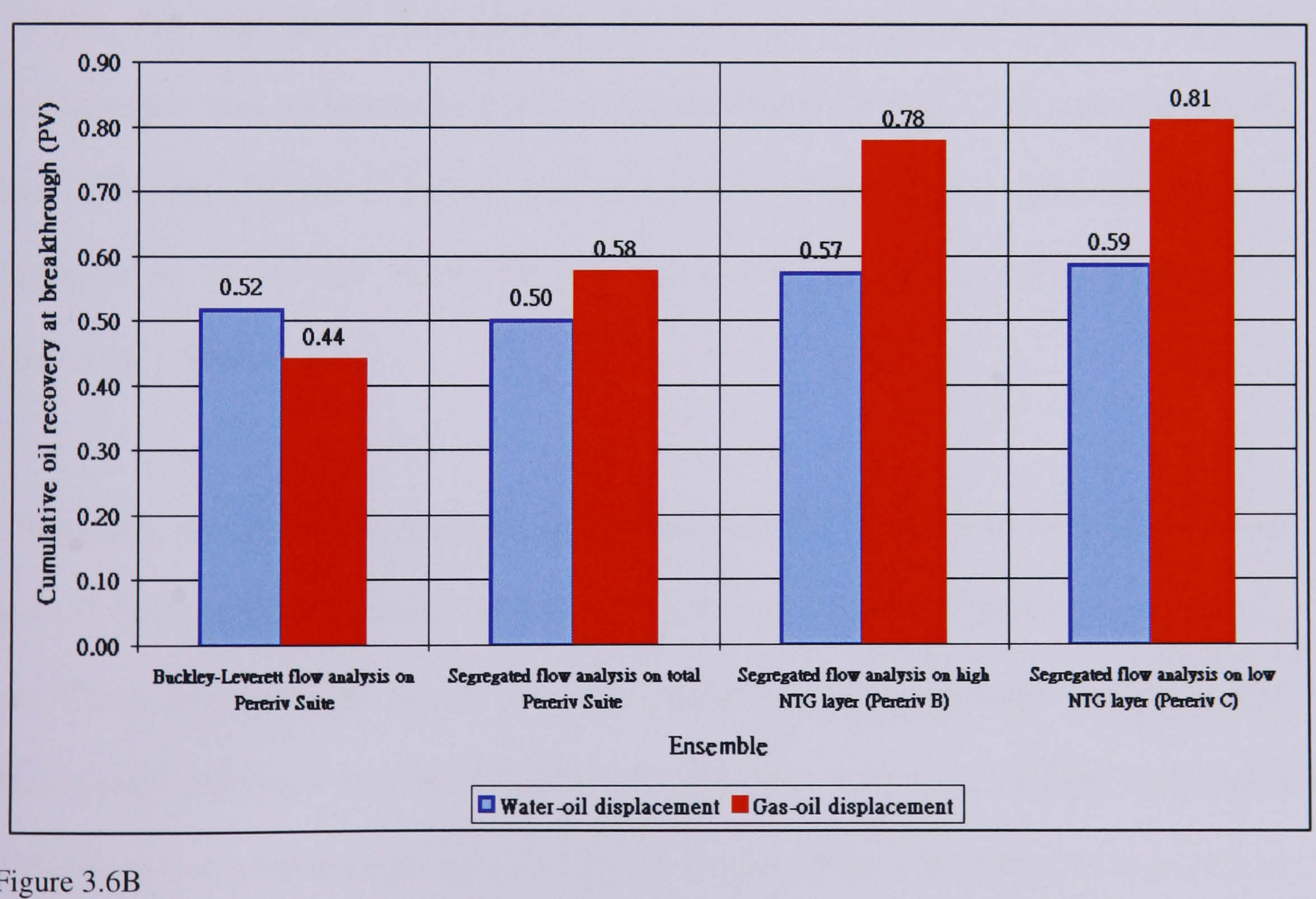


Figure 3.6B

Figure 3.6. Summary of the breakthrough time (A, top) and cumulative oil recovery at breakthrough (B, bottom) in each ensemble under gas and water injection. The results are estimated by Buckley-Leverett flow and segregated flow model.

3.6.2. Segregated flow analysis

Following the Buckley-Leverett flow analysis, the reservoir performance can also be studied using the segregated flow model. As mentioned earlier, one of the approaches to studying displacement within Azeri Field was to assume that the entire Pereriv Suite acted as a single reservoir (see Table 3.1). The second approach was used to study each sub-divided Pereriv Suite layer independently. Pereriv B and C were selected to represent a high and low NTG interval in the Pereriv Suite. Both Pereriv B and D high NTG (NTG>70%), whereas Pereriv A,C and E have low NTG (NTG<70%) (section 2.2.2).

Under the segregated flow model, the time to breakthrough under water-oil displacement was estimated as 6.31 year (Total Pereriv Suite), 7.25 year (Pereriv B) and 7.39 year (Pereriv C layer). The cumulative oil recovery at breakthrough was estimated to be 0.5 PV (Total Pereriv Suite), 0.57 PV (Pereriv B) and 0.59 PV (Pereriv C) (Figure 3.6).

Similarly, the breakthrough time and cumulative oil recovery at breakthrough for gas-oil displacement was also estimated. Under gas-oil displacement by considering the whole Pereriv Suite as one reservoir, displacement mechanism, the segregated flow model predicted that the breakthrough time was 7.28 years and the cumulative oil recovery at breakthrough was 0.58 PV. In Pereriv B the cumulative oil recovery at breakthrough was 0.78 PV after 9.82 years of injection. In Pereriv C the breakthrough time was 10.21 years and the cumulative oil recovery at breakthrough was 0.81 PV. The results of both breakthrough time and cumulative oil recovery at breakthrough under segregated flow model are summarised in Figure 3.6.

3.6.3. Stability analysis

The stability analysis indicated that the end-point mobility (M) of the water-oil displacement was 0.63 therefore it was mobility stable (M<1) regardless of production rate. On the other hand, the gas-oil displacement was mobility unstable because of the large difference in fluid viscosity. For the gas-oil displacement, the end-point mobility ratio (M) was 21 which was mobility unstable, however the displacement could be stabilised by gravity. As mentioned in section 3.5, the gas-oil displacement stability, therefore, depends on the production rate and the reservoir properties. Table 3.3 shows Dietz's critical rate for each model. The range of possible values of M and G are shown in Table 3.4. Since the offtake rate was proportional to the kH of each layer, the dimensionless gravity number G was the same for each ensemble. The detailed demonstration of the relationship between the dimensionless gravity number G and the mean permeability related production rate is shown on the supplementary note in Appendix 1.

	All Pereriv	Pereriv A	Pereriv B	Pereriv C	Pereriv D	Pereriv E
Production rate per well (mrbd)						
Proportional to kH of each layer	29.19	1.80	12.88	4.50	9.18	0.83
Critical rate (mrbd)						
Assuming north flank dip angle is 25°	24.15	1.49	10.65	3.72	7.59	0.69
Assuming north flank dip angle is 35°	32.77	2.02	14.46	5.05	10.30	0.94
Assuming north flank dip angle is 45°	40.40	2.49	17.83	6.23	12.70	1.15

Table 3.3. Critical well rates.

	Pereriv Suite
North flank (gas injection)	M=21
Assuming north flank dip angle is 25°	G=16.5
Assuming north flank dip angle is 35°	G=22.5
Assuming north flank dip angle is 45°	G=27.7
South flank (water injection)	M=0.63

Table 3.4. End point mobility ratio and dimensionless gravity number.

The gas-oil displacement stability was sensitive to the reservoir properties (equation 3C). The results shown in Figure 3.5 and 3.6 were obtained under the assumption that the north flank dip angle was 35°, for which the current production rate was equivalent to c.89% of the Dietz's critical rate. The estimated stability condition could be changed by variations in the oil production rate. Moreover, updating reservoir properties would also affect the stability estimation. Therefore the variation in displacement stability conditions was also studied. Applying the same production rate to models with different dip angle was equivalent to testing the reservoir performance with production rate grater or less than the Dietz's critical rate.

The reservoir performance with these different dips is summarised in Figure 3.7 and 3.8. When the north flank dip angle was assumed to be 45° (equivalent to 72% of Dietz's critical rate) the time of gas breakthrough for the whole Pereriv Suite was 10.13 years and yielded 0.80 PV at breakthrough. On the other hand, if the dip angle

was assumed to be 25° the same offtake rate was equivalent to 121% of Dietz's critical rate, the estimated breakthrough time was reduced to 2.52 year and the CORB was yielded 0.20 PV.

All the results are summarised in Figure 3.6 and Figure 3.8 in order to compare: 1.) different assumptions on reservoir layering; 2.) different flow models; 3.) different displacement mechanisms and 4.) different stability conditions.

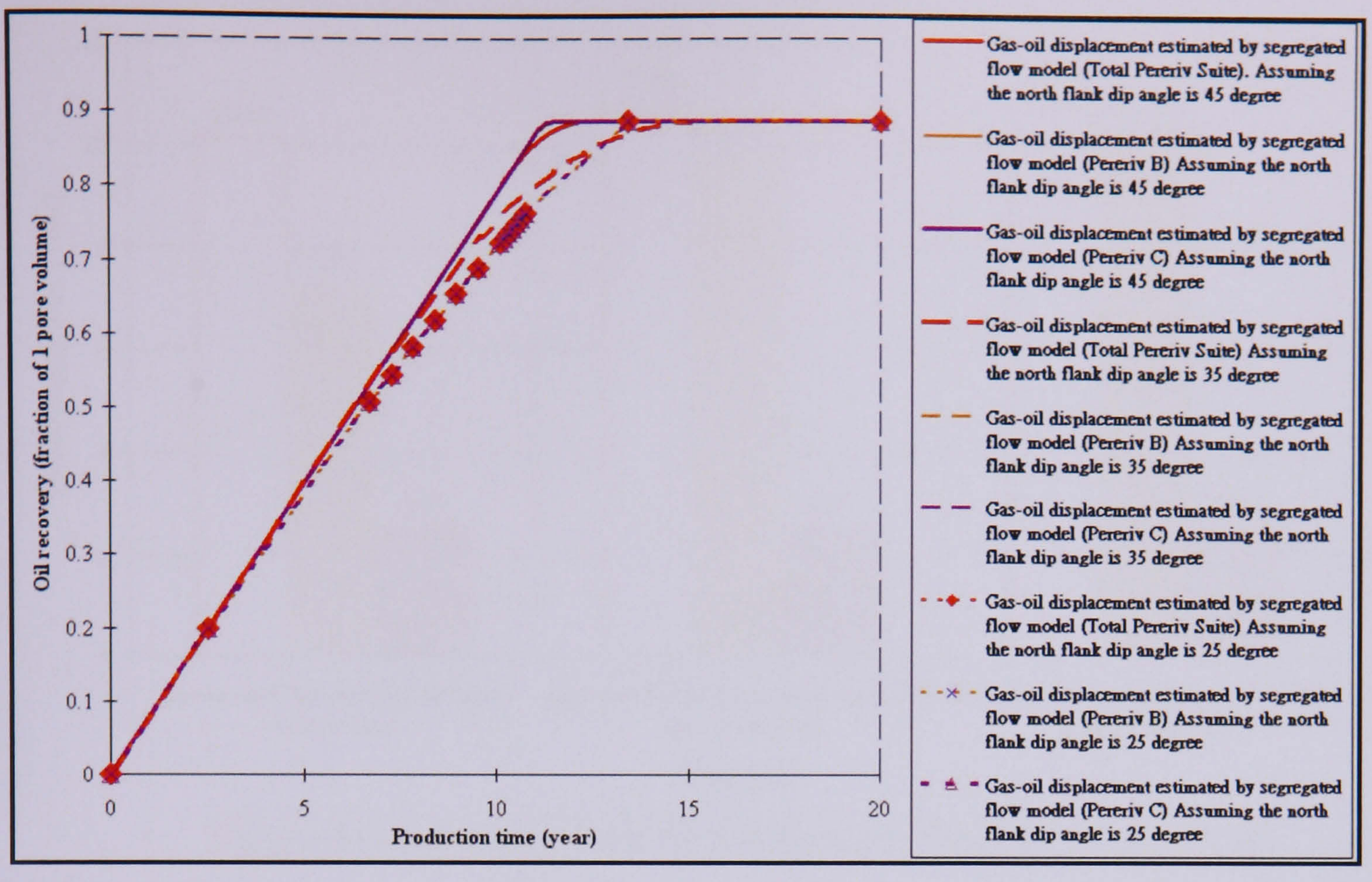


Figure 3.7A

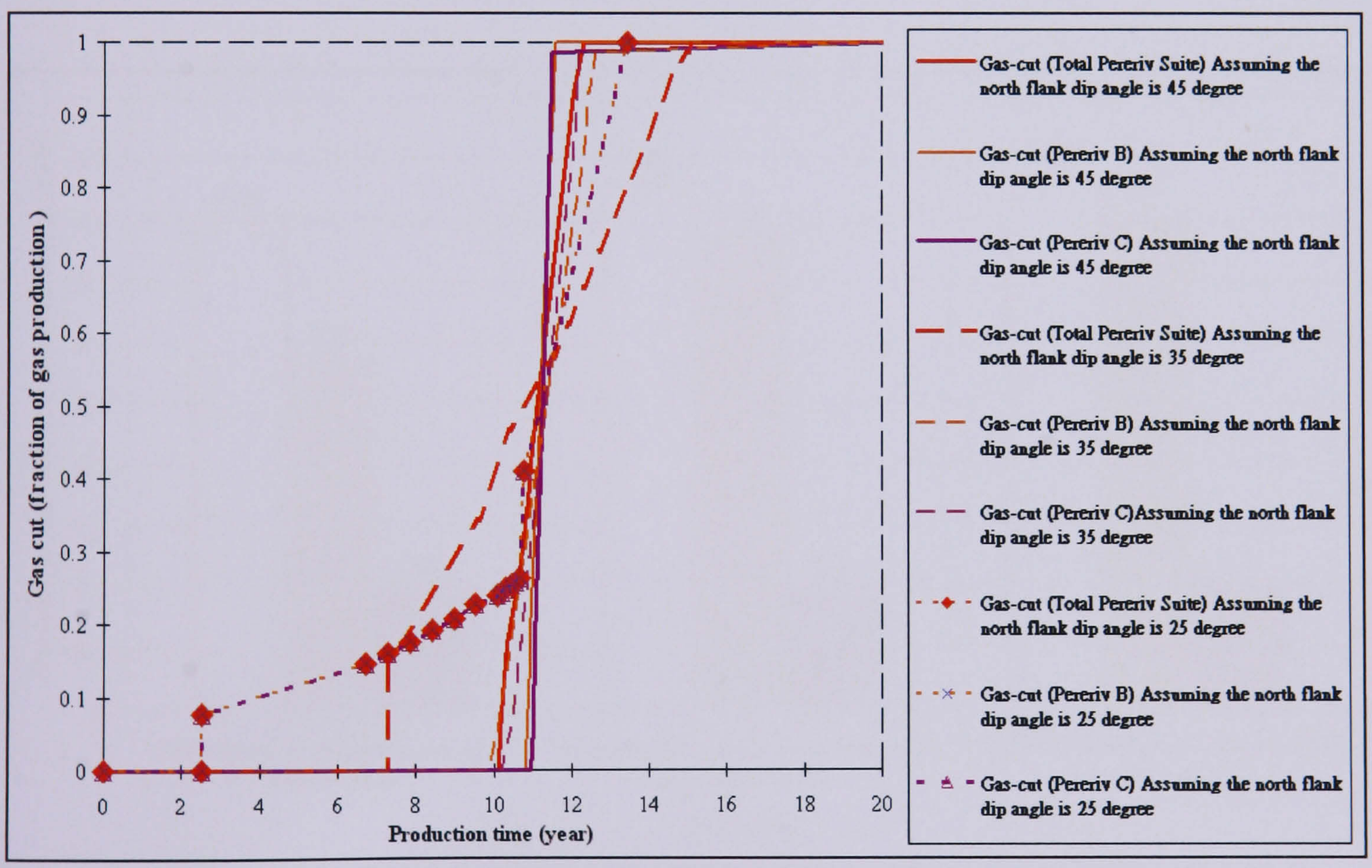


Figure 3.7B

Figure 3.7. The estimation of the dimensionless cumulative oil recovery profile (pore volume) **(A, top)** and gas cut **(B, bottom)** profile for the ensembles under different stability assumptions. The figures covered the case when the north flank has different dip angles that equivalent to apply a range of different Dietz's critical rate for the displacement. For the range of dip angles from 45°, 35° to 25° the current the production rate is equivalent to c. 72%, 89% and 121% Dietz's critical rate.

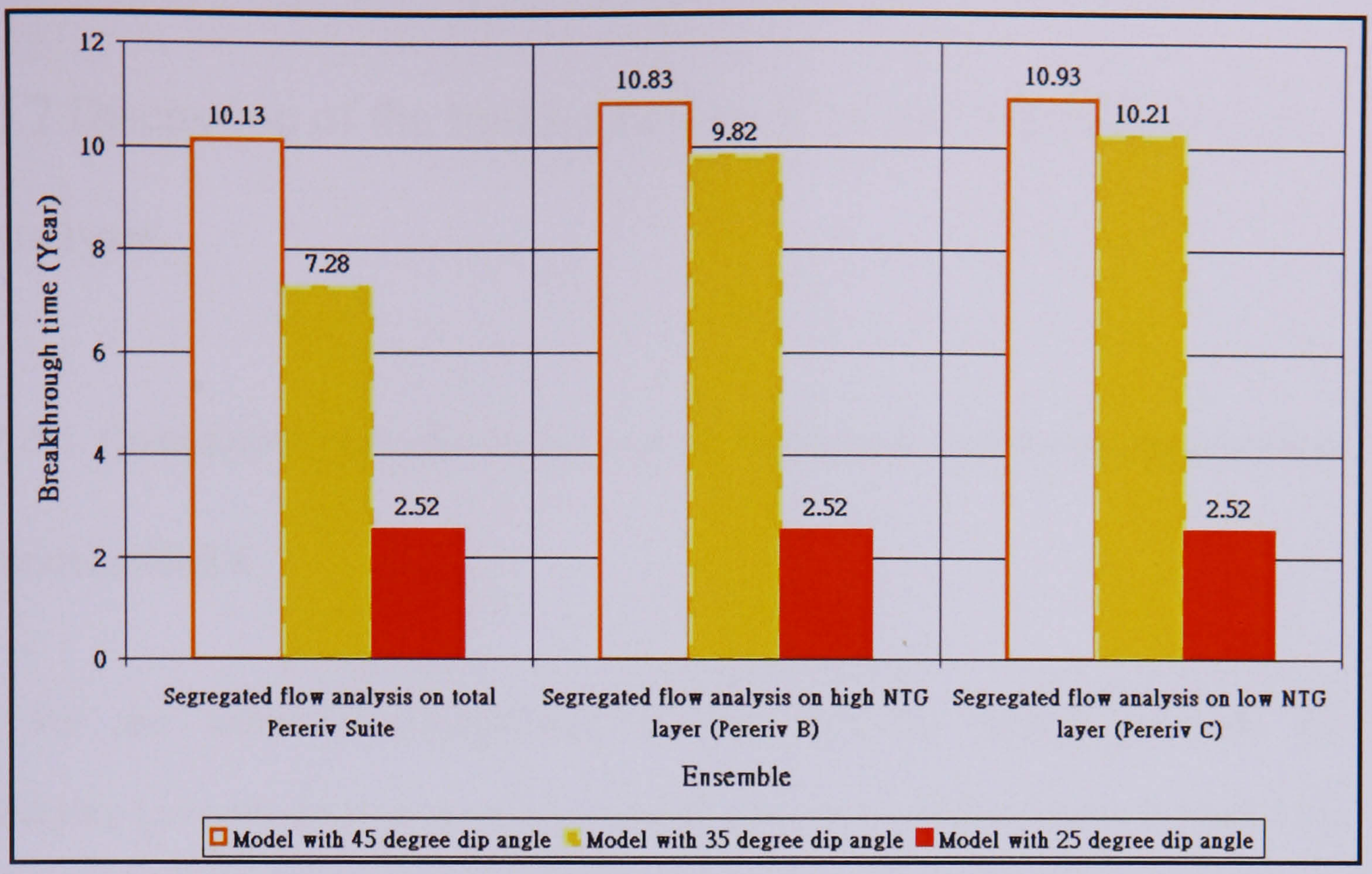


Figure 3.8A

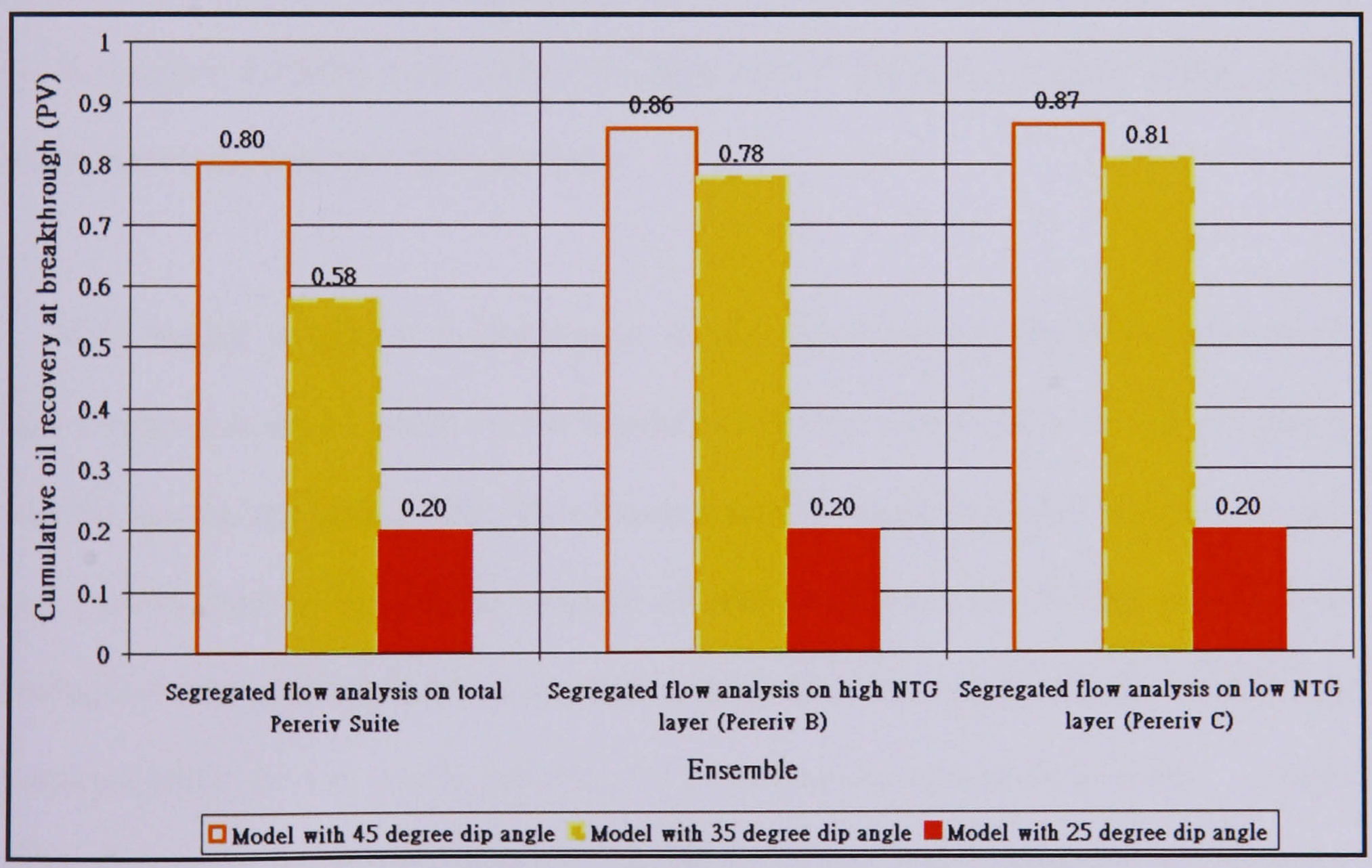


Figure 3.8B

Figure 3.8. Summary of the breakthrough time **(A, top)** and cumulative oil recovery at breakthrough **(B, bottom)** in each ensemble under gas injection. The results estimated using a segregated flow model. The current offtake rate applies to reservoir models that have a dip angle equal to 45° , 35° and 25° respectively; that is equivalent to 72%, 89% and 121% Dietz's critical rate that is applied to the model.

3.7 Discussion of the Buckley-Leverett flow and segregated flow analysis

3.7.1. Comparison of the Buckley-Leverett flow model and the segregated flow model analysis

For the water-oil displacement, the oil recovery profile predicted by Buckley-Leverett and segregated flow models were very similar (Figure 3.5 and 3.6), although Buckley-Leverett flow and segregated flow models are based on different assumptions. However, because of the limited vertical segregation that occurs within the favourable mobility ratio water-oil displacement, there was a good match of the results between these two flow analyses.

With regard to gas-oil displacement, it was observed that the Buckley-Leverett flow model predicted a much earlier breakthrough time and a lower CORB compared with the segregated flow model. This was because the north flank has a high dip angle and gravity had a favourable impact on the displacement. Within the current production rate and reservoir properties assumptions, the gas-oil displacement was predicted to be gravity stable (section 3.6.3). In the segregated flow model, vertical cross flow was taken into account, so the over-ride gas tongue in the mobility unstable displacement was stabilised by the force of gravity and the sweep efficiency was increased in the north flank Azeri Field. Therefore, compared with the 1D Buckley-Leverett flow model that assumes zero vertical cross flow, the segregated

flow model was more suitable to represent the gas-oil displacement mechanism in the north flank Azeri Field.

3.7.2. Comparison of water-oil displacement against gas-oil displacement

Water displacement had a later breakthrough time and higher recovery under the Buckley-Leverett flow prediction. This was because under the Buckley-Leverett flow model gas flooding had lower sweep efficiency in comparison with water flooding as gas was more mobile than water so that gas swept less oil from its invaded zone compared with water flooding schemes. Within the prediction of the segregated flow model, it was observed that gas-oil displacement, in general, has a higher oil recovery at breakthrough time and ultimate cumulative oil recovery compares with water-oil displacement (Figure 3.5 and 3.6).

It was considered that the reason for lower ultimate cumulative oil recovery under water-oil displacement was due to the lower maximum movable oil saturation under water-oil displacement (Figure 3.2). From the recovery profile (Figure 3.5), it was found that both gas and water injection mechanisms reached the maximum movable oil recovery in year 15. Therefore, the magnitude of the ultimate cumulative oil recovery was determined by the maximum movable oil saturation which was determined by the relative-permeability curves. From the relative permeability curves (Figure 3.2), it was observed that when water saturation reached 0.73 the oil relative-permeability was practically zero. Therefore, it was considered that the maximum oil that could be recovered was c.0.615 of the pore volume (given that

connate water was 0.112; Figure 3.4); whereas under gas-oil displacement mechanisms the maximum movable oil was 0.888 of the pore volume.

3.7.3. Comparison of the different Pereriv Suite model

Three different reservoir models were used (Total Pereriv Suite, Pereriv B and Pereriv C) to represent different assumptions of the reservoir geology. Since offtake rate was proportional to kH of each layer, the results for Buckley-Leverett flow model analysis obtained the same results regardless of the different model size all the ensembles (Appendix 1). However, with the segregated flow assumption, both gas and water-oil displacement show that a higher CORB was obtained in a thinner layer, although each layer had the same G and M value. This was because of the geometry effect. Shook et al., (1992) showed that in a dipping reservoir, the thinner the model the higher the CORB value if an immiscible mobility unstable displacement had achieved vertical equilibrium. This factor will be discussed in more detail in Chapter 5 and 6.

3.7.4. Comparison of the different dip angle

Applying the same offtake rate to the reservoir with the lower the dip angle is equivalent (in stability terms) to applying a higher rate to the reservoir with the original dip angle (equation 3.C). For unfavourable mobility ratio displacements with production rate above Dietz's critical rate, the displacement is gravity unstable. Thus a gas tongue is formed that lead to early gas breakthrough. The results (Figure 3.7 and 3.8) showed that the unfavourable stability conditions had a negative influence on the time of breakthrough and the cumulative oil recovery.

However, current production in the north flank provides conditions for the gas displacement that were very close to the gravity stable rate boundary. The current production rate was c. 89% of Dietz's critical rate, assuming the dip angle was c. 35°. Any variation in the conditions (e.g. variation in rock and fluid properties) could lead to the displacement becoming unstable. Dietz's stability analysis can be used to indicate if a displacement is gravity stable. However, such indication only applies on a gravity dominated displacement in which the displacement is under a vertical equilibrium (VE) condition.

3.7.5. Limitation of analytical solutions on gravity assisted displacement

Most of the previous studies on gravity assisted displacement were based on the assumption that VE is achieved (Ekrann 1990, 1992, Yortsos 1992). Fayers and Muggeridge 1990 extended Dietz's theory in tilted and anisotropic reservoir. However their theory was also limited to the condition that the vertical anisotropy was not too small (Kv:Kh > 0.3). VE is achieved when maximum vertical cross flow is possible. The degree of vertical cross-flow can be indicated by the effective aspect ratio R_L (Yortsos 1991, 1992 and Shook et al. 1992). In a homogeneous system without the influence of capillary force, VE will be achieved when gravity dominates the displacement.

Effective aspect ratio $$R_L = \frac{L}{H}\sqrt{\frac{k_v}{k_h}}$$ equation 3.E

However, if the offtake rate of a displacement becomes too large, gravity effects are reduced and viscous force eventually dominates the displacement. Then no vertical cross flow occurs within the displacement and VE is not achieved. The balance between viscous and gravity forces in a displacement can be indicated by the buoyancy number N_g (Shook et al. 1992).

Buoyancy number $$N_g = \frac{k_h \lambda_{ro} \Delta\rho g \cos\theta H}{u_T L}$$ equation 3.F

Hence displacement is influenced both by the balance between gravity and viscous force (via rate) and by the effective aspect ratio R_L. The dimensionless R_L impacts VE is influenced by the Kv:Kh ratio and the length and thickness ratio of a reservoir (Ekrann 1990, Yortsos 1991, 1992 and Shook et al. 1992). Any geological heterogeneity factor that reduces Kv:Kh of a reservoir such as discontinuous shales (Begg and King 1985) may reduce the chance of a displacement to achieve VE. However, there has been limited research on the combined influence of geological heterogeneities and different balance of gravity and viscous force on displacement. Chapter 1 and 2 demonstrate that there are large numbers of studies showing how the heterogeneity has a large influence on recovery. However, heterogeneities exist in various length scales and it is not well known how they influence recovery. The next chapter will look at which heterogeneity has the largest influence on reservoir performance.

3.8. Conclusion

- A Buckley-Leverett flow model predicted earlier gas breakthrough and lower cumulative oil recovery for unfavourable mobility ratio gas-oil displacements. Buckley-Leverett flow model under-estimated the sweep efficiency for a displacement with offtake rate below Dietz's critical rate. As the vertical segregation was omitted, the sweep efficiency was only dependent on viscosity rate and relative permeability. The advantage of gravity stable displacement was not taken into account.
- However the Buckley-Leverett and segregated flow model yielded very similar results on the time of breakthrough and recovery profile estimation for the mobility stable water-oil displacement.
- For segregated flow, it was found that the thinner the reservoir the higher the cumulative oil recovery at breakthrough (CORB). At the same gravity stability condition, the fluids interface contact angle was the same, the thinner reservoir, the higher proportion of oil will be recovered at breakthrough.
- The proposed production rate in the north flank was close to the critical rate which meant that the gas-oil displacement was very close to the stability limit.
- Unfavourable stability conditions have negative impact on breakthrough time and CORB.
- All the analyses were done in a homogeneous environment. However, no reservoir in reality is completely homogeneous. The next question to be addressed is how these geological heterogeneities affect the production.

Chapter 4
Screening study of reservoir-unit scale heterogeneities

4.1. Introduction

Certain types of heterogeneity can result in a different effect on reservoir behaviour depending on the mobility ratio of the fluids, PVT properties, aquifer strength, dip angle and method of production (Weber 1986). It is not yet clear how the genetic bodies within a fluvial deltaic reservoir have an impact on displacement and recovery mechanism. Also, it is not yet clear how they should best be represented in a reservoir model.

The internal structure of fluvial deltaic reservoirs is complex. As discussed in Chapter 2, heterogeneities occur over a range of length scales within a given depositional environment; from the variation in NTG in different regions of the reservoir to the variation of the pore structure. Many researchers have defined different ways to draw the boundaries between different length scales. This thesis applied the length scale defined by Weber (1986) (for details see Chapter 2). By using a 'top-down' approach, this investigation starts from a study of the impact of the reservoir-unit scale geological heterogeneities on reservoir performance.

At reservoir-unit scale, the boundary of the genetic bodies within a fluvial deltaic environment such as channel sand bodies or extensive shales control sand body

connectivity as well as both vertical and areal sweep efficiency. In order to improve reservoir performance, it is necessary to identify which geological heterogeneities have major impacts on oil recovery during gas or water flooding so that the reasons behind these impacts can be understood. Achieving this goal can be assessed by a range of 3D geological models in conjunction with experimental design techniques, in order to develop a screening process to rank the impact of selected heterogeneities on oil recovery.

4.2. Aims

1. Identify the heterogeneities at the reservoir-unit scale which have potential impact on oil recovery.
2. Develop a screening process to rank the impact of selected heterogeneities on oil recovery.
3. Understand the interaction between different heterogeneities and displacement to explain the rank order.

4.3. Reservoir-unit scale heterogeneities in fluvial-deltaic reservoirs

The description of heterogeneities at reservoir-unit scale are based on subsurface core data measurements, production reports for the Azeri and Chirag reservoirs (Jones and Jerauld 2005), other examples of fluvial deltaic reservoirs (such as the Bahar field in the southern Caspian region or Prudhoe Bay field in Alaska) and outcrop analogues (e.g. Balakhany Quarry and Yasamal Valley) that were described in Chapter 2.

Six heterogeneities were selected for investigation in this screening study. The decision was driven by firstly considering which features were more likely to influence the reservoir performance under a given recovery process. Secondly whether such features had already demonstrated a strong influence on recovery in previous reservoir development examples (e.g. Abdullaev et al. 1998; Jones et al. 1994; Weber and van Geuns 1990). The selected heterogeneities are summarized in Table 4.1 and described briefly below.

Factor (heterogeneity)	Setting 1	Setting 2
Channel Orientation	Channel-fill sandbodies are oriented oblique (49°) to tectonic dip	Channel-fill sandbodies are oriented parallel to tectonic dip
Channel Sinuosity	Channel sinuosity = 1.73(Pereriv B) 1.67 (Pereriv C) ; 1.64 (Pereriv D)	Channel sinuosity = 1.0 (Pereriv B, C and D)
Channel Stacking	Channel-fill sandbodies treated explicitly as stacked, multistorey channel-belt sandstones	Channel-fill sandbodies treated explicitly as individual, single-storey channel-fill sandstones
Channel Dimensions	Small channel-fills: (1) single-storey channel-fill sandbodies = 6m thick, 100m wide (2) multistorey channel-belt sandbodies = 10m thick, 600m wide	Large channel-fills: (1) single-storey channel-fill sandbodies = 6m thick, 200m wide (2) multistorey channel-blet sandbodies =15m thick, 600m wide
Interlayer connectivity	Sandbodies are free to connect between layers Pereriv B,C and D	No connectivity between sandbodies in layers Pereriv B,C and D
Lateral variation of NTG within Pereriv C	Local NTG =0% in Pereriv C	Local NTG =45% in Pereriv C

Table. 4.1. Factors (heterogeneities) investigated in the sensitivity analysis. The impact of these six factors is investigated by observing the percentage change in average response when each factor is varied from setting 1 to setting 2.

4.3.1. Channel orientation

Paleocurrent measurements from channel-fill sandstones in the Pereriv Suite reservoir in Azeri and Chirag are generally directed towards the south with a range of angles that vary from parallel to the tectonic dip, to a 49° offset to the east. In the nearby Bahar Field (Abdullaev et al. 1998), it was found that channel orientation

within the Pereriv Suite is a major uncertainty on oil recovery. The same may be found in the Azeri field. Gas injected into the north flank of the Azeri structure may flow along the channel orientation down the flank instead of displacing directly to the nearest producer. In such a case, the injected gas would experience a less steep dip angle. Assuming that the average dip angle of north flank Azeri is c.31°, the injected gas would experience c.21.5° dip only. A shallower dip angle could push the proposed gas-oil displacement scheme out of the range of stability (the stability analysis of gas injection in Azeri north flank is showed in Chapter 3). If the displacement fails to be stabilized by gravity, it will lead to lower sweep efficiency and early gas breakthrough. Examples comparing various settings of channel orientation in static reservoir models are shown in Figure 4.1A and 4.1B.

4.3.2. Channel sinuosity

From outcrop analogue data, it is observed that the channel sand bodies generally lack lateral accretion surfaces, and the subsurface core and the palaeo-current data also show little variation (Reynolds et al. 1998, Reynolds et al. 2003; Reynolds and Riley 2003). These data suggest that the channels could have a low sinuosity. By using the methodology developed by Le Roux (1992) the sinuosity was estimated from the subsurface palaeo-current core data. Previous research has demonstrated that channel sinuosity has a significant impact on the connectivity of a channel system with low NTG (Larue and Hovadik 2006; Jones et al. 1995), therefore it was selected for the screening study. Since the range of channel sinuosity is uncertain, therefore two end-members of channel sinuosity (highly sinuous channels and straight channels) were selected for the screening study. Examples comparing various settings of channel sinuosity in the static reservoir models are shown in Figure 4.1A and 4.1B.

4.3.3. Channel stacking

The outcrop analogue data demonstrated examples of individual single-storey channel sandstones and also stacked multi-storey channel belt sandstones. In a low NTG environment, the variation of stacking pattern has a large impact on connectivity (Larue and Hovadik 2006; Jones et al. 1995) as well as the dimensions and aspect ratio of the effective flow path of the displacement. Examples comparing various setting of channel stacking patterns in static reservoir models are shown in Figure 4.1C and 4.1D.

4.3.4. Channel dimensions

The outcrop analogue and sub-surface data showed that the dimensions of single-storey and multi-storey channel sandbodies vary in width between c. 100-600m and c. 6-15m in thickness (Reynolds et al. 2003; Reynolds and Riley 2003). The thickness of the single-storey channels is 6m on average and their widths are between 100-200m, whereas the multi-storey channel belt is c. 10-15m thick and 600m wide. Jones et al. (1995) and Larue and Hovadik (2006) demonstrated that channel sandstone dimensions have a significant impact on connectivity in a low NTG channelised environment and variation in size has a large influence on cumulative oil recovery. Examples comparing various settings of channel dimensions in static reservoir models are shown in Figure 4.1C and 4.1D.

4.3.5. Interlayer connectivity

It is not clear from the overall data whether mudstone sheets completely subdivide the Pereriv Suite into five sub-layers, or whether there is communication between the layers. The outcrop study by Reynolds et al. (1998) and the geological studies on the nearby Bahar Field (Abdullaev et al. 1998) indicated that there are lateral mud-sheet barriers within the Pereriv Suite. However, sub-surface pressure data (see Chapter 2) showed that the inter-layer boundary is not completely sealing. Abdullaev et al. (1998) suggested that such laterally extensive barriers have a major influence on fluid displacement. If cross flow is possible, then injected gas or water would leak from one layer to another. This phenomenon could reduce the sweep efficiency and lead to earlier breakthrough. Examples of static reservoir models with different settings of interlayer connectivity between sub-Pereriv layers are shown in Figure 4.1E and 4.1F.

4.3.6. Internal variation of NTG within Pereriv C

NTG is observed to vary from 0% to c.50% in the Pereriv C layer. On average the NTG value of Pereriv C is c. 45% (Table 3.1). Jones et al. (1994) demonstrated that variation in NTG has a large influence on cumulative oil recovery. In the regions with high NTG, oil recovery may be increased because of the presence of the higher volume of oil in place. The presence of sand within Pereriv C may also increase oil recovery because it enhances cross-flow between the overlying and underlying Pereriv B and D layers. However, Pereriv C may also act as a thief zone and reduce the sweep efficiency in Pereriv B and D. Examples of static reservoir models with different settings of the internal variation of NTG within Pereriv C layer are shown in Figure 4.1E and 4.1F.

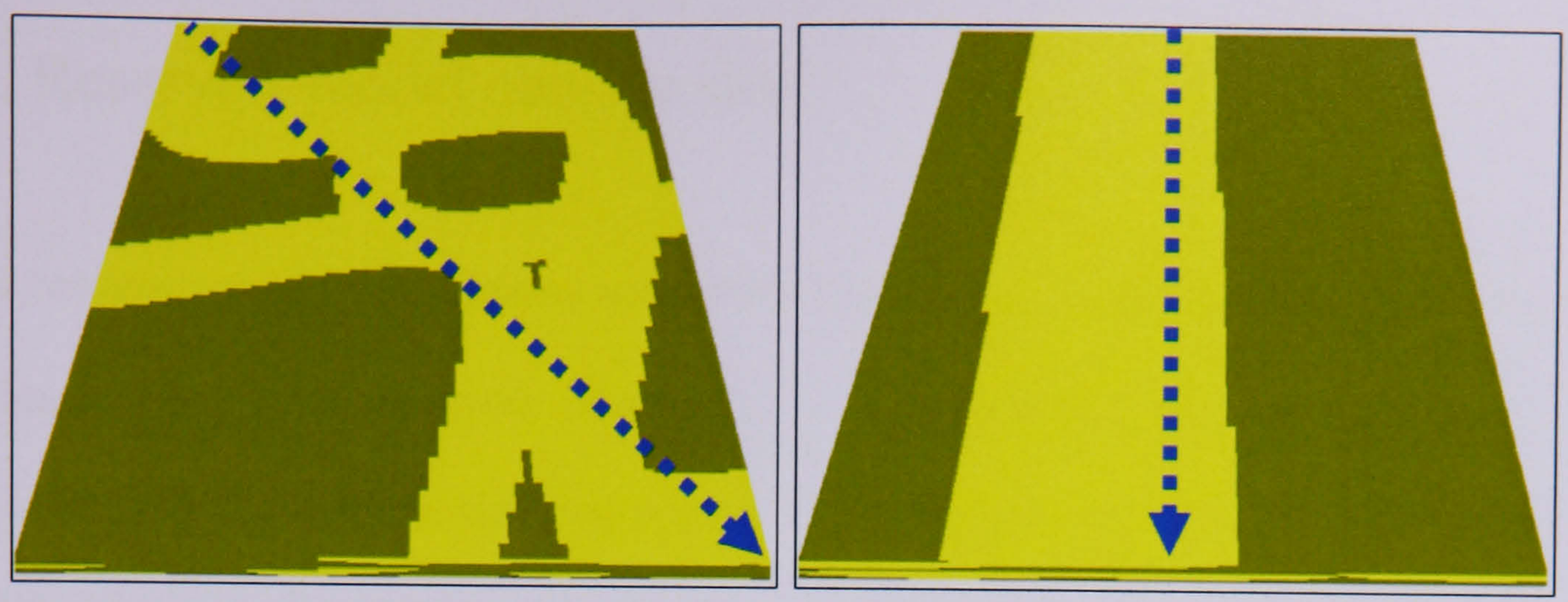


Figure 4.1A

Figure 4.1B

Figure 4.1C

Figure 4.1D

Figure 4.1E

Figure 4.1F

Figure 4.1. 3D images of north-flank static reservoir models that were used to conduct the 1st, 2nd and 3rd screening studies. The models demonstrate the different settings of reservoir-unit scale heterogeneities that were examined. For example, a model with sinuous channels oblique to the tectonic dip (with 49° offset) **(A)** is compared with a case where straight channels are aligned parallel to the tectonic dip **(B)**. The blue arrow shows the overall channel orientation. A model with several multistorey large channel-fill sandbodies **(C)** is compared with a model containing many small, single-storey channel-fill sandbodies **(D)**. Figures **A-D** were captured from low NTG models (Pereriv C). Figures **E** and **F** demonstrate lateral variations in NTG within the Pereriv C layer when the static models include Pereriv B, C and D layers. The green dotted lines demonstrate boundaries between each sub-Pereriv layer, which were set either to allow no connectivity between Pereriv B, C and D layers **(E)** or to allow sandbody connectivity across the layer boundaries **(F)**.

4.4. Reservoir model construction

The reservoir model dimensions were driven by the inter-well spacing that currently applies to the Azeri reservoir (Figure 1.1.). The current well setting in Azeri is approximately 1 injection well supporting 2 production wells. In order to keep the model representative, the distance between model boundary and production wells is symmetrical; the width of each model was 1500m which is double the distance between each production well. The length of each north flank model was 1900m, and for each of the south flank model the length of the model was 478m (Figure 1.1). The thickness of each model varied according to the reservoir interval included in the model. For example, models that contain Pereriv B, C and D are 104m on the Z coordinate the sum of the three reservoir intervals (Pereriv B at 42m, C at 30m and D at 32m). The dip angle in north flank models was c.31° and c.21° in south flank models.

The dimension of each grid cell was c.12m (north flank models) and c.11m (south flank models) in length, c.20m in wide and 1m thick. Reservoir model information was summarized in Table 4.2. It is known that grid resolution has a great influence on the reliability of the simulation results (Baker and Moore 1996; Haajizadeh and Begg 1993; Prevost et al. 2005). In Appendix 2, a study of grid resolution in different simulation settings was demonstrated to support the grid resolution used in this chapter.

Heterogeneity model	Coordinate	Grid number	Model length /m	Grid block size/m
North Flank	X	160	1900	12
	Y	75	1500	20
	Z	104	104 (Sum of Pereriv B,C and D)	1
		Total: 1248000		
South Flank	X	45	478	11
	Y	75	1500	20
	Z	104	104 (Sum of Pereriv B,C and D)	1
		Total: 351000		

Table. 4.2. Information on reservoir model setting for 1st screening study. Same grid block size is applied to all 3 screening study.

Object-based algorithm was used for reservoir modelling. The advantage of using object-based algorithm was described in Chapter 2. The algorithm models channel sand bodies stochastically in a mudstone background. The distribution of sand bodies was according to the experimental design matrix; each model contained a different combination of the geological features that are described in section 4.3. The experimental design methodology will be described a later in section 4.6. In this section the internal geological features (e.g. Kv:Kh ratio) within channel sand bodies were neglected in order to honour the 'top-down' method. The combination of reservoir-unit scale and genetic-unit scale heterogeneities will be studied in Chapter 5.

4.5. Fluid flow simulation

Simplified flow conditions were applied for the displacement simulation. Incompressible flow and no dissolved gas in the oil was assumed. With the simplified flow properties of the Azeri hydrocarbons, it was feasible to use a streamline simulator that included gravity effects (Batycky et al. 1996). The advantage of using a streamline simulator was that the displacement process could be simulated using a

model with large number of grid cells that directly include refined grid features. Models with a large number of grid cells could not be simulated by using a conventional simulator. The impact of the underlying aquifer and overlying gas cap was also neglected and it was assumed that the displacement schemes on each flank were isolated thus they were simulated separately.

The production rate of each south flank model was c.9% of the model STOIIP per year, which was the target production rate for the Azeri field. In the north flank, 93.3% of the Dietz's critical rate was chosen as the production rate of each model, given that the target field production rate was between 72% and 120% of Dietz's critical rate, because of the variation in dip angle along the north flank (Chapter 3). A streamline simulation package (3DSL version 2.2 and 3.0) was used to conduct the screening studies. Throughout the screening study, the simulator was upgraded, which could introduce minor differences between data generated from different versions of the software. However, for an incompressible and immiscible displacement, such differences were minor and would not affect the main results and conclusions of the screening study.

4.6. Screening study design

Experimental design and analysis methods (Jones et al. 1995; Box et al. 1978; Damsleth et al. 1991; Montgomery 2005; Salhi et al. 2005; White and Royer 2003) and analysis of variance (Box et al. 1978; Montgomery 2005) were applied to conduct a screening study in order to identify the key heterogeneities which had a major impact on recovery. Since a large number of simulations would be required to investigate all the possible combinations of factors, experimental design was used to

determine a limited number of experiments which best reveal the aspects to be investigated.

A two-level fractional factorial design was employed; known as a 2^{k-p} design. With the two-level fractional factorial design, each heterogeneity factor can take one of two settings denoted (1) and (2). These setting reflect two end-members from a range of observations obtained from either subsurface measurements or outcrop analogues. For example, the degree of connectivity between sandbodies in each layer of the Pereriv Suite is uncertain, and the impact of sandbodies being connected (1) or unconnected (2) across these layer boundaries. By comparing the results of a suite of models that investigate end-member settings for multiple heterogeneity factors, it was possible to rank the heterogeneity factors based on their influence on the performance of the Pereriv Suite reservoir models. By using experimental design methods, one can rapidly identify the factor that has the largest influence on the objective measure. However the method does not explain the reason behind the results. For more details on the advantages and the limitation of experimental design see Chapter 2. In section 4.3 the explanations of the setting for each factor were discussed and they are summarized in Table 4.1. The reservoir-unit scale screening study was divided into three parts:

4.6.1. First screening study: Analysis of Pereriv B, C and D

The reservoir-unit scale screening study begins by considering models which included Pereriv B, C and D layers. It was considered that these three layers represent the entire Pereriv Suite, as these layers are the 3 largest productive intervals within the Pereriv Suite. The Pereriv A and E layers were neglected. The impact of the six

reservoir-unit scale fluvial-deltaic heterogeneities (see Table 4.1) on production by gas or water injection was studied. A 2^{6-2} resolution IV experimental design was used (the setup of the simulations is shown in Table 4.3) to quantify the impact of each heterogeneity on production.

Parameter	1	2	3	4	5	6
Runs						
1	2	1	1	1	1	2
2	1	2	1	1	2	1
3	1	1	2	2	1	1
4	2	2	1	2	1	1
5	1	2	2	1	1	2
6	2	1	2	1	2	1
7	2	2	2	2	2	2
8	1	1	1	2	2	2
9	1	2	2	2	2	1
10	2	1	2	2	1	2
11	2	2	1	1	2	2
12	1	1	2	1	2	2
13	2	1	1	2	2	1
14	1	2	1	2	1	2
15	1	1	1	1	1	1
16	2	2	2	1	1	1

Table. 4.3. Experimental design matrix for 1st sensitivity screening study. The parameter row denotes the heterogeneity factor; 1: Channel orientation; 2: Channel sinuosity; 3: Channel stacking; 4: Channel dimensions; 5: Inter-layer connectivity; 6: Lateral variation of NTG within Pereriv C.

4.6.2. Second screening study: Analysis of Pereriv B, C and D (models with net sand in Pereriv C)

The second sensitivity analysis was focused on regions where there is net sand in the Pereriv C layer (i.e. the NTG within Pereriv C was fixed to be c.45% in each reservoir model). A 2^{5-1} resolution V experimental design was used. The experimental design matrix is shown in Table 4.4 and it was used to quantify the impact of the remaining 5 heterogeneities (Table 4.1) on oil recovery.

Parameter	1	2	3	4	5
Runs					
1	1	2	2	2	1
2	2	2	2	1	1
3	1	2	1	2	2
4	2	1	1	1	1
5	1	1	2	2	2
6	1	2	2	1	2
7	1	2	1	1	1
8	2	2	2	2	2
9	2	1	2	2	1
10	2	1	2	1	2
11	2	1	1	2	2
12	1	1	1	1	2
13	2	2	1	2	1
14	2	2	1	1	2
15	1	1	2	1	1
16	1	1	1	2	1

Table. 4.4. Experimental design matrix for 2nd sensitivity screening study. The parameter row denotes the heterogeneity factor; 1: Channel orientation; 2: Channel sinuosity; 3: Channel stacking; 4: Channel dimensions; 5: Inter-layer connectivity.

4.6.3. Third screening study: Analysis of Pereriv B and C layers in isolation

The third sensitivity analysis focused on high and low NTG layers separately. This part of the screening study aimed to explore the impact of the same type of heterogeneities on oil recovery within environments that have different NTGs. This approach assumed that the results from Pereriv B could represent another high NTG layer in Azeri, Pereriv D. Given that Pereriv A and E were neglected, therefore the Pereriv B results could also represent the entire Pereriv Suite in the region where zero NTG is found in Pereriv C. A 2^{4-1} resolution IV experimental design was used, which required 8 simulation experiments for each displacement process to quantify the impact of heterogeneities in Pereriv B and C. The same experimental design matrix has been used for both high and low NTG layers and is shown in Table 4.5.

Parameter	1	2	3	4
Runs				
1	1	1	2	2
2	1	2	1	2
3	1	2	2	1
4	2	2	1	1
5	1	1	1	1
6	2	2	2	2
7	2	1	2	1
8	2	1	1	2

Table. 4.5. Experimental design matrix for 3rd sensitivity screening study. The parameter row denotes the heterogeneity factor; 1: Channel orientation; 2: Channel sinuosity; 3: Channel stacking; 4: Channel dimensions.

4.6.4. Impact of uncertainty

Three stochastic realizations of each reservoir model were generated, in order to investigate the significance of the response from each heterogeneity factor compared to stochastic uncertainty. Estimates of stochastic uncertainty would be improved by generating more realizations. In Appendix 3, a study of the stochastic uncertainty and the number of stochastic realizations was conducted. The investigation studied up to 15 stochastic realizations of each reservoir model in order to demonstrate the reliable number of realization that should be used to overcome for the screening study. It was observed that although the magnitude of the response would be different when different numbers of realization were used, however the screening process can always pick up the factor that is the most significant to the objective measure when three or more realisations is being used. The results therefore suggested that three realisations were reliable for the screening study. For more details see Appendix 3.

4.7. Results

4.7.1. First screening study: Analysis of Pereriv B, C and D

Figures 4.2A to 2D show the oil recovery, cumulative GOR and cumulative water cut by gas and water injection for each of the 16 simulations conducted for the north and south flank models. The variation of oil recovery and breakthrough time shows the impact of the ensemble of geological heterogeneities on reservoir performance. Both gas and water injection recovery processes yield high oil recovery (more than 60% after 20 years of injection) and the range of recovery is small; c.10% in both flanks (north flank: c. 70%-80% after 20 years injection; south flank: c. 60%-70% after 20 years injection). The range of cumulative GOR and water cut of both recovery processes are similar. The cumulative GOR in the north flank models is c. 100% - 165%. In the south flank models, the cumulative water cut is c. 59% - 64% after 20 years injection. The high recovery is because the recovery is dominated by the high NTG layers. Compared with low NTG layers, Pereriv B,D with high NTG have all the sand connected therefore high NTG layers do not have sand connectivity problems thus all the movable oil in high NTG layer can be swept and recovered. Moreover, given that genetic-unit heterogeneities are not included in this part of study, high NTG layers are therefore have lower tortuous effective flow path compare with low NTG layer. It can then be concluded that the variation of recovery is controlled by the variation in NTG in Pereriv C layer. Figure 4.3A demonstrates that by modelling Pereriv C with a NTG of 45%, the oil recovery increases by c.14% in both flanks.

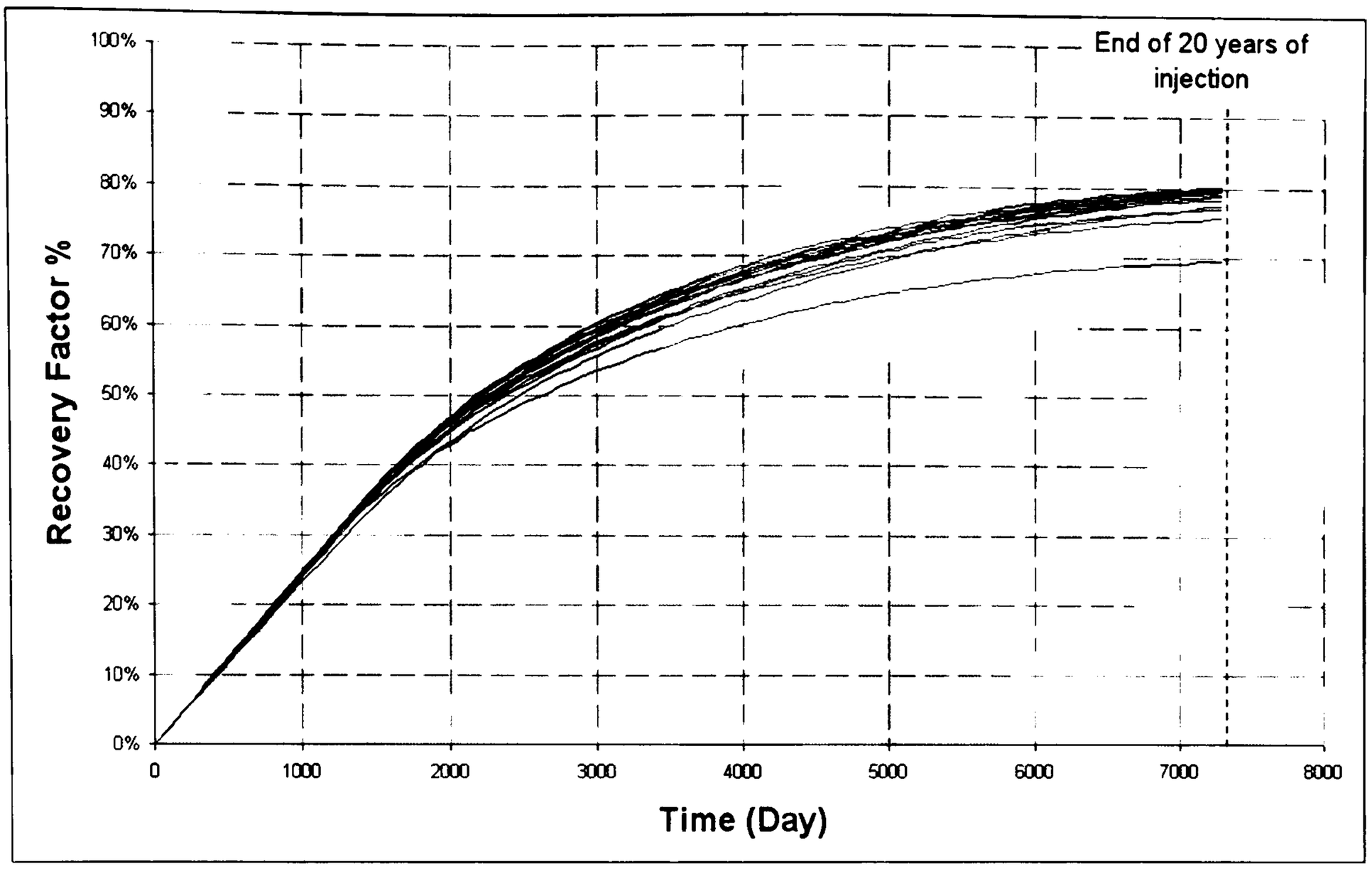


Figure 4.2A

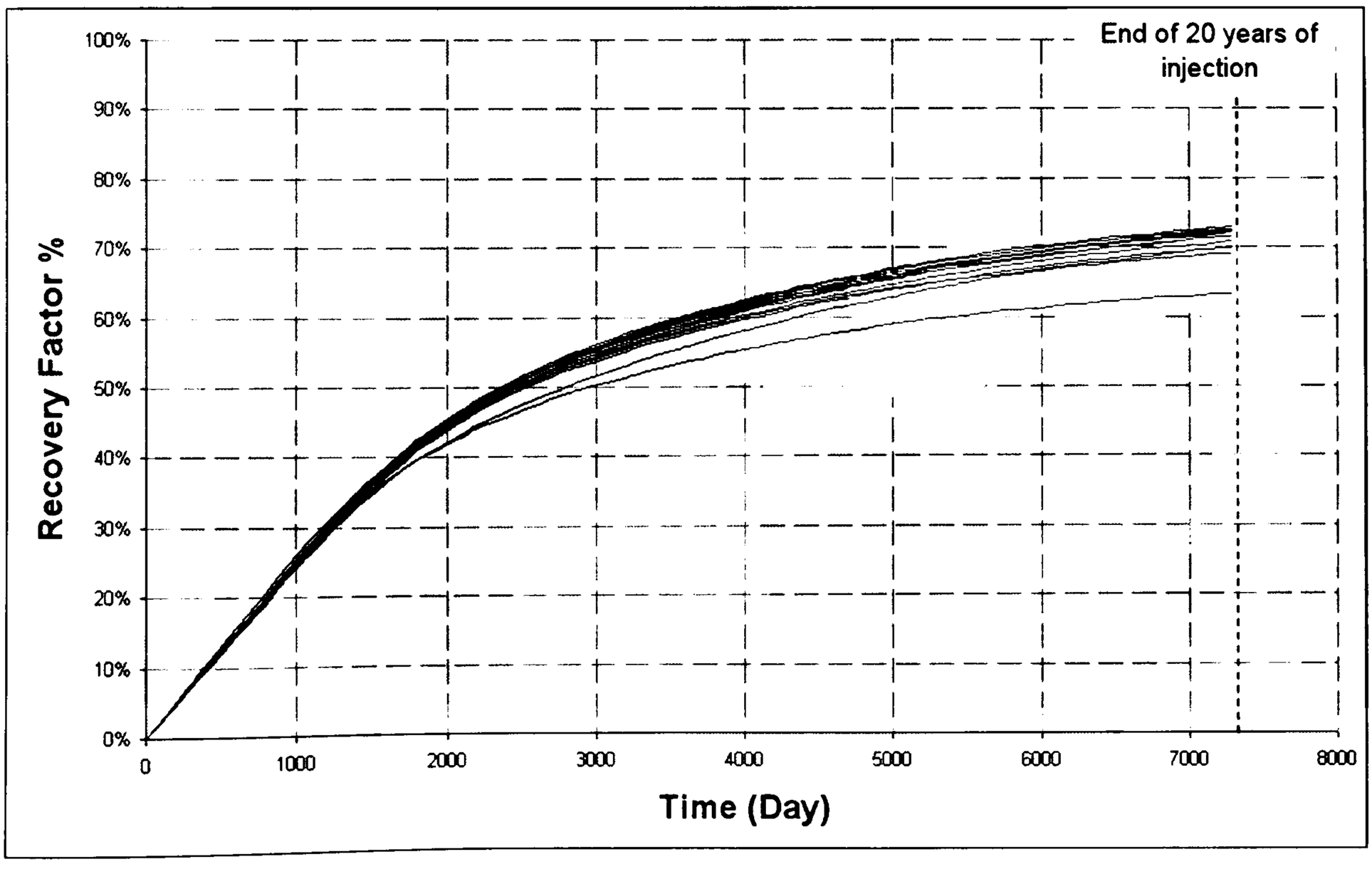


Figure 4.2B

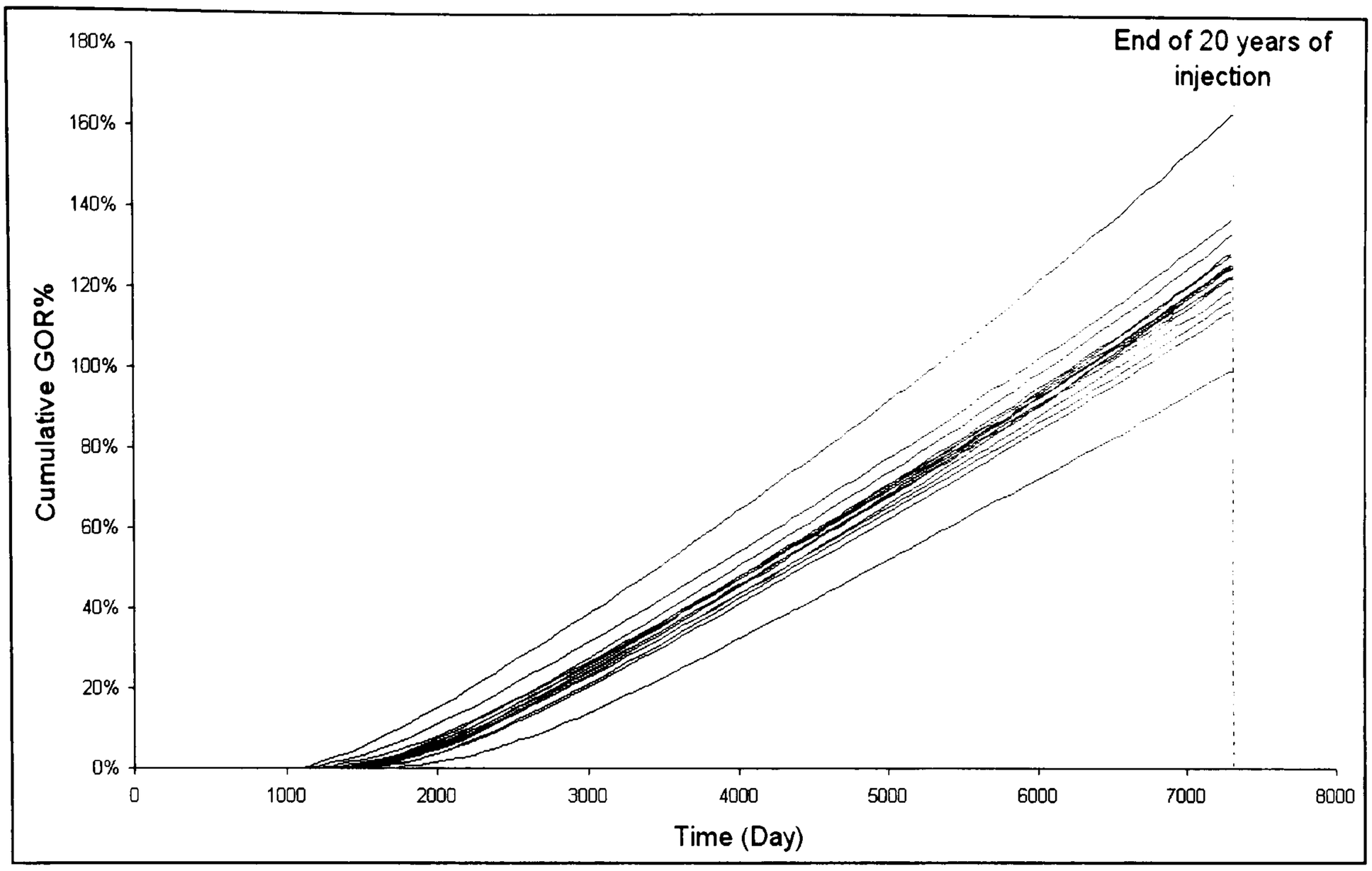


Figure 4.2C

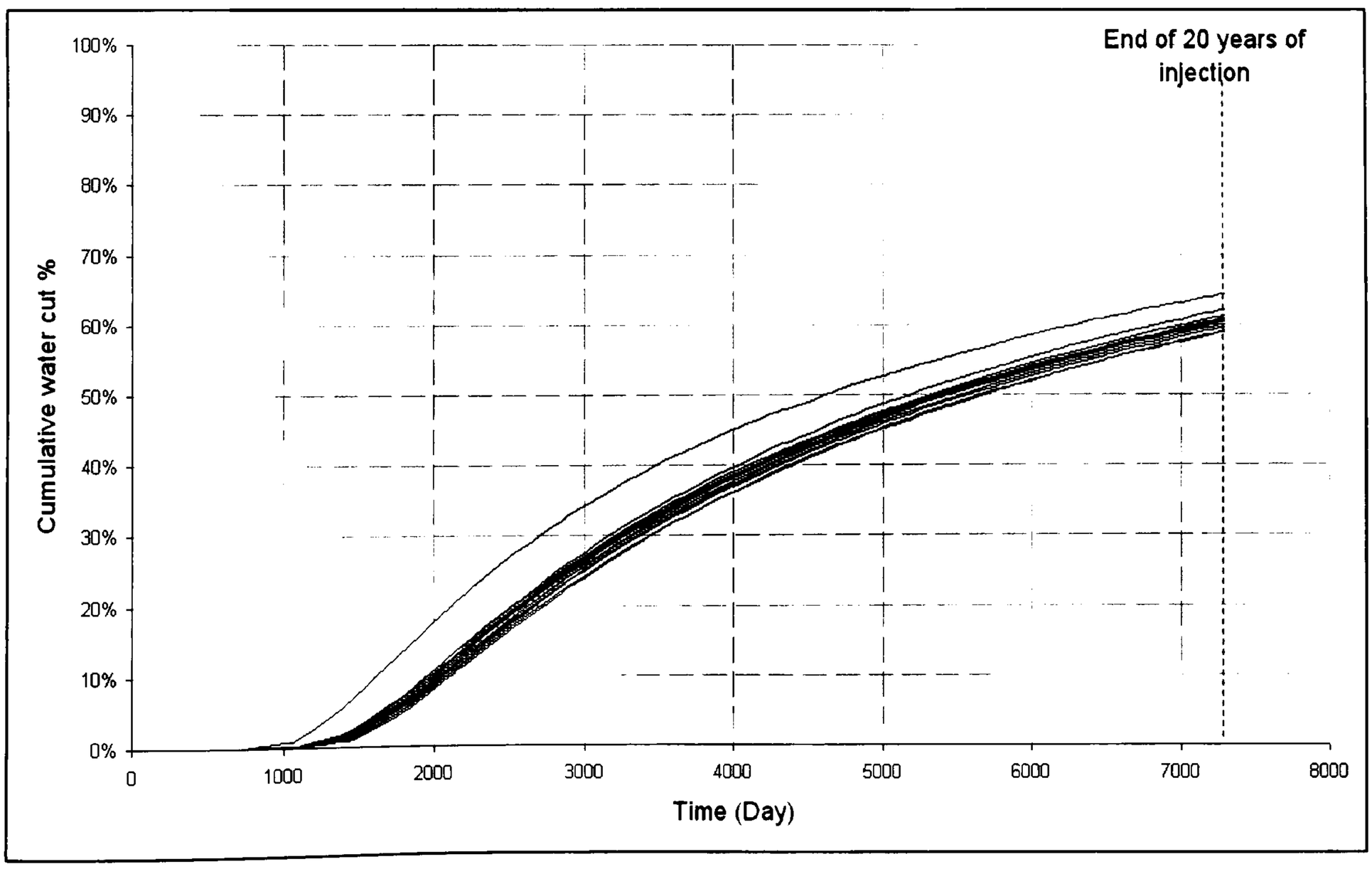


Figure 4.2D

Figure 4.2. Recovery factor, cumulative gas oil production ratio (GOR) and cumulative water cut from gas injection **(A,C)** and water injection **(B,D)** as a function of time for each of the 16 simulation experiments run in the first sensitivity analysis on the Pereriv B, C and D layers. Analysis of these curves yielded the responses shown in Figures 4.3.

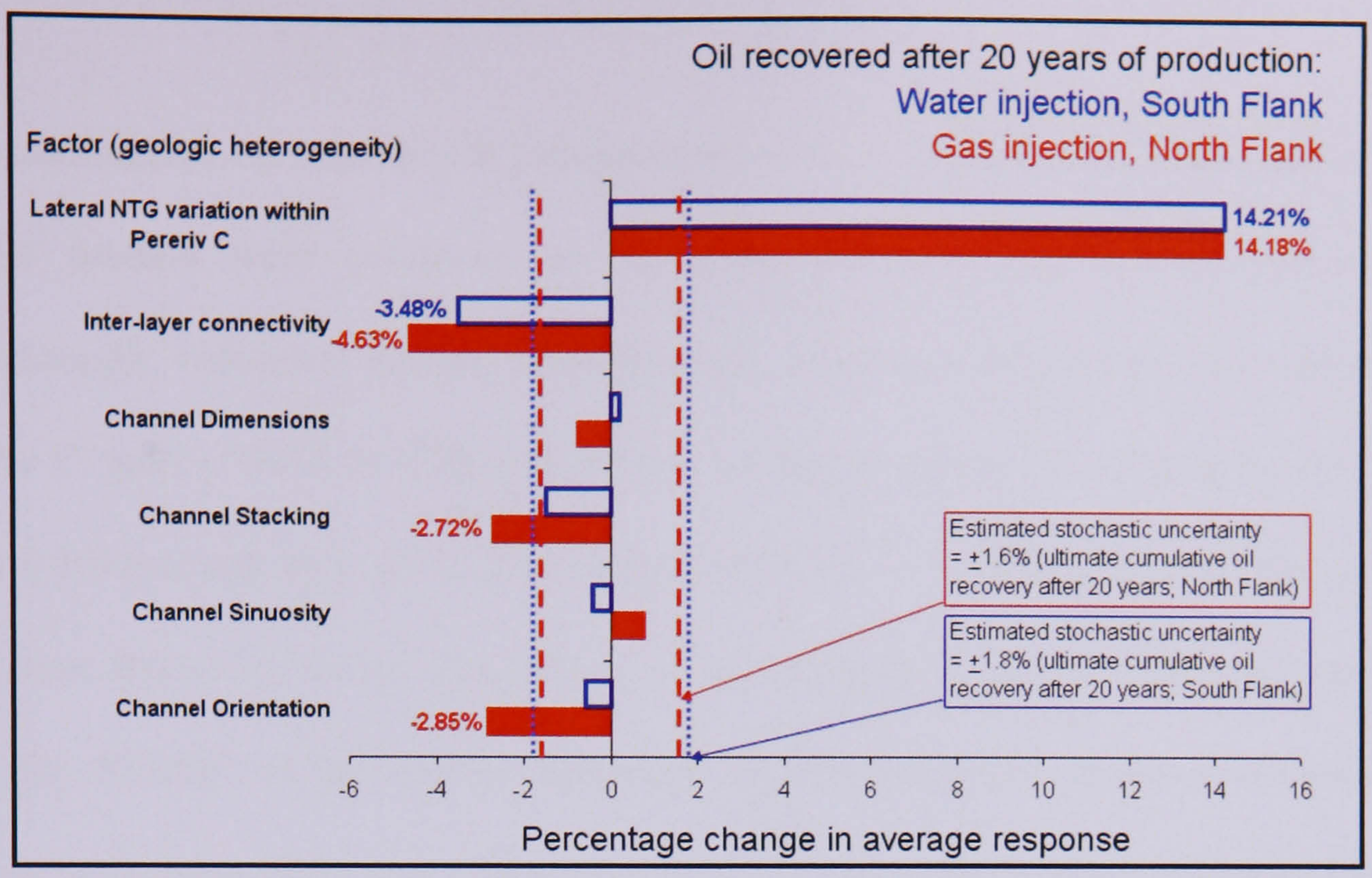


Figure 4.3A

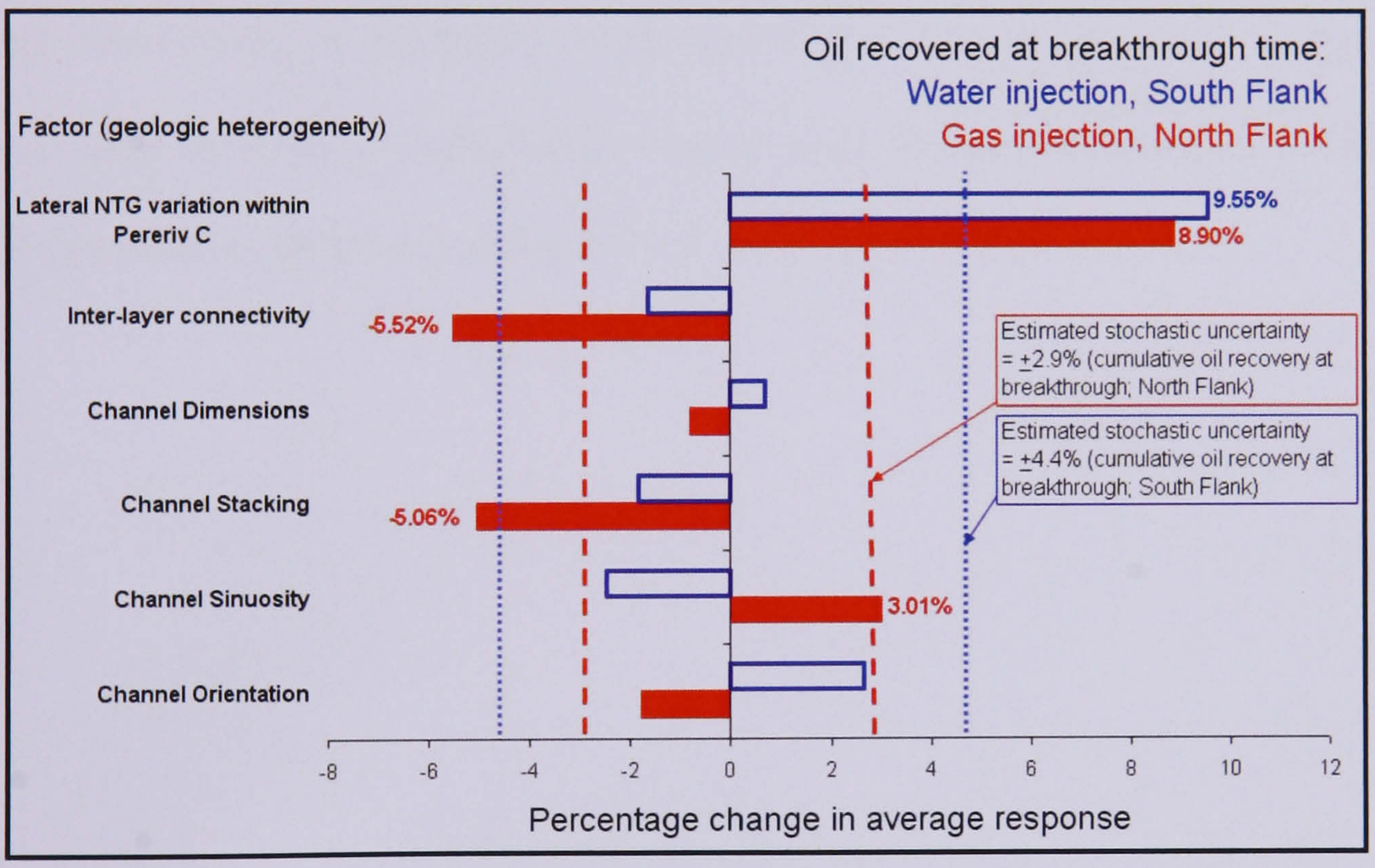


Figure 4.3B

Figure 4.3. Results of 1st screening study, average percentage change in **(A, top)** oil recovered after 20 years, and **(B, bottom)** oil recovered at breakthrough of gas (north flank) and water (south flank), observed when each factor in the sensitivity analysis is varied from setting 1 to setting 2 (Table 4.1). Pereriv B, C and D layers are included in the models. If the bar lies to the right then the change is positive. For example, modelling Pereriv C with 45% NTG (setting 2) increases cumulative oil recovery by c. 14% compared with modelling it with zero NTG (setting 1). The dashed lines denote the average percentage change observed from different stochastic realizations. If the impact of varying a factor is at or below the level of stochastic uncertainty then modelling decisions are unimportant for the chosen range of parameters.

The cumulative oil recovery at breakthrough was a proxy for breakthrough time, as all the models were produced at the same constant rate. Lower recovery at breakthrough indicates earlier breakthrough. Figure 4.3B shows that modelling Pereriv C with a NTG of 45% caused gas breakthrough to be delayed by c.9% and water breakthrough by c.10%. This suggested that a low NTG layer does not act as a thief zone. Recovery factor was defined as the percentage of cumulative oil recovered from the STOIIP of the model. Although oil recovery was increased if sand was present in the low NTG layer (Figure 4.3.A), this increased recovery comes from an increased STOIIP and the overall recovery factor decreased. This effect was due to the poor connectivity of sandbodies in the low NTG layer, which caused the recovery factor to drop by c.4% in both flanks (Figure 4.4). The connectivity of sandbodies will be discussed in detail in section 4.7.3.2.

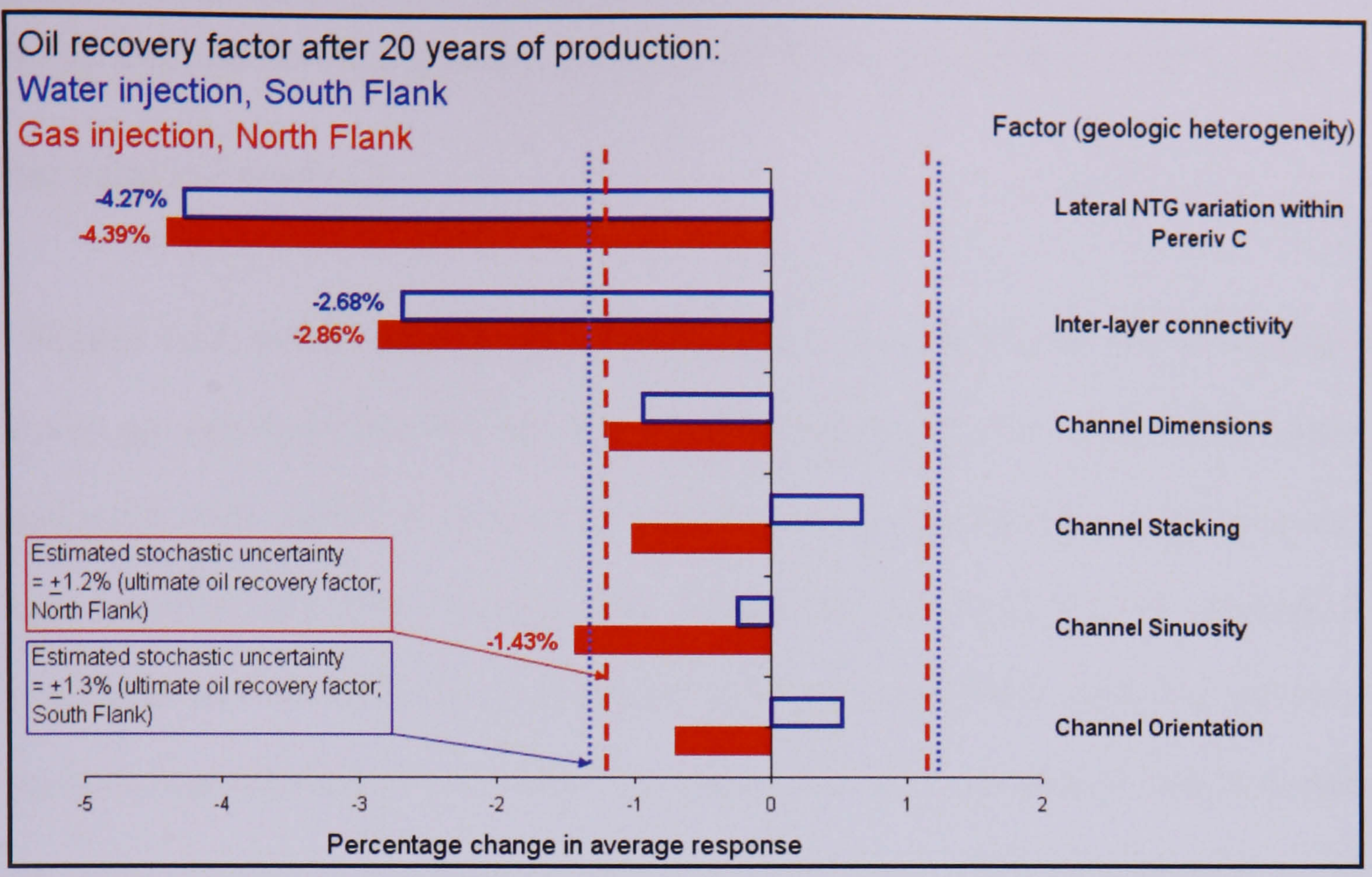


Figure 4.4. Result of 1st screening study, average percentage change in oil recovery factor after 20 years, observed when each factor in the sensitivity analysis is varied from setting 1 to setting 2 (Table 4.1). Pereriv B, C and D layers are included in the models. If the bar lies to the right then the change is positive. Recovery factor was defined as the cumulative oil recovered over the STOIIP of the model. As poor connectivity of sandbodies in the low NTG layer (Pereriv C), therefore the overall recovery factor reduced if more net sand was introduced into this layer.

Figures 4.3 to 4.4 demonstrated that the impact of varying most of the heterogeneity factors was close to or below the level of stochastic uncertainty in both flanks. The results suggested that modelling decisions were not important for the chosen range of parameters. However, in models that had sand in the Pereriv C layer, the average impact of the heterogeneity factors was significantly larger than the models that had no sand in the Pereriv C layer. The standard deviation of the cumulative recovery factor of the models that had net sand in Pereriv C is 4.1%, whereas the standard deviation of the cumulative recovery factor of models that had no sand in Pereriv C was only 0.43%. It was therefore necessary to refine the screening study. In the next section, the screening analysis is focused only on regions where there was net sand in Pereriv C.

4.7.2. Second screening study: Analysis of Pereriv B, C and D (models with net sand in Pereriv C)

Figures 4.5A to 5D show the oil recovery, cumulative GOR and cumulative water cut by gas and water injection for each of the 16 simulations conducted for the north and south flank models in the second screening study. The variation of oil recovery and breakthrough time showed the impact of the ensemble of geological heterogeneities on reservoir performance. Both gas and water injection recovery processes yielded high oil recovery (more than 60% after 20 years of injection) and the range of recovery was small, c. 14% in north flank and c. 9% in south flank (north flank: c. 66%-80% and south flank: c. 64%-73% after 20 years injection). The range of cumulative GOR and water cut of both recovery processes were similar in both flanks. The cumulative GOR in the north flank was c. 111% - 177% after 20 years injection. In the south flank, the cumulative water cut was between c. 61% - 66% after 20 years injection. Since all the models contained both high and low NTG layers, the high recovery was because the recovery is dominated by the high NTG layers and as explained in section 4.7.1. The variation of recovery was mainly controlled by the inter-layer connectivity between Pereriv B, C and D.

Figures 4.6A and 4.6.B show the average percentage change in cumulative oil recovery and total gas (north flank) and water (south flank) produced after 20 years of injection. In this set of screening studies, it was observed that inter-layer connectivity has the most significant impact on oil recovery under both displacement schemes. It was found that when the reservoir layers were completely isolated, oil recovery was reduced by c.8% in the north flank (gas injection) and c.4.5% in the south flank

(water injection). Moreover, in reservoir models with no interlayer connectivity. gas production was increased by c. 6% in the north flank (Figure 4.6A) and water production was increased by c. 3% in the south flank (Figure 4.6B). The results suggested that the vertical cross flow of gas and water between layers did not reduce sweep efficiency. This was demonstrated by the fact that the cumulative oil recovery was increased when the layers were connected (Figure 4.3A). The channel sand bodies in Pereriv C could be poorly connected to the injection and/or production wells because of the low NTG in this layer. In this case, recovery could be improved by pressure support via Pereriv B and/or D, so recovery was improved when there was inter-layer connectivity.

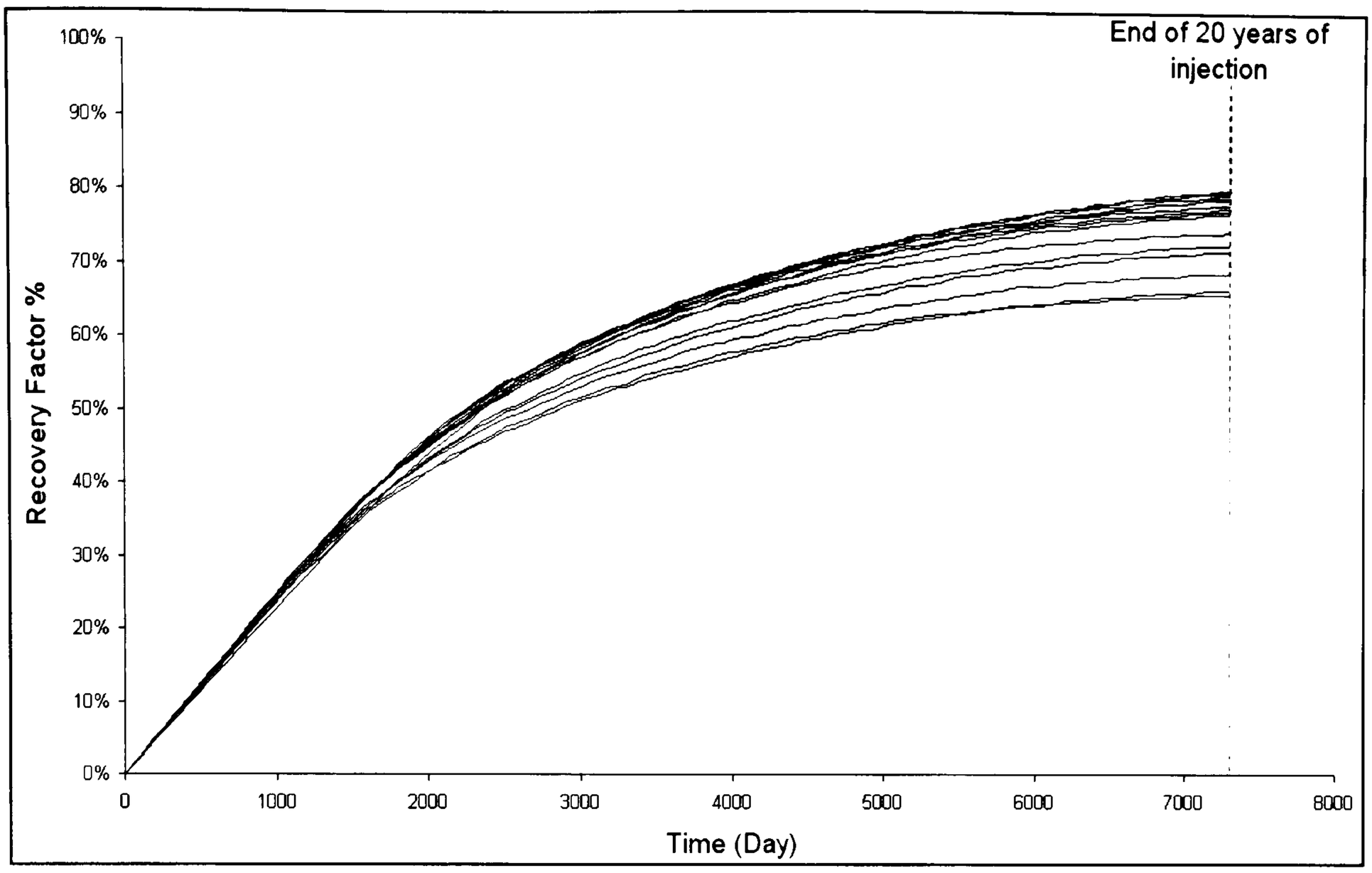


Figure 4.5A

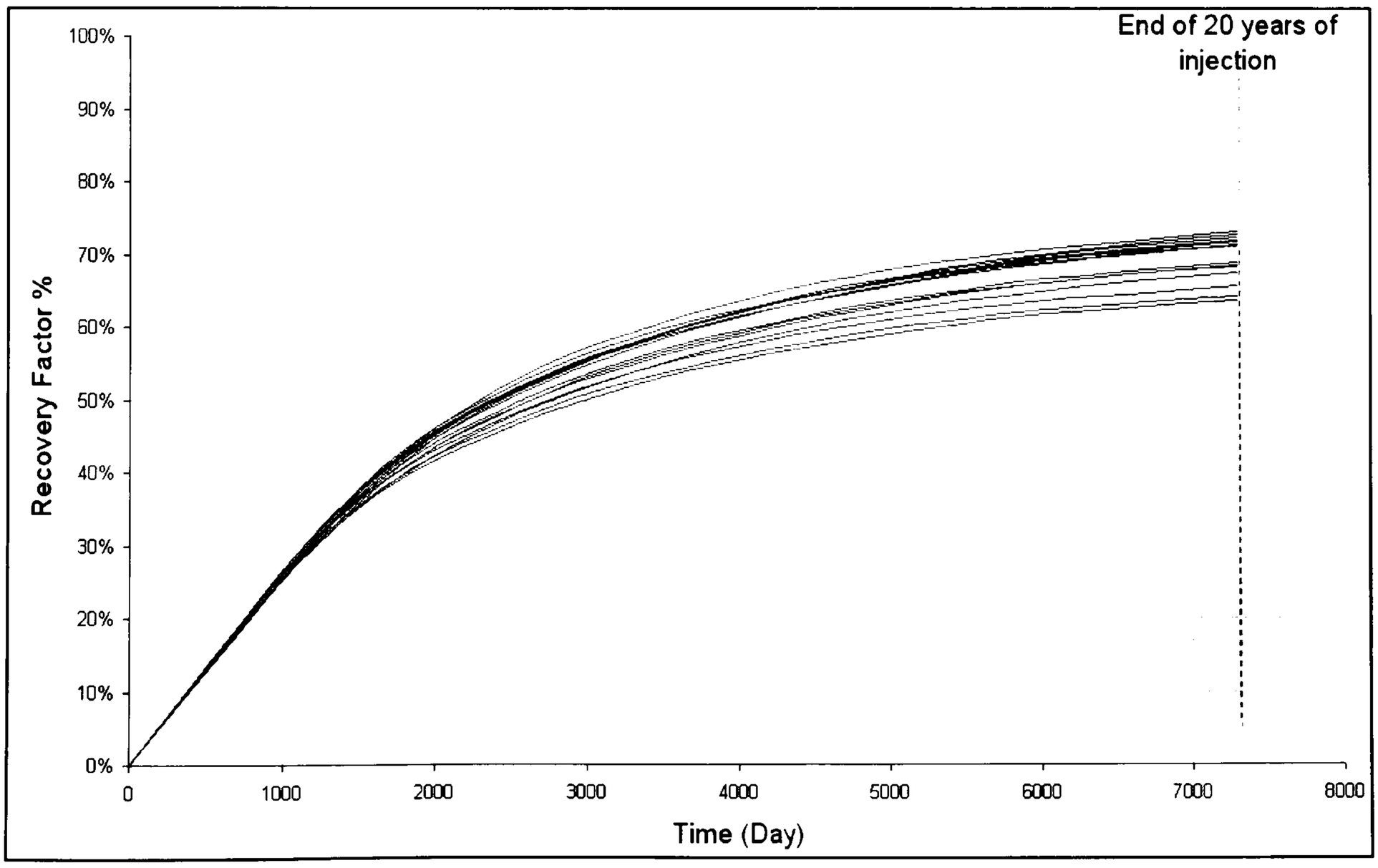


Figure 4.5B

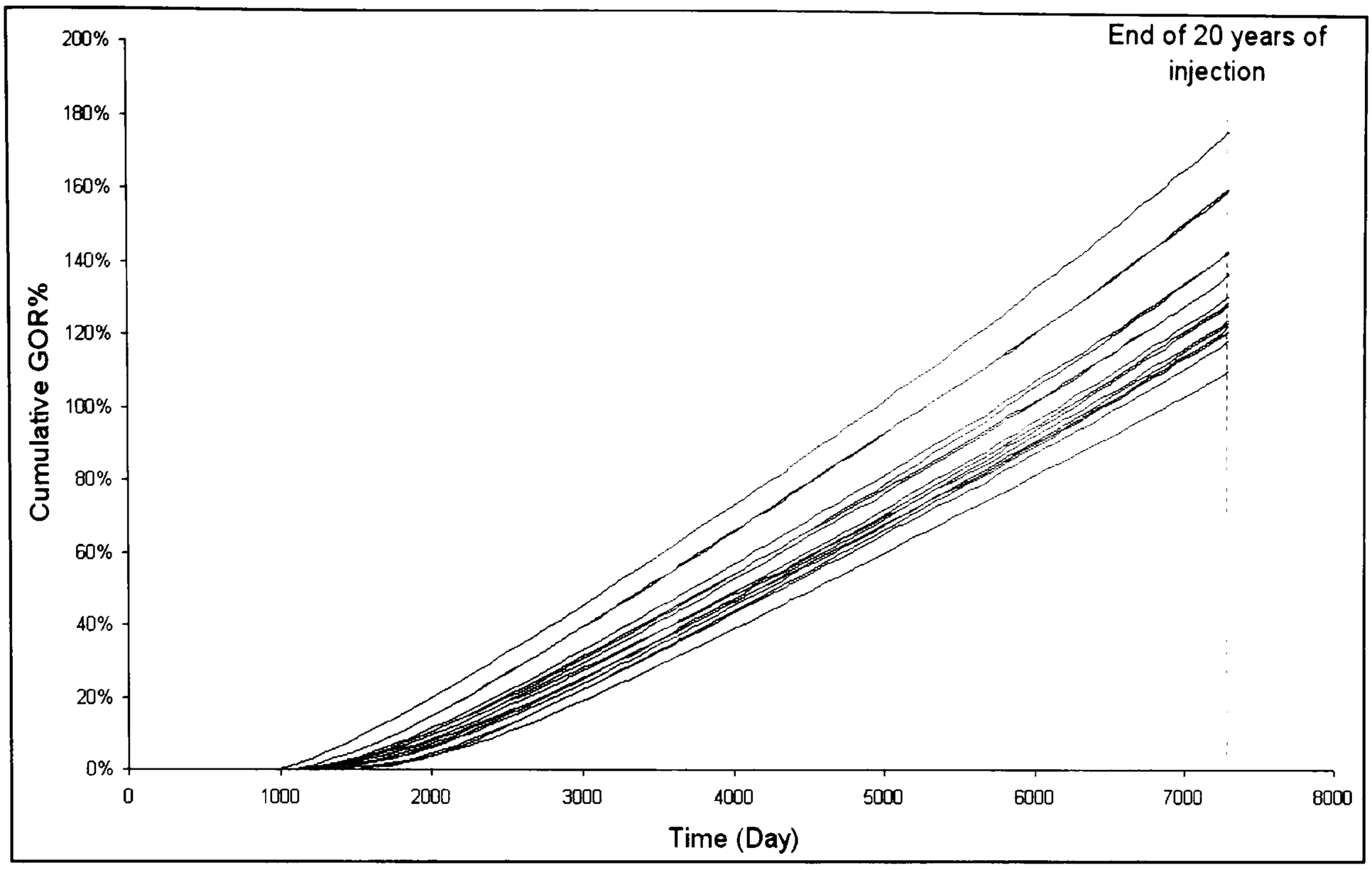


Figure 4.5C

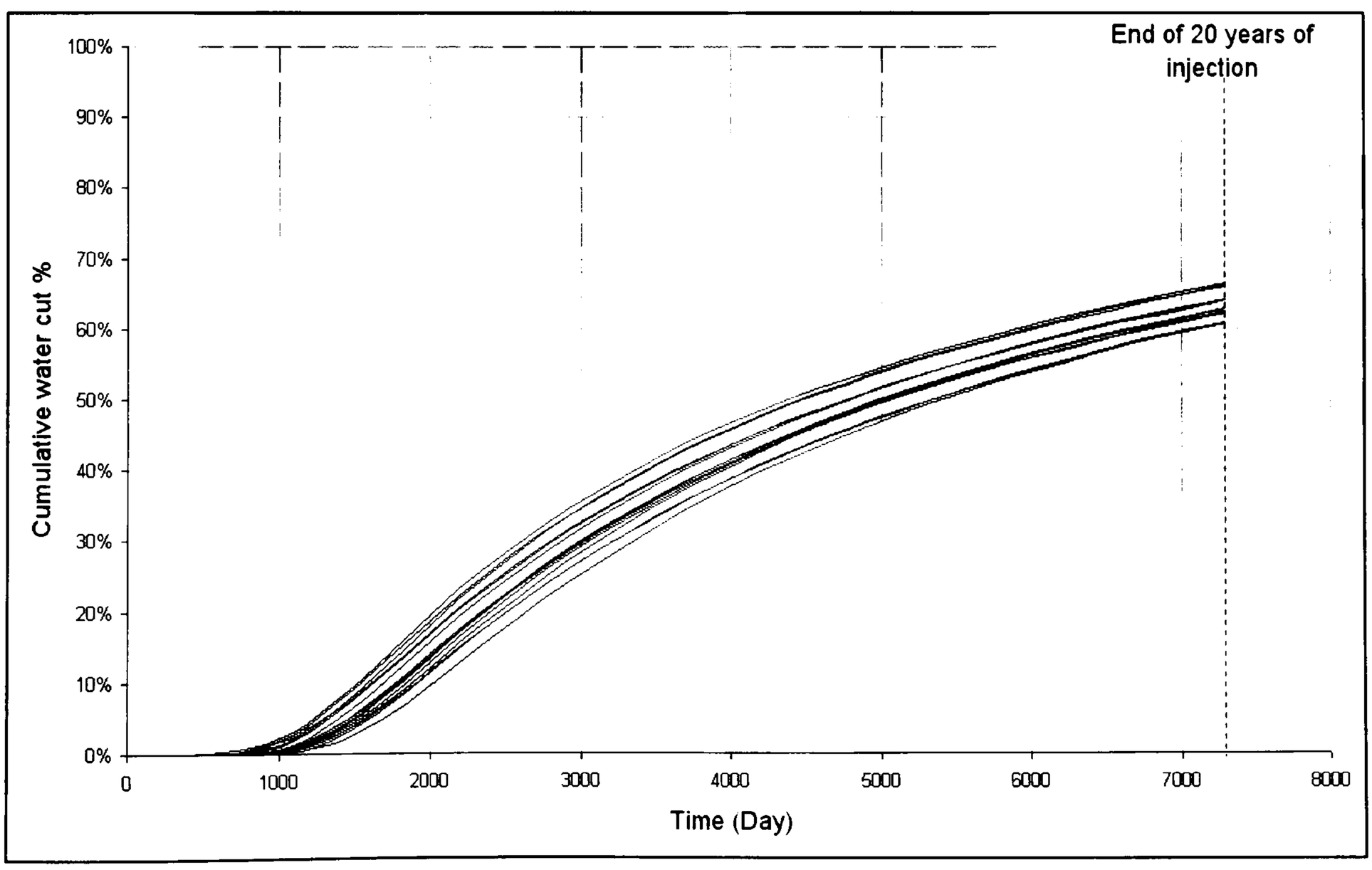


Figure 4.5D

Figure 4.5. Recovery factor, cumulative gas oil production ratio (GOR) and cumulative water cut from gas injection **(A,C)** and water injection **(B,D)** as a function of time for each of the 16 simulation experiments run in the second sensitivity analysis on the Pereriv B, C and D layers. Analysis of these curves yielded the responses shown in Figures 4.6.

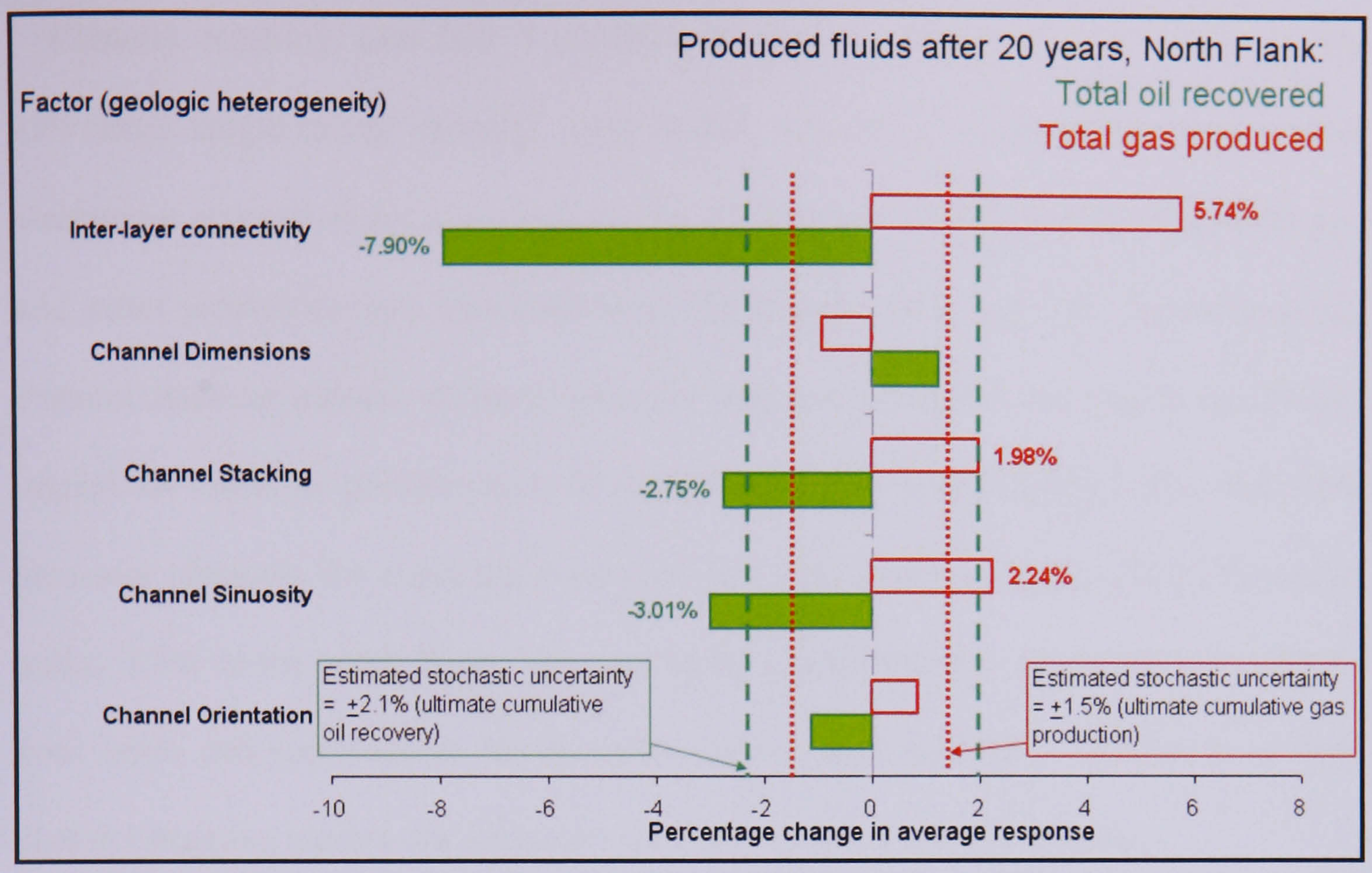


Figure 4.6A

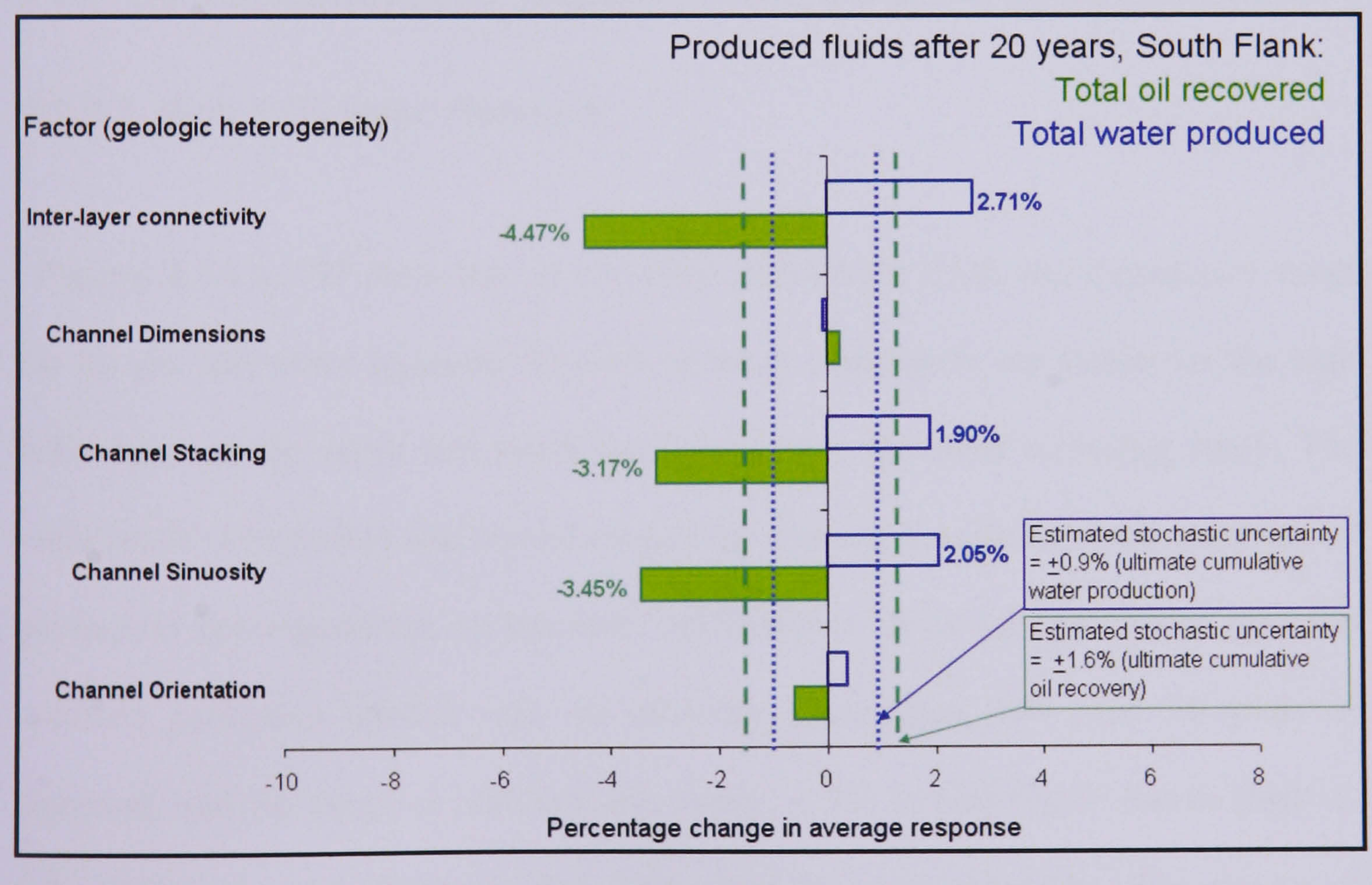


Figure 4.6B

Figure 4.6. Result of 2nd screening study, average percentage change in oil recovered and total gas (north flank) and water (south flank) produced after 20 years in **(A, top)** north flank models, and **(B, bottom)** south flank models, observed when each factor in the sensitivity analysis is varied from setting 1 to setting 2 (Table 4.1). Pereriv B, C and D layers are included in the models; Pereriv C is modelled with a fixed NTG of 45%.

Channel stacking also had a significant impact. Many reservoir models with individual single-storey channel sand bodies instead of multistorey channel belt sandstones showed oil recovery reduced by c.3% in both flanks and the volume of gas and water production was increased by c. 2% (Figure 4.6A and 6.B). Apart from the channel stacking pattern, channel sinuosity was another factor that had a significant impact on reservoir performance. In reservoir models with straight rather than low sinuosity channels the cumulative oil recovery was decreased by c. 3% in the north and c. 3.5% in the south flank. Gas and water production was increased by c. 2% in both north and south flanks. In the next section there will be a discussion of how channel stacking pattern and channel sinuosity control sweep efficiency.

4.7.3. Third screening study: Analysis of Pereriv B and C layers in isolation

4.7.3.1. High NTG layer: Pereriv B

Figures 4.7A to 7D show the oil recovery, cumulative GOR and cumulative water cut by gas and water injection for each of the 8 simulations conducted for the high NTG layer of the north and south flank models in the third screening study. The variation of oil recovery and breakthrough time showed the impact of the ensemble of geological heterogeneities on reservoir performance. Both gas and water injection recovery processes yielded high oil recovery (more than 70% after 20 years of injection) and the range of recovery was small, c. 3% in both flanks (north flank: c. 77%-79% and south flank: c. 70%-73% after 20 years injection). The ranges of cumulative GOR and water cut of both recovery processes are similar in both flanks. The cumulative GOR in the north flank was c. 108% - 120% after 20 years injection. In the south flank, the cumulative water cut was c. 61% - 63% after 20 years injection. The high recovery resulted in the high NTG layer which has low tortuous

effective-flow paths compared with the low NTG layer in the absence of genetic-unit scale heterogeneities.

The results from Pereriv B could be used to represent the other high NTG layer, Pereriv D, and the entire Pereriv Suite in regions where there was no sand recorded in the Pereriv A,C and E layers. Figures 4.8A and 4.8B show that heterogeneities had a different impact on the north and south flanks. In north flank models with high NTG, it was found that the impact of all heterogeneities on oil recovery and gas production is below the stochastic uncertainty. This suggested that the chosen reservoir-unit scale heterogeneity factors were unimportant for modelling gas injection in high NTG layers. However, in the south flank models, it is found that channel orientation has the most significant impact on cumulative oil recovery and water production; although the magnitude is small (all responses were less than 2%). Figure 4.8B shows the results of the screening study on the south flank high NTG layer; it was found that when channel sand bodies were oriented parallel to the tectonic dip, the cumulative oil recovery increased by c.1.5% and the cumulative water production decreased by c.1%. The next most important heterogeneity factor was channel sinuosity. However, the impact was found to be very close to the stochastic noise.

Channel orientation was found to be the most significant heterogeneity factor on the south flank high NTG layer. This was because when the channel sand bodies were oriented parallel to the tectonic dip, it provided a direct route between injector and producer wells; whereas when the models contained channels that were offset from the tectonic dip, the water-oil displacement was subtly moved from one channel to another, decreasing the areal sweep efficiency. Figure 4.9 shows an example of the

saturation distribution of the movable oil in two reservoir models with different channel orientations.

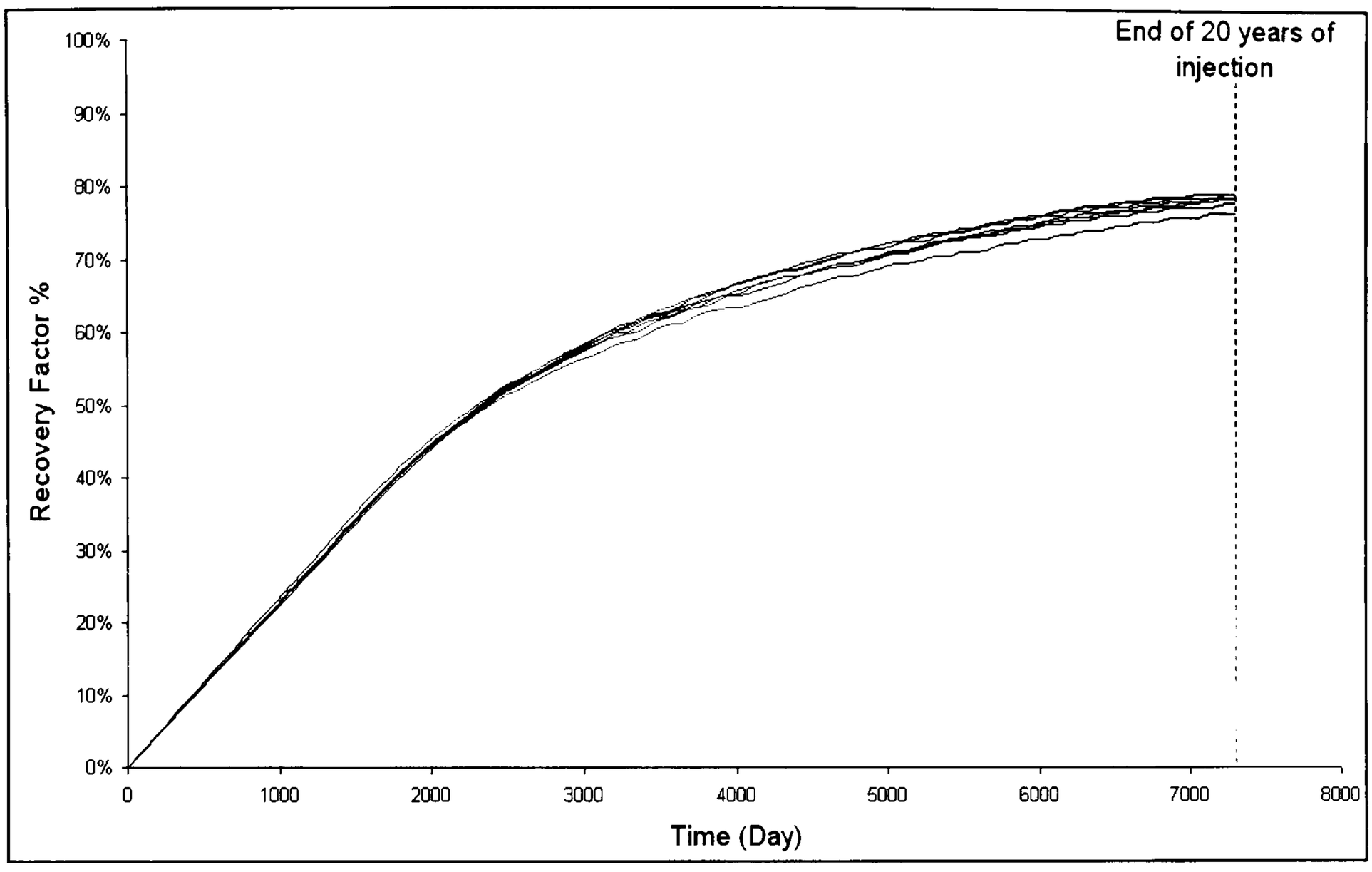


Figure 4.7A

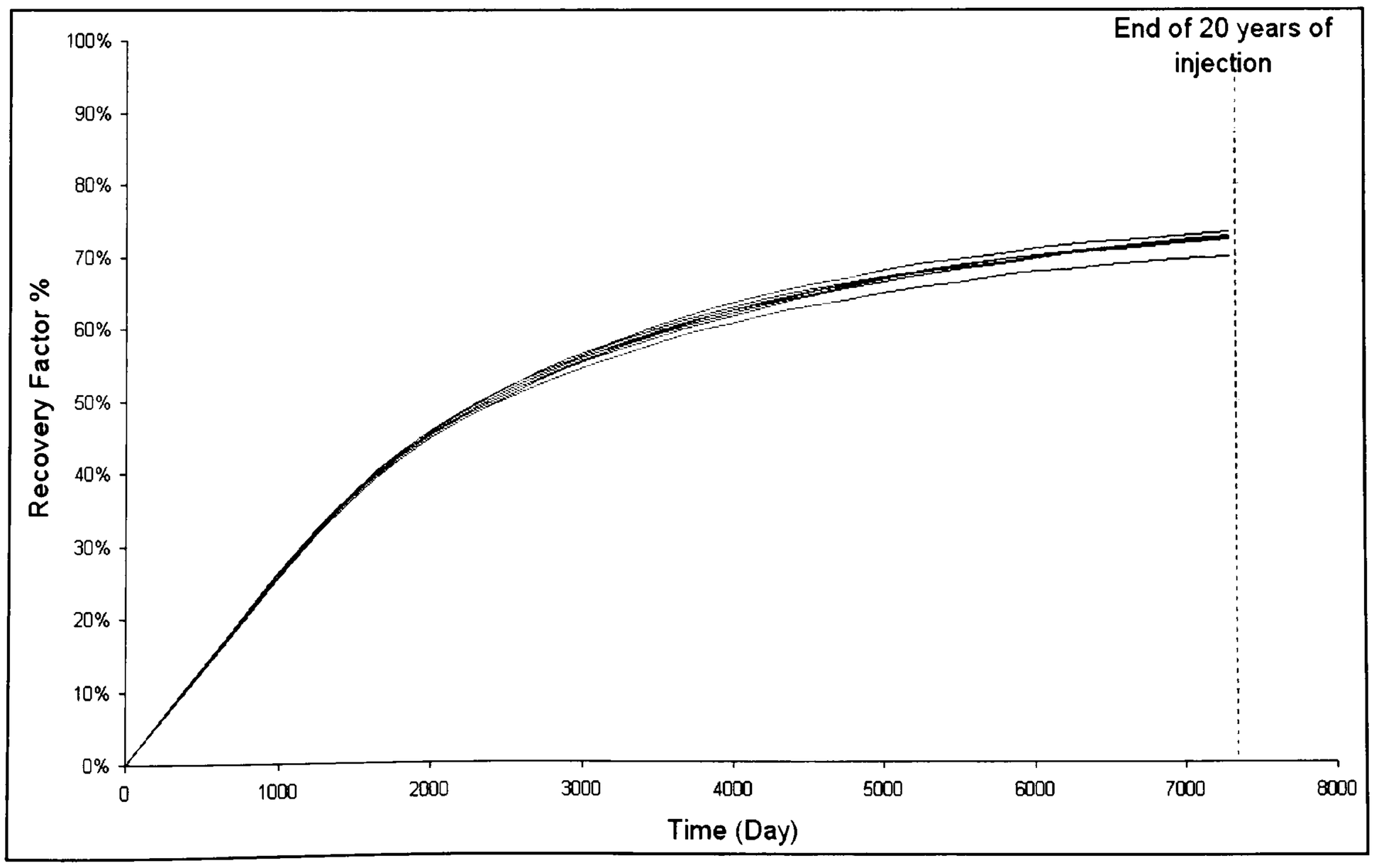


Figure 4.7B

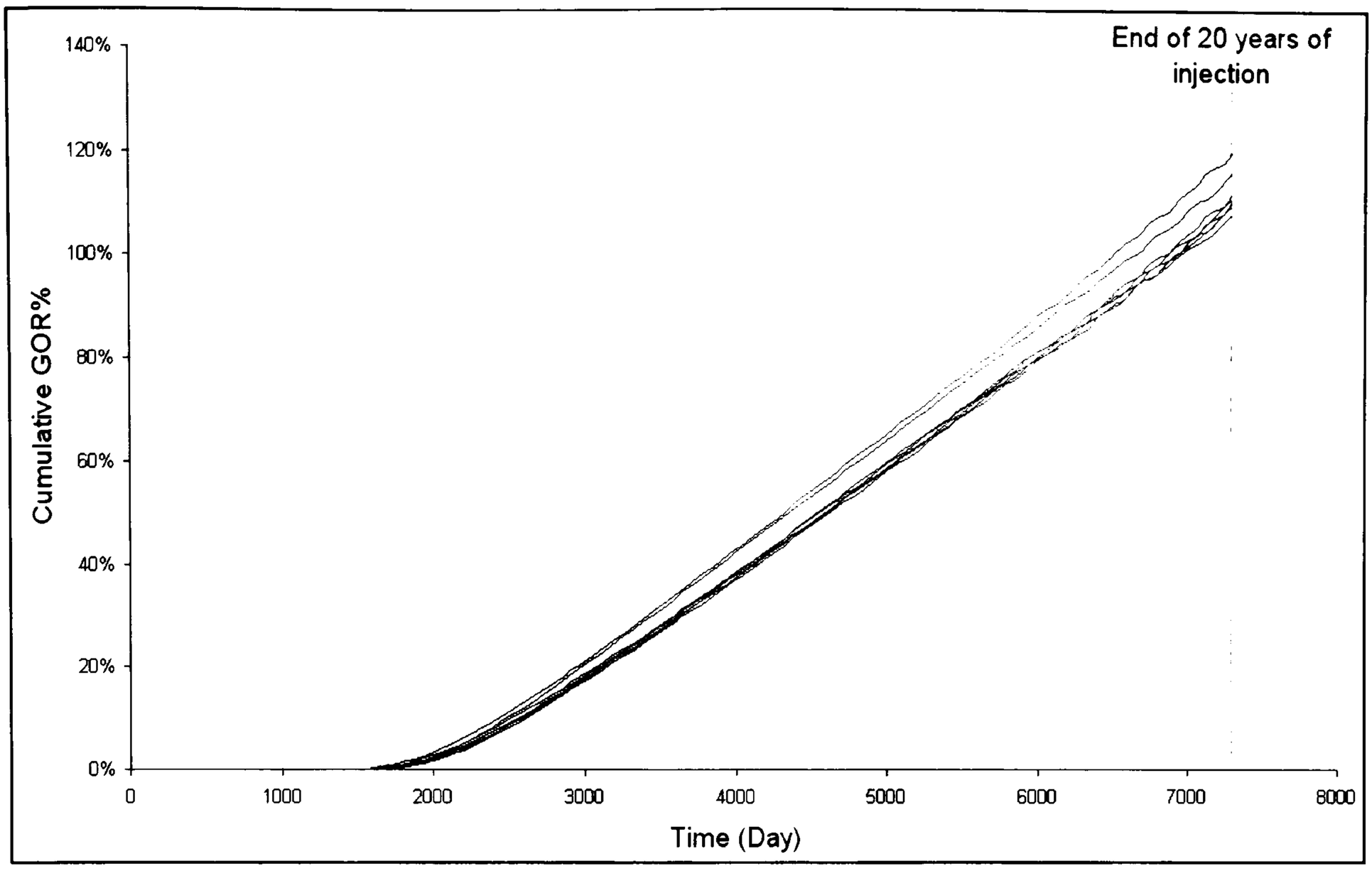


Figure 4.7C

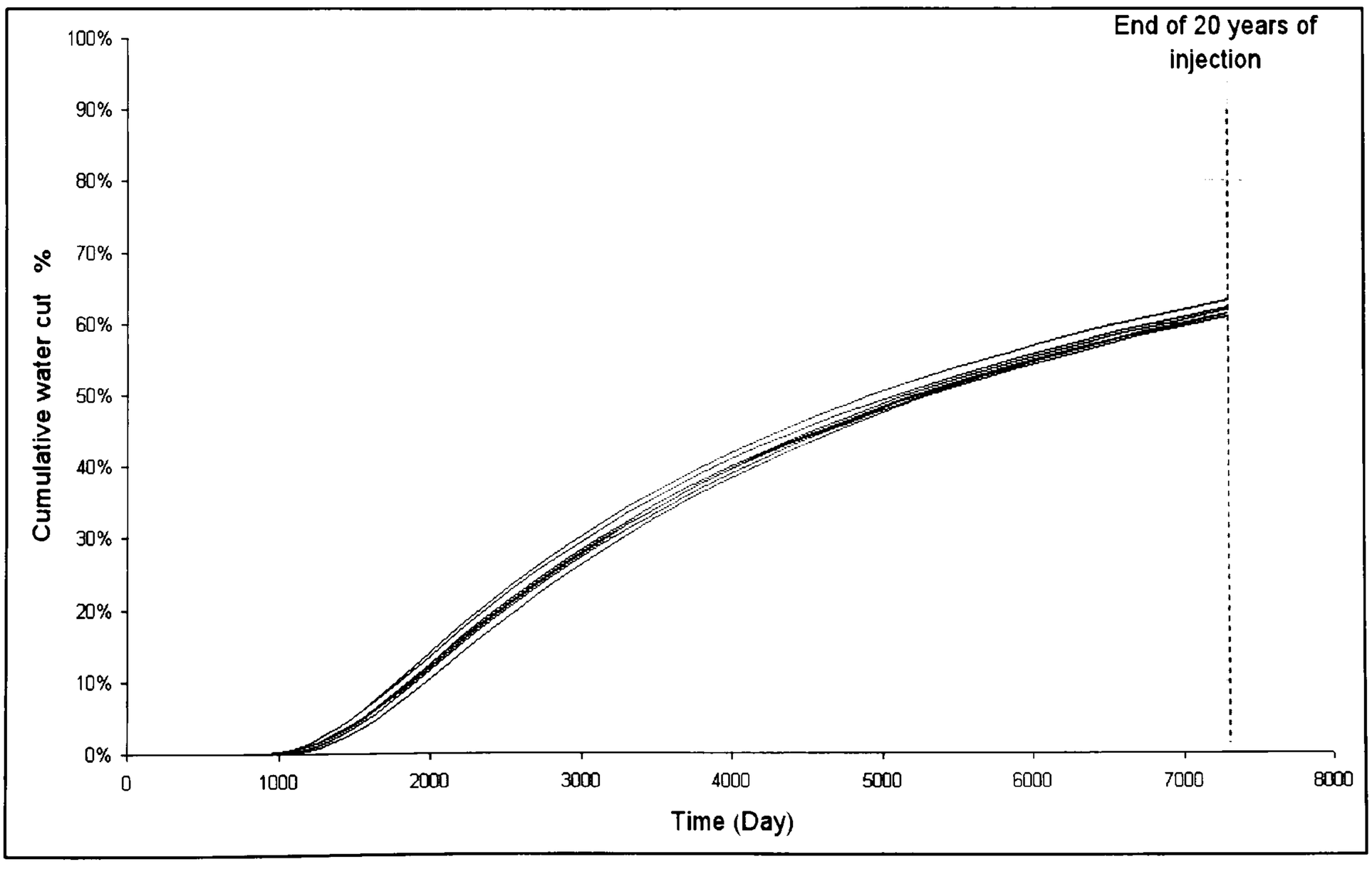


Figure 4.7D

Figure 4.7. Recovery factor, cumulative gas oil production ratio (GOR) and cumulative water cut from gas injection **(A,C)** and water injection **(B,D)** as a function of time for each of the 8 simulation experiments run in the third sensitivity analysis on the Pereriv B layers. Analysis of these curves yielded the responses shown in Figures 4.8.

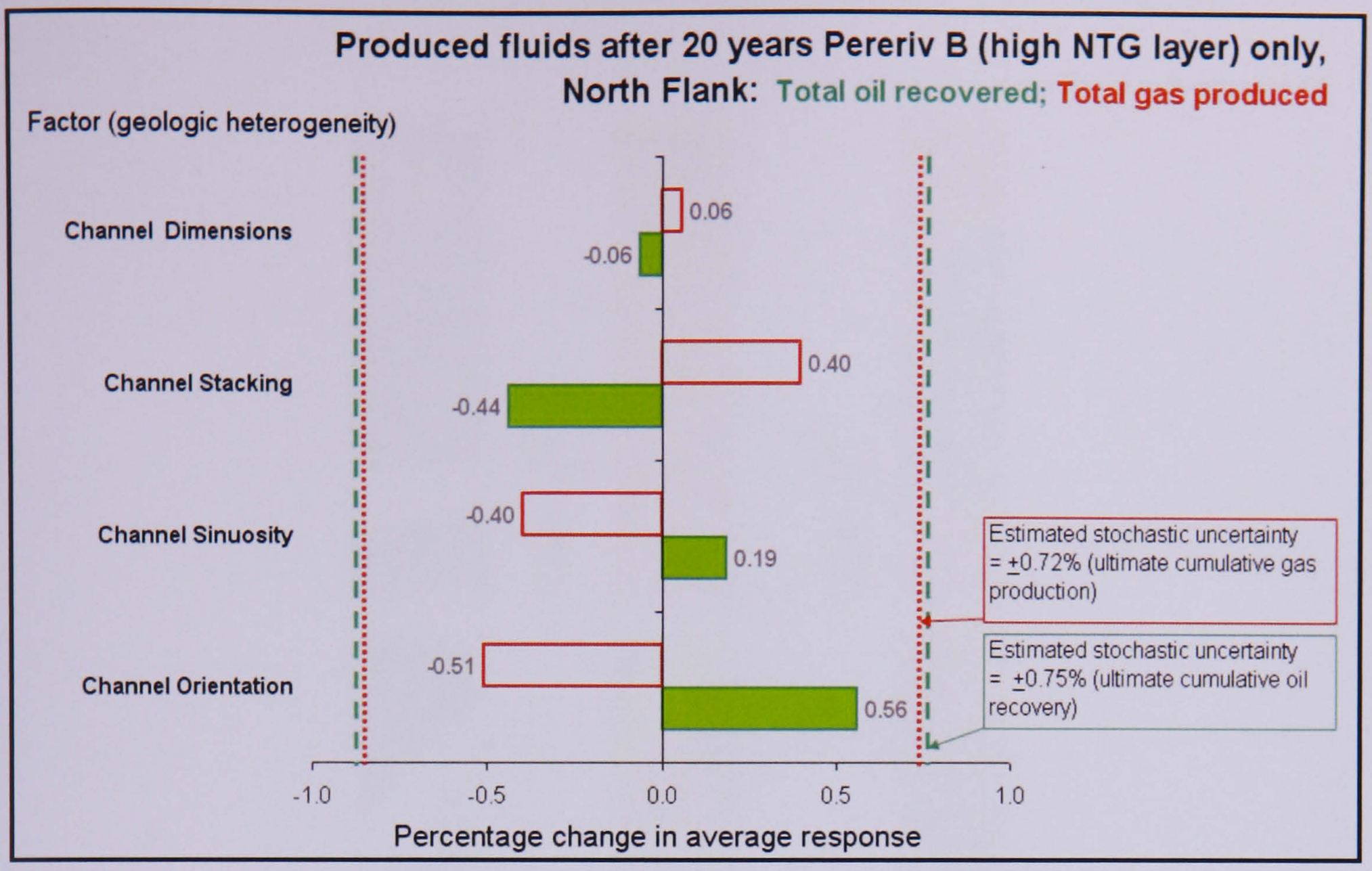


Figure 4.8A

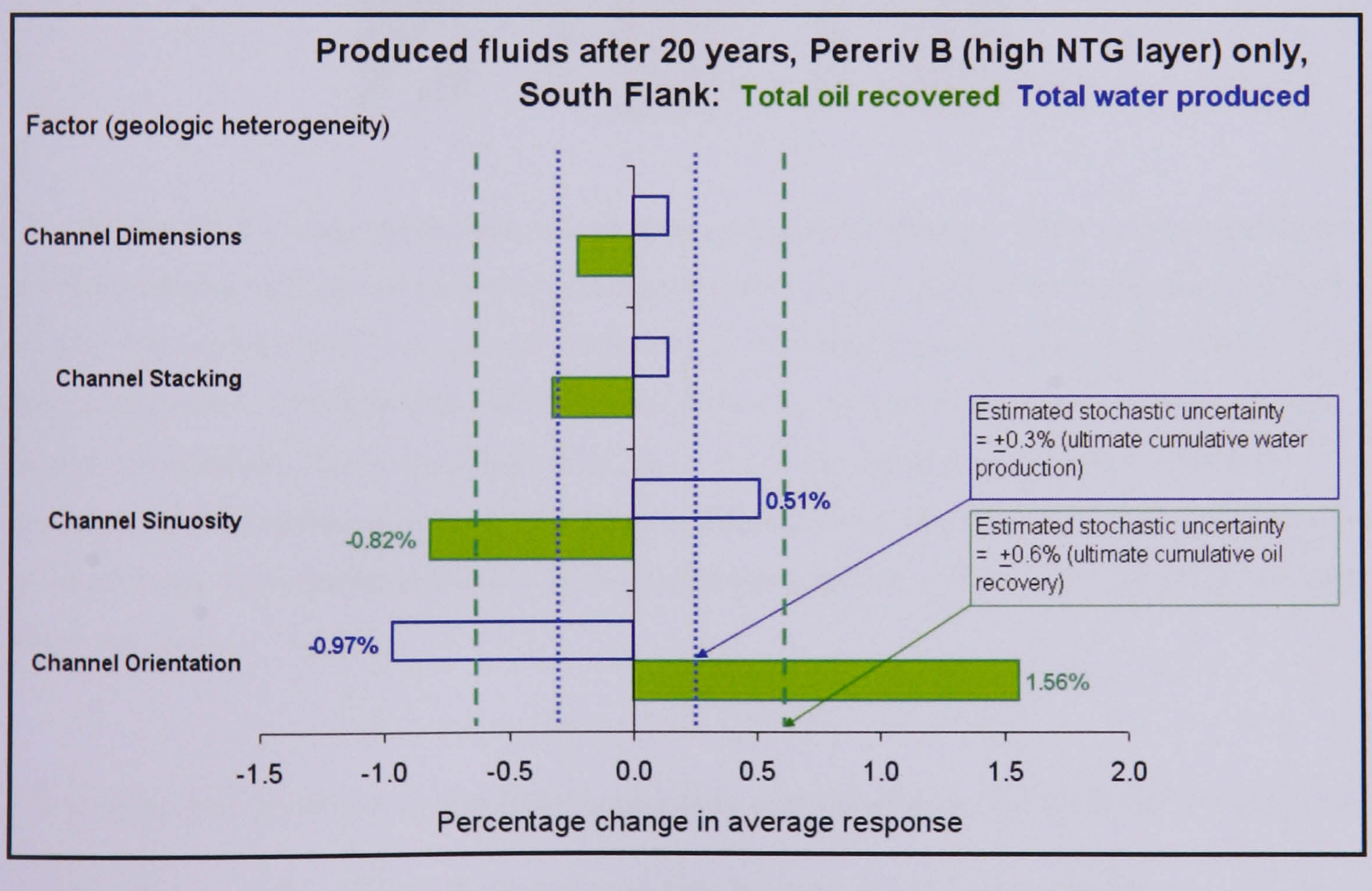


Figure 4.8B

Figure 4.8. Results of 3rd screening study (Pereriv B), average percentage change in oil recovered and total gas (north flank) and water (south flank) produced after 20 years in **(A, top)** north flank models, and **(B, bottom)** south flank models of Pereriv B only, observed when each factor in the sensitivity analysis is varied from setting 1 to setting 2 (Table 4.1).

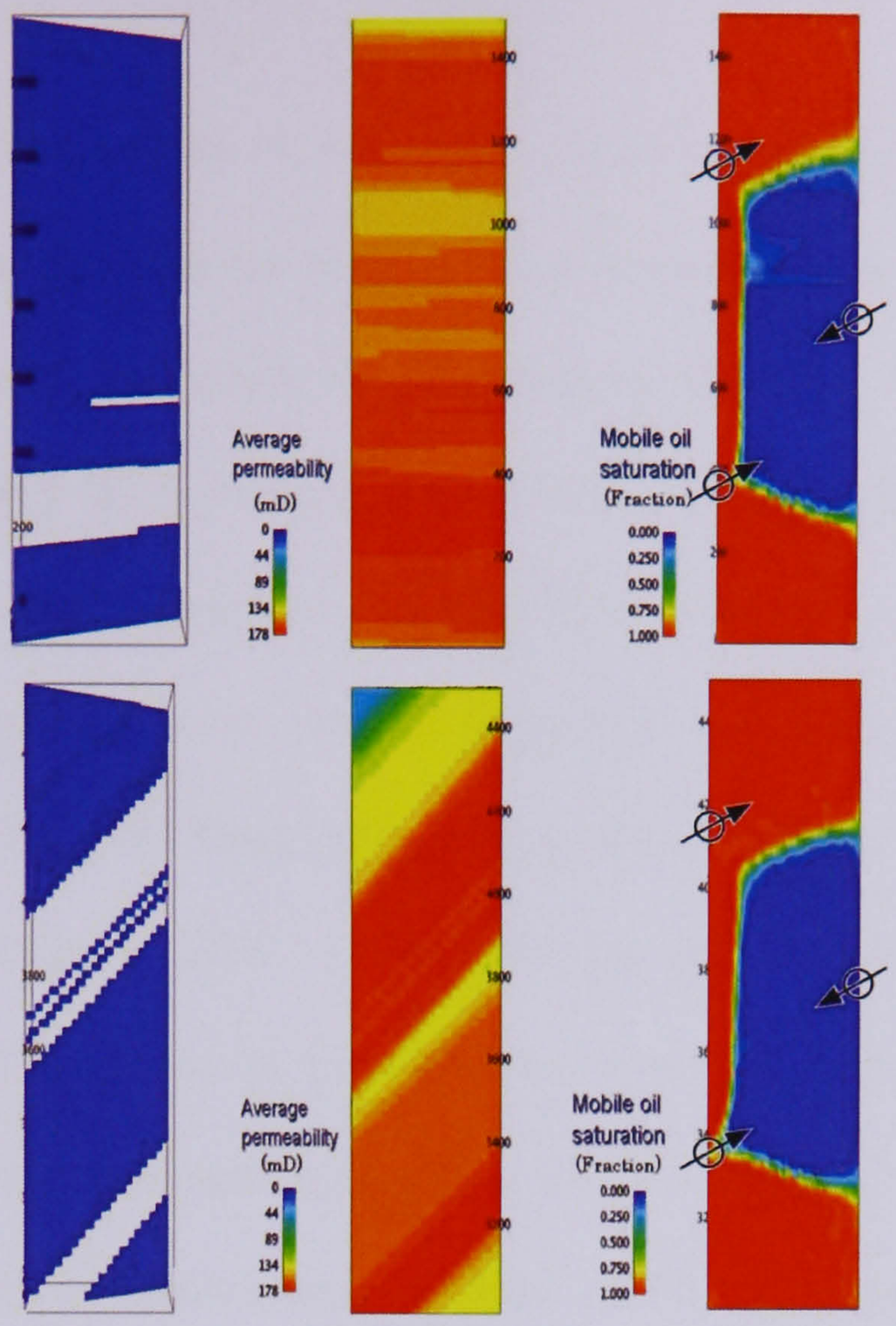


Figure 4.9. Plan views of **(left column)** shale distribution; **(center column)** thickness-averaged permeability; and **(right column)** thickness-averaged mobile oil saturation after 5 years of water injection in **(top row)** south-flank model of Pereriv B with channel belts parallel to the tectonic dip and **(bottom row)** south-flank model of Pereriv B with channel belts oblique to the tectonic dip (with a 49° offset to the east). The two producers and one injector are also labeled. The model with channel belts oblique to the tectonic dip exhibits a wider range of thickness-averaged permeability **(bottom center)**. Thus, for this model, sweep efficiency is subtly decreased because of a wider range of flow path lengths. Earlier breakthrough occurs in the model **(bottom right)** as a result of this subtle decrease in areal sweep efficiency.

The different response to the heterogeneities was related to the different mobility of water and gas. The effect of heterogeneities in high NTG layers under gas injection was relatively small because the mobility of displacing gas was much higher than that of water.

4.7.3.2. Low NTG layer: Pereriv C

Figures 4.10A to 10D show the oil recovery, cumulative GOR and cumulative water cut by gas and water injection for each of the 8 simulations conducted for the low NTG layer of the north and south flank models in the third screening study. The variation in oil recovery and breakthrough time showed the impact of the ensemble of geological heterogeneities on reservoir performance. Wide ranges of oil recovery and gas and water production were yielded from gas and water injection recovery processes, c. 40% in the north flank and c.55% in the south flank (north flank: c. 35% - 76% and south flank: c. 20% - 75% after 20 years injection). The range of cumulative GOR and water cut for both recovery processes were wide in both flank. The cumulative GOR in the north flank was c. 111% - 365% after 20 years injection. In the south flank, the cumulative water cut was c. 57% - 90% after 20 years injection. The wide ranges of recovery and gas/water production occurred because the influence of connectivity and flow path tortuosity in the low NTG layers caused some mobile oil not to be swept and recovered.

Figures 4.11A and 4.11B show the average percentage change in oil recovery and total gas and water production after 20 years of injection. The impact of varying the modelling parameters clearly had a larger magnitude compared with the results obtained from the high NTG Pereriv B layer. For example, in the north flank low NTG Pereriv C layer, channel sinuosity was the most significant heterogeneity factor on total oil recovery and gas production. Modelling straight channels decreased cumulative oil recovery by c. 35% and increased the total gas production by c. 23%; whereas all the heterogeneities had an impact below the level of stochastic noise in the high NTG layer. Similarly, in the south flank low NTG Pereriv C layer, the most

significant heterogeneity factor on reservoir performance was also the variation of channel sinuosity. By modelling straight channels, the cumulative oil recovery was reduced by c. 55% and increased the total water production by c. 23%. In contrast, channel sandbody orientation had only a small impact (below stochastic noise) on total oil recovery in low NTG layer (Figure 4.11A and 4.11B) when it was the most significant heterogeneity in high NTG layers (Figure 4.8A and 4.8B).

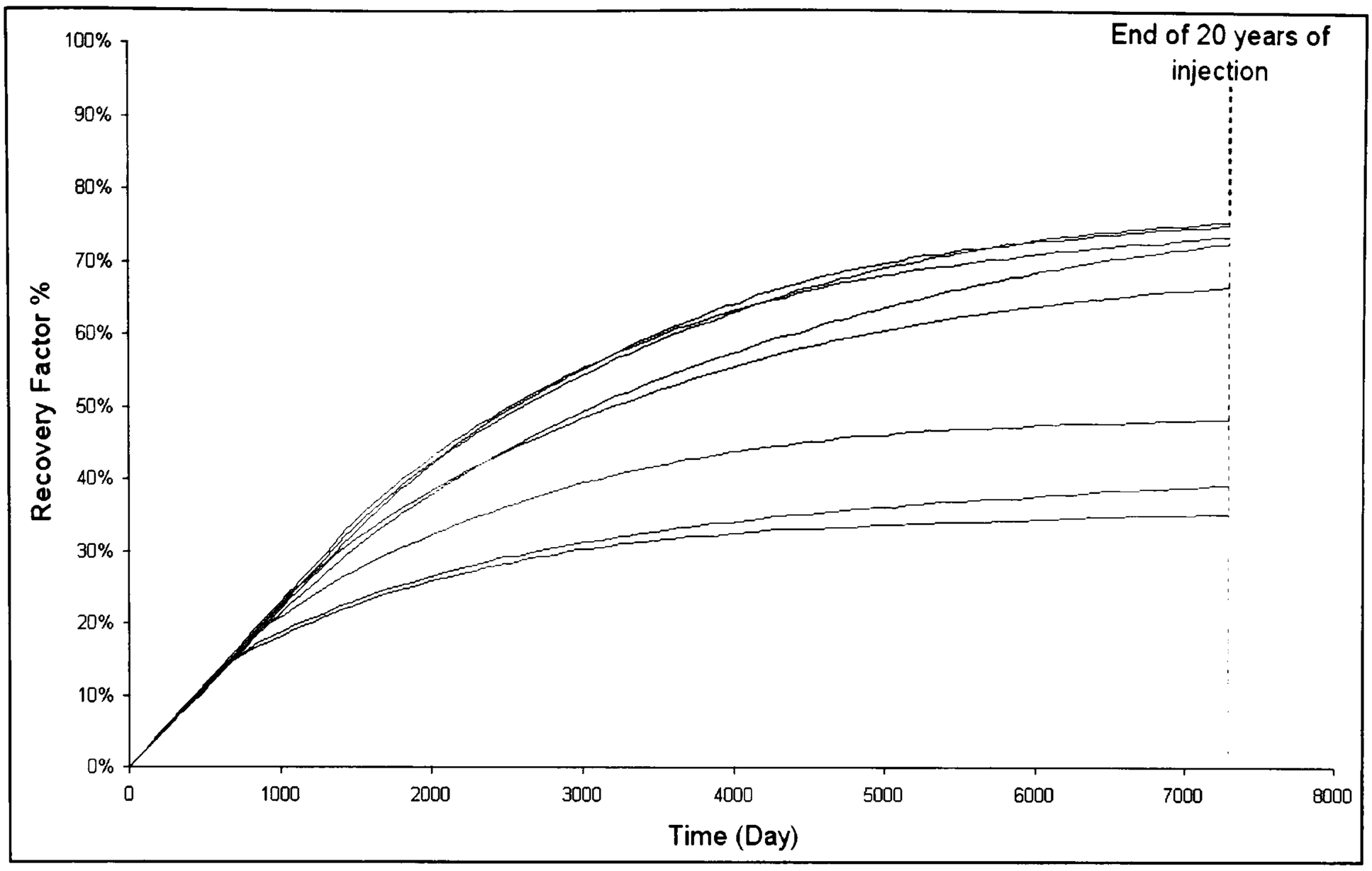


Figure 4.10A

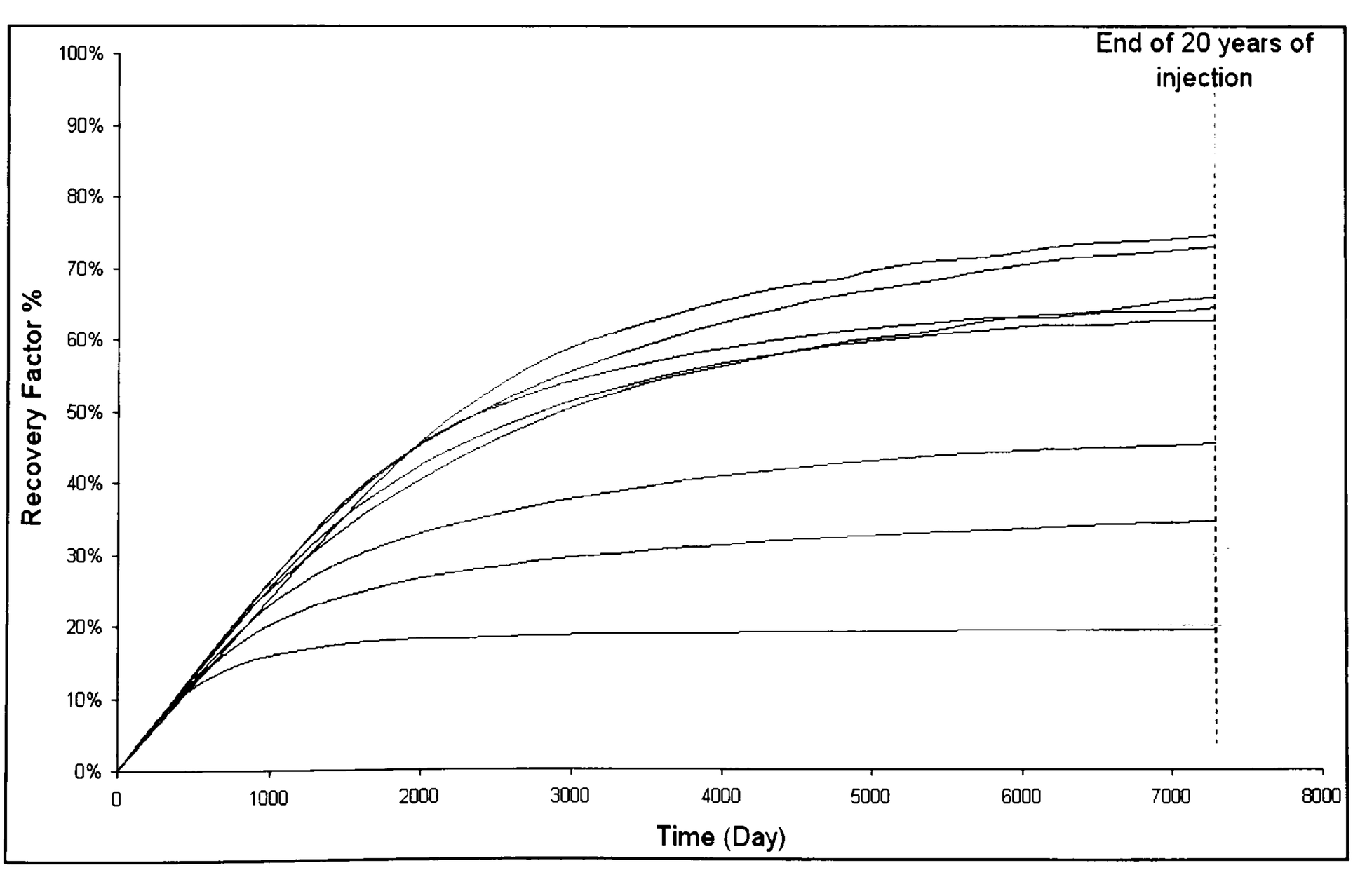


Figure 4.10B

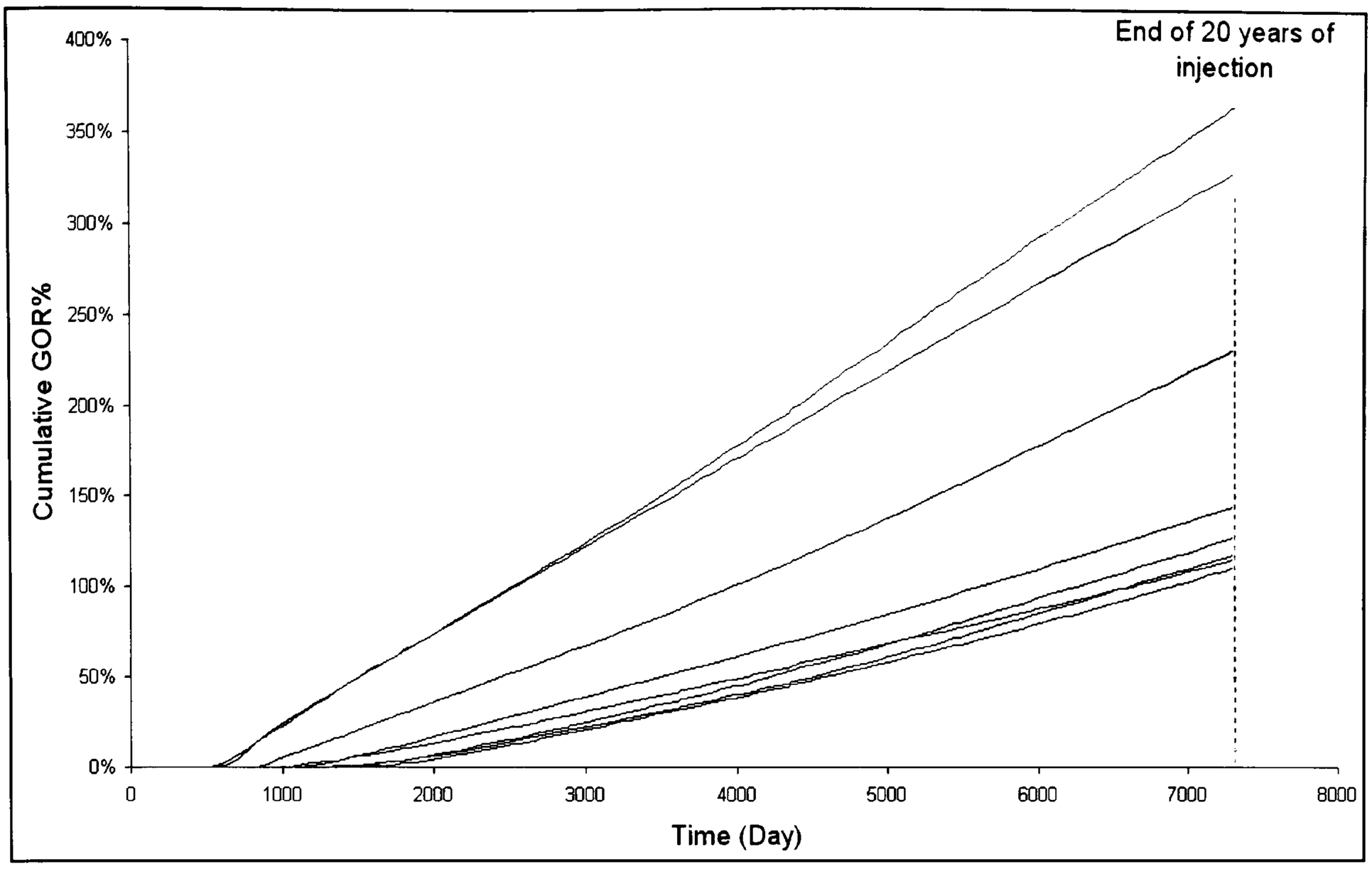


Figure 4.10C

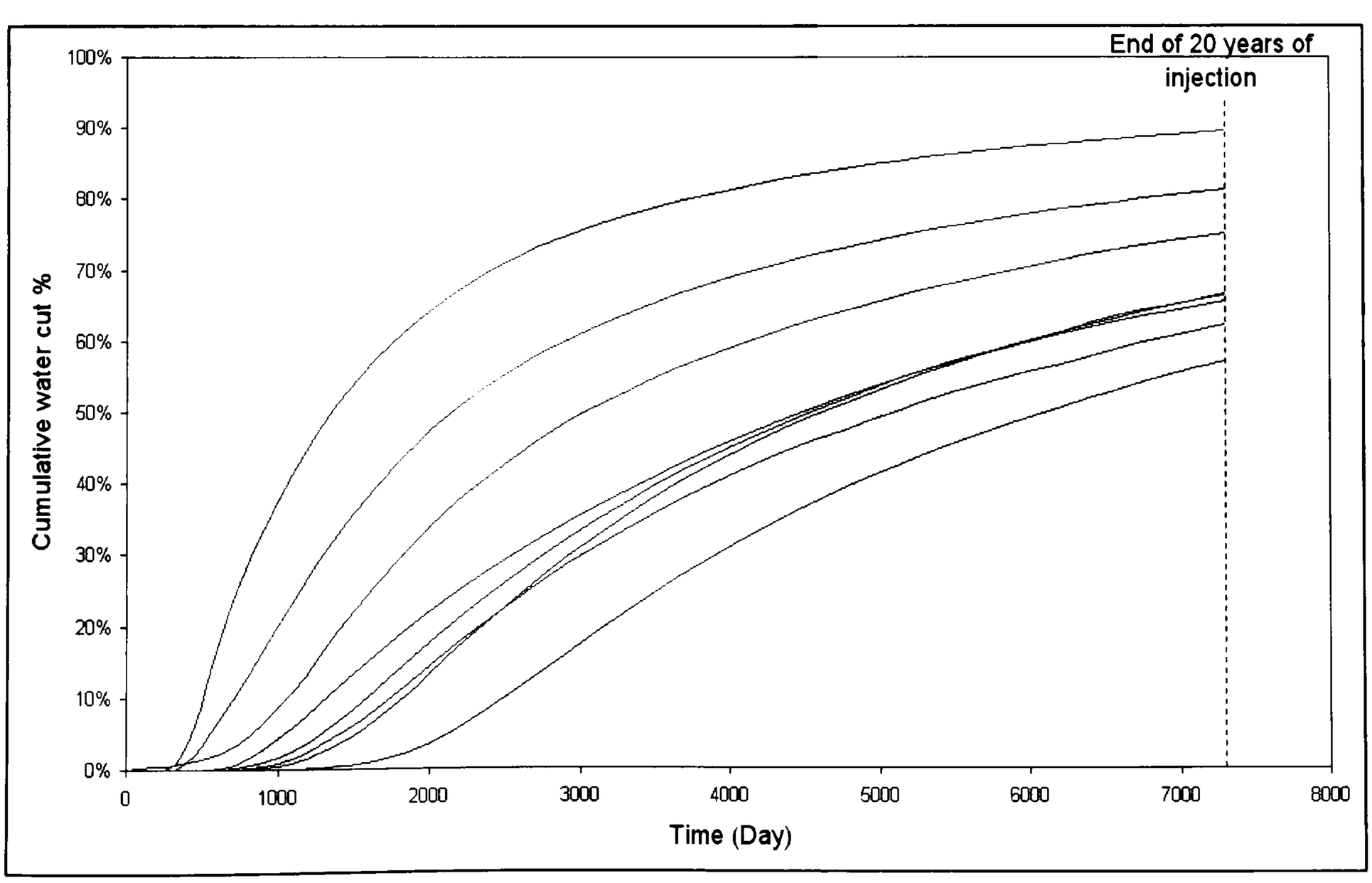


Figure 4.10D

Figure 4.10. Recovery factor, cumulative gas oil production ratio (GOR) and cumulative water cut from gas injection **(A,C)** and water injection **(B,D)** as a function of time for each of the 8 simulation experiments run in the third sensitivity analysis on the Pereriv C layers. Analysis of these curves yielded the responses shown in Figures 4.11.

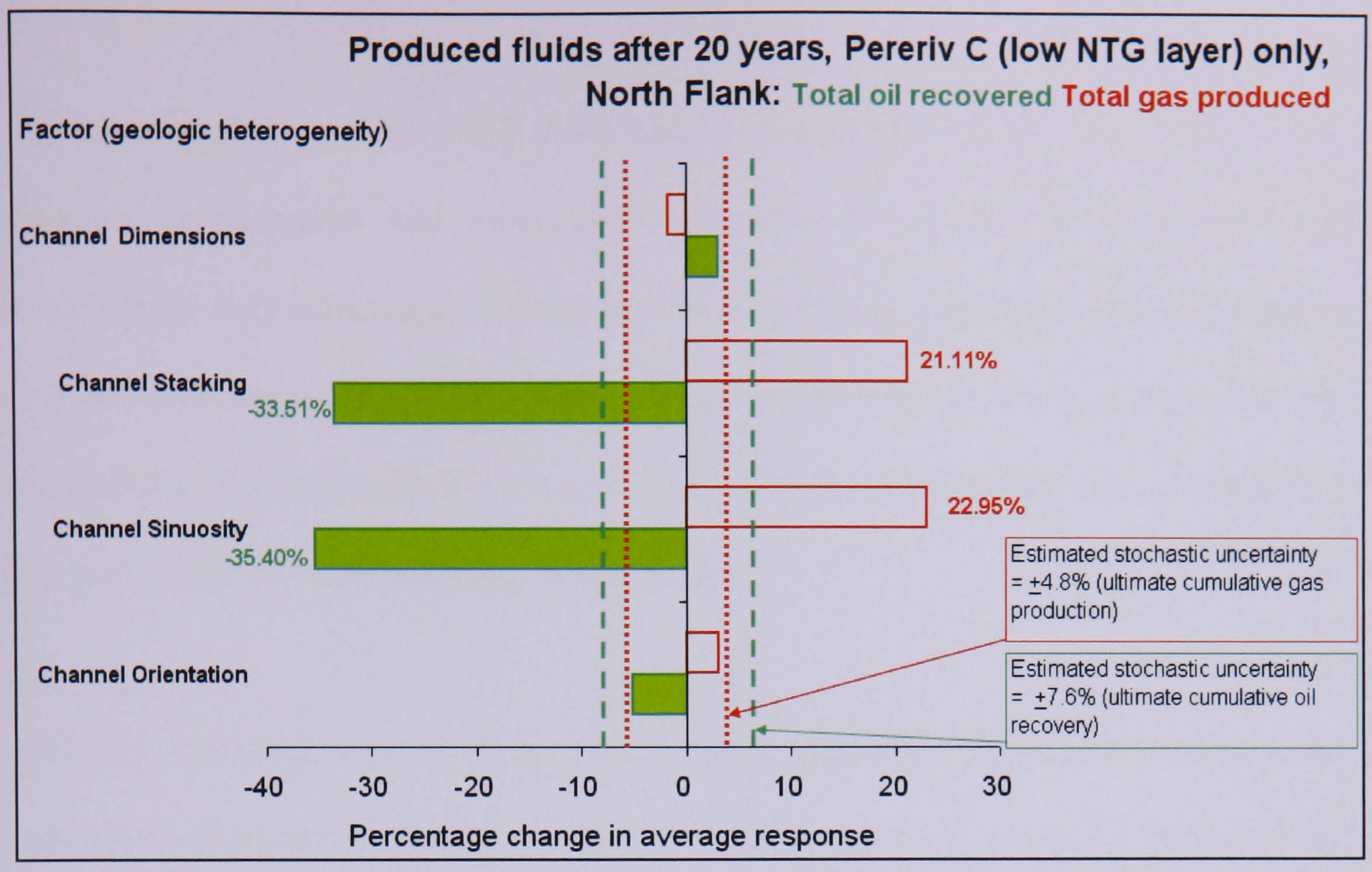


Figure 4.11A

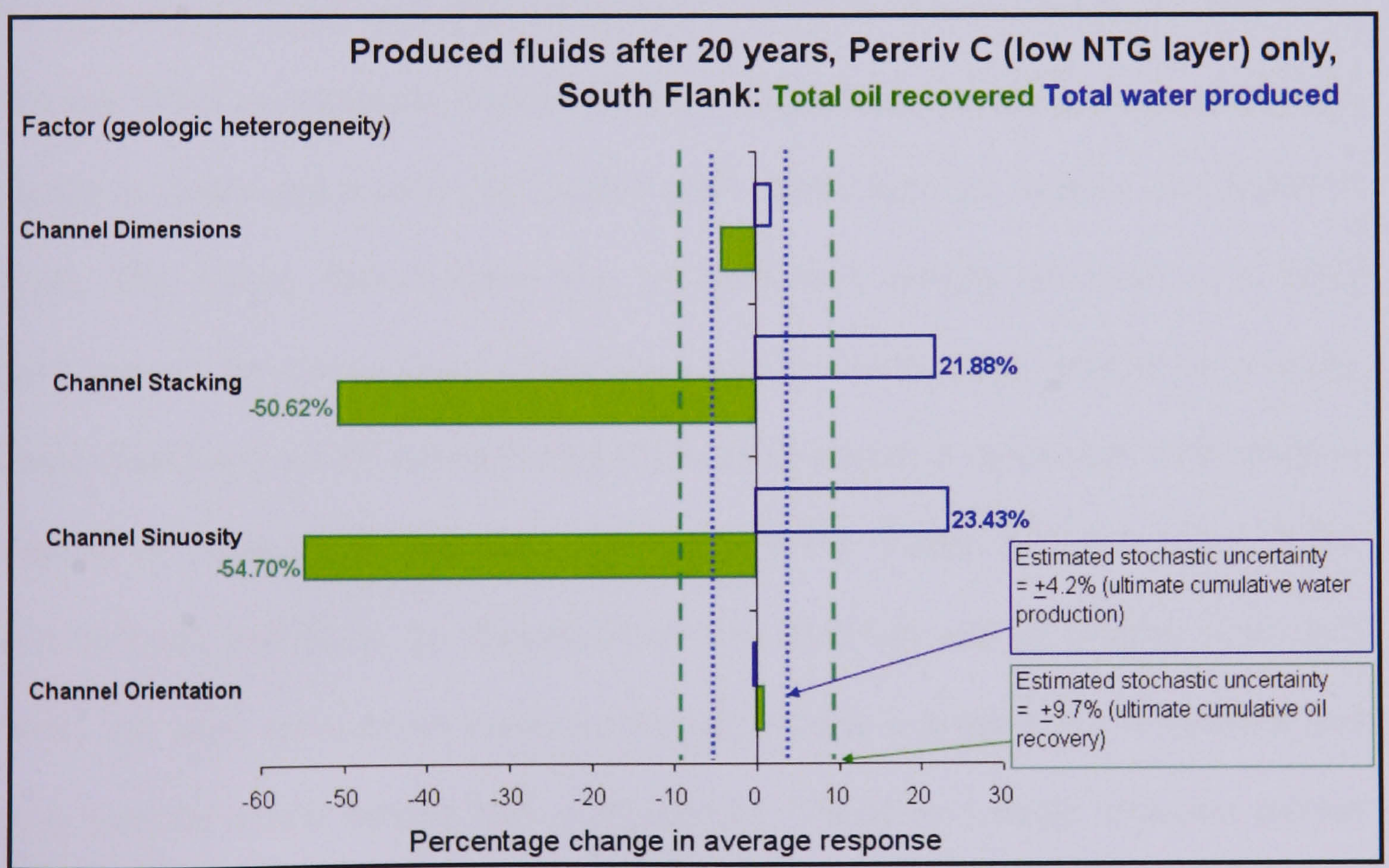


Figure 4.11B

Figure 4.11. Results of 3rd screening study (Pereriv C), average percentage change in oil recovered and total gas (north flank) and water (south flank) produced after 20 years in **(A, top)** north flank models, and **(B, bottom)** south flank models of Pereriv C only, observed when each factor in the sensitivity analysis is varied from setting 1 to setting 2 (Table 4.1).

As mentioned in section 4.6.3 these results underestimated the true range of the reservoir architectures and associated production behaviours. It is because the investigation only selected the realizations in which there was connectivity of channel sand between the injector and at least one producer well. In many realizations, the connectivity between wells was zero; in some models, well location was adjusted by a few grid blocks in order to ensure connectivity.

Channel sinuosity was found to be the most significant factor that controls the reservoir performance under both gas and water injection schemes, followed by channel stacking pattern. The variations in channel sinuosity significantly changed the connectivity of the channel sand bodies between the injector and production wells in a low NTG environment. Figures 4.12A and 4.12B shows the average percentage change in connected fraction of channel sand bodies between injector and producer wells. The results demonstrated that by modelling straight channels in a NTG environment, the connectivity of the sand and the wells were reduced by c. 9.5% (north flank) and c.22% (south flank). These results were in agreement with previous studies of channelized reservoirs with low NTG. Larue and Hovadik, (2006) demonstrated that when the channels have low sinuosity and are parallel with each other, the areal intersection between channels within a given layer is reduced and such systems would behave like a 2D system. Therefore straight channels caused poor connectivity.

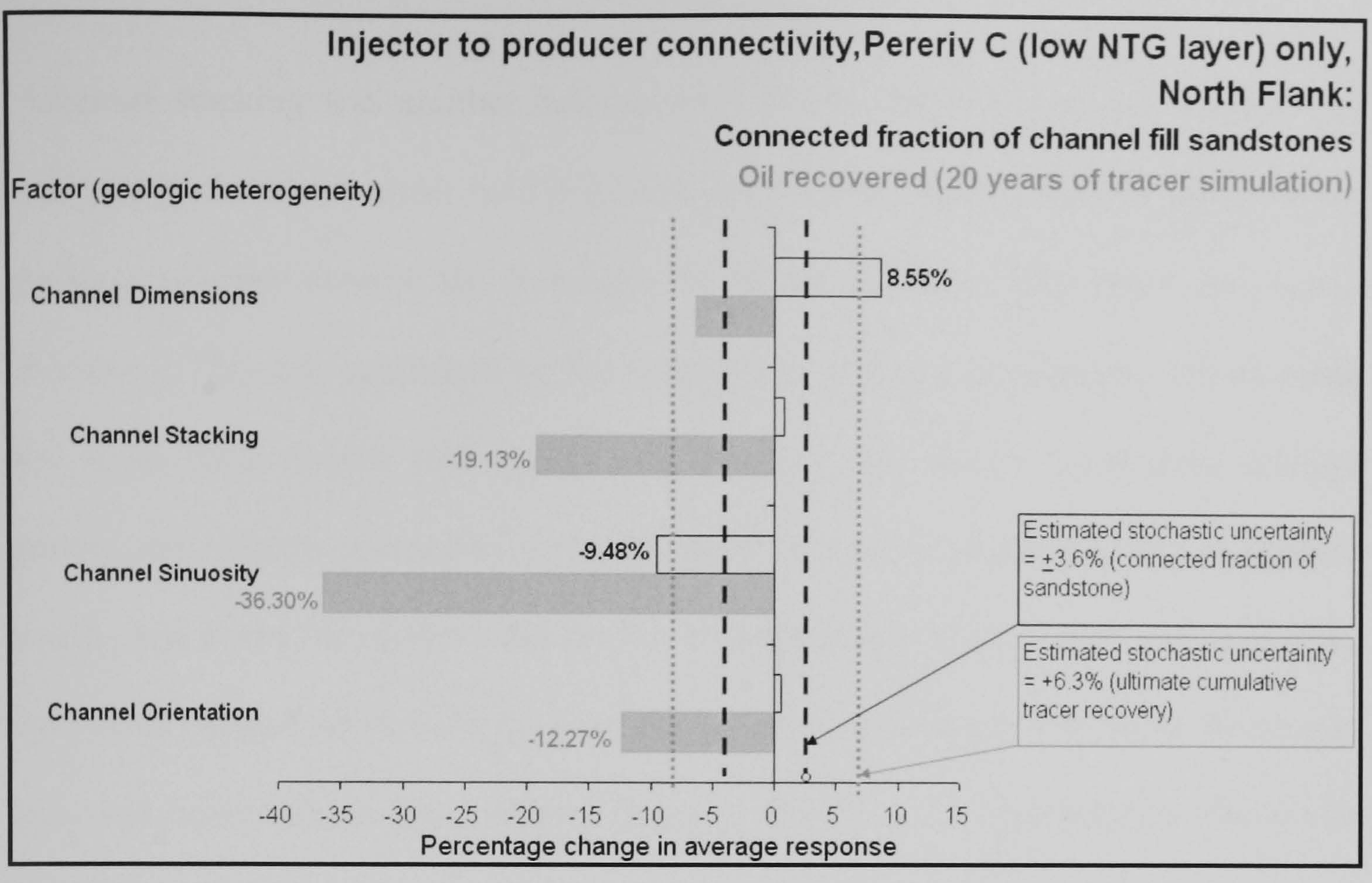


Figure 4.12A

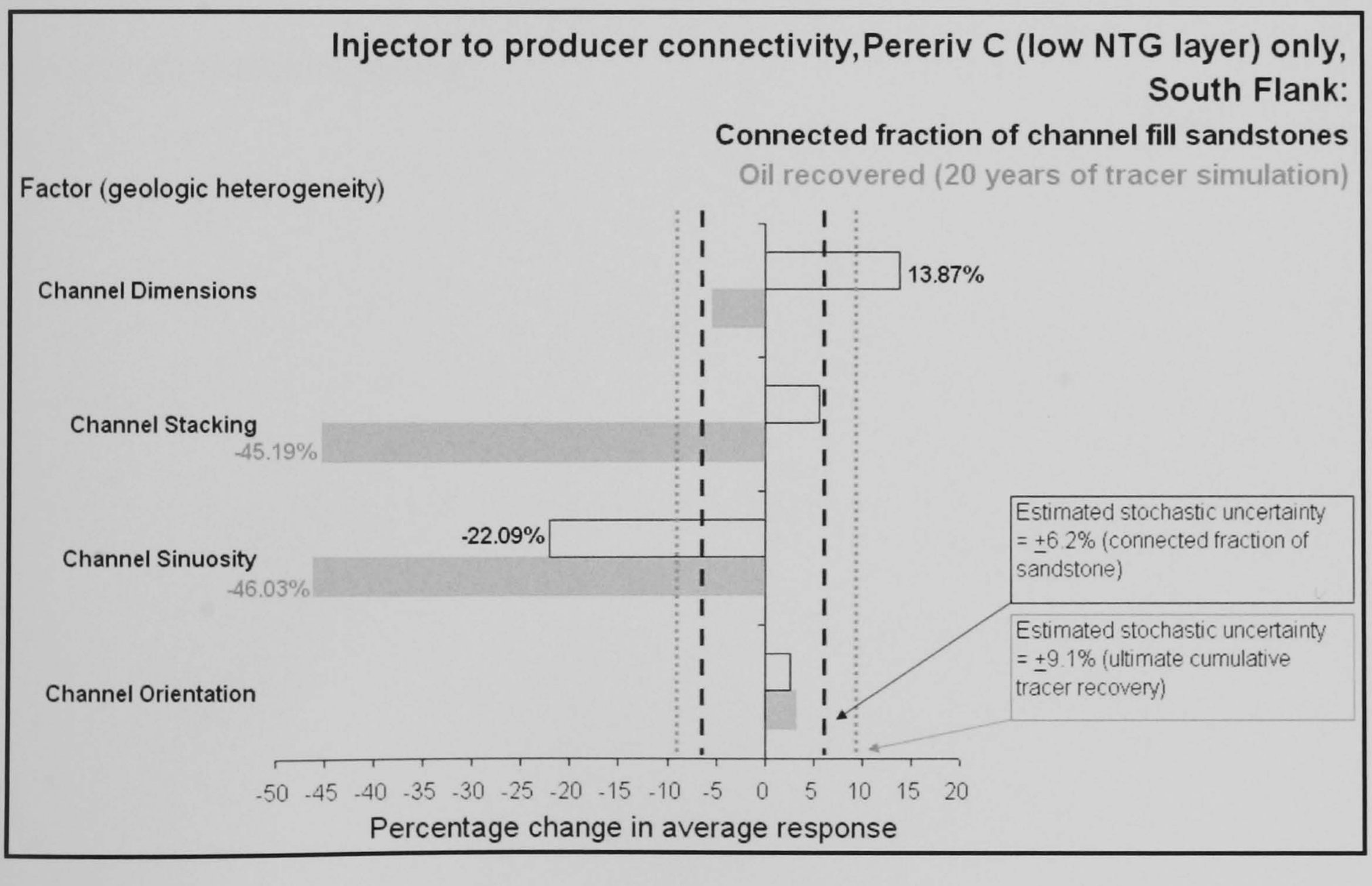


Figure 4.12B

Figure 4.12. Results of 3rd screening study (Pereriv C), average percentage change in connected fraction of channel-fill sandstones between injection and production wells, and oil recovered after 20 years of tracer injection, in (**A, top**) north flank models, and (**B, bottom**) south flank models of Pereriv C only, observed when each factor in the sensitivity analysis is varied from setting 1 to setting 2 (Table 2).

Channel stacking was another heterogeneity factor that had significant impact on reservoir performance under both displacement schemes. This is because the different stacking patterns control the tortuosity of the flow paths, and hence the sweep efficiency. This was confirmed by the comparison of tracer simulations in both north and south flank models (see Figure 4.12A and 4.12B) Tracer simulations omitted gravity and relative permeability effects and they were a measure of the streamline lengths and hence the results reflected the flow tortuosity. It was found that modelling individual channels decreased the recovery in tracer simulations. Therefore the results indicated reduction of the sweep efficiency. Figure 4.13 demonstrates the tracer saturation plot in models with individual channel and multistorey channel belts. It was found that models containing individual channels had a more tortuous flow path, so more oil remained unswept.

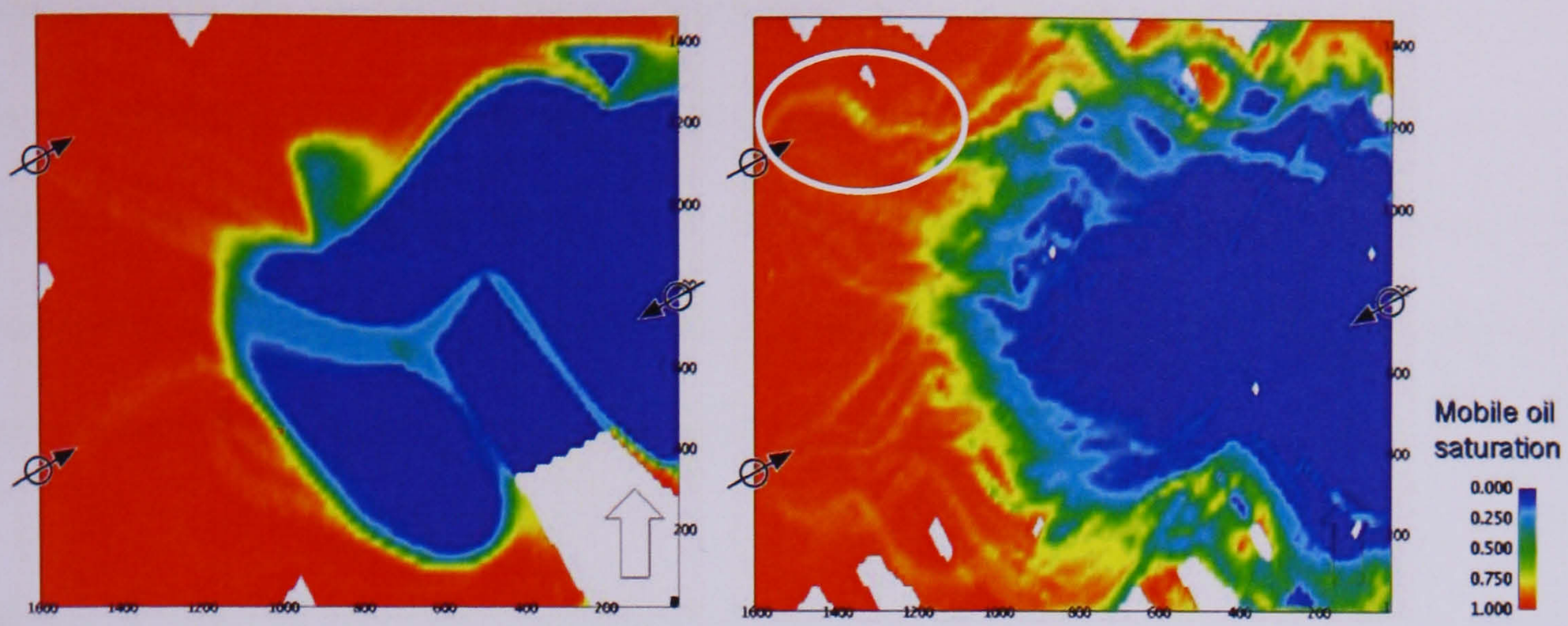


Figure 4.13. Plan view of thickness-averaged oil saturation after 5 years of tracer injection in **(left)** north-flank model of Pereriv C with multistorey, channel-belt sandbodies and **(right)** north-flank model of Pereriv C with individual, single-storey channel-fill sandbodies. The two producers and one injector are labeled. Where the figures show thickness averaged mobile oil saturation less than 1 indicated that one or more layers at that location is occupied by the injected fluid. This plot could enable identification of individual flow paths within the model (e.g. a flow path of injected fluid moving towards the producer was identified by a white circle). Flow paths in the single-storey model **(right)** were more tortuous, resulting in poorer areal sweep of the oil. Therefore, earlier breakthrough results from modelling single-storey channel-fill channel sandbodies. Hence, the cumulative oil recovered is lower for such a modelling setting. On average when single-storey channel-fill sandbodies were modelled, oil recovery was c. 19% lower than in when multistorey channel-fill sandbodies were modelled.

4.8. Discussion

4.8.1. Impact of NTG variation in Pereriv C

From the first screening study (section 4.7.1), it was found that in general the recovery from models that contained Pereriv B, C and D was high and the range of recovery was small. This was because the recovery was dominated by the high NTG layers where all the sand were connected and the layer had low tortuous flow path. From the third screening study on Pereriv B layer in isolation (section 4.7.3.1), it was found that modelling decisions in the high NTG layer affect recovery by less than 2%. The variations in recovery from Pereriv Suite models were dominated by the

variations in the modelling approach adopted in the low NTG Pereriv C. Since this layer contributes to a relatively small proportion of the total recoverable oil, its impact on the overall recovery was small. The overall cumulative oil recovery increased if there was net sand present in Pereriv C because of the larger amount of oil volume in place; however the recovery factor was reduced.

4.8.2. Impact of interlayer connectivity

When there was communication between low NTG Pereriv C and high NTG Pereriv B and D layers, therefore the cumulative oil recovery increases. Moreover, the production of injected water or gas was reduced. This suggested that having communication between layers with different NTG did not penalize production. Some realizations of the low NTG Pereriv C layer models had zero connectivity between injector and producer. In such a case, interlayer connectivity enhanced oil recovery, because sand bodies within the low NTG layer could be connected with the high NTG layer and hence provides pressure support and a flow path to produce the oil in the low NTG layer. By simulating recovery from high and low NTG layers alone, it was possible to gain understanding of the key heterogeneities which controlled the displacement in each environment without being affected by another layer. For example the impact of heterogeneities in Pereriv C on production was masked by co-mingling with the larger and more productive Pereriv B and D layers. The effects of inter-layer heterogeneities are discussed below.

4.8.3. Impact of heterogeneities within low NTG layers

The results in this chapter demonstrated that modelling decisions in the low NTG layer (Pereriv C) had a much higher impact on oil recovery compared with the high NTG layers (Pereriv B and D). Channel sinuosity and stacking pattern were found to be the two dominant factors that influence oil recovery in this low NTG environment. The variation of channel sinuosity was important to the cumulative oil recovery as it controls sand body connectivity. Whereas the variation of the channel stacking pattern controls the flow path tortuosity and hence the sweep efficiency. The results from the screening study on Pereriv C were consistent with previous studies on channelized reservoirs with low NTG (Jones et al. 1995; Larue and Hovadik 2006). Although Pereriv C contributes only a small fraction of the total production in Azeri, the screening study results from Pereriv C could be applied in similar fluvial deltaic environments with low NTG, for example the overlying Balakhany reservoirs in the ACG field and other reservoirs with low NTG in the southern Caspian Basin.

4.8.4. Impact of heterogeneities within high NTG layers

As mentioned in section 4.8.1. modelling decisions in high NTG layers had a small influence on oil recovery. There was only a subtle variation in areal and vertical sweep efficiency that depended on channel orientation and stacking pattern. When models contained individual channel storeys which were oriented obliquely to the tectonic dip, the flow paths were more tortuous than in models containing multistorey channel belts that were oriented parallel to the tectonic dip. Since the latter models provided a direct flow path between wells, the recovery of models with individual

channel sand bodies oriented obliquely to the dip yield a slightly lower recovery (Figure 4.9).

In the north flank high NTG screening studies (gas-oil displacement), all the models yielded high recovery with insignificant impact of heterogeneities (Figure 4.8A). It was found that the impact of heterogeneities on recovery under gas-oil displacement was below stochastic noise. This is mainly due to the high mobility of the displacing gas. In the south flank high NTG screening studies (water-oil displacement), heterogeneities had a larger but still small impact. Indeed, the mobility ratio had a large impact on recovery in high NTG reservoirs. The results in high NTG layers from this chapter were similar to those obtained by Larue and Friedmann (2005) These workers investigated the reservoir architecture (channel sandbody geometry and spatial distribution) and permeability heterogeneity (variation in permeability within channel sandbodies) on waterflooding in channelised reservoirs. They found that in a high NTG environment the reservoir architecture had only a small impact on water-oil displacement, as its connectivity is high. However, in their research the impact of gravity forces was not significant. The most important control on recovery was found to be the end-point mobility ratio. In Chapter 5, an investigation will be conducted to study the impact of different mobility ratios in reservoir models that contain more detailed geological features within high NTG layers during recovery by gas-oil displacement.

4.8.5. Impact of different displacement schemes

It was found that in most cases, the same heterogeneities had a significant impact on both gas-oil and water-oil displacements. This might be because both displacements

are stable (the water-oil displacement is mobility stable in the south flank and the gas-oil displacement was stabilized by gravitational forces in the north flank). This explanation was supported by the results of applying single phase tracer simulations. Figures 4.14A and 4.14B show that tracer simulations produced a very similar rank order of key heterogeneities in both flanks. This suggested that when the two different displacement schemes were considered to be stable (either mobility stable or gravity stable) they would yield the same interaction with heterogeneity. Therefore the stability of a displacement could be one of the most important factors that controls its interaction with heterogeneity. Another possible explanation was that the variation in recovery was dominated by sand body connectivity and the tortuosity of the flow path, and that the displacement stability had only a small impact on the ranking order of the heterogeneity factors. This interpretation suggested that even if the displacement was unstable, a similar response would be obtained. In Chapter 5, an investigation will be conducted to study the impact of geological heterogeneity on gas-oil displacements under different stability conditions.

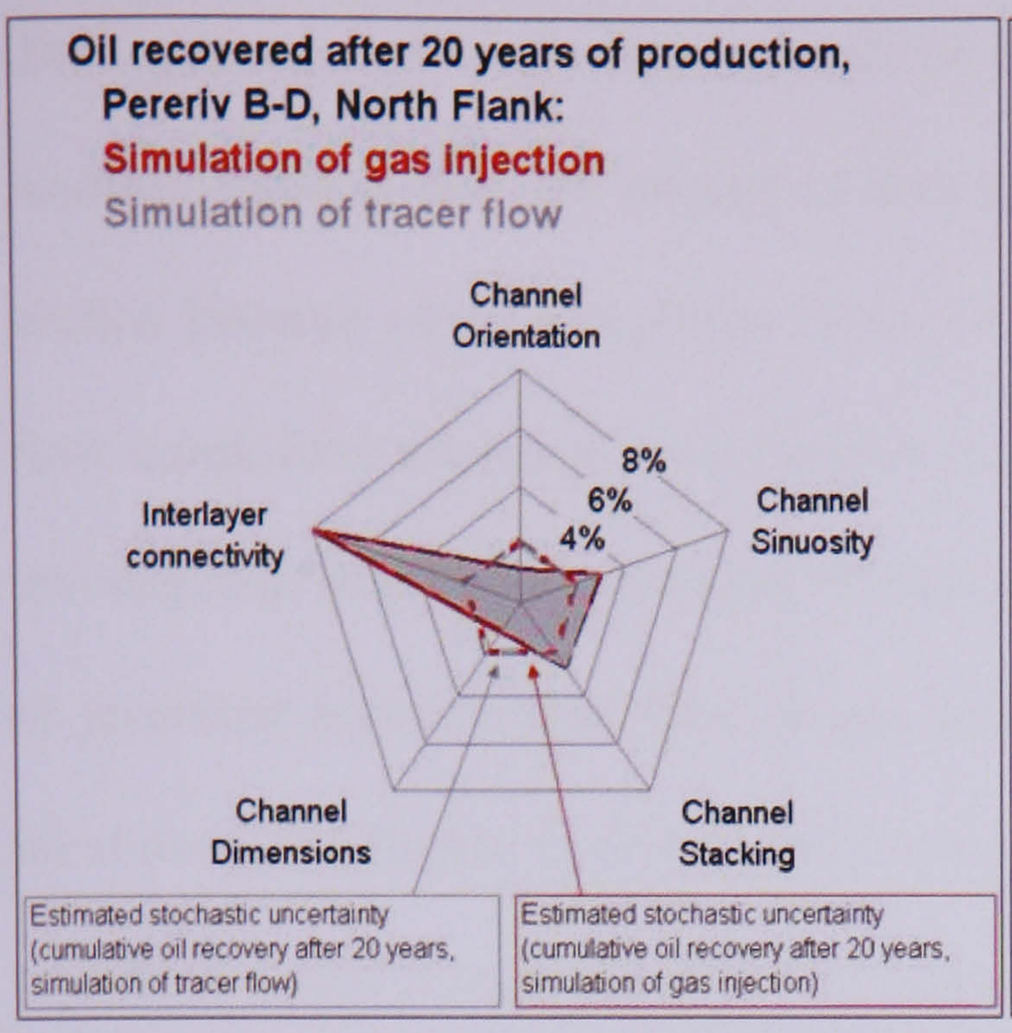


Figure 4.14A

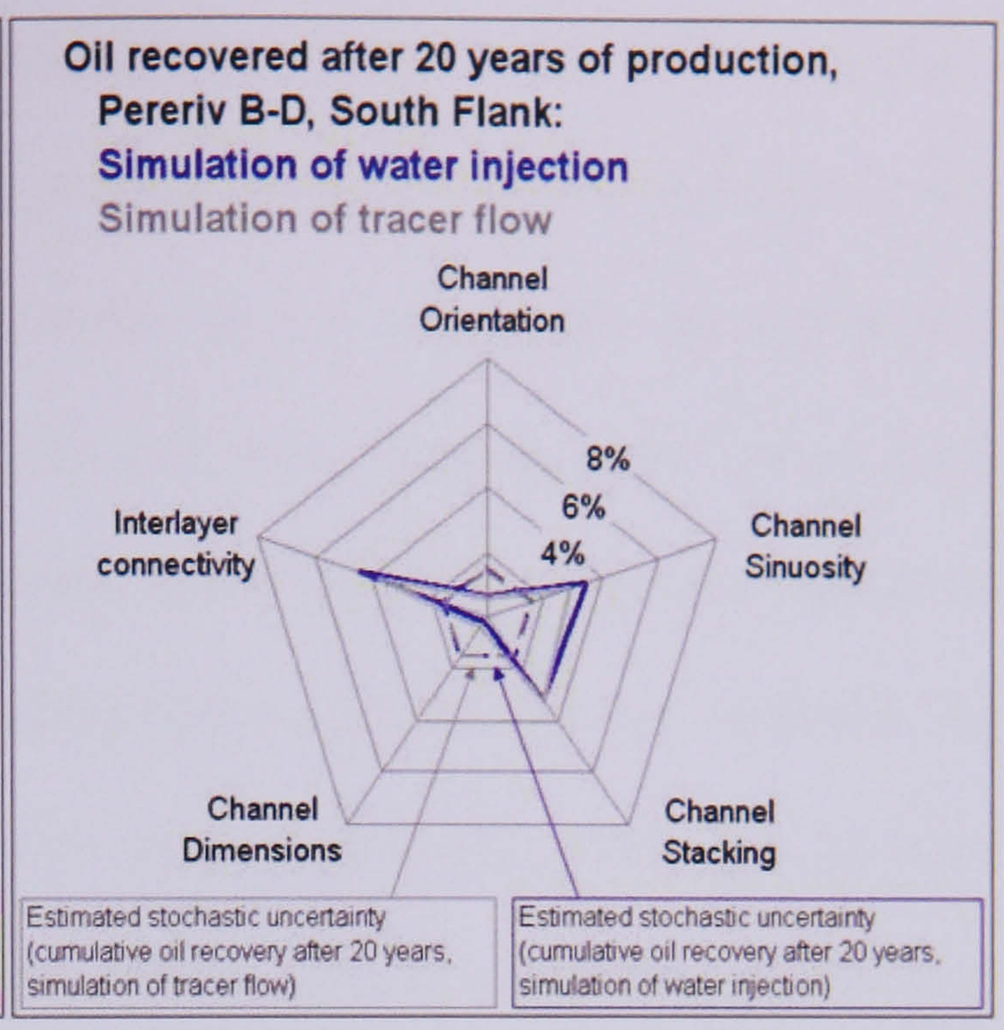


Figure 4.14B

Figure 4.14. Impact of different heterogeneities on flow within Pereriv B, C and D in **(A, left)** the north flank and **(B, right)** the south flank. Absolute percentage change in oil recovered after 20 years was plotted as distance from the center of the chart for each heterogeneity, to enable comparison between the previous simulations of tracer flow, gas injection, and water injection. The area around the center of each chart represents the average percentage change observed from different stochastic realizations. The tracer simulations captured the ranking order above stochastic uncertainty for both gas-oil and water-oil displacements, suggesting that gravity segregation, and relative permeability effects, were small.

4.8.6. Wider application to ACG reservoir.

In this chapter the reservoir-unit scale heterogeneities have been studied. However, the models were relatively simple, thus the results should be interpreted accordingly. A number of the heterogeneities at genetic-unit scale were not modelled in this chapter. For example, upward-fining trends within channel sandbodies may affect sweep efficiency; also mud-clast lags along channel bases can significantly reduce the effective vertical permeability. Moreover, the permeability heterogeneity within sand bodies (Kv:Kh) has also been demonstrated to significantly control recovery during water flooding (Friedmann et al., 2001; Larue and Friedmann, 2005). Therefore all

these genetic-unit scale heterogeneities will be investigated in the next chapter. Another issue is that the impact of heterogeneities could be underestimated in this section because of the simplified flow conditions applied. Simulating incompressible flow conditions means that the impact on the reservoir pressure cannot be properly investigated. In addition, because of simulating 'dead oil' PVT properties, variations of reservoir pressure that lead to gas evolving from solution are not captured. As mentioned in Chapter 1, with Azeri's reservoir pressure at bubble point, any pressure reduction would release gas from the solution, thus producing a significant volume of gas. In Chapter 5, the impact of modelling more realistic fluid properties will be assessed.

4.9. Conclusion

This part of the project has investigated the impact of the reservoir-unit scale heterogeneities that are found in fluvial deltaic environments on gas and water flooding under simplified PVT assumptions.

The following is a summary of the findings in this section:

- The local variation in NTG within Pereriv C and the interlayer connectivity between low NTG layers and the adjacent high NTG layers are the principal controls on oil recovery under both gas and water injection scheme.
- In most cases, the same significant heterogeneities impact are found in both water and gas displacements because both displacements are stable at the planned production rates.

- When sand is present in low NTG layers, the overall recovery increases because it locally increases the STOIIP. However the overall recovery is reduced because of poor sweep efficiency and sand bodies connectivity within the low NTG layers.
- In regions that have net sand in the low NTG layer, recovery is increased if there is communication between the high and low NTG layers. This is because the sand bodies are poorly connected to the wells, so if there is communication between adjacent high and low NTG layer, the pressure support from adjacent high NTG layers to improve the overall recovery. There is also an associated benefit in the reduction of the production of the injected water or gas.
- In the low NTG layers, it is found that recovery is primarily controlled by the connectivity of the channel sand bodies to the wells, and by sweep efficiency within the connected sand bodies.
- Channel sinuosity is found to be the factor that controls the connectivity of the sand bodies to injector and producer wells. The connectivity increases as the channel sinuosity increases.
- Channel sand body stacking pattern is found to be the factor that controls the sweep efficiency within connected sand bodies. The sweep efficiency increases when the channel sands are stacked together to form multistorey channel belts.
- Geological heterogeneities within high NTG layers have only a relatively small impact on recovery when genetic-unit scale features are not considered.

- The variation in channel sandbody orientation and stacking pattern subtly controls the areal and vertical sweep efficiency within high NTG layers and hence recovery is affected by these parameters.

Chapter 5
Combined screening study of genetic-unit and reservoir-unit scale heterogeneities

5.1. Overview

The investigation in the previous chapter was to find which geological heterogeneities at reservoir-unit scale have the most significant impact on total oil recovery and total gas/water production. It was demonstrated that geological features such as inter-layer connectivity, channel sinuosity and the variation of channel stacking patterns have significant influence on oil recovery, because these features control the connectivity of the sand bodies and the tortuosity of the resulting flow paths. However, in high NTG reservoir layers none of the reservoir-unit scale heterogeneities had a significant influence on displacement. Does this mean that it is possible to model these layers as homogeneous?

At the genetic-unit scale (Chapter 2), the distribution of internal barriers or permeability zonation controls the vertical and areal sweep efficiency (Jones et al. 1994; 1995). This chapter compares the influence of heterogeneities at different scales on reservoir performance. This chapter also identifies which genetic-unit scale heterogeneity has the largest impact on reservoir performance and investigates when genetic-unit scale heterogeneity factors are modelled, whether or not reservoir-unit scale heterogeneities have significant influence on the reservoir performance.

From the outcrop analogues (Balakhany Quarry and Yasamal Valley, see Chapter 2) and core data collected from the Azeri Field (Reynolds et al. 2003; Reynolds and Riley 2003), a number of geological features at smaller length scales (genetic-unit scale) were observed. Typical features include mud-clast lags at channel bases, upwards-fining grain size trends, impermeable shales, and variable ratio of vertical permeability to horizontal permeability (Kv:Kh). Previous research has demonstrated that the internal geological features within a channel sand body can have a large influence on displacement (e.g. Weber 1986; Jones et al. 1994; Jones et al. 1995; Hartkamp-Bakker 1993; Ringrose et al. 1993).

Geological heterogeneity at genetic-unit scale potentially has an influence on displacement. For example, a mud-clast lag at a channel base, because of its low permeability, may act as a vertical flow barrier, or increases the vertical flow tortuosity. This effect is similar to that of discontinuous shales on displacement (Haldorsen and Lake 1984; Begg et al. 1985; Begg and King 1985; Haldorsen and Chang, 1985; Begg et al. 1987). Other researchers (Richardson et al. 1977; Jones et al. 1994) also suggested that during an immiscible displacement, oil is often bypassed by the displacing fluid in regions close to isolated shales. Fayers and Muggerldge (1990) and Shook et al. (1992) have shown that the variation in Kv:Kh within a sand body has a direct influence on the vertical equilibrium. The vertical equilibrium (VE) represents a stage of maximum cross flow occurring in the vertical direction (Shook et al 1992). The Shook et al. (1992) suggested it is necessary to include such features in flow simulation studies, because they can influence the breakthrough time and cumulative oil recovery prediction.

Within any point of the Azeri Field the reservoir pressure is at the bubble point pressure. Any pressure reduction would result in gas coming out of solution. In the previous chapter, a simplified fluid PVT description (e.g. incompressible flow and fluids properties independent of pressure) was used. However, using a more realistic fluid PVT description such as gas evolved from solution when reservoir pressure dropped below the bubble point pressure may influence how the reservoir performance responds to the geological heterogeneity. In this chapter, a realistic fluid PVT description of the Azeri Field was applied in the screening study in order to compare the results with those of the simplified fluid PVT description. The impact of different fluid PVT description is thus understood. As discussed in Chapter 3, the stability of gas-oil displacement was controlled by the balance of gravity force and viscous forces, which is influenced by the offtake rate. In last chapter, the same rank order of influence of heterogeneities on both water and gas displacement was found. It was hypothesized that the reason was due to the stable displacements in both cases (water-oil displacement is mobility stable, and the gas-oil displacement is gravity stable for the proposed offtake rate). Under different stability conditions, the geological heterogeneity factors may have a different degree of influence on the displacement. For example, previous work (e.g. Weber 1986; Haldorsen 1986 and Fayers and Muggerldge 1990) showed that vertical flow barriers or a lower Kv:Kh ratio can have a positive influence on gravity unstable displacements, by increasing the vertical sweep efficiency. However such factors may have a negative influence on a gravity stable displacement. Therefore , there is a need to investigate the response of both gravity stable and unstable displacement with different heterogeneities. In this chapter a range of offtake rates were used to capture the mobility unstable gas-oil displacement to conduct the screening study.

5.2. Aims

1. Identify the heterogeneities at the genetic-unit scale which have a potential impact on oil recovery.

2. Develop a screening process to rank the impact of selected heterogeneities on oil recovery.

3. Understand the interaction between different heterogeneities and gas-oil displacement in relation to the rank order.

4. Apply a realistic fluid PVT description to the screening study in order to evaluate the PVT impact on the rank order of geological heterogeneities.

5. Investigate the relationship between displacement stability and recovery response for the studied heterogeneities.

5.3. Combination of genetic-unit scale and reservoir-unit scale heterogeneities in a fluvial deltaic reservoir

The information about heterogeneities at the genetic-unit scale was mainly based on the outcrop analogues (Balakhany Quarry and Yasamal Valley) that were described in Chapter 2. Subsurface pressure, well log and core data from the Azeri and Chirag Field (Reynolds et al. 2003; Jones and Jerauld 2005) were also taken into account. Previous research on channelised reservoirs were also used for reference (Jones et al. 1994 and 1995).

Four genetic-unit scale heterogeneities were selected for investigation in this screening study (Table 5.1). This selection was based on a consideration of features that were widely recognized to have a large influence on reservoir performance by

previous researchers, production geologists and reservoir engineers (e.g. Haldorsen and Lake 1984; Begg and King 1985; Begg et al. 1985; Kortekaas 1985; Haldorsen and Chang 1986; Weber 1986; Stalkup and Ebanks 1986; Begg et al. 1987; Fayers and Muggeridge 1990; Shook et al .1992; Reynold et al. 2003; Jones and Jerauld 2005).

Factor (heterogeneity)	Setting 1	Setting 2
Mud-Clast lags	No mud-clast lag at channel base	Mud-clast lag at each channel base
Kv:Kh ratio	Kv:Kh = 0.1	Kv:Kh = 1
Upward Fining Trend	A single value of permeability is assigned to the channel-fill sandbodies (the mean permeability of 178mD)	Channel-fill sandbodies with upward reduction in permeability from 346mD at the channel base 10mD at the top of the channel (the mean permeability of 178mD)
Extensive shales	No extensive shale within high net-to-gross layers	Extensive shale presence in high net-to-gross layers
Channel Dimensions	Small channel-fills: 6m thick, 100m wide	Large channel-fills: 6m thick, 200m wide
Channel Stacking	Channel-fill sandbodies treated explicitly as stacked, multistorey channel-belt sandstones	Channel-fill sandbodies treated explicitly as individual, single-storey channel-fill sandstones
Channel Orientation	Channel-fill sandbodies are oriented parallel to tectonic dip	Channel-fill sandbodies are oriented oblique (49°) to tectonic dip

Table 5.1. Factors (heterogeneities) investigated in the sensitivity analysis. The impact of these seven factors is investigated by observing the percentage change in average response when each factor is varied from setting 1 to setting 2.

5.3.1. Reservoir-unit scale heterogeneity factors

Three reservoir-unit scale heterogeneities were chosen to be re-examined in this chapter from the range investigated in the previous chapter. These were channel orientation, stacking pattern and dimensions. It was found that they had an insignificant influence on reservoir performance in the previous chapter. However, when more detailed genetic-unit scale geological features were modelled, these reservoir-unit scale factors could be inter-linked with the genetic-unit scale factors; thus they might have a larger influence on reservoir performance than indicated in

Chapter 4. For example, channel geometry influences the size of the mud-clast lag at channel bases; large channels have more continuous and larger mud-clast lags, whereas smaller channels will have less extensive and more distributed lags.

These reservoir-unit scale factors were introduced and discussed in the previous chapter. It was found that with a simplified fluid PVT description, together with high NTG layers, the response of these factors to recovery and breakthrough werer within stochastic noise level. However, the influence of these factors might be significant if more realistic fluid PVT description applied. All the channels that were modelled in this chapter have low sinuosity (P=1.21). This provided a reasonable base case for Azeri as low channels sinuosity was estimated for Azeri (Reynolds et al. 2003) and no reservoir is likely to have completely straight channels.

5.3.1.1. Channel orientation

Paleocurrents from channel-fill sandstones in the Pereriv Suite reservoir in Azeri are generally directed towards the south, with a range of angles that varies from parallel to the tectonic dip to a 49° offset to the east (Reynolds et al. 2003). In an earlier study of other southern Caspian Fields showed that channel orientation within the Pereriv Suite was a major uncertainty in reservoir characterization (Abdullaev et al. 1998). It was recognized that if channels have an offset angle to the tectonic dip, the injected gas could experience a reduced dip angle. A shallower dip angle has a negative influence on the displacement stability. It was shown in Chapter 4 that the variation of channel orientation had insignificant influence on reservoir performance. However, when the reservoir contains genetic unit scale features, such as an upwards-fining permeability trend, or mud-clast lags at channel bases, channel

orientation could have a more significant impact on the gas displacement; for example, early gas breakthrough might occur in those models having channels offset to the east and with high permeability at the base of each channel.

5.3.1.2. Channel stacking

The outcrop analogue data presented in Chapter 2 demonstrated examples of individual single-storey channel-fill sandbodies and stacked multi-storey channel-belt sandbodies present within the deposition environment. Some of the genetic-unit scale features are associated with channel-fill sandbodies. Therefore, the channel stacking pattern influences the geometry and pattern of the genetic unit scale features. For example, the channel stacking pattern will affect the spatial distribution of mud-clast lags. Therefore, the variation in channel stacking pattern was re-examined in this chapter.

5.3.1.3. Channel dimensions

The outcrop analogue and sub-surface data presented in Chapter 2 demonstrated that the single-storey channel sand bodies vary in width between 100-200m. From the outcrop analogue data it was observed that variation in channel thickness was generally small, the thickness of the individual channels were c.6m. Previous work (Jones et al. 1995; Larue and Hovadik 2006) demonstrated that channel dimension has a large influence on cumulative oil recovery in a channelised environment. Channel dimensions control the geometry of genetic-unit scale features such as

mud-clast lags at channel base. Therefore, the variation in channel dimensions was re-examined.

5.3.2. Extensive shale within high NTG layers

Production geologists observed impermeable shales within high NTG layers in core data. At the corresponding depth, RFT data also recorded a small pressure break across the shales (Reynolds et al. 2003). It is not clear how extensive these shales are. The pressure break across the shales suggested a possibility that minor flooding surfaces may be present in the high NTG interval due to the rapid lake level changes in the Caspian Basin (Chapter 2). Shales associated with the flooding surfaces could be extensive enough to divide the high NTG interval into separate layers. In order to test the influence of the presence of extensive shales in a high NTG interval on reservoir performance, this chapter compared the case when there was no extensive shale present in the high NTG layer, with a case when extensive impermeable shales divided the reservoir laterally into thinner intervals.

5.3.3. Upward-fining trends within channel-fill sandbody

Upward fining trend of the grain size within each channel-fill sandbody were often observed in the Pereriv Suite (Reynolds et al. 2003; Reynolds and Riley 2003). Upward-fining trends result in an upward reduction in permeability within each channel-fill sandbody. Such variations in permeability could have a large influence on recovery, as unswept or bypassed oil could remain in the low permeability upper part of the sandbody (Weber 1986; Weber and van Geuns 1990). This study compared two cases, one with only a single value of permeability was assigned to the entire

channel-fill sandbody (178mD) and the other one with the permeability valuez reducing upward within each channel-fill sandbody. In the second scenario, the permeability reduced linearly from 346mD at the channel base to 10mD at the top of the channel, resulting the same mean permeability within the channel of 178mD.

5.3.4. Ratio of vertical and horizontal permeability within channel-fill sandbodies (Kv:Kh)

One of the major uncertainties in the Pereriv Suite reservoir, or any fluvial-dominated deltaic reservoir, is the Kv:Kh ratio within individual sandbodies. Previous studies (e.g. Fayers and Muggerldge 1990; Shook et al. 1992) suggested that Kv:Kh ratio was the most important factor that controls displacement behavior when the displacement was mobility unstable but gravity stable, because the Kv:Kh ratio determined the rate of vertical segregation of a displacement. Gravity stability of a mobility unstable displacement is fundamentally controlled by vertical segregation. Therefore the Kv:Kh ratio has the potential to influence the gas-oil displacement performance.

In this study, two extreme Kv:Kh ratios were considered. In the previous chapter it was assumed that the sandbodies were isotropic with Kv:Kh equal to one. In the case when sandbodies contained small scale geological features such as cross-bedding or lamination (Reynolds et al. 2003), they are normally anisotropic. There were no reliable Kv:Kh measurements available from the Azeri Field sands. Therefore a Kv:Kh value was assumed for the anisotropic sandbodies. Previous studies of high and low NTG fluvial reservoirs (Jones et al. 1994 and 1995) applied Kv:Kh equal to 0.1 for channel-fill sandbodies containing similar types of small-scale heterogeneities

to Azeri Field such as cross-bedding or lamination which were also found in the Azeri Field (Reynolds et al. 2003; Reynolds and Riley 2003). Therefore, a KvKh ratio of 0.1 was assumed to represent the anisotropic sandbodies in this study.

5.3.5. Mud-clast lags at channel bases

In outcrop analogue and core data, lags of mud clasts were observed at the base of many channel-fill sandbodies. Mud-clast lags have low transmissibility and they are relatively thin compared with each channel sand body (<1m thick). Therefore mud-clast lags behave like discontinuous shales, preventing vertical cross flow. There are numerous studies (e.g. Haldorsen and Lake 1984; Begg et al. 1985; Begg and King 1985) which demonstrated that discontinuous shales have a large influence on displacement due to the reduction of the vertical permeability (see section 5.3.4). This chapter investigated the influence of the presence of mud-clast lags at the channel base. The shape, geometry and continuity of the mud-clast lags were correlated with the channel geometry and stacking pattern. Channels were stochastically distributed in the reservoir model (Chapter 4). To represent mud-clast lags, channel bases were assigned to have zero vertical transmissibility. Therefore, the mud-clast lag geometry and distribution were related to the channel geometry and stacking pattern. For small single storey channels, the mud-clast lags were smaller and were distributed more evenly compared with the case when large channels were stacked together. Since all the channels were stochastically distributed in the reservoir model, some channels were eroded by later channels, therefore mud-clasts were often found to be discontinuous. This is consistent to outcrop and subsurface observations reported in the sedimentology study (Reynolds et al. 2003). The selected heterogeneities are summarized in Table 5.1

5.4. Screening study design

A two-level fractional factorial design was employed again in this chapter. The details of the method can be found in section 4.6 and in previous studies (e.g. Box et al. 1978; Montgomery 2005). This part of the screening study aimed to explore the impact of the heterogeneities across a combination of reservoir-unit and genetic-unit scales on the cumulative oil recovery, gas production and the total oil recovery factor in a high NTG reservoir layer. As discussed in section 4.6.3, the results from the high NTG layer study presented here can be applied to Pereriv B and D given that these two layers have high NTG (>85%). The high NTG results can also represent the entire Pereriv Suite in regions where Pereriv A,C and E have zero NTG. A 2^{7-3} Resolution IV experimental design was used. Such a design requires 16 simulation experiments in order to quantify the impact of seven factors. The same experimental design matrix was used for all the screening studies reported in this chapter (Table 5.2).

Parameter	1	2	3	4	5	6	7
Runs							
1	2	1	2	2	1	1	2
2	1	1	1	1	1	1	1
3	2	2	2	1	2	1	1
4	2	2	1	1	1	2	2
5	1	1	1	2	1	2	2
6	2	2	1	2	1	1	1
7	1	2	2	2	1	2	1
8	2	1	1	1	2	1	2
9	1	1	2	1	2	2	2
10	2	1	2	1	1	2	1
11	1	1	2	2	2	1	1
12	1	2	2	1	1	1	2
13	1	2	1	2	2	1	2
14	1	2	1	1	2	2	1
15	2	2	2	2	2	2	2
16	2	1	1	2	2	2	1

Table 5.2. Experimental design matrix for 4th sensitivity screening study. The parameter row denotes the heterogeneity factor; 1: Channel orientation; 2: Channel stacking; 3: Channel dimensions; 4: Extensive shales; 5: Upward fining trend; 6: Kv:Kh ratio; 7: Mud-clast lags .

Similar to Chapter 4, three stochastic realizations of each reservoir model was generated, in order to determine the significance of the response from each heterogeneity factor compared with the stochastic uncertainty.

5.5. Reservoir model construction

A more realistic fluid PVT description was applied in this screening study. For this purpose, a conventional simulator had to be used, because the streamline simulator was considered not an ideal tool to simulate fluid PVT properties that changes with reservoir pressure (such as fluid compressibility and evolved gas from solution). These features are potentially important for reservoir behavior and the influence of heterogeneity on flow could be different if these physical mechanisms

were included. Hence a conventional simulator (VIP) was used so that a more realistic description of Azeri Field fluids could be included.

The symmetry element reservoir model which represented the inter-well region had more than 500,000 grid cells (Chapter 4). It was not feasible to simulate such a large number of grid cells with the conventional simulator. A subset of the reservoir model was therefore used for conventional simulation. The subset models were 950m long, 750m wide and 21m thick, and were extracted from the symmetry element models which were 1900m long, 1500m wide and 42m thick. With this design, the subset models contained a total of 62,160 cells.

In order to ensure that the results from the subset models were comparable to the symmetry element models, the volume, flow rate and production time had to be scaled appropriately. It has been demonstrated that two reservoir systems were comparable when they have the same key dimensionless numbers (Shook et al. 1992). Any two immiscible displacements are considered to be identical, if they sharing the same values in respect to the following six dimensionless numbers. In other words, the difference in these six numbers indicates the difference between two displacements.

Effective aspect ratio

$$R_L = \frac{L}{H}\sqrt{\frac{k_v}{k_h}} \qquad \text{equation 5.A}$$

Dip angle group

$$N_\theta = \frac{L}{H}\tan\theta \qquad \text{equation 5.B}$$

Buoyancy number

$$N_g = \frac{k_h \lambda_{ro} \Delta\rho g \cos\theta H}{u_T L} \qquad \text{equation 5.C}$$

End-point mobility ratio $$M = \frac{\lambda_{rf}}{\lambda_{ro}}$$ equation 5.D

Capillary number $$N_{Pc} = \frac{\lambda_{ro}\sigma}{Lu_T}\sqrt{\phi k_h}$$ equation 5.E

Density number $$N_{\rho} = \frac{\rho_f}{\Delta\rho}$$ equation 5.F

Nomenclature	
L : length, F : force, t : time, m : mass; [=] means 'has units of'	
L	Reservoir length [=] L
H	Reservoir thickness [=] L
A	Cross-sectional area [=] L^2
g	Gravitational acceleration [=] L/t^2
σ	Fluids interfacial tension [=] F/L
ϕ	Sandbody porosity [=] fraction
θ	Reservoir dipping angle [=] radians or degrees
k_h	Horizontal permeability [=] L^2
k_v	Vertical permeability [=] L^2
ρ_j	Density of phase j [=] m/L^3
μ_j	Viscosity of phase j [=] $(F\text{-}t/L^2)$
λ_{rj}	Relative mobility of phase j [=] $(F\text{-}t/L^2)^{-1}$
q	Volumetric flow rate [=] L^3/t
S	Saturation [=] fraction
kr'_j	End-point relative permeability of phase j [=] fraction
u_T	Displacement velocity [=] L/t
Subscripts	
o	Oil phase
f	Displacing fluid phase (i.e gas or water)
or	Residual oil
wc	Connate water

Table 5. 3. Table of nomenclature.

Shook et al. (1992) demonstrated that the variation in density number (N_ρ) does not influence the recovery. Moreover, in this investigation the capillary force was assumed to be negligible; therefore, both the capillary number (N_{pc}) and the density number (N_ρ) were ignored in this study.

The volume of the subset model was chosen to keep the key dimensionless numbers (R_L, N_θ) the same between the subset model and the symmetry element model. Since the volume of the model changed, the rate and the injection time were also scaled

down in order to keep N_g the same. The end-point mobility (M) was not affected by the variation of the model volume. Therefore all the dimensionless numbers were matched between the subset model and the symmetry element model. The details of the scaling calculations are reported in Appendix 4 and it was found that the variation in model volume has negligible effect on the screening study. Reservoir model information is summarized in Figure 5.1 and Table 5.4.

Heterogeneity model	Coordinate	Grid number	Model length /m	Grid block size/m
North Flank: Sector model	X	80	950	12
	Y	37	750	20
	Z	21	21	1
		Total: 62160		

Table 5.4. Information on subset reservoir model setting.

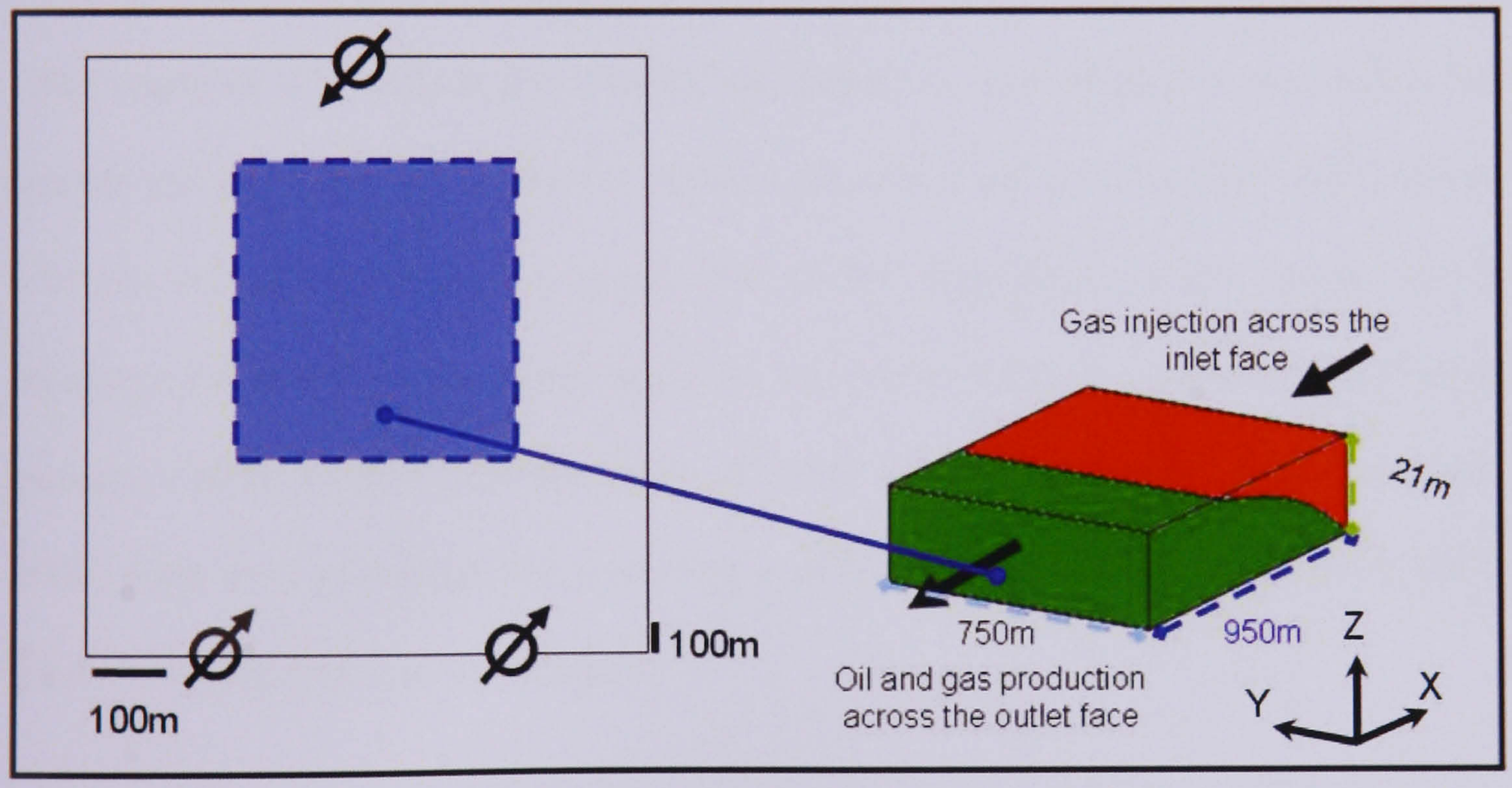


Figure 5.1. The setting of the subset reservoir models mimics the displacement mechanism in the symmetry element model.

5.6. The design of the displacement simulations.

The investigation in this chapter started by conducting the geological screening study under simplified fluid PVT description. In the second part of this chapter, realistic Azeri fluid PVT description was applied to the screening study. All the screening studies were conducted in subset models with reviewed relative permeability curves, which were designed specifically to study gas-oil displacements in the central north flank of the Azeri Field. In order to compare with the results from Chapter 4, the influence of the variation in model's geometry and the variation in relative permeability curves are reported in Appendix 4 and 5 respectively. Table 5.5 summarizes all the screening studies in this chapter under various conditions.

The study in this section was similar to Chapter 4. The impact of the underlying aquifer and overlying gas cap were omitted and it was assumed that the displacement schemes on each flank were isolated, thus all the simulations in this chapter solely represent Pereriv B in the north flank of the Azeri Field. A streamline simulation package (3DSL version 2.2) and finite different simulation package (VIP Lankmark 2006) were used to conduct the screening studies under simplified and realistic Azeri fluid PVT description in this chapter.

Section of screening study	Fluids description	Production rate	Well control scheme
Section 5.6.1	Simplified fluid description	93.3% Dietz's critical rate	No well control scheme applies
Section 5.6.2	Realistic fluid description	93.3% Dietz's critical rate	No well control scheme applies
Section 5.6.3	Realistic fluid description	46.7% to 186.7% Dietz's critical rate	No well control scheme applies
Section 5.6.4	Realistic fluid description	46.7% to 186.7% Dietz's critical rate	Well control scheme applies

Table 5.5. Summary of screening studies under various conditions.

5.6.1. Gas-oil displacement in a high NTG layer with simplified fluid PVT description

The first part of this investigation is similar to the studies that were conducted in Chapter 4. This part of the screening study aimed to explore the impact of the combination of reservoir-unit scale and genetic-unit scale heterogeneity on reservoir performance within a high NTG environment (Pereriv B). Simplified fluid PVT description of incompressible flow, constant fluid properties and dead oil were assumed so a streamline simulator could be used. The advantages of using a streamline simulator were discussed in section 4.5.

5.6.2. Gas-oil displacement in a high NTG layer with realistic fluid PVT description

A more realistic fluid PVT description was used in this study, i.e. fluids properties are dependent on pressure. Figure 5.2A - 5.2E show the reservoir fluid properties against pressure. Geological heterogeneity may not only influence the movement of not only the injected gas, but also the movement of evolved gas from solution.

Geological heterogeneity could therefore influence the reservoir performance differently in simulations that capture more physical phenomena in the displacement.

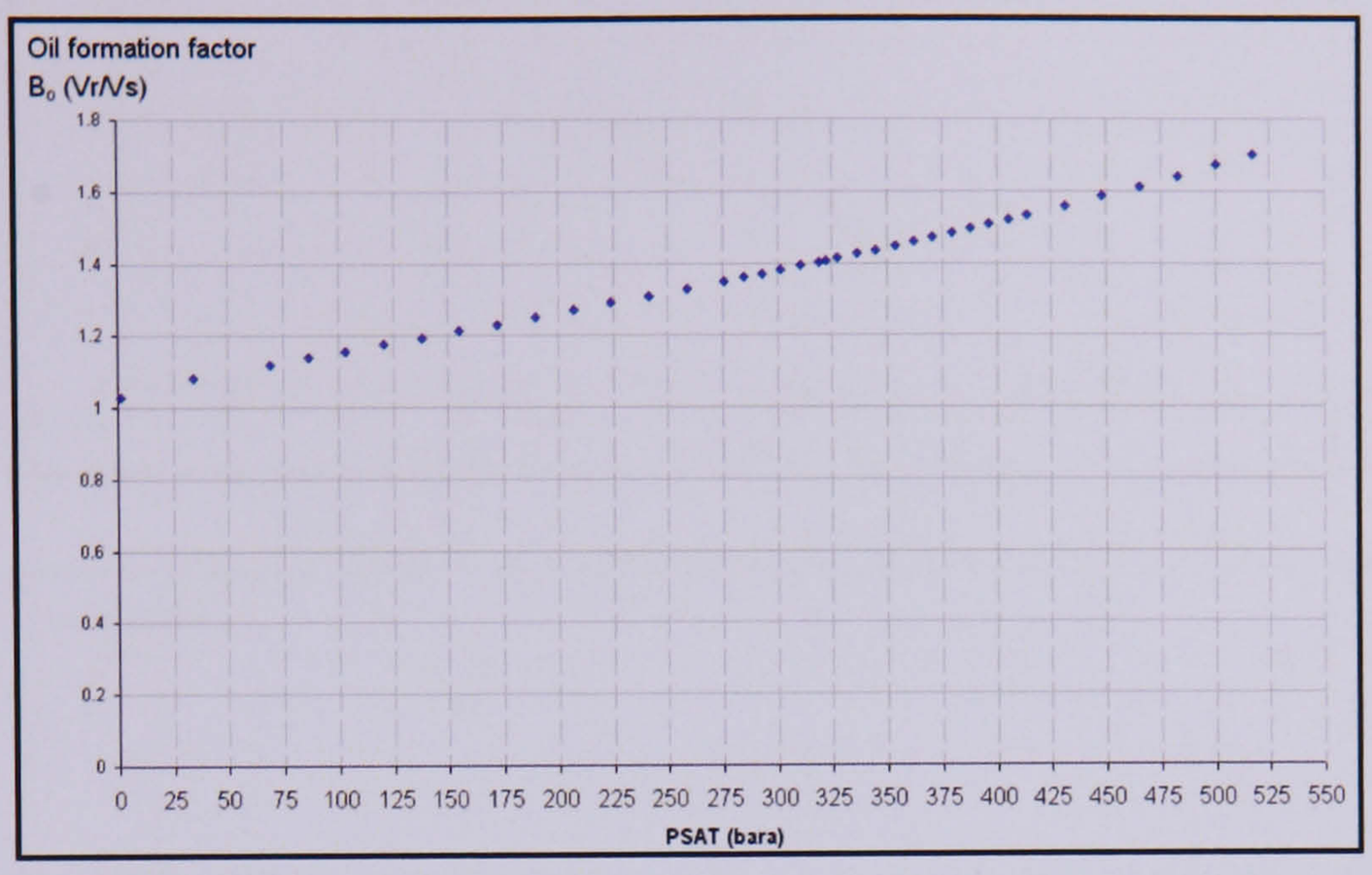


Figure 5.2A

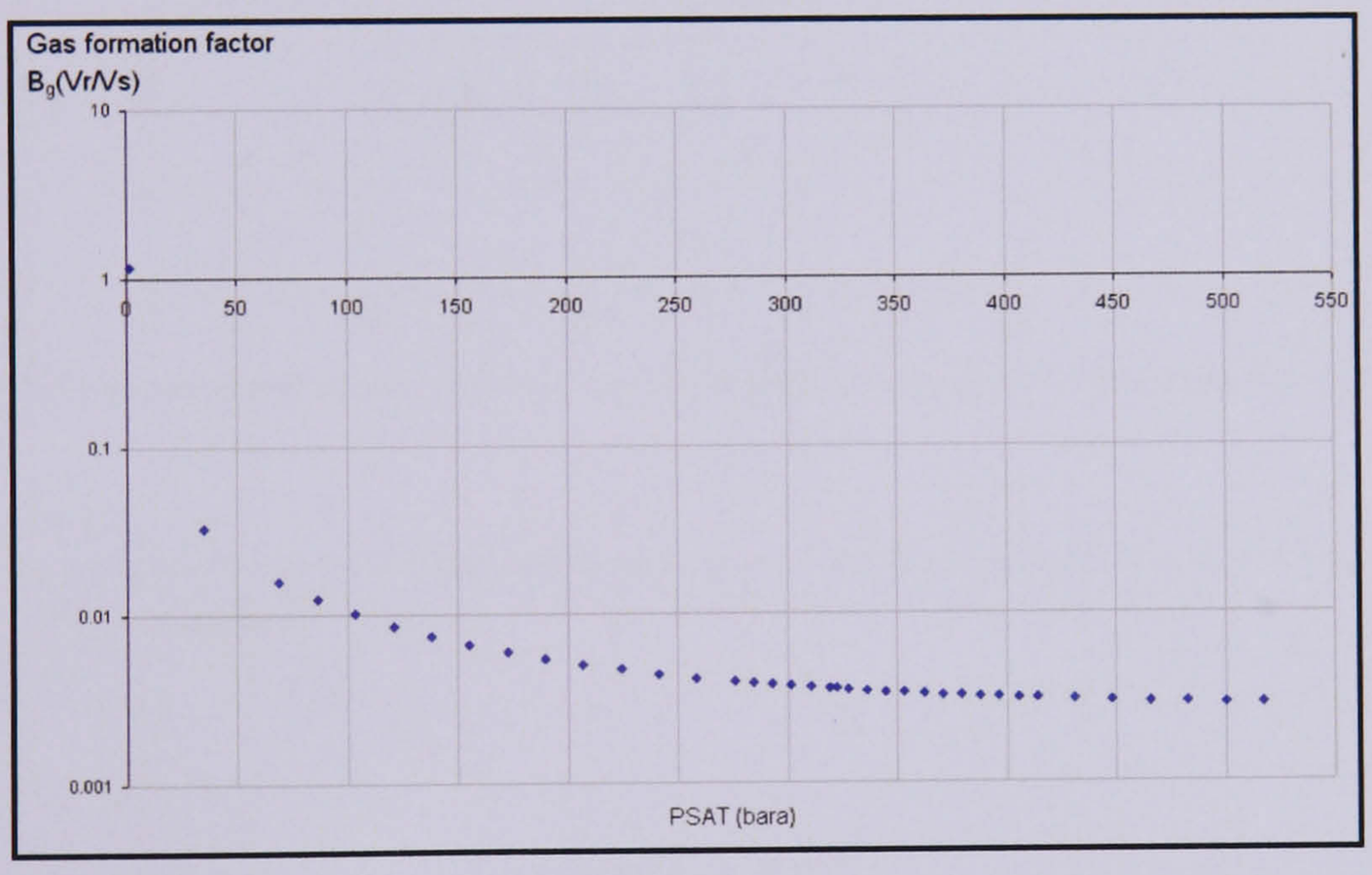


Figure 5.2B

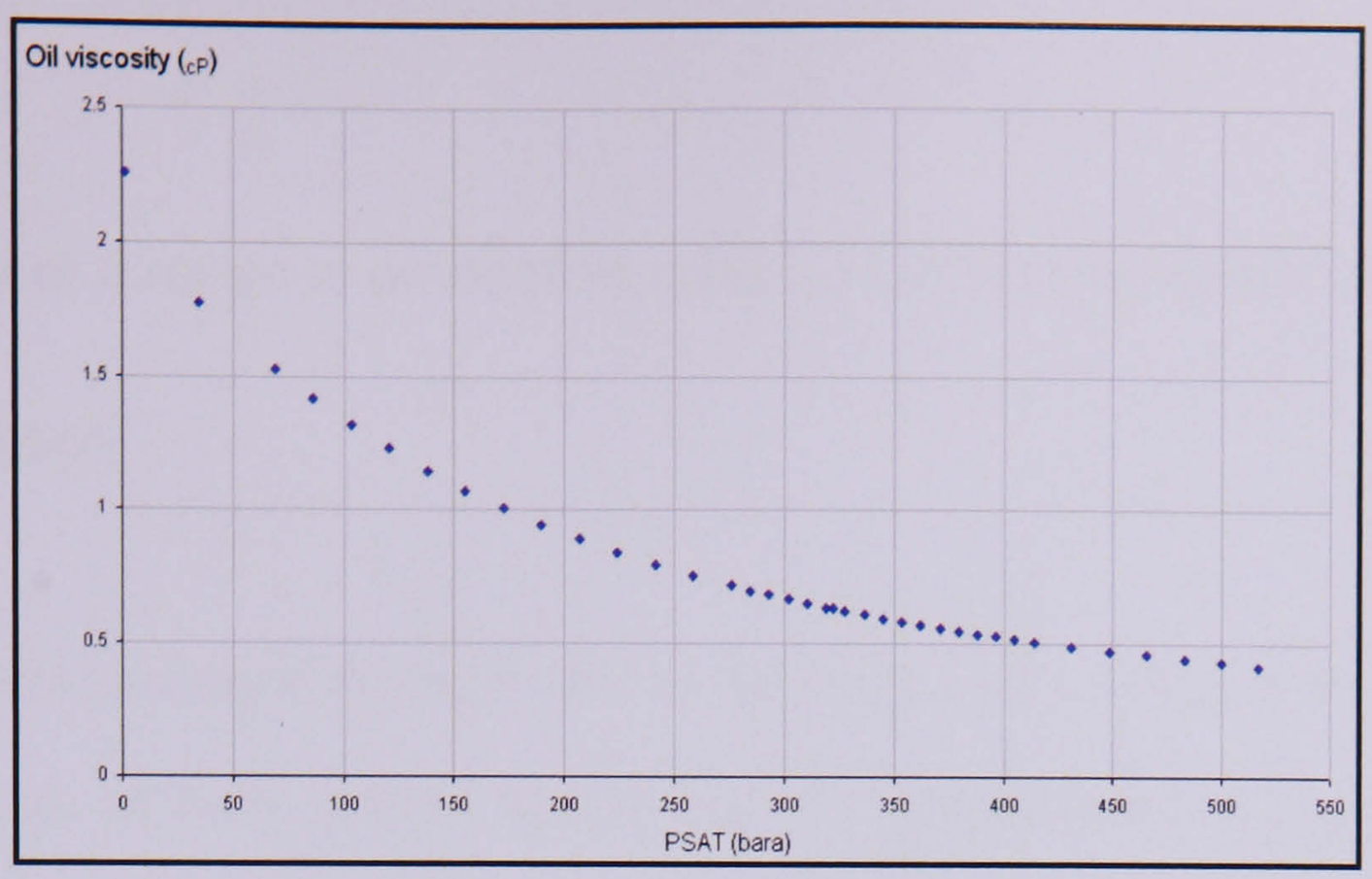


Figure 5.2C

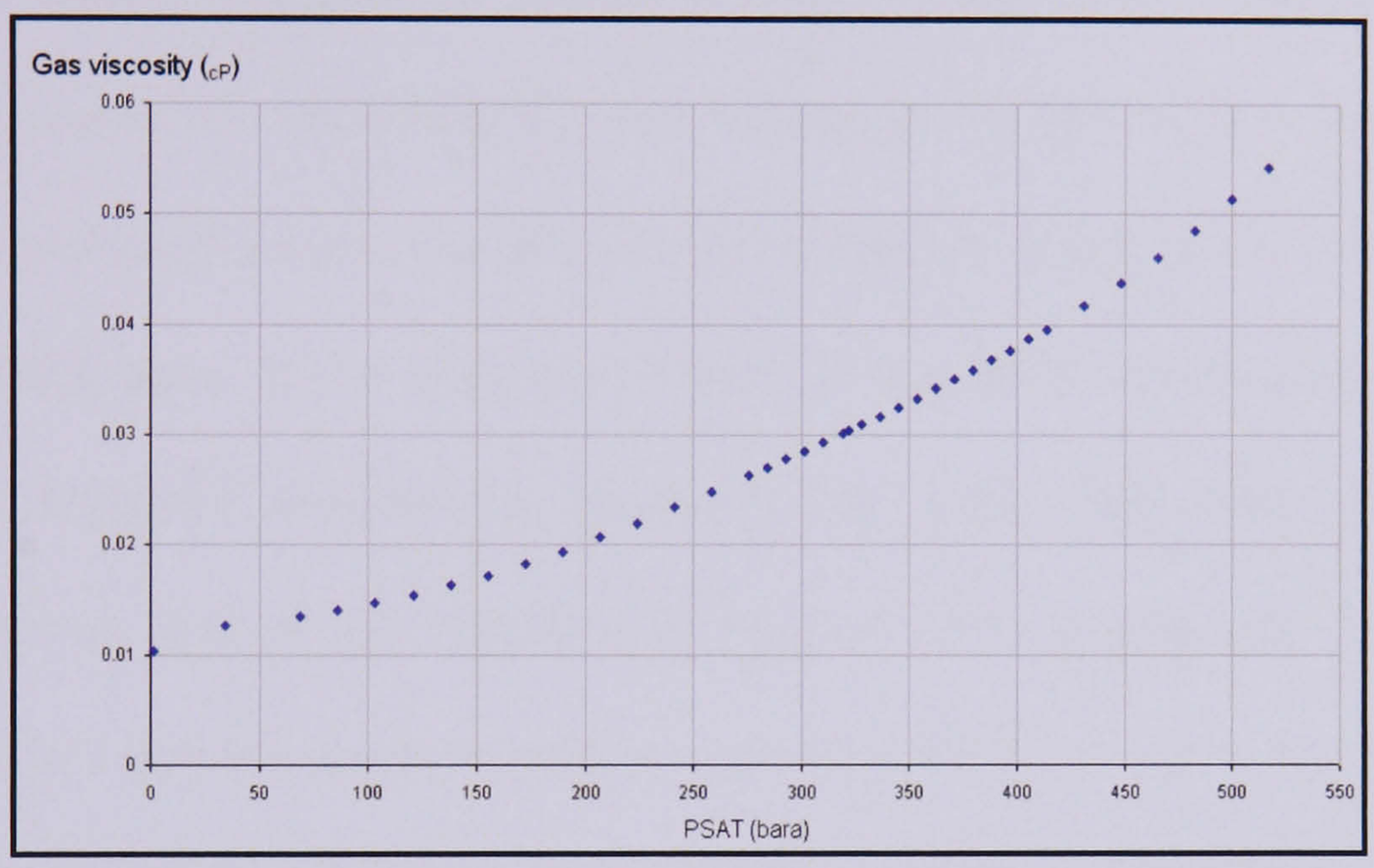


Figure 5.2D

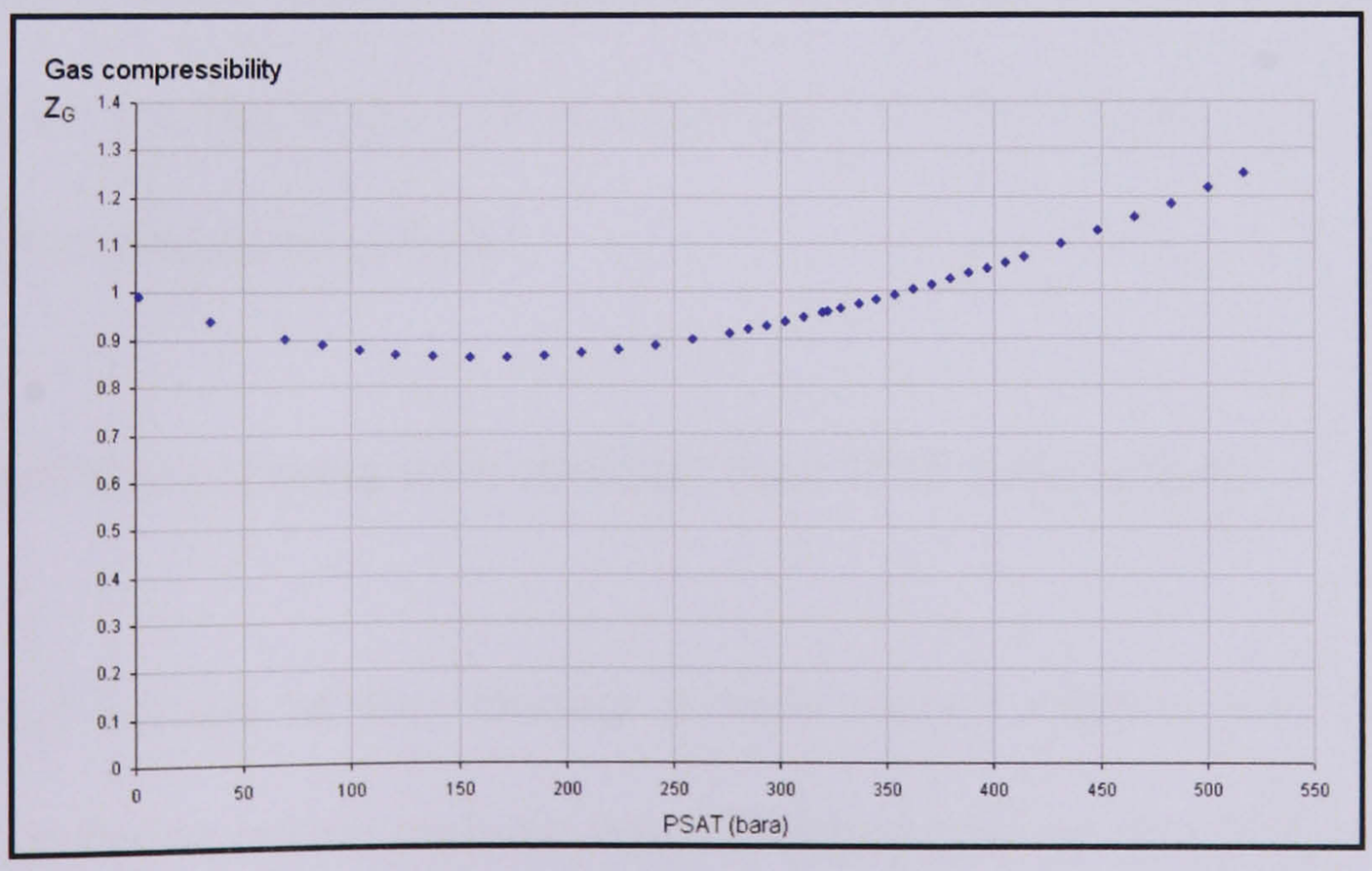


Figure 5.2E

Figure 5.2 (A-E). Azeri reservoir fluids description at different reservoir pressure. **(2A)** Oil formation factor; the reservoir bubble point pressure is approximately 302 bara **(2B)** Gas formation factor; **(2C)** Oil viscosity **(2D)** Gas viscosity **(2E)** Gas compressibility measured in the Azeri reservoir. The fluids sample tests were done at c. 342K.

5.6.3. Study of a range of production rates on both simplified and realistic fluid PVT description

In the previous simulations, 93.3% of the Dietz's critical rate was chosen as the production rate of each model. At this rate the displacement was gravity stable. However, in reality, because of uncertainty in the reservoir properties (e.g. rock permeability, reservoir architecture) and variations in production rate related to economic or technical issues, the displacement stability might not be able to achieve and vary through time. In the previous chapter, it was demonstrated that the mobility stable water injection simulations produced the same rank order of geological heterogeneities as that of gas injection. It was not clear whether the similar results were because the gas-oil displacement was gravity stable, or the same ranking order was independent of the displacement stability. A range of production rates (from 46.7% to 186.7% of the Dietz's critical rate) was applied in this screening study. The purpose was to test the impact of displacement stability on the impact of various geological heterogeneities on flow.

5.6.4. Well control scheme with realistic fluid PVT description

In the final section of this chapter a well control scheme was applied to the simulation in order to mimic realistic Azeri Field operations, in which the production is constrainted to gas handling capacility. If the gas-oil-ratio (GOR) is higher than a platform can handling capacity, the production well has to be choked back. In this part of study, a well GOR control scheme was applied in the simulations together

with realistic fluid PVT description. The GOR limit of each well was set to be 534 m^3 (gas)/m^3 (liquid), which is the maximum GOR that a platform can handle in the Azeri Field. If such a limit was exceeded, the production well was shut in. After the well was shut in, the potential GOR on production was tested every 30 days. If the potential GOR productions fell below this limit, then the well was re-opened. This part of the study investigates the variation in the rank order of geological heterogeneities when more realistic operating conditions were applied. In this section, the simulation was focused on a region that was near the production well (Figure 5.3) in order to study the influence of the well control scheme on the simulated flow behaviour.

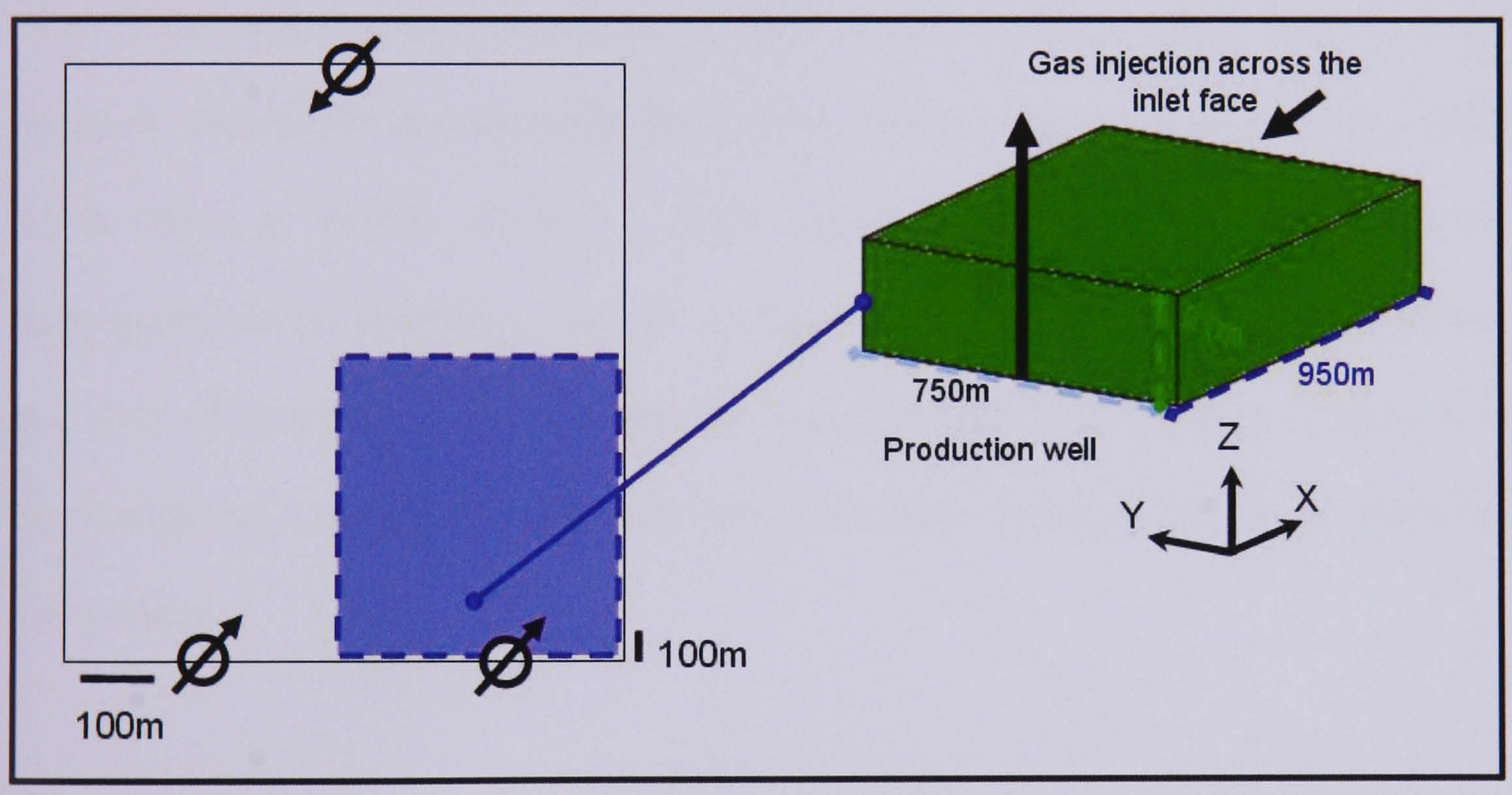


Figure 5.3. The setting of the subset reservoir model to mimic displacement mechanism close to the production well in order to study the influence of well control on the screening study.

5.7. Results and Discussion

5.7.1. Gas-oil displacement in a high NTG layer with simplified fluid PVT description

The first set of screening studies was conducted under the simplified fluid PVT description. Figures 5.4A to 5B shows the recovery factor and cumulative GOR by gas injection for each of the 16 simulations in the fourth screening study. The variations of oil recovery and breakthrough time showed the impact of the ensemble of geological heterogeneities on reservoir performance. The range of recovery was c. 59% - 72% and that of the cumulative GOR was c. 137% - 193% after 10 years injection. The results demonstrated that genetic-unit scale heterogeneity in high NTG layers (such as Pereriv B) had a much larger impact than reservoir-unit scale heterogeneitoes on simulated recovert. Compared with the range of recovery factors that were obtained from the 3rd screening study on high NTG layer in Chapter 4, it was found that with genetic-unit scale heterogeneities included, a lower oil recovery was yielded.

The variation in Kv:Kh ratio and the presence of mud-clast lags at channel bases were found to be the two most dominant factors that influence oil recovery. Figure 5.5 demonstrate that by modelling Kv:Kh ratio equal to 1, the recovery factor was increased by c.14.3% and total gas production decreased by c.7.9%. Modelling mud-clast lags at channel bases was found to be the second most significant factor that controls the reservoir performance under gas injection. By including mud-clast

lags in the model, the recovery factor decreased by c.3.2% and total gas production increased by c. 2.5%.

The results demonstrated that the impact of varying most of the reservoir-unit scale heterogeneity factors was close to or below the level of stochastic uncertainty. This suggests that the modelling decisions for these parameters were not important for the chosen range of parameter values. The results from this chapter were consistent with the results that were found in the 3rd screening study reported in the Chapter 4.

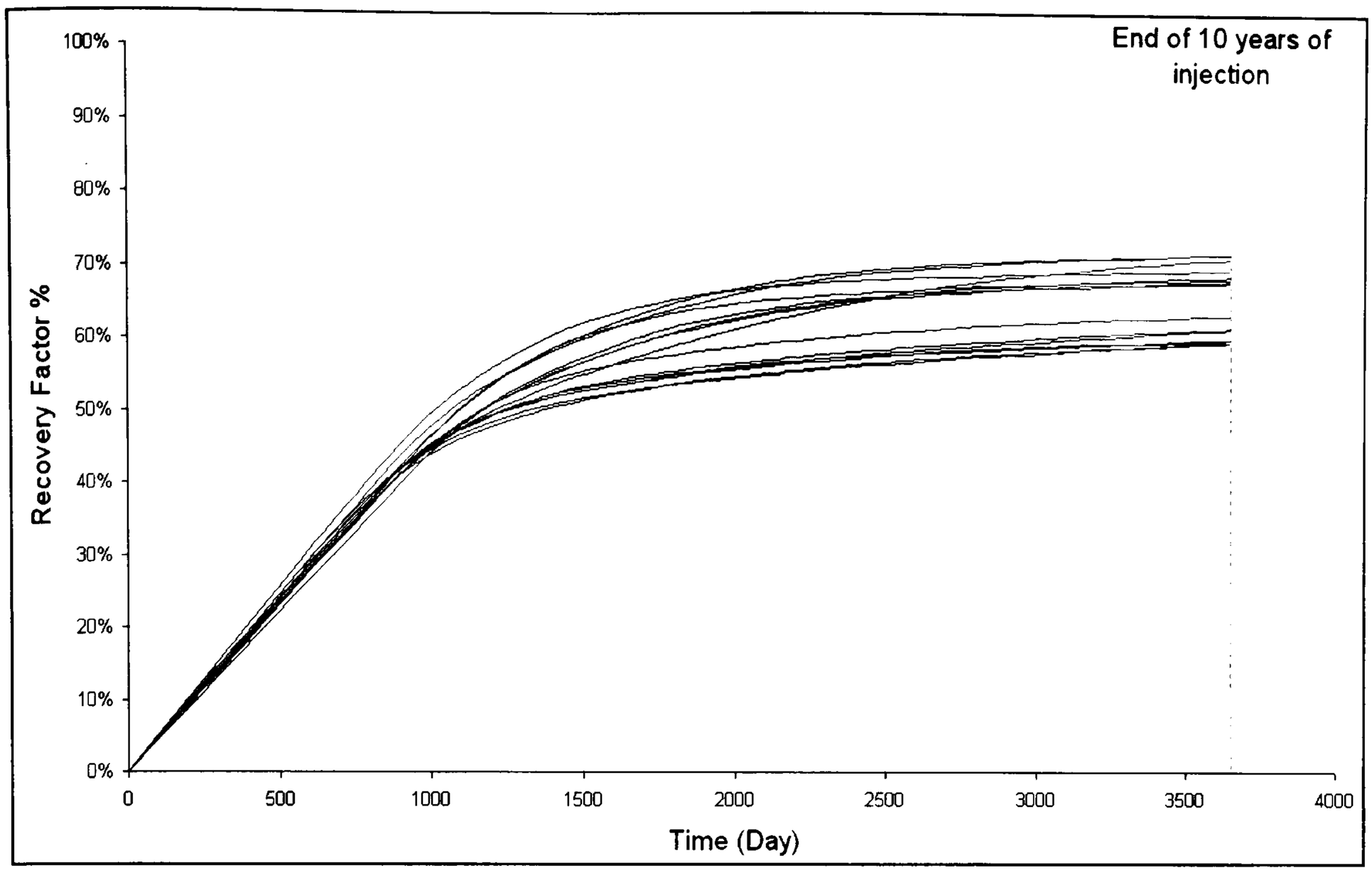


Figure 5.4A

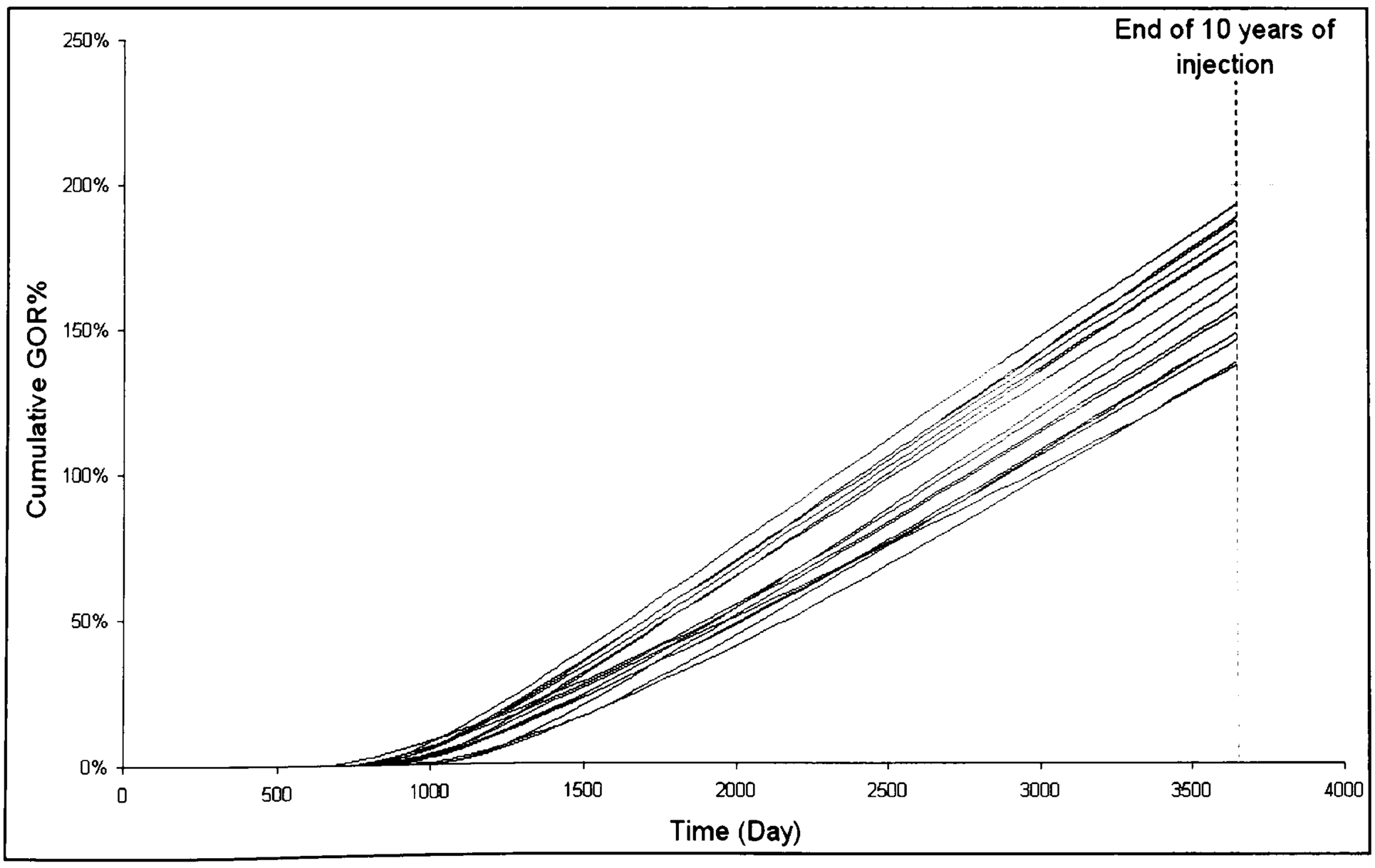


Figure 5.4B

Figure 5.4. Recovery factor **(A)** and cumulative gas oil production ratio (GOR) **(B)** as a function of time for each of the 16 simulation experiments run in the fourth sensitivity analysis on the Pereriv B layers based on simplified fluid PVT description. Analysis of these curves yielded the responses shown in Figures 5.5.

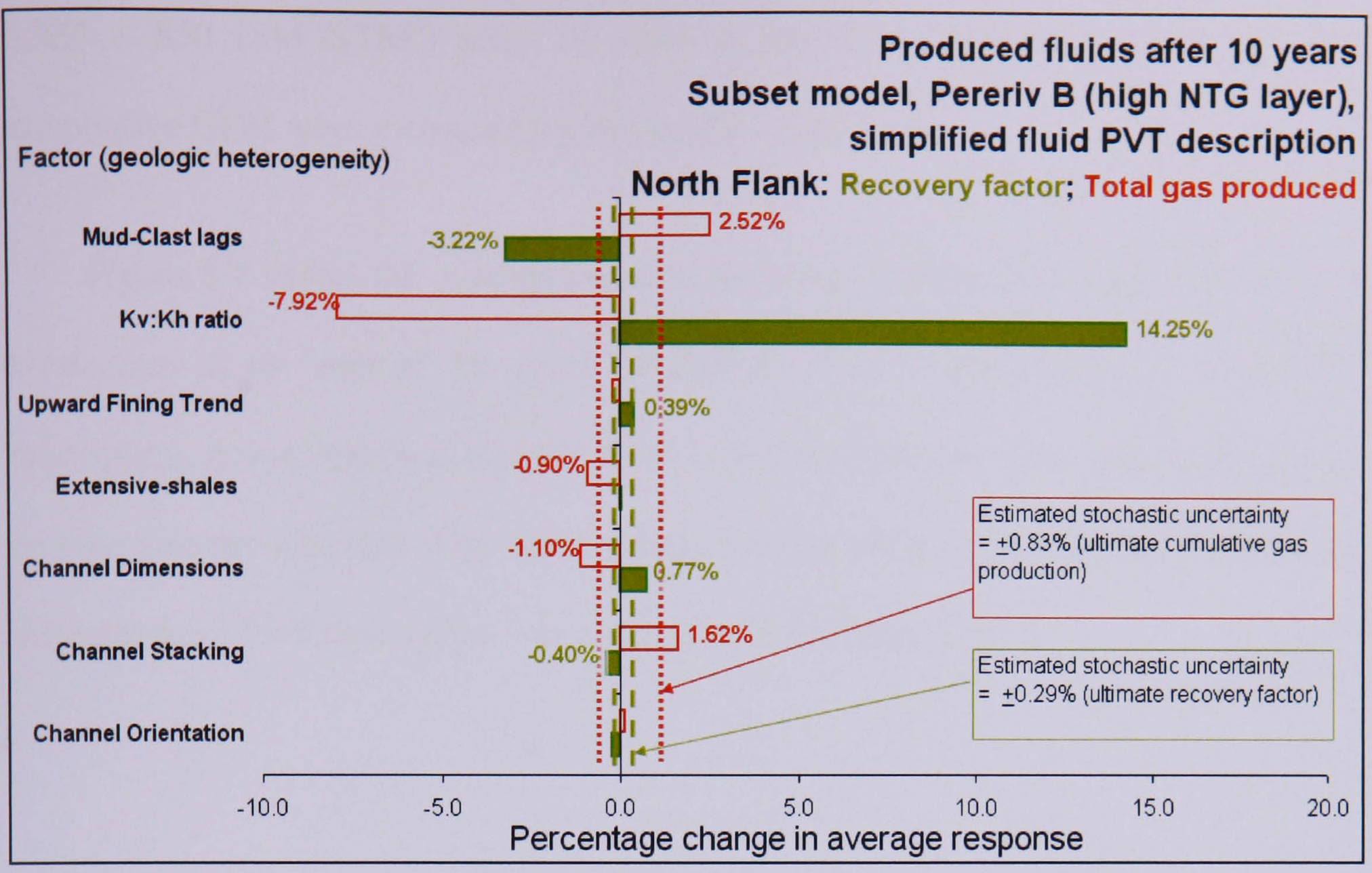


Figure 5.5. Average percentage change in recovery factor in subset models with simplified fluid PVT description after 10 years in north flank subset models of Pereriv B, observed when each factor in the sensitivity analysis is varied from setting 1 to setting 2 (Table 5.1). If the bar lies to the right then the change is positive. For example, modelling the channel sand Kv:Kh ratio equal to 1 (setting 2) increased recovery factor by c. 14.3% compared with modelling it equal to 0.1 (setting 1). The dashed lines denote the average percentage change observed from different stochastic realizations. If the impact of varying a factor is at or below the level of stochastic uncertainty then modelling decisions are unimportant for the chosen range of parameters.

5.7.2. Gas-oil displacement in a high NTG layer with realistic fluid PVT description

Figure 5.6 shows the recovery factor and cumulative GOR by gas injection for each of the 16 simulations in the fourth screening study under realistic fluid PVT descriptions. The variations of oil recovery and breakthrough time showed the impact of the ensemble of geological heterogeneities on reservoir performance. The range of recovery factor was between c. 65% - 82% and that of the cumulative GOR was

c.535 – 850 (SM^3/STM^3) after 10 years of injection. Both recovery factor and cumulative GOR were measured under standard conditions.

Figure 5.7 shows the average percentage change in recovery factor and total gas production at the end of 10 years production. With a more realistic fluid PVT description, it was observed that the Kv:Kh ratio still had the most significant impact on reservoir performance. The direct comparison between both screening studies with different fluid PVT description was summarized in Figure 5.8.

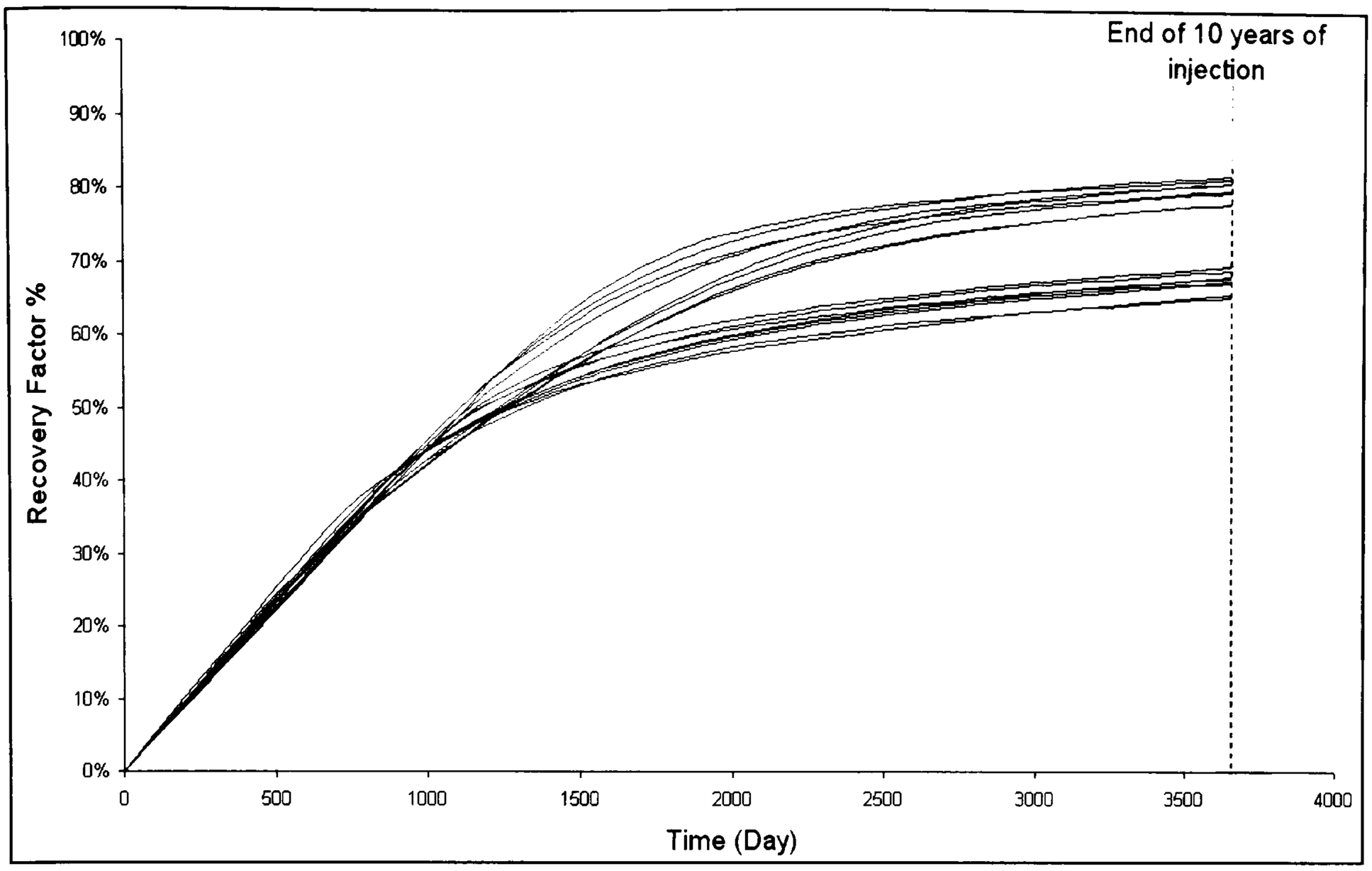


Figure 5.6A

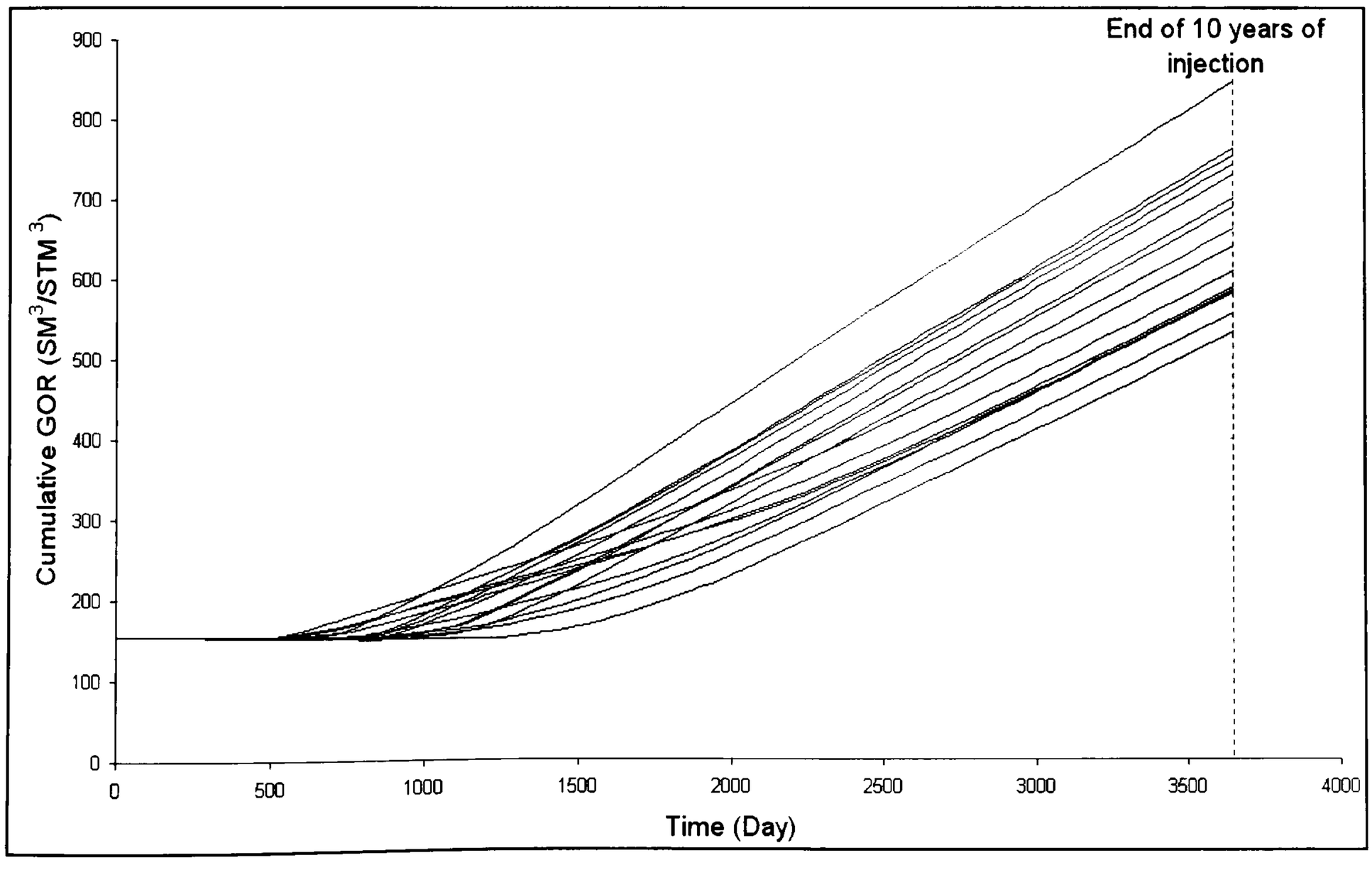


Figure 5.6B

Figure 5.6. Recovery factor **(A)** and cumulative gas oil production ratio (GOR) **(B)** as a function of time for each of the 16 simulation experiments run in the fourth sensitivity analysis on the Pereriv B layers based on realistic fluid PVT description. Analysis of these curves yielded the responses shown in Figures 5.7.

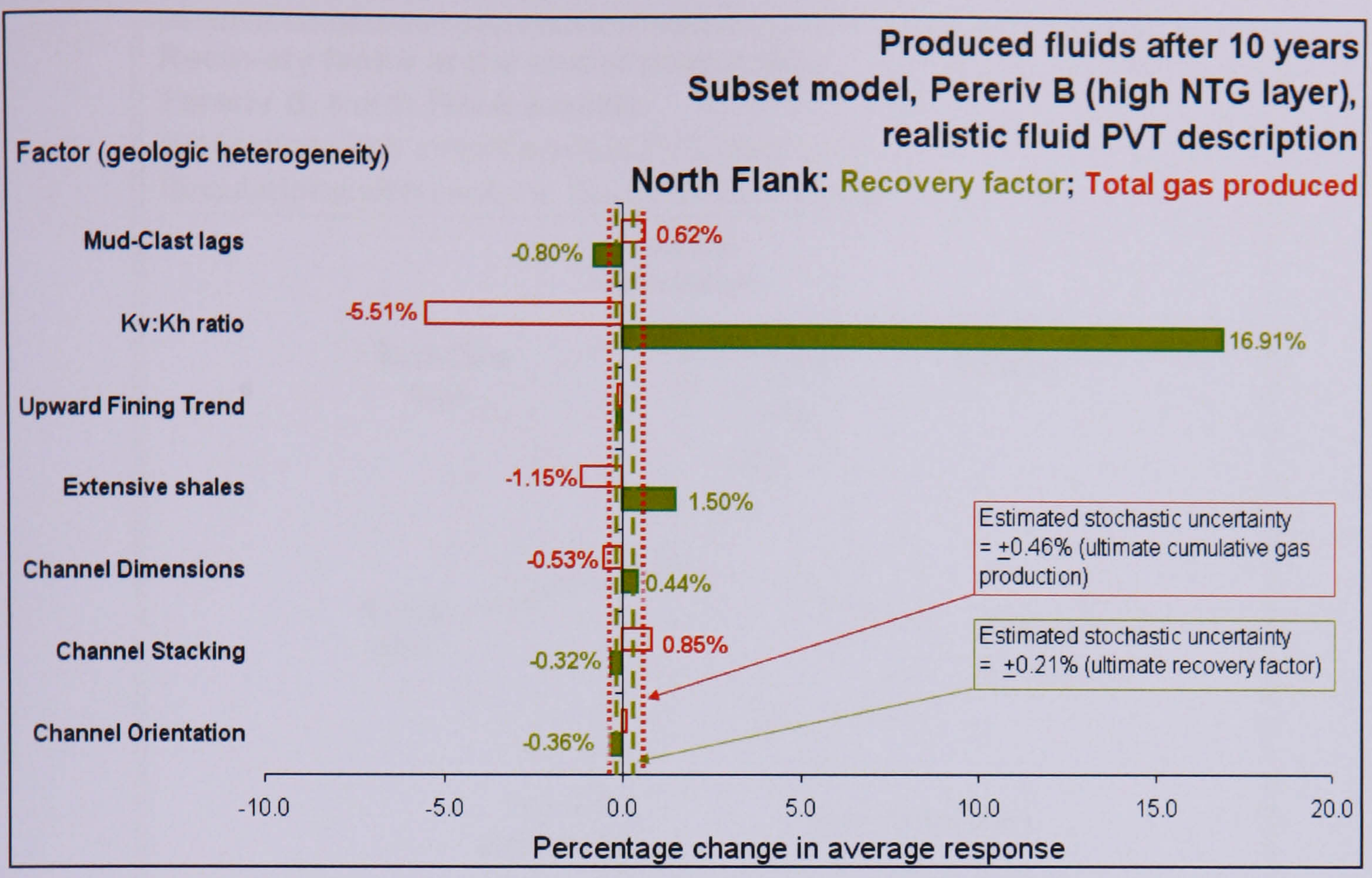


Figure 5.7. Average percentage change in recovery factor and total gas produced in subset models with realistic fluid PVT description after 10 years in north flank subset models of Pereriv B, observed when each factor in the sensitivity analysis is varied from setting 1 to setting 2 (Table 5.1). The realistic fluid PVT description (Figure 5.2) is applied.

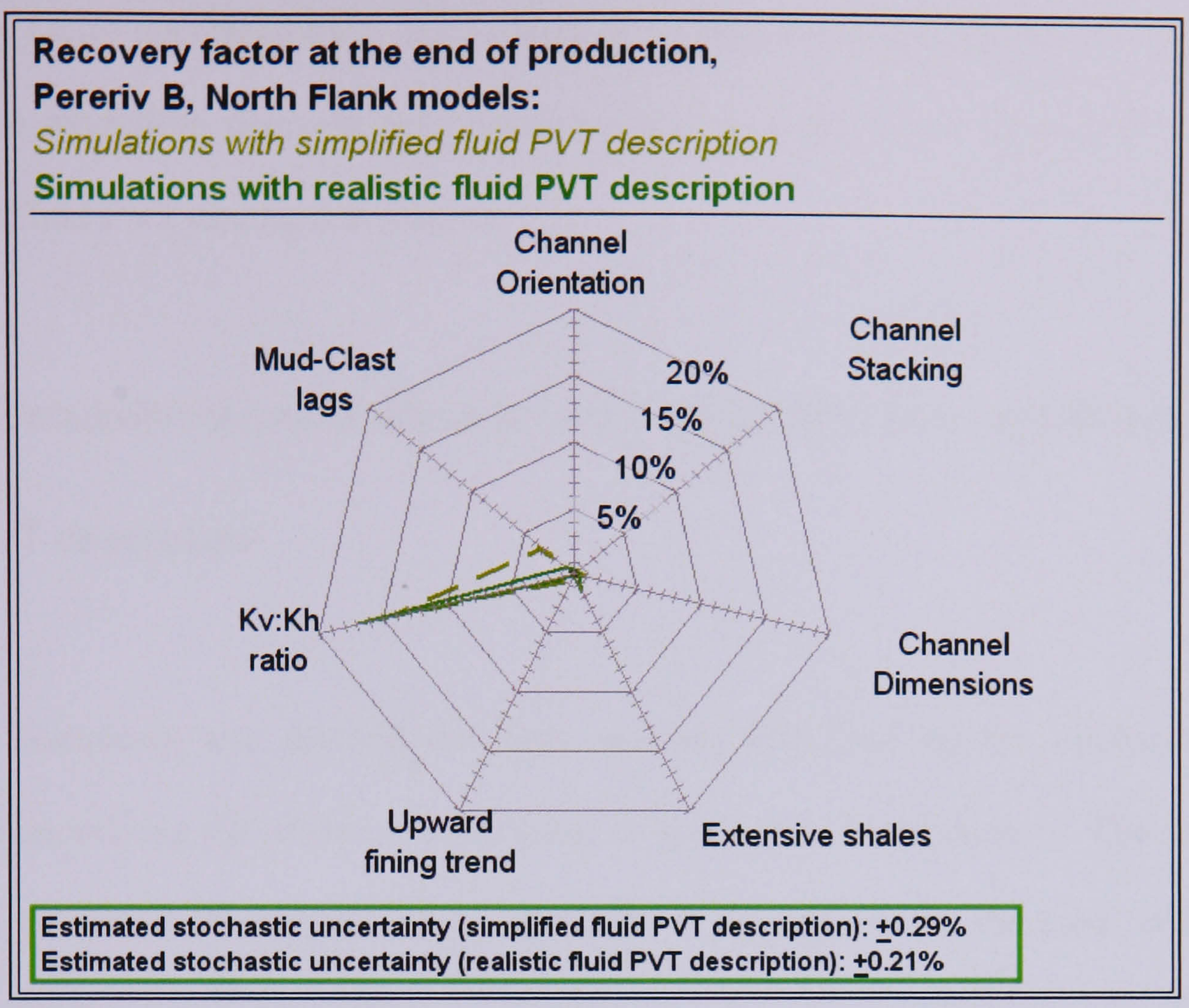


Figure 5.8. Absolute percentage change in recovery factor at the end of production period is plotted as distance from the centre of the chart for each heterogeneity, to enable comparison between simulations with simplified and realistic fluid PVT description.

Under the realistic fluid PVT description, by increasing the Kv:Kh ratio from 0.1 to 1, the recovery factor increased by c. 16.9% and the total gas production decreased by c. 5.5%. The influence of extensive shales on recovery factor was the second largest factor under realistic fluid PVT description. In this case extensive shales were modelled within the high NTG layer, the recovery factor increased by c.1.5% and the total gas production decreased by c. 1.2%. This demonstrated that the impact of extensive shale became more significant under realistic fluid PVT description.

Mud-clast lags also influenced reservoir performance. However, with the realistic fluid PVT description, the magnitude of the influence of mud-clast lags was smaller compared with the case when simplified fluid PVT description was applied. The

recovery factor decreased by c. 3.2% under simplified fluid PVT description, whereas the same modelling decision only decreases the recovery factor by c. 0.8% under realistic fluid PVT description (Figure 5.7).

5.7.3. Discussion of gas oil displacement in a high NTG layer with different fluid PVT description

This discussion was divided into two sections. The first section, discussed the reasons underlying the observed rank order of geological heterogeneity. The second section discussed the impact of the fluid PVT description on the rank order of heterogeneity.

5.7.3.1 Impact of the sand Kv:Kh ratio

The sand Kv:Kh ratio was the most significant heterogeneity regardless of the fluid PVT description (section 5.7.1 and 5.7.2). If the Kv:Kh ratio was equal to one that means maximum cross flow could be achieved within a displacement. Whilst if the Kv:Kh ratio was much less than one, the majority of gas would move along the bulk flow direction instead of segregating upwards in vertical direction. This effect was captured by the effective aspect ratio R_L (expression 5.A). R_L is a function of Kv:Kh ratio; when R_L is small, vertical cross flow is reduced hence the VE condition is less likely to be achieved. VE is important for mobility unstable (gas-oil) displacement, because the gravity stable condition is controlled by the degree of fluid vertical segregation.

If VE is not achieved, gas does not sweep the reservoir as efficiently, so the lower the Kv:Kh the lower the oil recovery. In the most extreme case when Kv:Kh becomes zero, the flow model becomes Buckley-Leverett type. There was no variation in saturation perpendicular to the reservoir dip. This phenomenon of vertical segregation was more obvious when the gas-oil average shock front mobility ratio was high (Figure A5.4).

Including mud-clast lags in the reservoir model yields a similar influence on displacement to reducing the sand Kv:Kh ratio. Mud-clast lags act like discontinuous shales, because of their low permeability and discontinuous shape,. As Begg and King (1985) suggested, discontinuous shales reduce the effective Kv:Kh ratio, because they increase the vertical flow tortuosity. Hence, including mud-clast lags in the reservoir model reduce the recovery factor and increases the total gas production under both simplified and realistic fluid PVT description.

5.7.3.2. Impact of the different fluid PVT description

By comparing Figure 5.5 and 5.7, a similar rank order was found from the screening studies with different fluid PVT description. Both sets of screening studies demonstrated that the Kv:Kh ratio was the most significant heterogeneity influencing oil recovery and total gas production. The Kv:Kh ratio was the most important heterogeneity factor because it controlled the efficiency of vertical cross flow; and this did not change when the more realistic fluid PVT description was applied. Mud-clast lags exert a similar influence by hindering vertical cross-flow, regardless of the PVT description.

However, with a more realistic fluid PVT description, the modelling decision to include extensive shales was more important than in the case with a simplified fluid PVT description. Figure 5.9 compared the gas saturation under different fluid PVT description in models with and without extensive shales (sand Kv:Kh ratio equal to 1). The results demonstrated that, under the realistic fluids description, the gas saturation within the invaded zone was slightly higher than under the simplified fluid PVT description. Also, under the simplified fluid PVT description, the gas moved more rapidly towards the production well.

Given that the reservoir pressure was very close to the bubble point, during production the reservoir pressure decreased below the bubble point. Therefore, gas was evolved from solution. Hence, more gas was generated under a realistic fluid PVT description. Figure 5.10 shows how the average reservoir datum pressure changed through time.

One might expect that extensive shales would also reduce recovery by preventing vertical cross flow. However, as these shales were laterally continuous, they effectively divided the reservoir into separate thinner intervals. Therefore with extensive shales in the system, the effective cross sectional area to flow was reduced and so the distance required for the gas to segregate upwards to the top of a sub-layer was decreased. Extensive shales improved oil recovery simply because of the geometrical effect. It was suggested by Shook et al. (1992) that a thinner reservoir yields a higher recovery factor because of its geometry. Figure 5.11A and 5.11B demonstrate two reservoirs with different layering geometries at breakthrough. The reservoir containing thin intervals defined by widespread barriers recovers more oil at breakthrough. This phenomenon could be described by the dip angle group

N_θ(equation 5.B). As suggested by Shook et al. (1992), under the VE condition, the larger the dip angle group the higher the recovery. The presence of extensive shales divided a reservoir into layers. Meanwhile the 'global' Kv:Kh becomes zero as gas injected at the base of the model would not segregate to the top. This phenomenon and the dip angle group will be discussed further in Chapter 6.

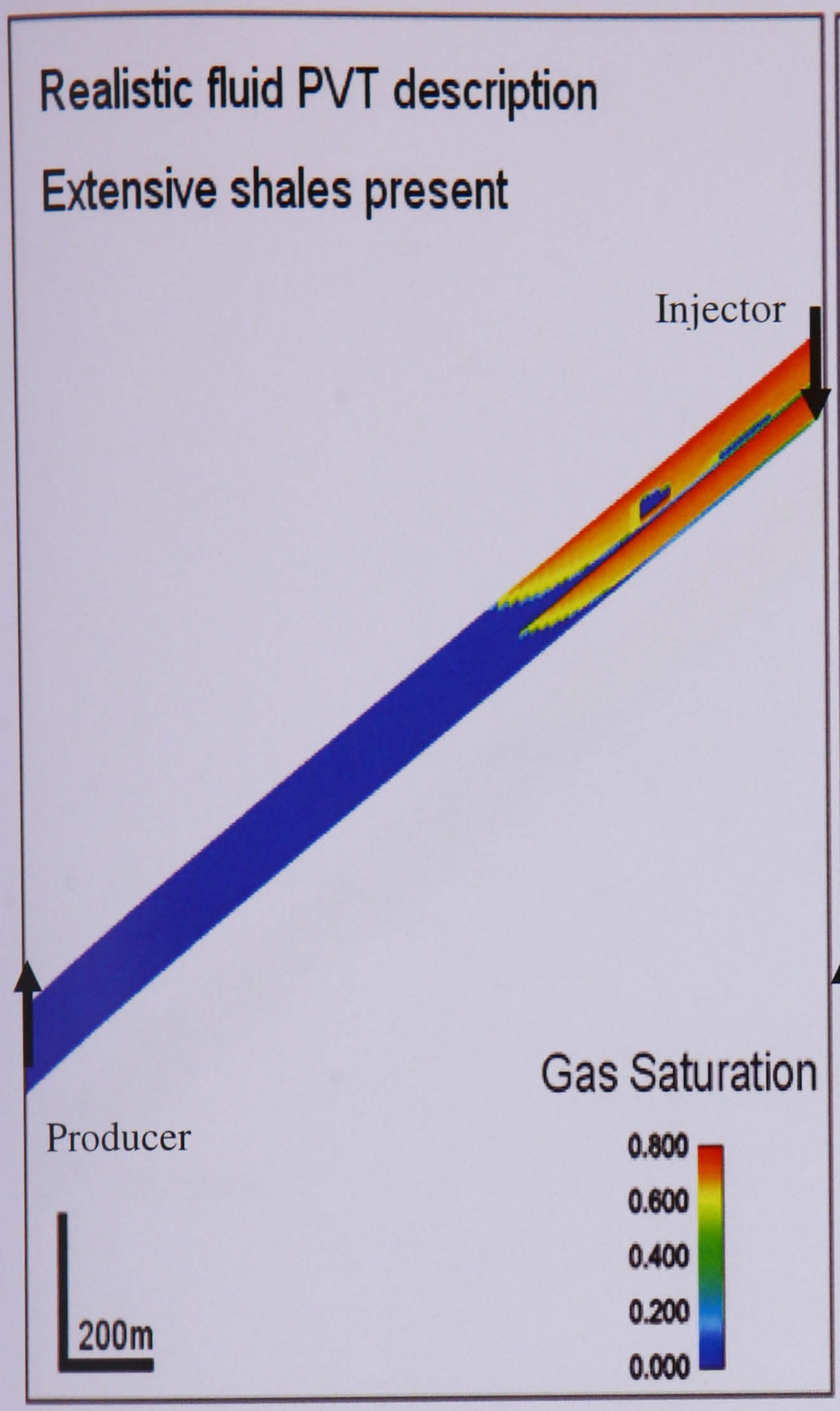


Figure 5.9A

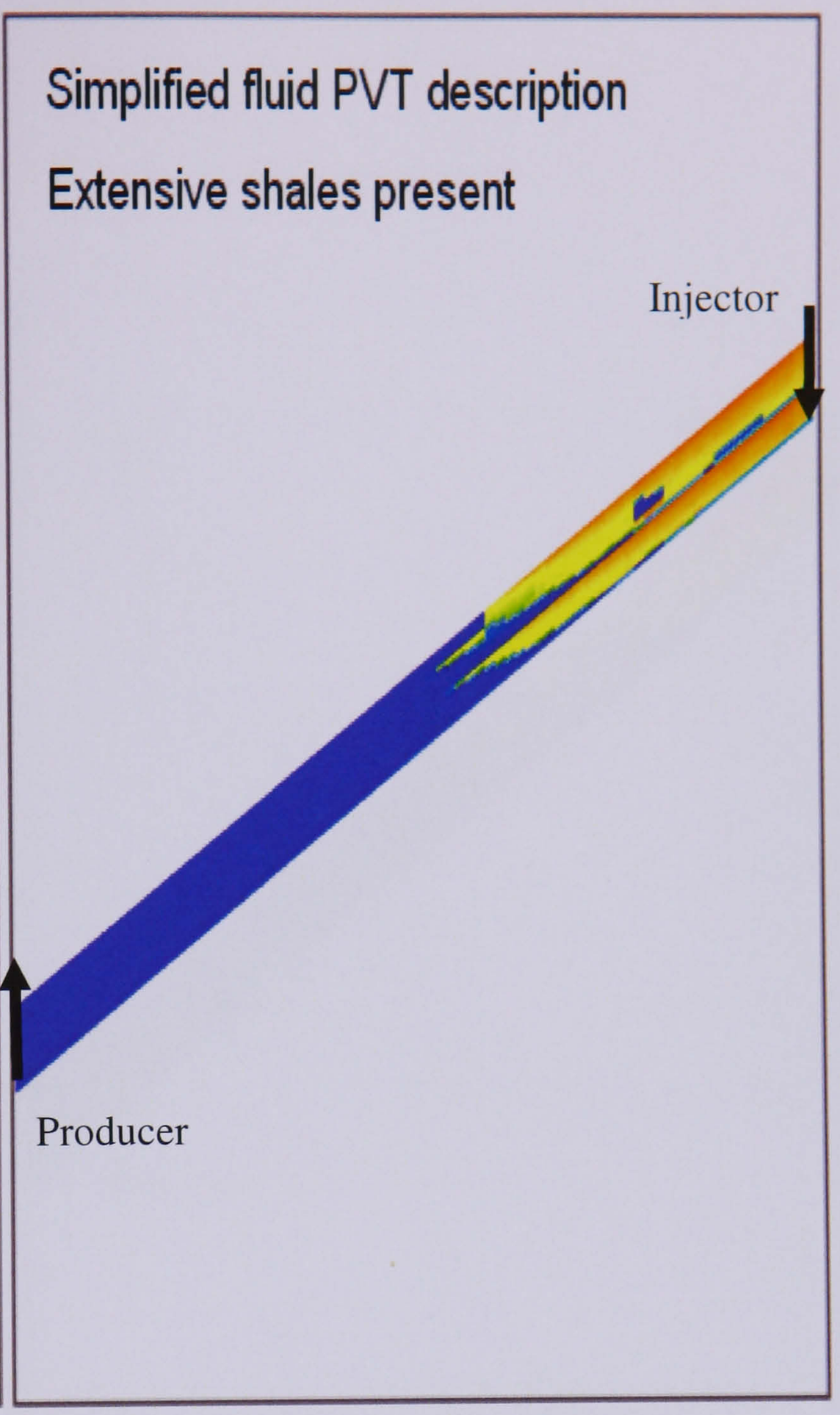


Figure 5.9B

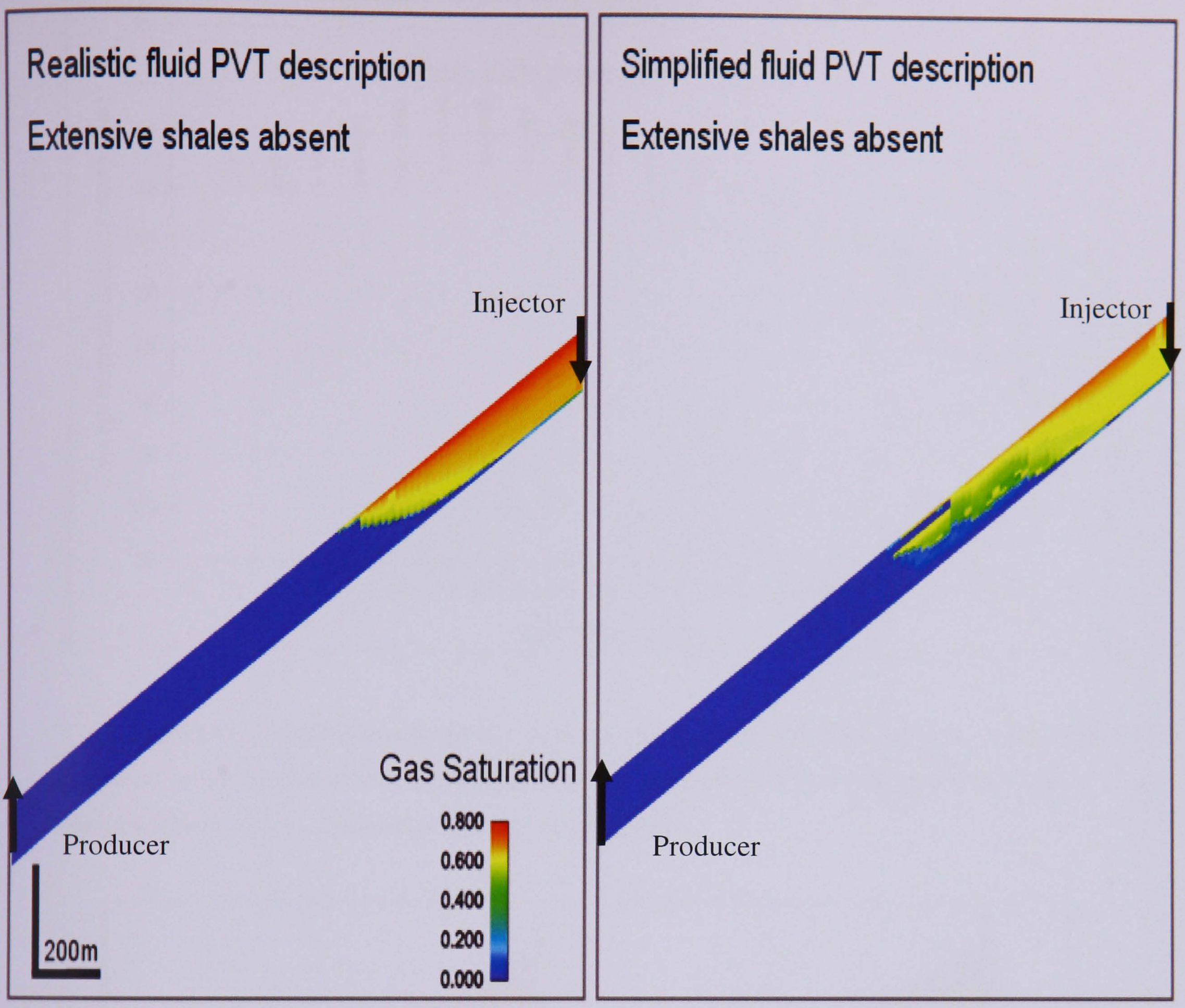


Figure 5.9C

Figure 5.9D

Figure 5.9. Cross section view of gas saturation after 3 years of production in Pereriv B. An extensive shale was present in the middle of the model and realistic fluid PVT description **(A)** and simplified fluid PVT description were applied **(B)**. Compared with the case where no extensive shale was present, and realistic fluid PVT description **(C)** and simplified fluid PVT description were applied **(D)**. The producers and injector were labeled. The plots showed that the gas saturation is higher in the invaded zone in the models containing the extensive shale **(A,B)** than in the models lacking the extensive shale **(C,D)**. With the extensive shale present, the gas saturation was subtly higher in the invaded zone. This effect is more obvious when realistic fluid PVT description was applied.

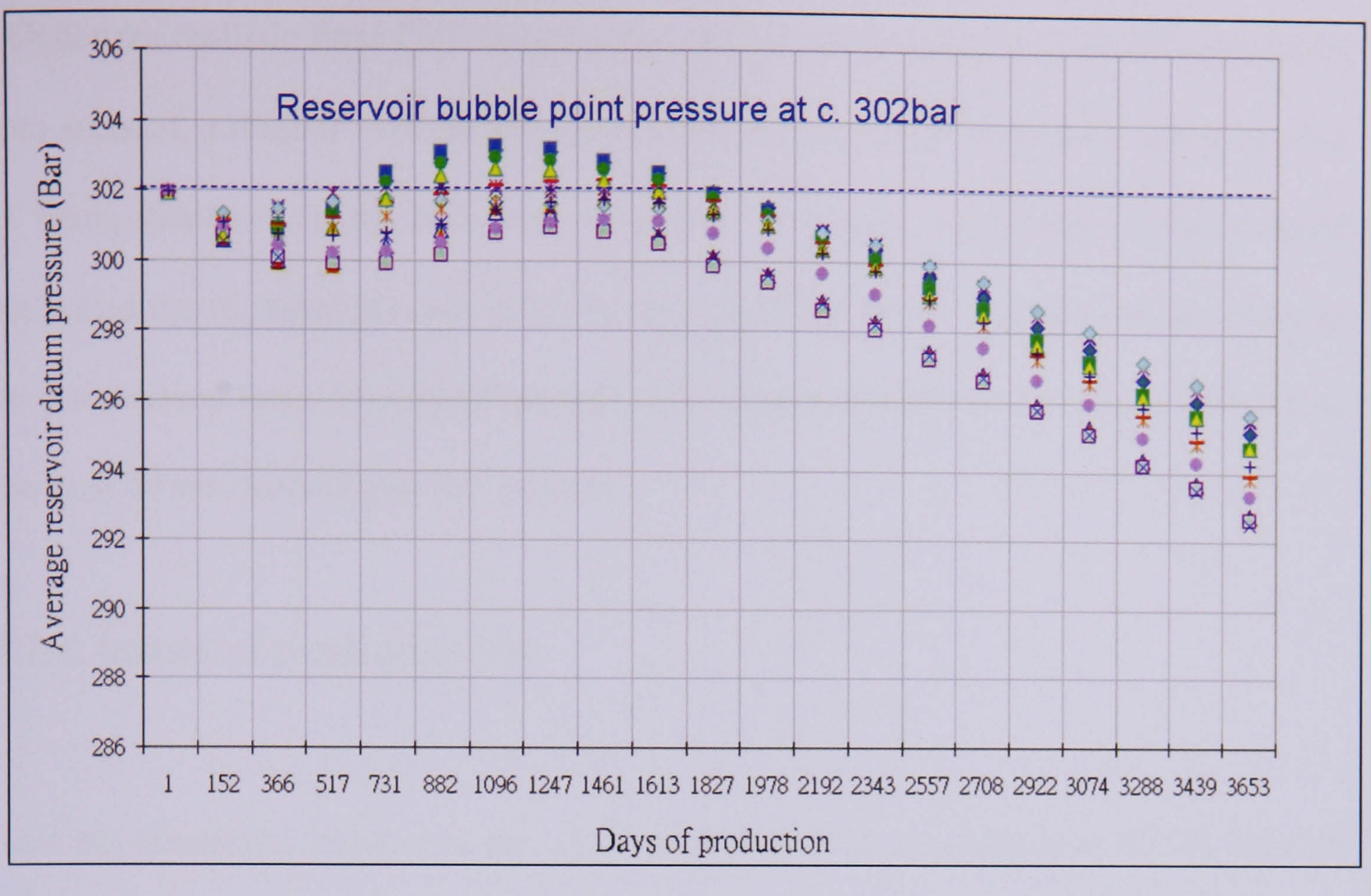


Figure 5.10. Average reservoir pressure at datum changes as a function of time for each of the 16 simulation experiments run with the realistic fluid PVT description. The reservoir datum pressure dropped below bubble point during the production period. Therefore gas was evolved out of solution.

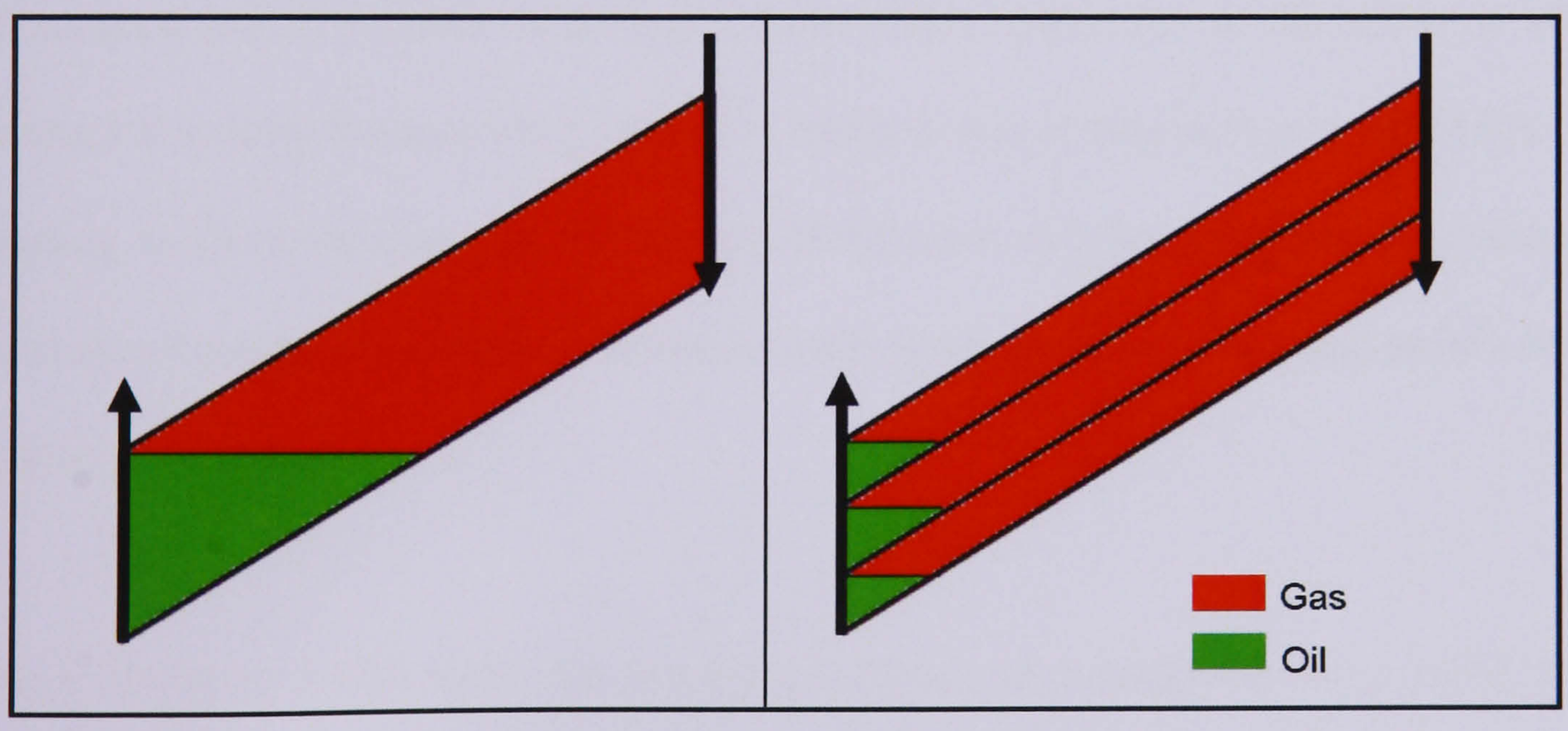


Figure 5.11A Figure 5.11B

Figure 5.11. Conceptual cross-section views of reservoirs with different layering geometry. Gas injection from the top (up-dip position) and a production well is located at the bottom of the model. The model with a thinner effective flow path (higher dip angle group N_θ, **11B, Right**) yielded higher breakthrough at oil recovery (BOR).

Under the realistic fluid PVT description, when evolved gas from solution was taken into account, a thinner vertical thickness helped the gas migrate upward faster instead of being displaced in the bulk flow direction. Therefore, modelling extensive shale increased the oil recovery. However in the simplified fluid PVT description, there is no gas evolved from solution (Figure 5.11B). Hence this effect was not as obvious as the case where evolved gas was present.

5.7.4. Impact of production rate

All the simulation studies so far were conducted with production at 93.3% Dietz's critical rate. Therefore all the displacements within the screening studies were considered to be gravitationally stable. The production rate can be varied according to the hydrocarbon demand. Moreover, because of uncertainty in reservoir properties the displacement stability could be different from initial expectations. Therefore, it was necessary to extend the screening study to a wider range of displacement stabilities. A screening analysis focusing on the impact of different stability conditions (governed by a range of production rates) on the rank order of the geological heterogeneities was covered in this section.

Figure 5.12A to 5.12D show the percentage change in average recovery factor and total gas production after 10 years of injection from simulation under both realistic and simplified fluid PVT description. A range of production rates has been applied in term of Dietz's critical rate. The figures show that the percentage change in average response is not strongly related to the production rate. Figures 5.12A and 5.12C show that Kv:Kh ratio is always the most important heterogeneity that influences recovery regardless of the fluid PVT description. Changing the sand Kv:Kh ratio from 0.1 to 1

yields an increase in recovery of c.16% at 46.7% Dietz's critical rate under both realistic and simplified fluid PVT description. At supercritical rates (186.7% Dietz's critical rate), the same modelling decision increased the recovery by c.13% under simplified fluid PVT description and by c.16% under realistic fluid PVT description. Increases in rate have a slightly larger influence on the response under simplified fluid PVT description; under the realistic fluid PVT description the recovery factor was less affected by the variation in rate.

For total gas production, although the ranking order of heterogeneities at different stability conditions appeared to be the same, the magnitude of the responses decreased when the production rate increased. For example, under realistic fluid PVT description and at 46.7% of Dietz's critical rate, modelling Kv:Kh equal to 1 decreases the total gas production by c. 15%. By contrast, at 186.7% Dietz's critical rate the same modelling decision only decreases the total gas production by c.3.3%. A similar impact was noticed under simplified fluid PVT description (Figure 5.12B, 5.12D).

The results suggested that the rank order was likely to be unchanged at different displacement stability. However, the magnitude of the response could change with the state of stability. If the displacement was gravity unstable, it was less likely to be affected by the geological heterogeneity. This was because the geological heterogeneity factor that controls the degree of the gravity stability has the largest influence on oil recovery and gas production. If the displacement was gravity unstable already, factors that affect VE became insignificant.

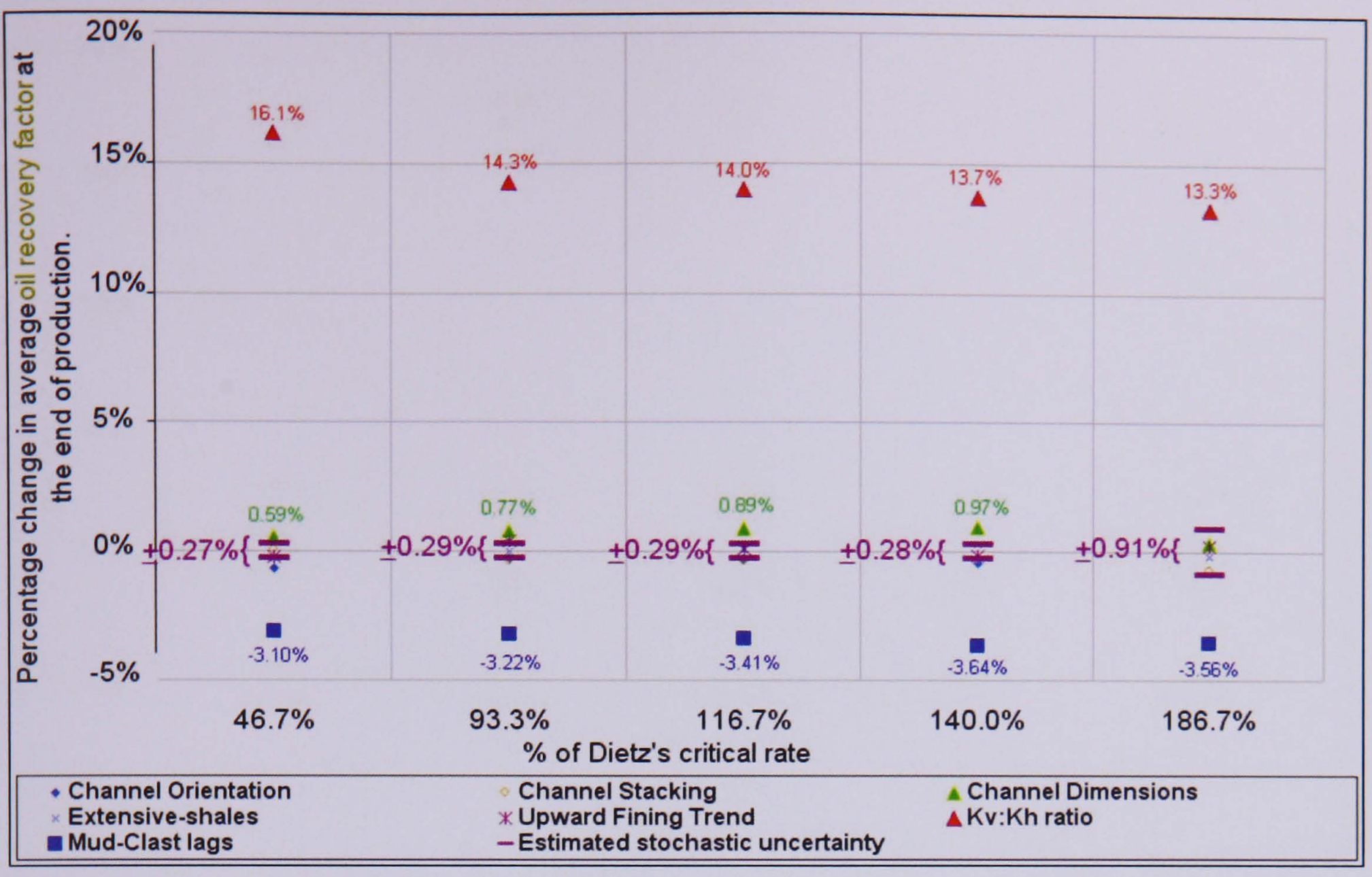


Figure 5.12A

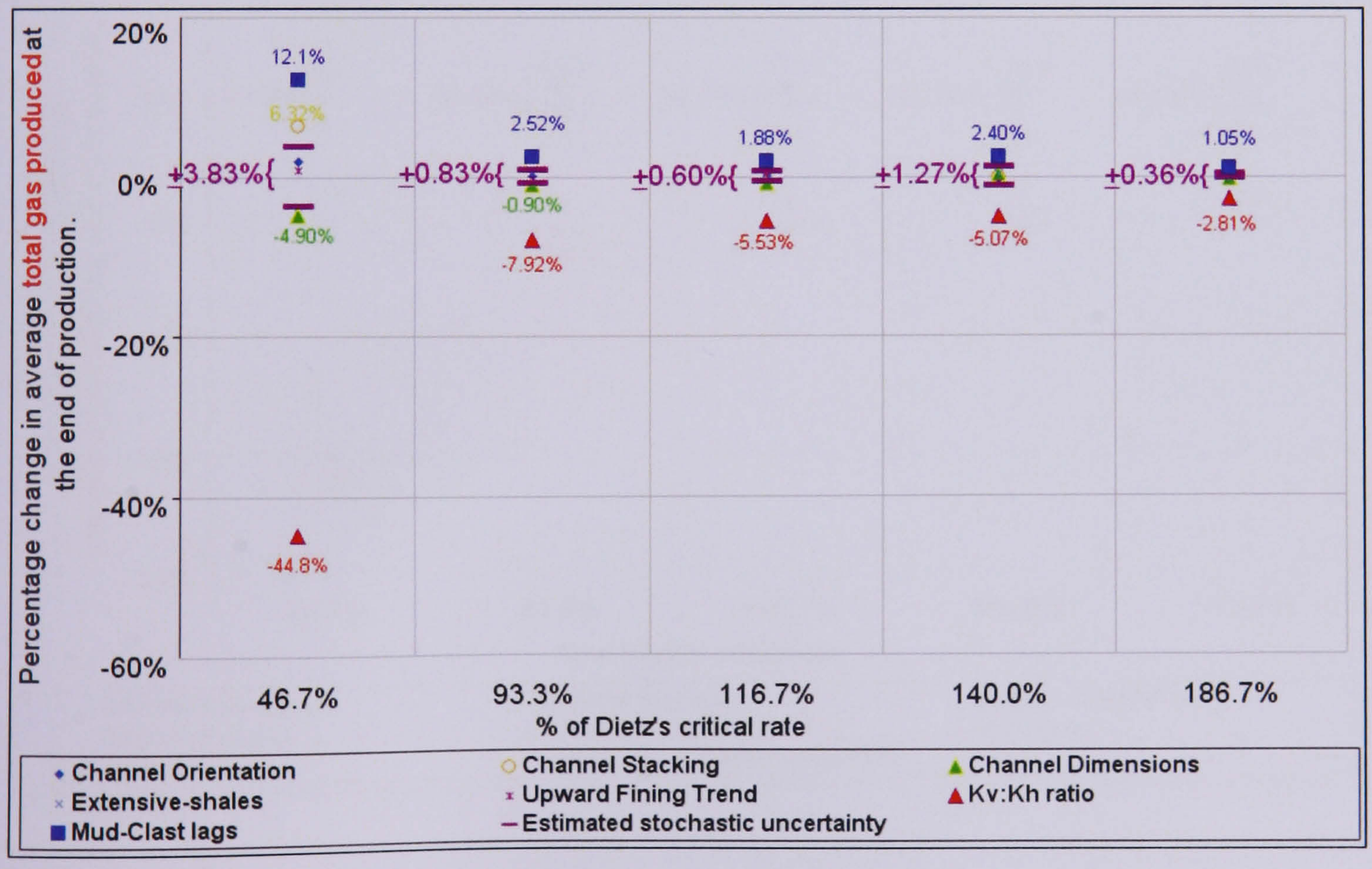


Figure 5.12B

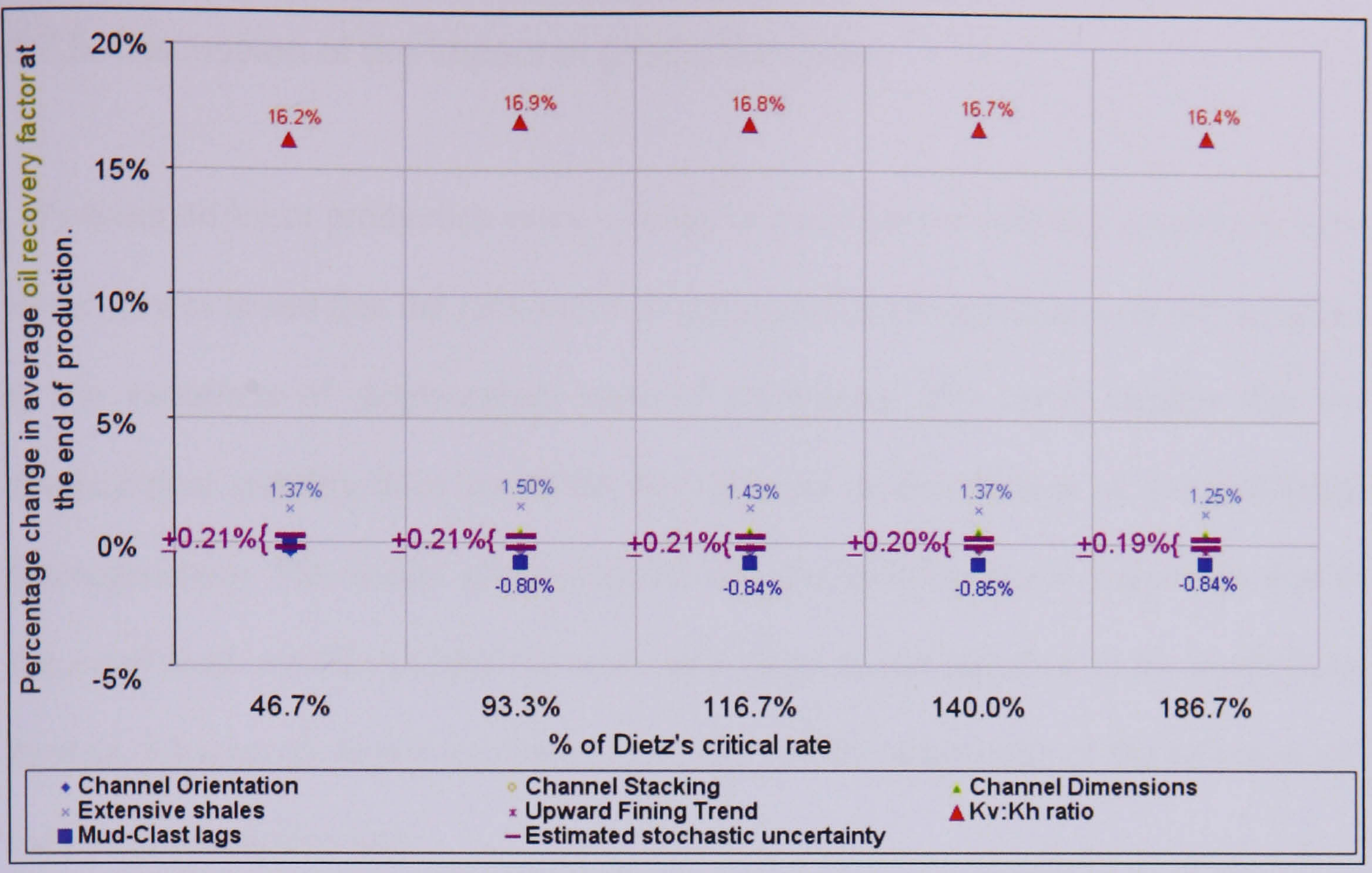


Figure 5.12C

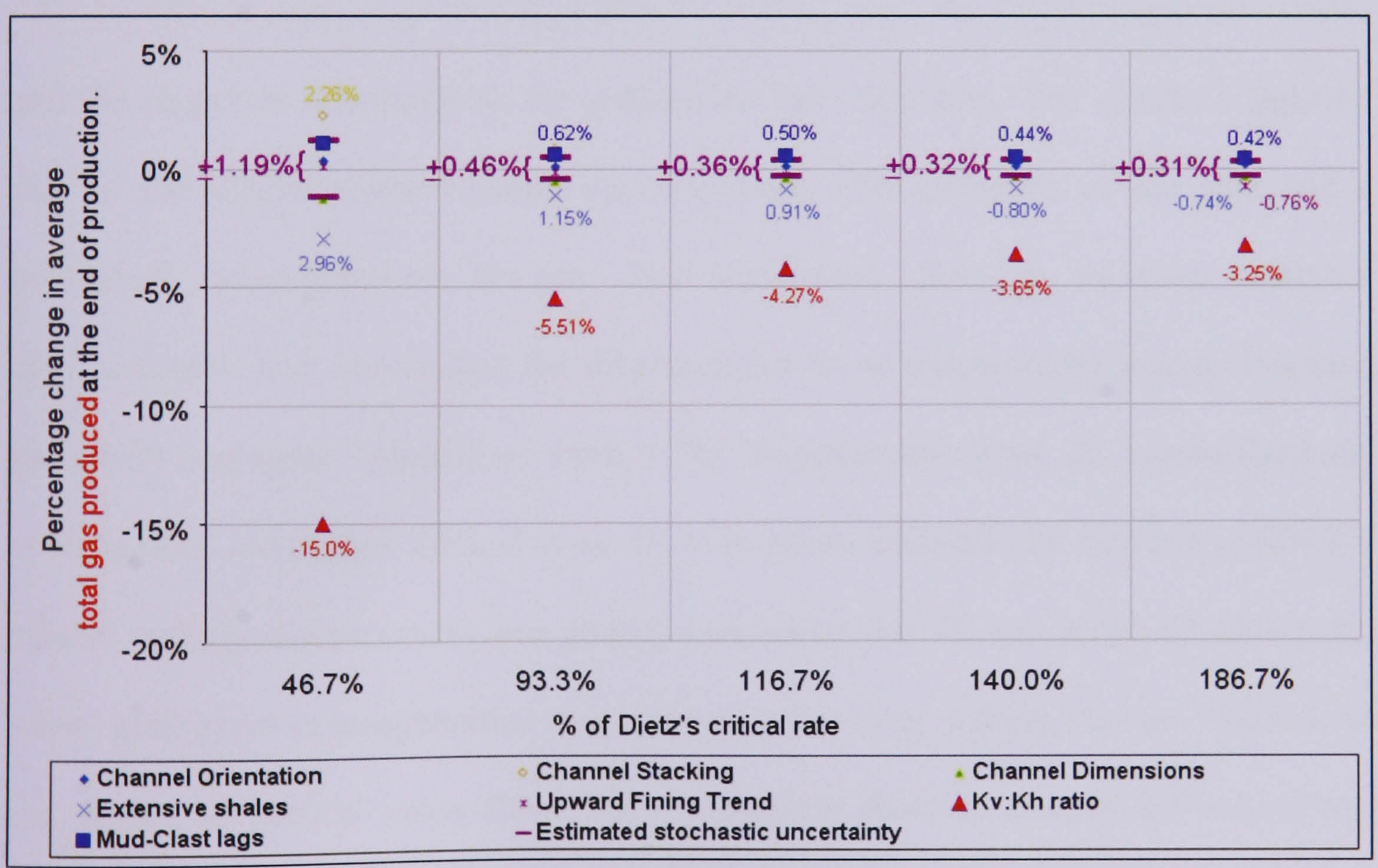


Figure 5.12D

Figure 5.12 (A-D). Average percentage change in recovery factor **(A, C)** and total gas produced **(B, D)** after 10 years of production. A range of production rates were applied with the simplified fluid PVT **(A, B)** and realistic fluid PVT properties **(C, D)**. The points plotted showed the response when each factor in the sensitivity analysis is varied from setting 1 to setting 2 (Table 5.1).

5.7.5. Discussion of the impact of production rate

By using different production rates, a range of gravitational stability conditions were tested. It was found that the rank order of geological heterogeneities was not sensitive to the variations of displacement stability conditions. The result implies that the displacement stability does not affect the recovery in the manner of the geological heterogeneities. The results also explained why the mobility stable water injection in the south flank models yielded the same rank order as gas injection in the north flank models (Chapter 4). However, it was observed that the magnitude of the response did vary with production rate.

At sub-critical rates (e.g. 46.7% of Dietz's critical rate), the largest response occurs, and the response decreased as the production rate increases. The results suggested that as the displacement became more unstable, the influence of the reservoir's geological heterogeneities became less significant. For the mobility unstable displacements, low rate helped the displacement to be stabilized by gravity because gas could segregate upwards to form a flat displacement front. In a homogeneous environment, maximum vertical cross flow occurred with offtake rate below Dietz's critical rate; the displacement was gravity dominated and VE was achieved. However, when geological heterogeneities were present, the heterogeneity factors influenced the degree of vertical cross flow. Such geological features directly influenced the state of VE in a displacement. For example, Kv:Kh controlled the degree of vertical cross flow. If gas could not segregate upwards freely even if the flow rate was below the Dietz's critical rate, the gas moved forward with the bulk flow direction. Previous studies have also shown that lower Kv:Kh has a positive impact on unstable displacements because vertical sweep efficiency is improved (Haldorsen 1986). For

mobility unstable displacement dominated by viscous forces, a high rate may magnify the influence of the geological features, e.g. fluids may channel through high permeability layers.

However, Figure 5.12 showed that the higher the offtake rate (less gravity stable), the heterogeneity became less significant for this mobility unstable gas-oil displacement. This was because the factors that control vertical segregation had the largest influence on the reservoir performance. The VE condition requires both vertical cross flow and gravity dominated flow. Compare with gravity unstable displacement, gravity stable displacements are more sensitive to heterogeneities that impede vertical segregation. If the displacement was gravity unstable already, gravity segregation can have very little influence. Even though gas can segregate upward freely, injected gas would form an over-riding gas tongue instead of forming a flat displacement front. Therefore the impact of the geological features on cross flow became less significant. Figure 5.12 shows that the higher the offtake rate (further away from stable condition) the less important the heterogeneity factors. This phenomenon was more obvious when simplified fluid PVT description was applied (Figure 5.12A-12B)

5.7.6. Impact of well control scheme

Figure 5.13 showed the recovery factor and cumulative GOR by gas injection for all the 16 simulations in the fourth screening study with realistic fluid PVT description. The results were generated at c. 93.3% Dietz's critical rate with a well control scheme applied. The variation of oil recovery and breakthrough time showed the impact of the ensemble of geological heterogeneities on reservoir performance.

The range of recovery factor was c. 58% - 74% and that of the cumulative GOR was c. 227 – 305 (SM^3/STM^3) after 10 years injection. Both recovery factor and cumulative GOR were measured under standard condition.

A production control scheme was now applied to the simulations such that the production well was shut in and re-opens based on the test of GOR. Figure 5.13A demonstrates that the sand Kv:Kh ratio still has the most significant impact on recovery factor, regardless of production rate. By switching sand Kv:Kh ratio from 0.1 to 1, the average recovery factor was increased by c.15% $\pm$1%. The results were similar to those in the previous section where no well control scheme was applied; it was observed that the magnitude of the response was not sensitive to the production rate (Figure 5.12C).

However, the impact of the heterogeneities on total gas production was very different in cases with or without the production control scheme. Figure 5.13B shows the impact of heterogeneity on total gas production when the well control scheme was applied (compare with Figure 5.12D). It was found that Kv:Kh ratio remains the most significant heterogeneity when the production rate was below or at Dietz's critical rate. However, when the production rate exceeded Dietz's critical rate, channel distribution and extensive shales became the two most significant heterogeneity factors that influenced the total gas production.

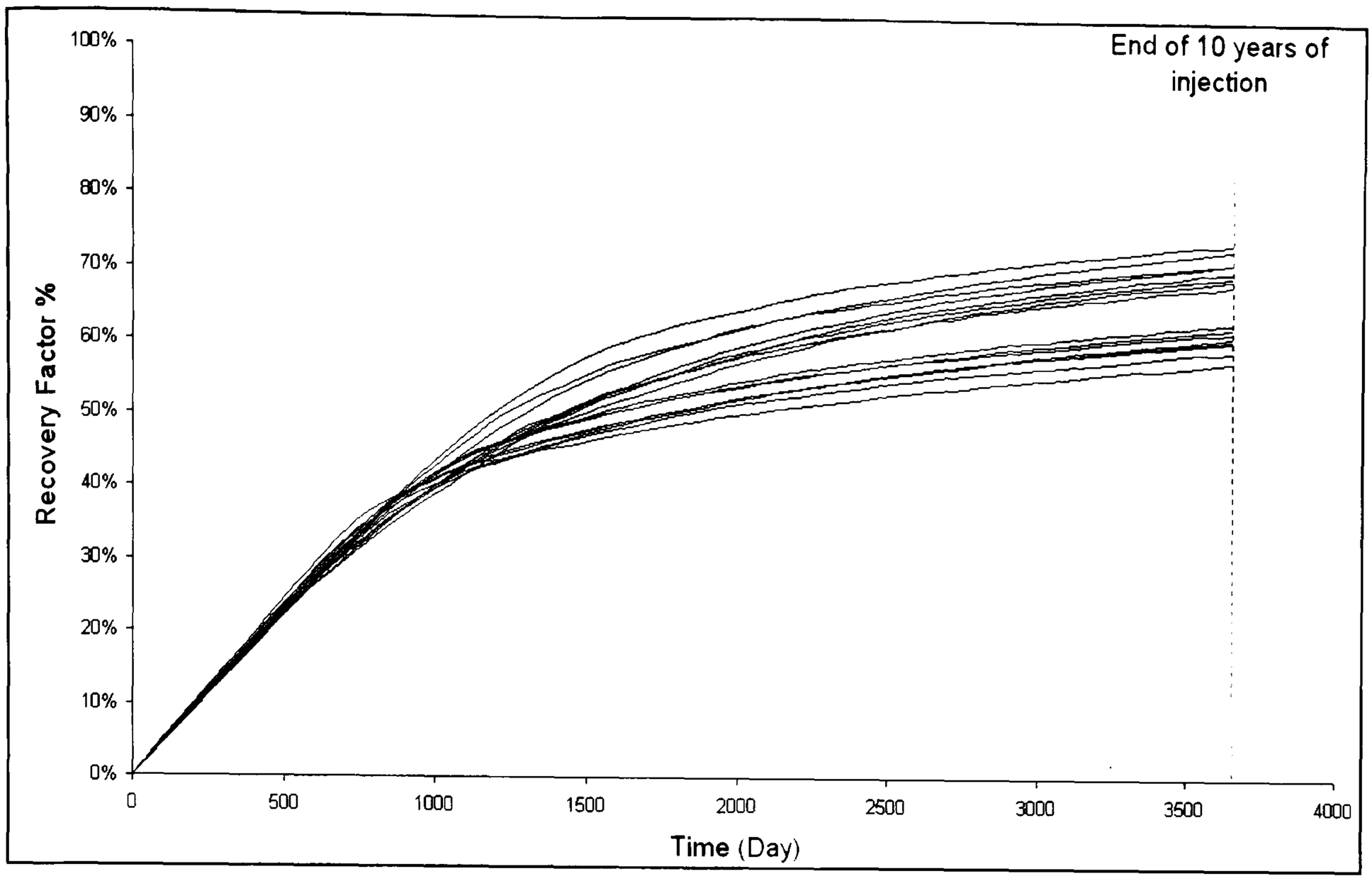


Figure 5.13A

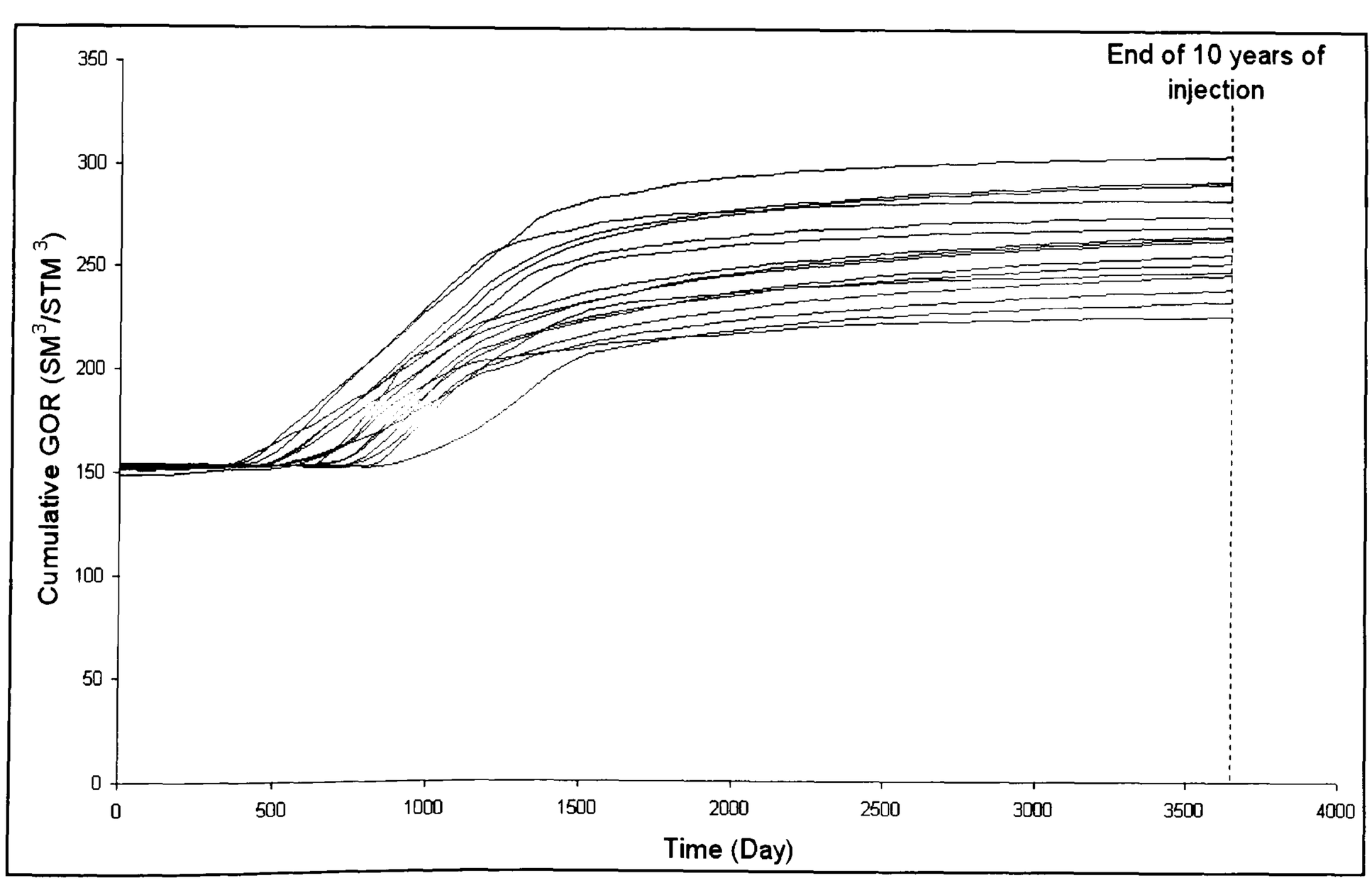


Figure 5.13B

Figure 5.13. Recovery factor **(A)** and cumulative gas oil production ratio (GOR) **(B)** as a function of time for each of the 16 simulation experiments run in the fourth sensitivity analysis on the Pereriv B layers based on realistic fluid PVT description: well control scheme was applied. The results were generated under c.93.3% of Dietz's critical rate. Analysis of these curves yielded the responses shown in Figures 5.14.

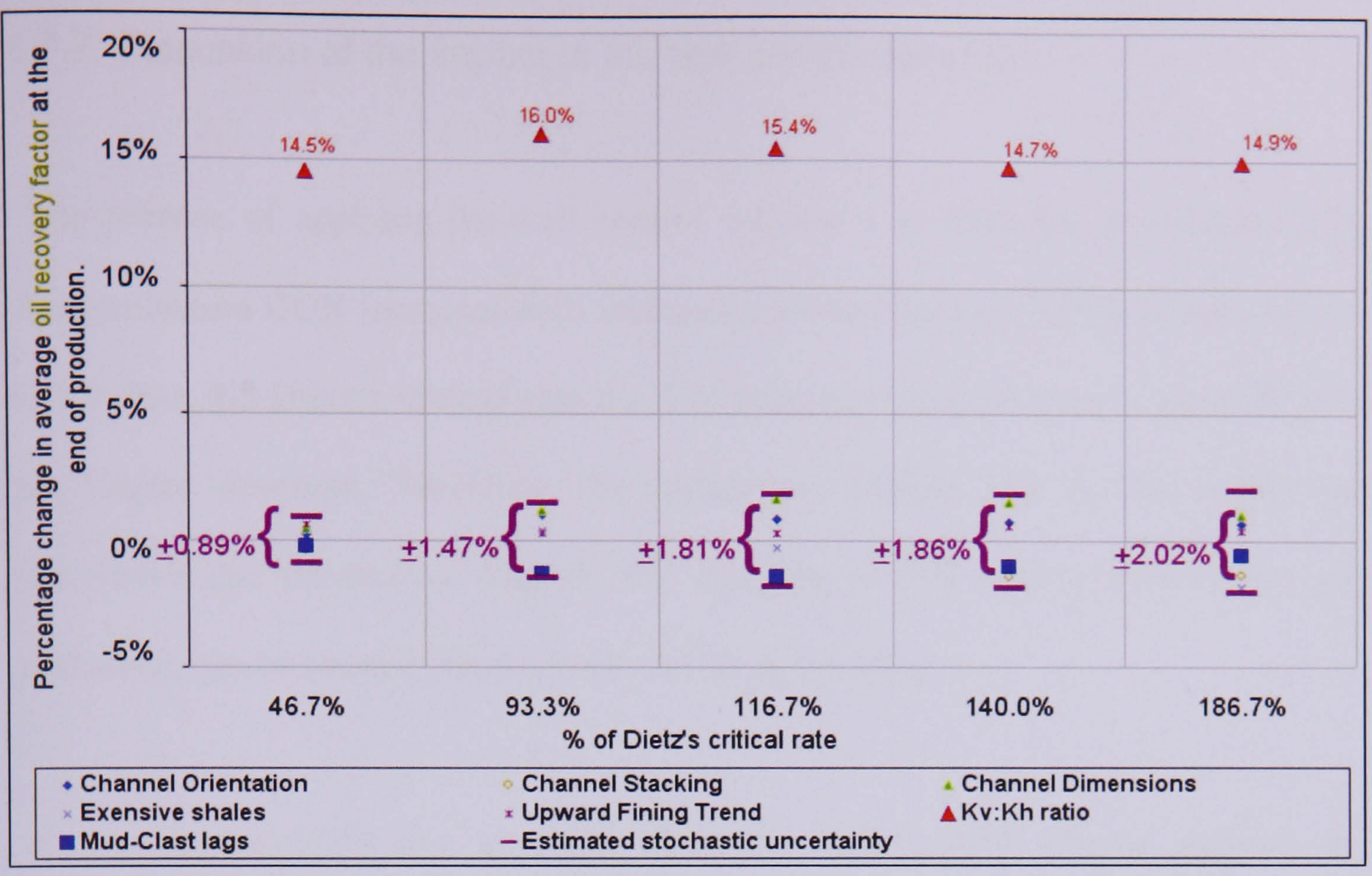


Figure 5.14A

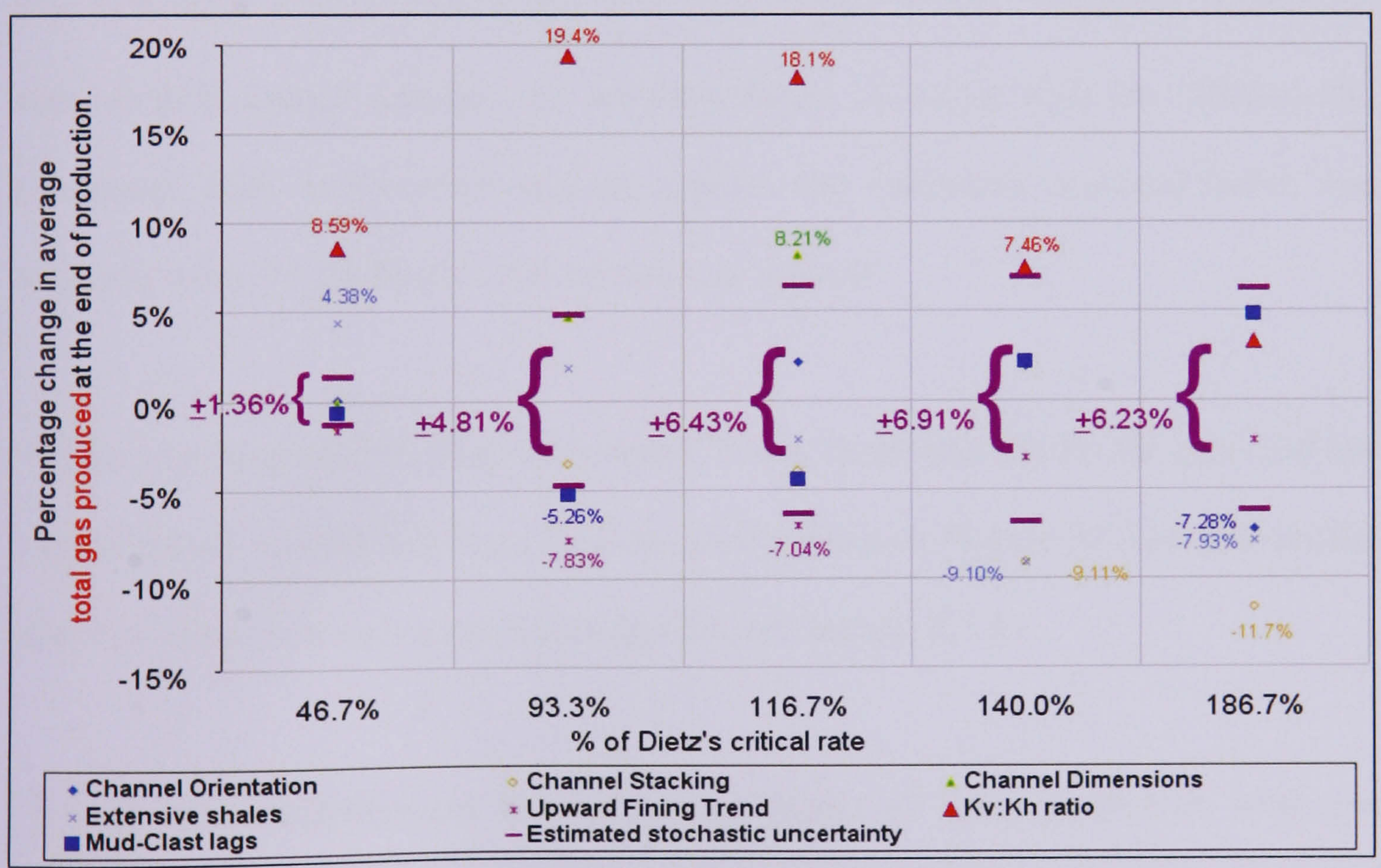


Figure 5.14B

Figure 5.14 (A-B). Average percentage change in recovery factor **(A, top)** and total gas produced **(B, bottom)** after 10 years of production in north flank subset models of Pereriv B. A range of production rates were applied with the realistic fluid PVT description and well control scheme. The points plotted show the response when each factor in the sensitivity analysis was varied from setting 1 to setting 2 (Table 5.1).

5.7.7. Discussion of the impact of the well control scheme

The purpose of applying the well control scheme is to limit the production GOR. The production GOR increases with increasing production rate. When offtake rates is higher than the Dietz's critical rate the displacement becomes gravity unstable so a gas tongue develops. Therefore, the higher the offtake rate is, the higher the cumulative gas production will be. By applying a well control scheme the gas production can be limited (Figure 5.6B, 5.13B and 5.15A).

It was demonstrated that in cases when the well control scheme applied, the recovery factor was reduced by c. 10%. This was because the production wells were shut-in from time to time due to the GOR limit (Figure 5.15B). Moreover, when there was no well control scheme, the recovery factor increased with the offtake rate. Otherwise, with well control scheme applied, the maximum recovery factor was achieved when 93.3% Dietz's critical rate was applied.

In the screening studies with well control, it was found that the Kv:Kh ratio had the largest impact on recovery regardless the production rate (Figure 5.13A). The results were the same if no well control was applied (see section 5.7.4).

It was not straightforward to explain the impact of heterogeneity on total gas production. When the displacement was stable, the sand Kv:Kh ratio was the most important factor for total gas production, as shown in the other screening studies. However, when production exceeded the critical rate, it was found that channel distribution became the most important heterogeneity factor for total gas production. The reason for this was not yet clear. Once the displacement became unstable, in

theory gas tongues were formed that lead to large amounts of gas being produced. When the well control scheme was applied, gas production was restricted because the production well was shut in. Therefore, gas would migrate back to higher positions (Figure 5.16E – 5.16I). The production well opened again once the amount of gas near the production well fell below the constrained GOR limit. The gas migration direction was a lot more complex than the case where no well control scheme was applied. Gas migration was related to how often the well was opened and how far the gas has migrated away from the well, so that the macroscopic gas displacement was not mainly driven by the production rate.

To understand the rank order, it requires a thorough study of the influence of heterogeneity on gas migration during shut-in, and to de-alias the responses due to the influence of heterogeneity during displacement. These studies were beyond the scope of this project and further work was needed.

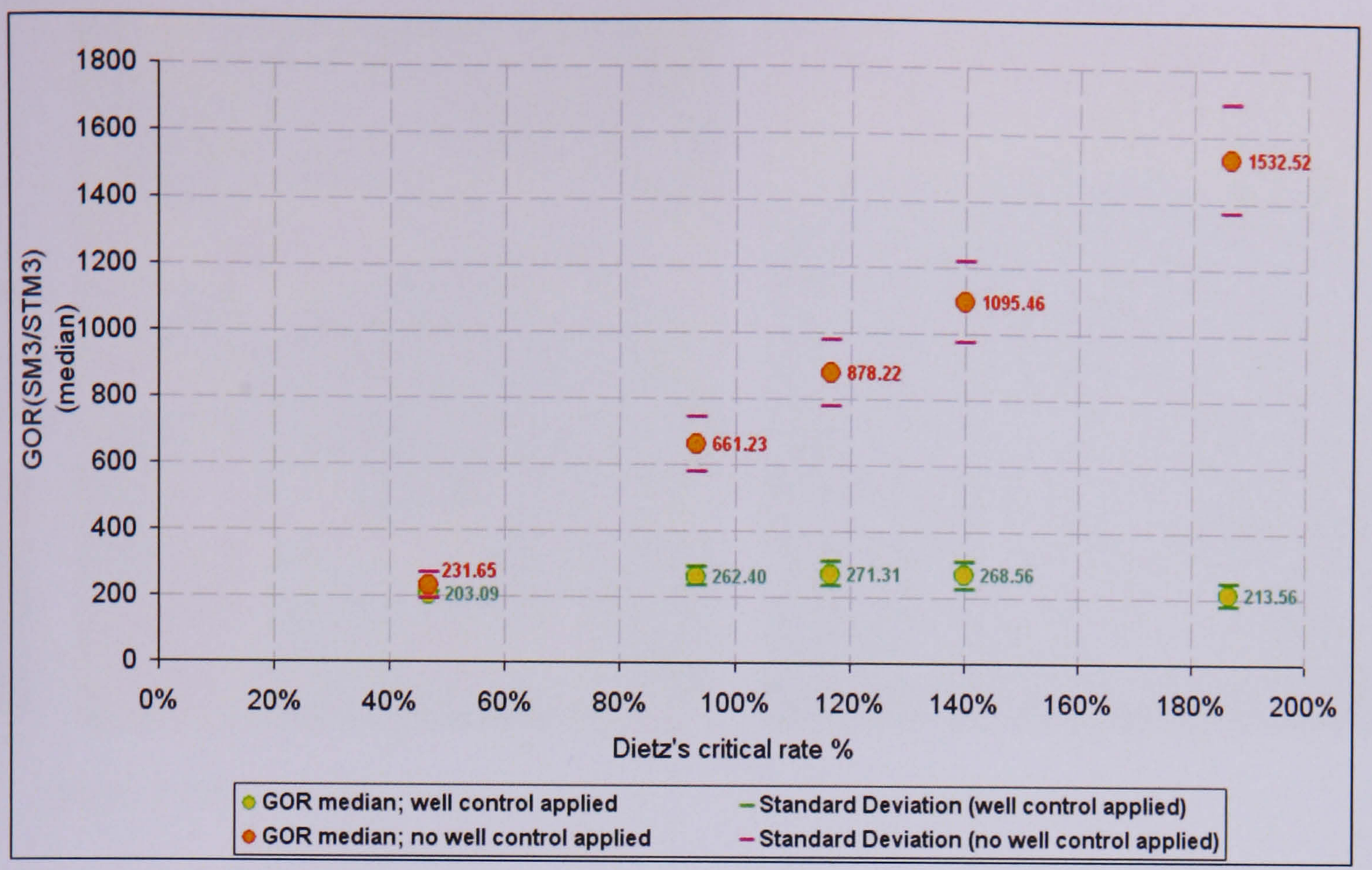


Figure 5.15A

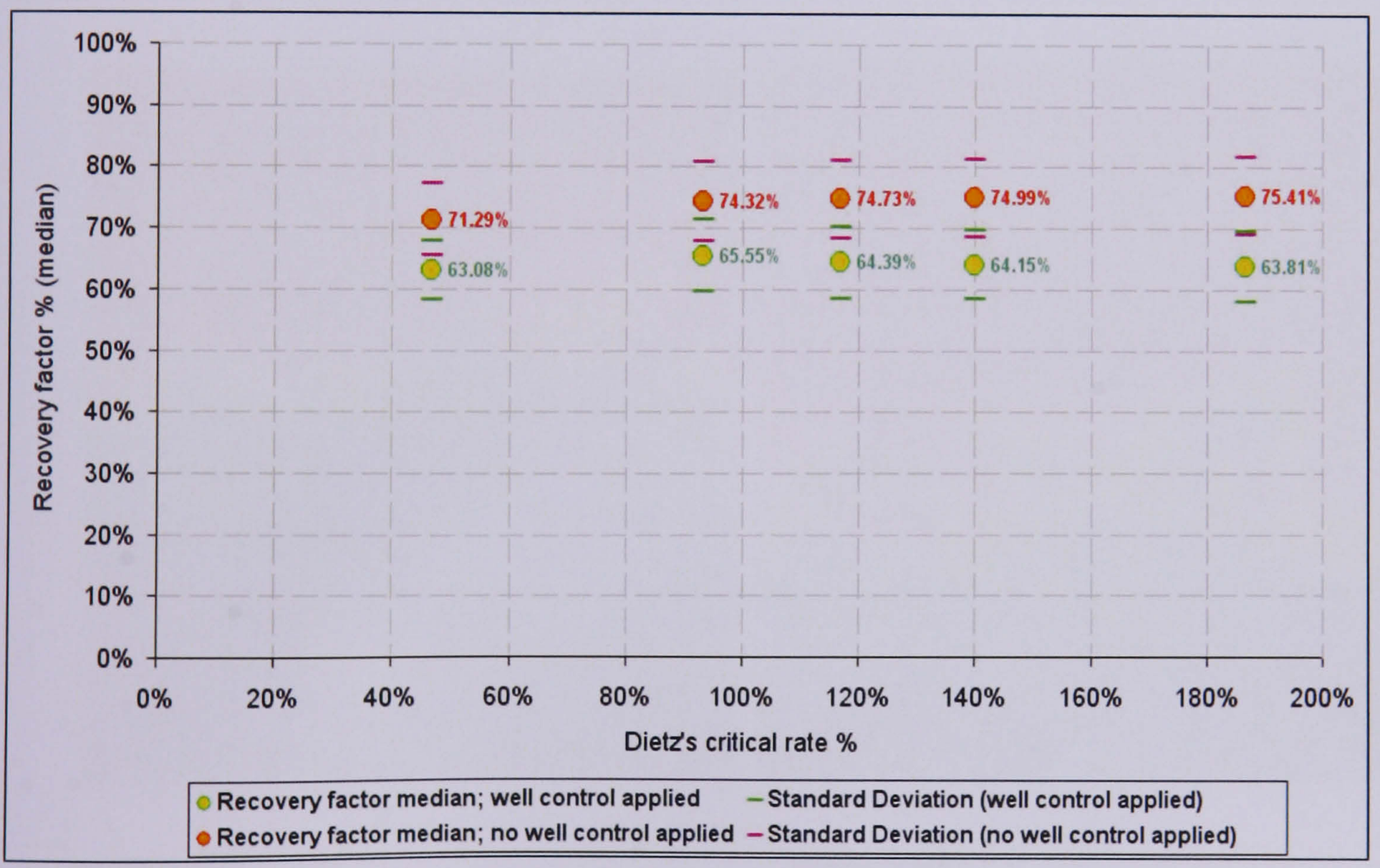


Figure 5.15B

Figure 5.15. Average GOR **(A, top)** and recovery factor **(B, bottom)** as a function of production rate when different well control scheme was applied. The cumulative recovery factor was found to be c. 10% higher than the case when well control scheme was applied. However the cumulative GOR was found to be much lower when the well control scheme was applied, and the highest cumulative GOR is found when c.116.7% Dietz's critical rate was used. Both simulations were conducted under realistic fluid PVT description.

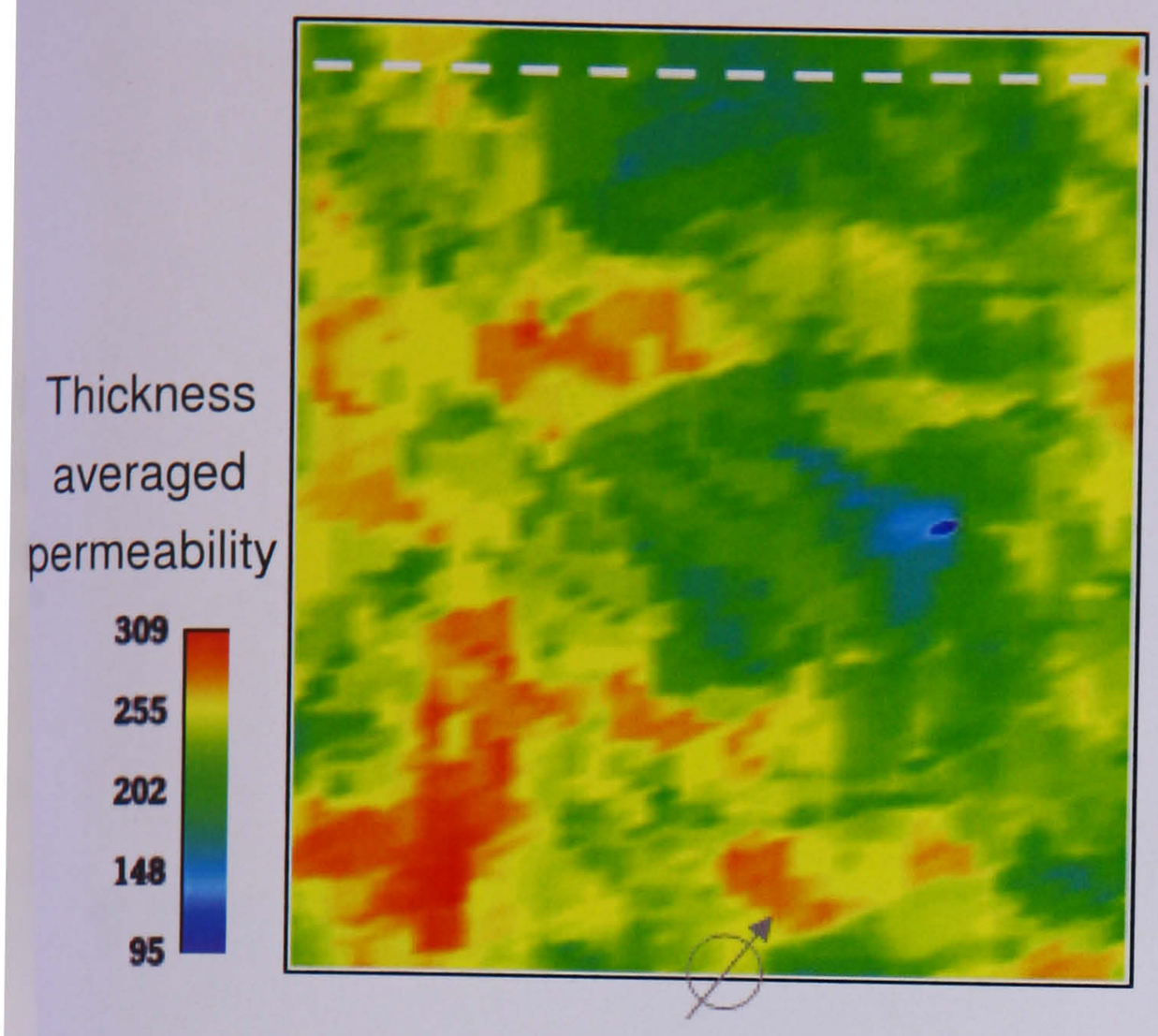


Figure 5.16A

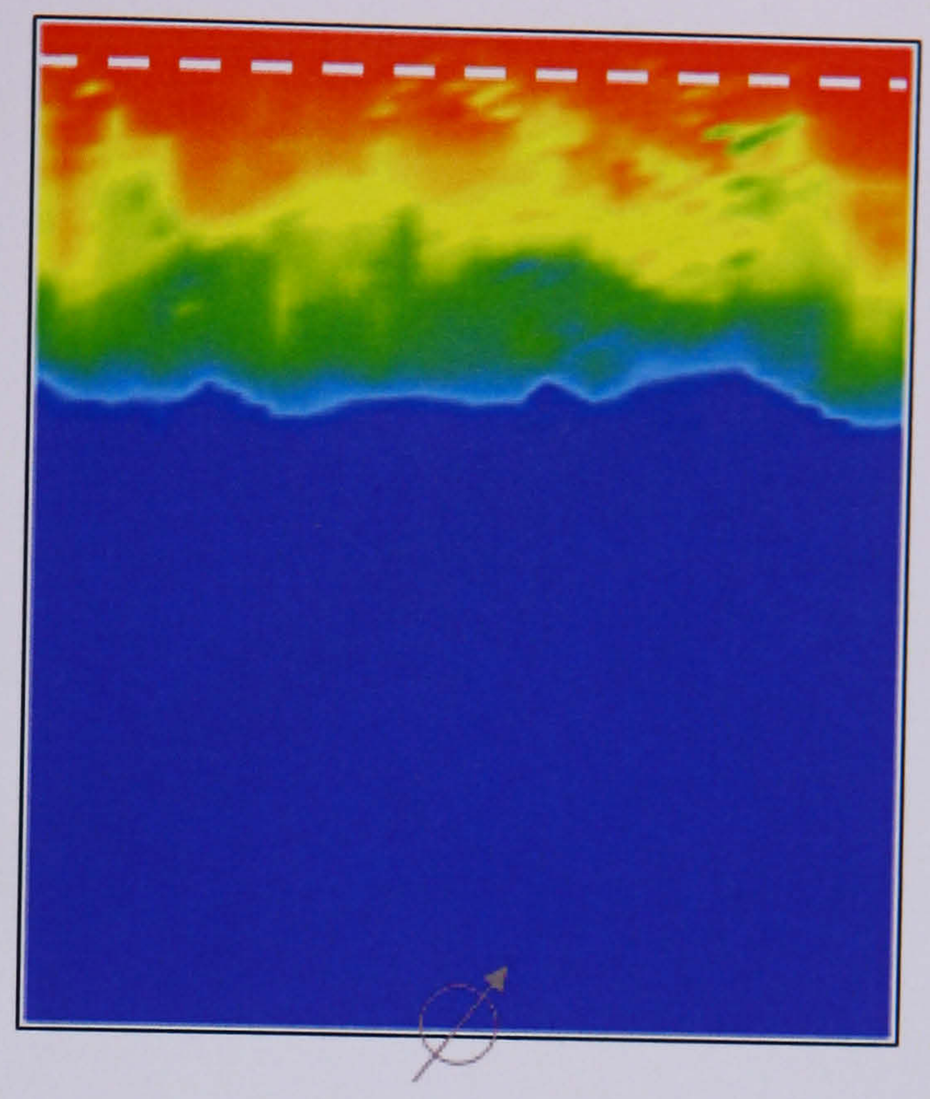


Figure 5.16B

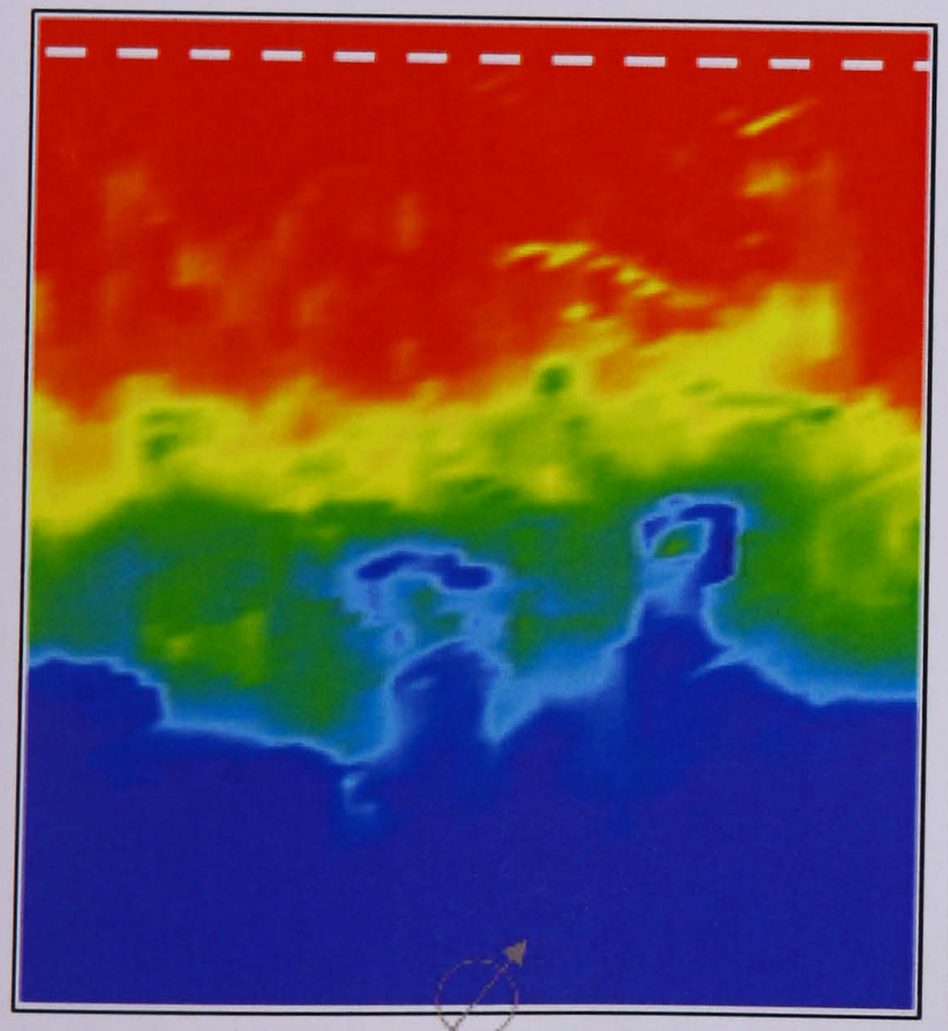


Figure 5.16C

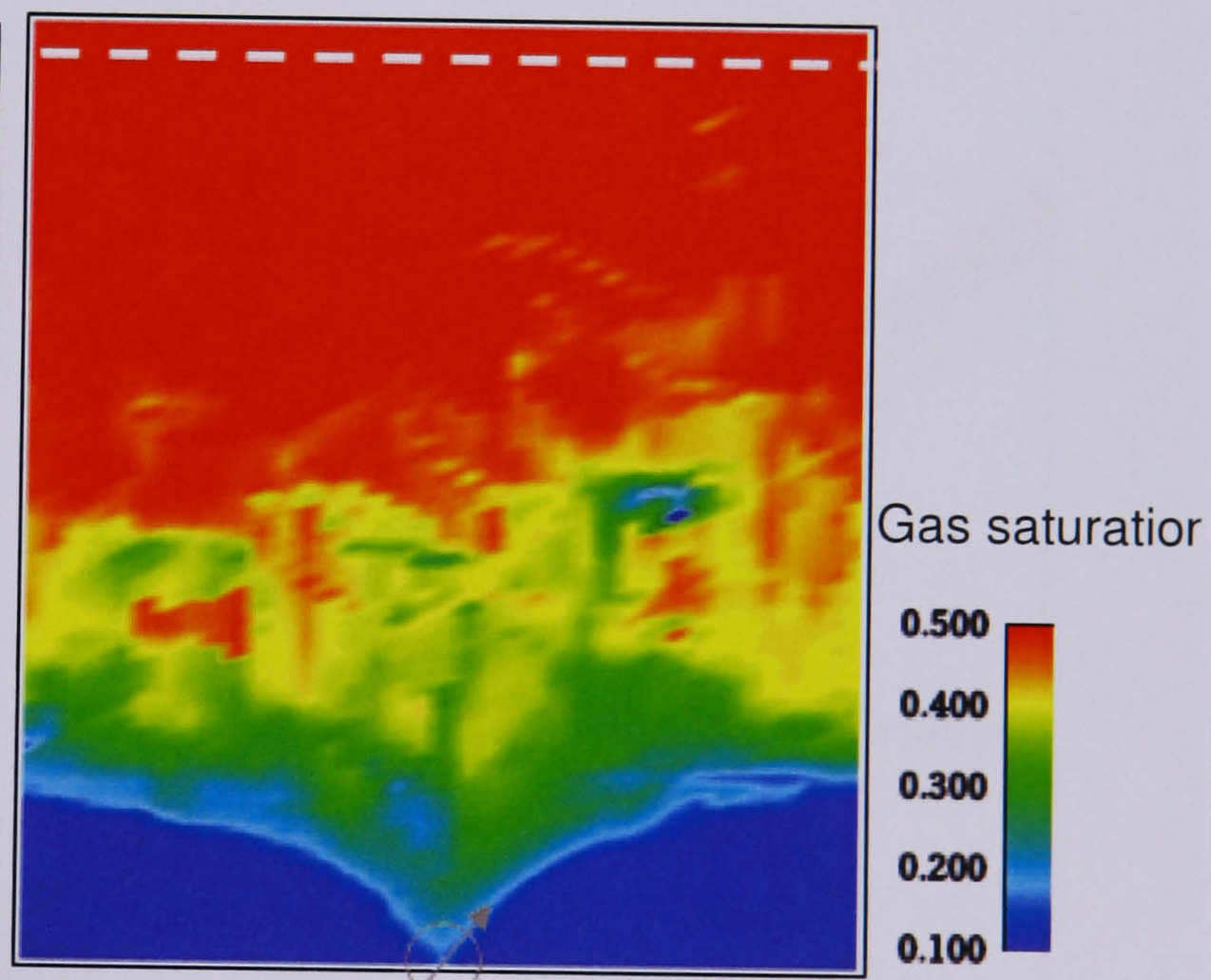


Figure 5.16D



Figure 5.16E

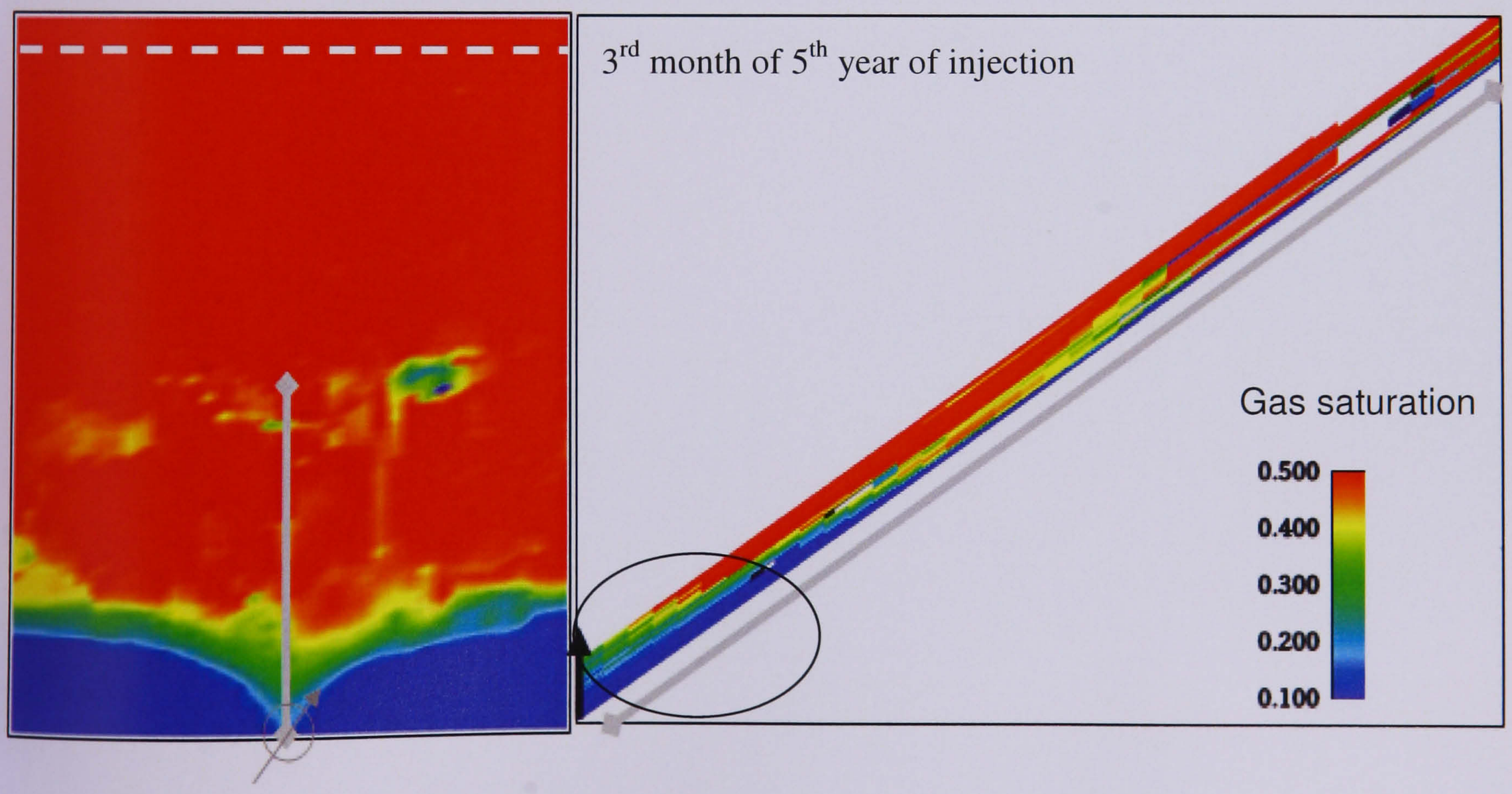


Figure 5.16F

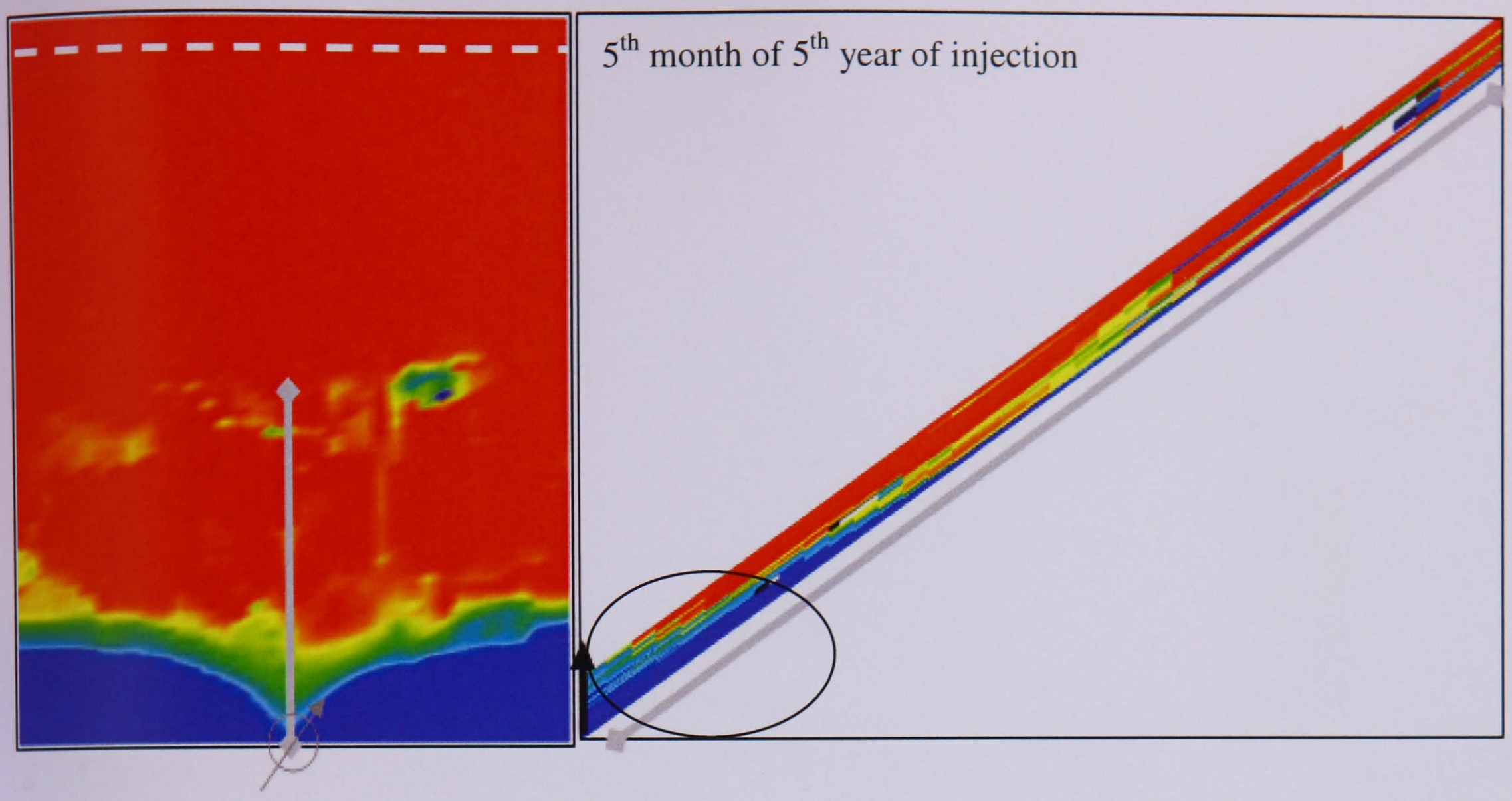


Figure 5.16G

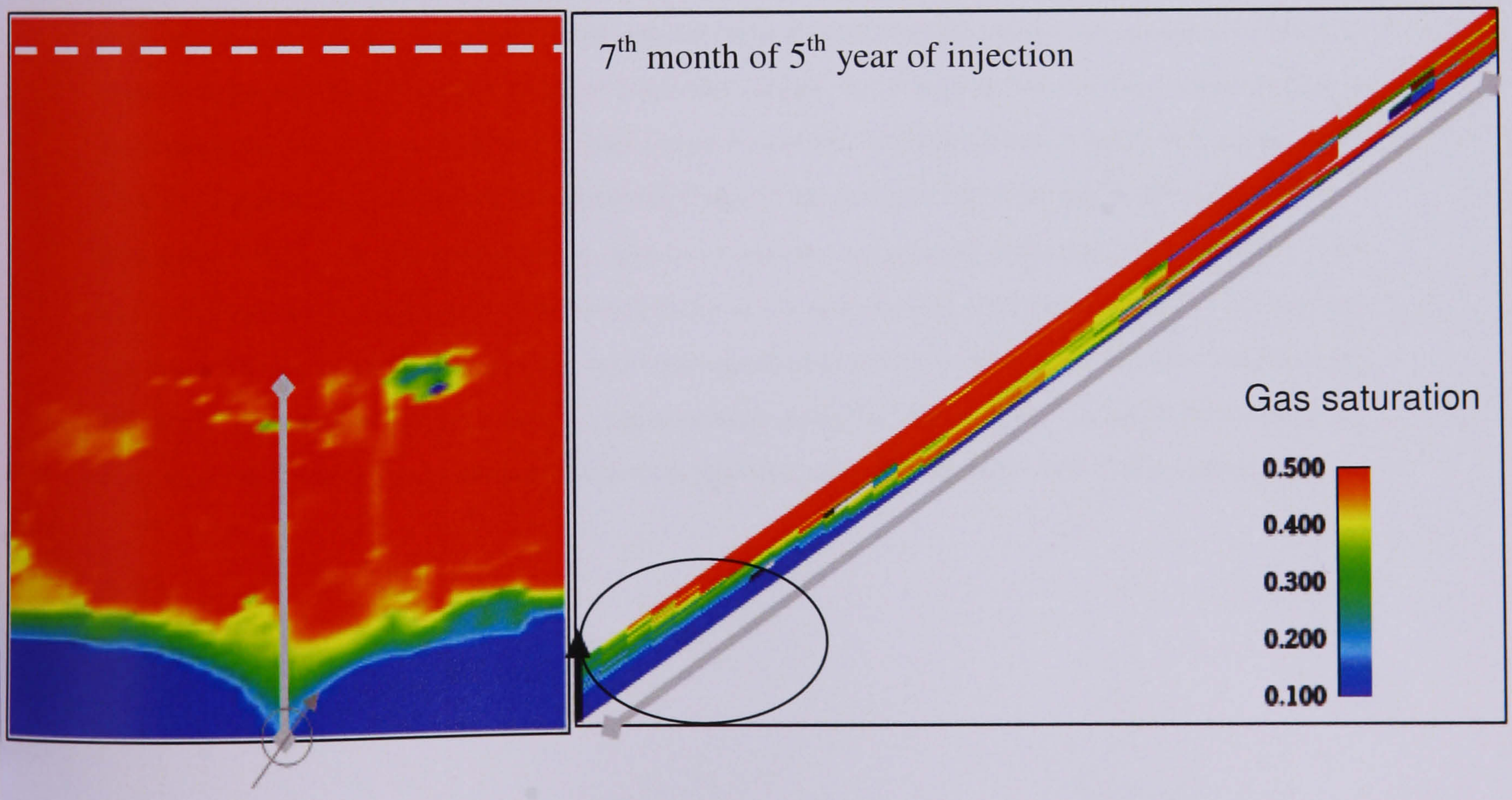


Figure 5.16H

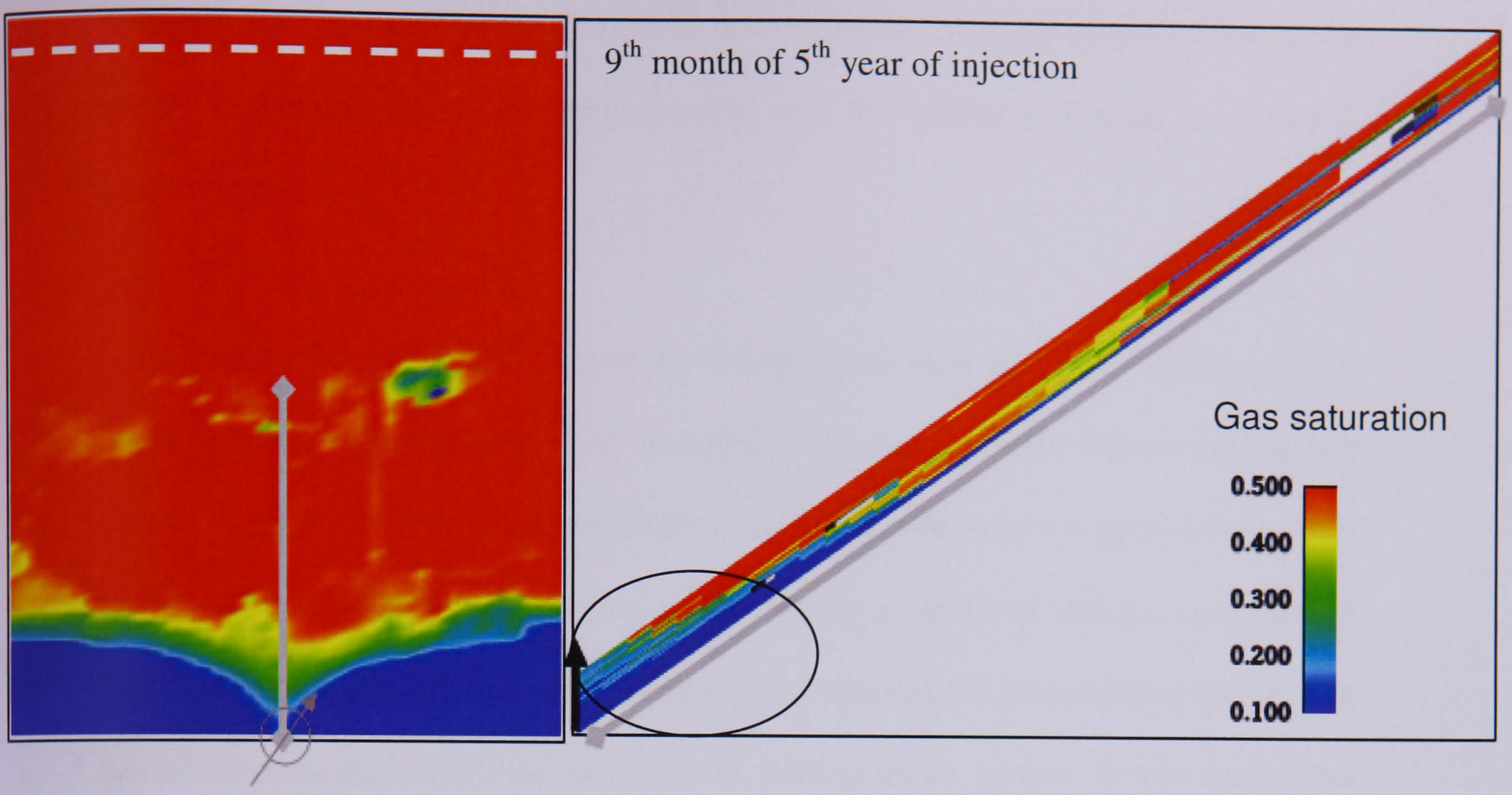


Figure 5.16I

Figure 5.16. Plan view of thickness-averaged permeability **(A)** ; and thickness-averaged mobile gas saturation plot of year 1 **(B)** , year 2 **(C)** , year 3 **(D)** and year 5 **(E-I)** of gas injection in a north-flank sector model of Pereriv B under realistic fluid PVT descriptions with a well control scheme applied. The white dotted line represents the inlet face of gas injection and the location of a producer well is also labeled. The 5th year of injection was focused in order to demonstrate the influence of well control. A cross-section view of gas saturation was also plotted for figure **E-I.** In the 5th year of injection, the producer was shut during the 1st **(E),** 5th **(G)** and the 9th **(I)** month and re-opened during the 3rd **(F)** and the 7th **(H)** month. The opening and shutting-in of the producer was based on the well's GOR constrain. There was a subtle variation of gas saturation between the shut-in and open periods; while the producer was closed, lower gas saturation was found near the producer and higher gas saturation was found at a higher position (black circle). The results demonstrated that gas moved to a higher position during the shut-in period. The figures demonstrated an example of the variation of gas saturation in one of the high NTG sector models under 93.3% Dietz's critical rate.

5.8. General discussion

The results discussed in this chapter show a similar rank order of the heterogeneity factors from the screening studies under both simplified and a more realistic PVT descriptions. This suggested that the realistic fluid PVT description had only a minor

influence on the rank order. Therefore the streamline simulator was adequate for identifying which geological heterogeneity had the largest influence on reservoir performance.

As mentioned in Chapter 3, gas-oil displacement was mobility unstable, but it could be stabilized by gravity when the offtake rate was below the Dietz's critical rate. However, reservoir offtake rate might be subject to the demand for hydrocarbon. This chapter discussed screening studies which covers a range of offtake rates. These studies were undertaken to test the relationship between the gravitational stability of gas-oil displacement and the rank order of heterogeneity factors. It was found that reservoir performance was less sensitive to heterogeneity under gravity unstable displacement compared with gravity stable displacement. Mobility unstable displacements could yield a high recovery if the displacement was under vertical equilibrium (VE) and a gravity stable condition. Perfect VE occurs when complete vertical segregation occurs in a gravity dominated displacement. It was found that the heterogeneity factor that controls the vertical segregation had a significant influence on immiscible mobility unstable displacement. Thus, a gravity stable displacement, was more sensitive to the factors that influence the vertical segregation in displacement such as sandbody Kv:Kh. It was because a gravity stable displacement required long enough time for injected fluid to establish VE, i.e. it required offtake rate below Dietz's critical rate. On the other hand, if the offtake rate was larger than the Dietz's critical rate, the different degree of vertical segregation became insignificant because the displacement was strongly influenced by viscous forces and eventually no longer in VE. Thus, the heterogeneity factors had less influence on a reservoir's performance when the offtake rate was higher than Dietz's critical rate. For viscous force dominated displacement, the variation in permeability yielded a

larger influence on sweep efficiency, compared with the factors that solely influence the fluids vertical segregation.

The influence of the 'non-reservoir' activity might be underestimated during the reservoir modelling process. In reality, reservoir performance is often affected by 'non-reservoir' factors, such as production well shut-in for pressure tests or because of equipment constraints (e.g GOR limit). The impact of well control schemes was considered in this chapter. The results from this investigation demonstrated that such activity affects the sensitivity of the reservoir performance response to the geological heterogeneity factors. This is because the 'non-reservoir' activity itself is also affected by the geological features. For example, the duration of a well shut-in period is related to both injected gas movement during the production period and in-situ gas migration during the production well shut-in period. However, the heterogeneity factor that has the largest influence on injected gas movement during a production period may not have the same influence on in-situ gas migration during the well shut-in period. Therefore if a 'non-reservoir' activity is introduced to the displacement process, the rank order of the influence of the heterogeneity factor on gas-oil displacement would be compounded with the impact of the 'non-reservoir' activity. It would be necessary to conduct screening study before and after 'non-reservoir' activity take place, e.g. well control scheme, as the reservoir condition would be different.

All the results showed that the genetic-unit scale heterogeneity factors in the Azeri environment had a larger influence on reservoir's performance than reservoir unit scale heterogeneity factors if no well control scheme has been applied. The results demonstrated that the heterogeneity factors on a larger scale did not necessarily have

a larger influence on flow. In fact, heterogeneity factor at any scale could have significant influence on reservoir performance. Hence, by using a 'top-down' modelling approach, it was possible to underestimate the uncertainty due to the smaller length scale heterogeneities. Therefore, the influence of the heterogeneity at all length scale should be studied.

5.9. Conclusions

This part of the project investigated the impact of a combination of genetic unit and reservoir unit scale heterogeneities on gas flooding in fluvial-deltaic reservoir.

The following is a summary of the findings in this section:

- The heterogeneities that control the approach to vertical equilibrium in this environment (Kv:Kh) were the most influential on the gas-oil displacement. The modelling sand Kv:Kh ratio below 1 and including mud-clast lags at channel bases decreased the oil recovery factor and increased the total gas production.
- When gas was evolved from solution, laterally extensive shales became more important because they reduced the vertical migration distance for the gas, and thus helped the gas to be stabilized by gravity. When extensive shales were present, total gas production decreased and the oil recovery factor increased compared with the homogeneous case.
- Variations in displacement stability did not change the rank order of the geological heterogeneities. However, different stability conditions changed the magnitude of the flow response to these heterogeneities. It was observed

that if the displacement was more gravity unstable, the reservoir performance was less sensitive to the influence of the geological heterogeneities.

- This screening study identified that the same significant geological heterogeneities had a greater influence on gas production when a well control scheme was applied. It happens when the production rate exceeds the Dietz's critical rate. However, the main reason was that these factors influence the total gas production was not yet fully understood. This needs to be investigated further.

Chapter 6
Rapid estimation of oil recovery

6.1 Overview

Currently there is no rigorous analytical method available which can predict oil recovery with a high degree of accuracy because of the large amount of uncertainty associated with reservoir geological properties and how it impacts flow behaviour. The usual method used is to conduct a number of numerical simulations that take different possible geological realisations and fluid properties into account. However, subsurface data are sparse, and reservoir architecture is often poorly understood. Moreover, not all geological heterogeneities have a significant influence on recovery. Using the numerical simulation based history-matching methods, it is possible to estimate reservoir performance using a 'trial and eliminate error' process, but this is both time consuming and unreliable. Developing an analytical method to estimate cumulative oil recovery can help quickly constrain reservoir performance. In order to develop a method to analytically estimate the range of recovery, it is first of all important to identify the geological heterogeneities that influence a displacement mechanism at a specific length scale.

The previous chapters identified that the factors affecting sandbody connectivity (Chapter 4), and the vertical equilibrium condition of a displacement (Chapter 5) had the most significant influence on fluvial deltaic reservoir performance. In this chapter, the investigation focused on the influence of the heterogeneities within Pereriv B and

D layers in the Azeri Field on gas-oil displacement, as an example of mobility unstable displacement. These layers had high NTG (NTG >85%) so all sandbodies were connected. Thus, connectivity was not a problem in these layers (theoretical connectivity threshold for a 3D reservoir model was c. 30-35% NTG; King 1990; Hovadik and Larue 2007). This chapter will first review the factors that influence an immiscible mobility unstable displacement mechanism influenced by gravity. From the previous chapter, it was found that the variation in length and distribution of mud-clast lags and Kv:Kh ratio had the largest influence on recovery in the high NTG reservoir. Therefore, reservoir heterogeneity was represented in terms of impermeable shales bodies. The second part of this chapter studied the impact of shale with different characteristics on mobility unstable gas-oil displacement and suggested a scheme that constrains the upper and lower boundary of cumulative oil recovery in Pereriv B and D interval.

6.2 Aims

1. Analyse the impact of various shale distribution and geometry on immiscible mobility unstable displacement.

2. Identify a scheme to give rapid estimation of the likely range of oil recovery, which incorporates the impact of shales.

6.3 The challenge of recovery prediction

Both Buckley-Leverett and segregated flow models are commonly used to describe the immiscible displacement mechanism. In the absence of capillary forces, the degree of vertical equilibrium (VE) indicates which flow model is the most suitable. VE is achieved when maximum vertical cross flow occurs and gravity dominates the displacement (Dake 1978; Shook et al. 1992). Previous studies (Dake 1978; Shook et al. 1992) suggested that the effective aspect ratio (R_L) and buoyancy number (N_g) are the two factors that indicate the degree of VE in a displacement. This is because R_L indicates the degree of vertical cross-flow whilst N_g indicates the balance between viscous and gravity forces in a displacement. In general, when the aspect ratio is small, vertical cross flow is less likely to occur and hence VE is unlikely to be achieved.

Effective aspect ratio $$R_L = \frac{L}{H}\sqrt{\frac{k_v}{k_h}}$$ equation 6.A

Similarly when N_g is large (e.g. offtake rate is less than the Dietz's critical rate) this indicates that the displacement is dominated by gravity force, whereas when N_g is small (e.g. offtake rate is a lot higher than the Dietz's critical rate) then the viscous force dominates the displacement. VE will not be achieved in a viscous force dominated displacement.

Buoyancy number $$N_g = \frac{k_h \lambda_{ro} \Delta\rho g \cos\theta H}{u_T L}$$ equation 6.B

If VE is perfectly satisfied and capillary forces are negligible, the segregated flow model is more suitable than the Buckley-Leverett flow model to describe a displacement (Dake 1978).

In the absence of capillary forces, immiscible displacement in a 2D anisotropic, homogeneous reservoir is also influenced by dip angle number (N_θ) and end-point mobility ratio (M) (Shook et al. 1992). These dimensionless numbers are used to indicate the difference between two displacements.

Dip angle group $$N_\theta = \frac{L}{H}\tan\theta$$ equation 6.C

End-point mobility ratio $$M = \frac{\lambda_{rf}}{\lambda_{ro}}$$ equation 6.D

The parameters in all the equations are summarised in Table 6.1.

Nomenclature	
L : length F : force t : time, m : mass [=] means 'has units of'	
L	Reservoir length [=] L
H	Reservoir thickness [=] L
A	Cross-sectional area [=] L^2
s	Number of shale per meter
l	Shale's length [=] L
Fs	Shale's density [=] fraction
t	Shale's thickness [=] L
T	Reservoir thickness [=] L
Ns	Number of shale
g	Gravitational acceleration [=] L/t^2
θ	Reservoir dipping angle [=] radians or degrees
k_h	Horizontal permeability [=] L^2
k_v	Vertical permeability [=] L^2
ρ_j	Density of phase j [=] m/L^3
μ_j	Viscosity of phase j [=] $(F\text{-}t/L^2)$
λ_{rj}	Relative mobility of phase j [=] $(F\text{-}t/L^2)^{-1}$
ϕ	Sandbody porosity [=] fraction
σ	Fluids interfacial tension [=] F/L
q	Volumetric flow rate [=] L^3/t
S	Saturation [=] fraction
kr'_j	End-point relative permeability of phase j [=] fraction
u_T	Displacement velocity [=] L/t
Subscripts	
o	Oil phase
f	Displacing fluid phase (i.e gas or water)
or	Residual oil
wc	Connate water

Table 6.1. Table of nomenclature.

As discussed earlier in Chapter 3, the end-point mobility ratio (M) indicates the displacement stability. For a mobility stable displacement the variation in VE condition has a negligible influence on recovery. The dip angle number (N_θ) indicates the influence of the reservoir geometry on recovery when VE is achieved. If the dip angle number is large (e.g. thin reservoir with highly dipping angle) and VE is achieved, the recovery would be increased for the gravity stable displacement as shown in Figure 5.9 and demonstrated by Shook et al. (1992). However, if the displacement is dominated by viscous forces, the variation of N_θ is insignificant. Therefore, recovery depends on both reservoir geometry and the state of VE.

A mobility unstable displacement can be stabilised by gravity as indicated by Dietz's stability analysis. The Dietz's gravity stable displacement condition is

indicated by the gravitational number (G) and end-point mobility ratio (M) (Chapter 3), that is based on the assumption that fluids with lower density can freely segregate upwards to form a sharp interface between the fluids which have different densities. Therefore Dietz's stability analysis assumes VE has been achieved. The analysis can be expressed in terms of end-point mobility ratio (M), dip angle group (N_θ) and buoyancy number (N_g). The following expressions demonstrate the gravity stable condition can be expressed in terms of the dimensionless numbers presented by Shook et al. (1992).

$$G = \frac{k_h \lambda_{rf}' A \Delta\rho g \sin\theta}{q}$$; gravity stable condition occurs when $G>M$-1 (equation 3.B and 3.C in Chapter 3)

$$N_g \times N_\theta \times M = \frac{A k_h \lambda_{ro}' \Delta\rho g \cos\theta}{q} \frac{H}{L} \times \frac{L}{H} \tan\theta \times \frac{\lambda_{rf}'}{\lambda_{ro}'} = \frac{k_h \lambda_{rf}' A \Delta\rho g \sin\theta}{q} = G$$

$$G = N_\theta \times N_g \times M$$

$$G' = \frac{G}{M} = \frac{k_h \lambda_{rf}' A \Delta\rho g \sin\theta}{q} = N_g \times N_\theta$$

Therefore the rearranged stability condition:

$$G > M - 1 \quad = \quad G' > 1 - \frac{1}{M} \quad = \quad N_\theta \times N_g > 1 - \frac{1}{M}$$

The expressions above show that recovery may be different with the same value of G (the N_θ and N_g can be different). For example, recovery would be different in a thin reservoir (larger dip angle group) with displacement at high offtake rate (small buoyancy number) and a thick reservoir (small dip angle group) with low offtake rate (large buoyancy number), although both cases would have the same value of G and M.

Recovery would be different because of the different geometry effect and the different balance of viscous and gravity forces.

6.4 Shale description and influence in high NTG sandstone reservoirs

Chapter 5 showed that impermeable barriers such as shales and mud-clast lags, and anistropic Kv:Kh of the sandbodies had the largest influence on mobility unstable gas-oil displacement in high NTG reservoir (Pereriv B/D). In order to obtain a rapid estimation of the likely range of recovery, using a model that could incorporate some geological heterogeneity, the Pereriv B/D model was simplified to a sand-shale reservoir. This is a common way of characterising a reservoir (Prats 1972; Richardson et al. 1977; Haldorsen and Lake 1982; Begg and King 1985; Haldorsen 1986; Haldorsen and Chang 1986; Begg et al. 1987; Borner et al. 1988; Ciammetti et al. 1995; de Riz and Muggeridge 1997; Jackson and Muggeridge 2000; Ringrose et al. 2005). Two end-members of shale character were used. One end-member was continuous shale whose length was longer than the interwell spacing - these shales reduced the effective flow path thickness (H). The other end-member had shales that were short and discontinuous, which controlled the effective Kv:Kh of the sandbody. Modelling and simulation time could be reduced by reducing complex geology to a simple sand and shale description. Another advantage of this method was to reduce the complex geological features into a quantitative parameter; therefore the method provided the possibility of representing the influence of geological features on reservoir performance in an analytical expression. Here, the presence of shale either affected the reservoir geometry (H:L) or vertical cross flow (effective Kv:Kh), hence

the influence of shales can be captured by R_L or N_θ. However, by reducing the complexity of the geological description, some of the fine scale heterogeneities, which may influence flow behaviour, are neglected.

The variation of VE is the main factor that controls the displacement. The areal displacement was not studied in this chapter. Therefore all work in this chapter refers to 2D models. King (1990) and Hovadik and Larue (2007) demonstrated that for a 2D system the connectivity threshold was c.55%-60% NTG. Sandbody connectivity reduced rapidly when the NTG of a 2D system was reduced to, or below, 60%. In case the connectivity below 100%, the geological features that influence connectivity became important for reservoir performance. Hence, in order to constrain the study in a high NTG 2D model, the investigation in this chapter considered the range of NTG varying from 60% to 100%.

6.5 Methodology and design of experiment

This investigation studied the influence of shale on a mobility unstable gas-oil displacement. Models with 31° of dip were used to conduct the experiment in order to mimic the Pereriv B/D interval in the Azeri Field. The descriptions of geological heterogeneity were simplified to sand (flow unit) and shale (no-flow unit). The same fluids and rock properties and relative permeability curves that were used in the preliminary displacement study in Chapter 3 were also applied here (Table 3.1 and Figure 3.1) with sandstone permeability equal to one Darcy.

The first series of 2D models (scheme A) explicitly contained discontinuous shales of different lengths. All the shales were one metre thick in Z coordinate and four

different shale lengths were modelled through a range of NTG to capture the influence of shale length on reservoir performance. All the shales were distributed randomly in this model. Eight realisations were generated in order to avoid a bias value from a particular realisation of shale distribution. Figure 6.1 shows two examples of scheme A models with different shale lengths.

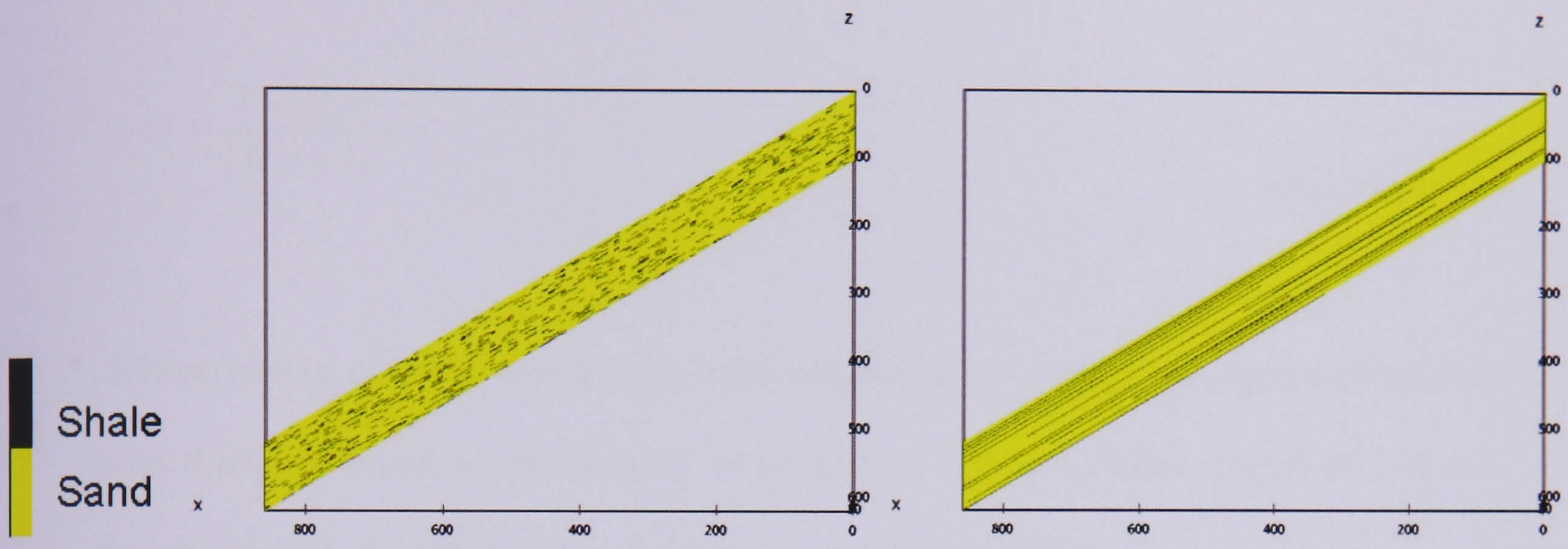


Figure 6.1A

Figure6.1B

Figure 6.1. Example of Scheme A model (explicitly modelled shales) in a reservoir of 90%NTG; **(A, left)** Left shows the case where the shale: reservoir length ratio equal to 0.01. **(B, right)** Right shows the case where the shale: reservoir length ratio equal to 0.8.

In the second series of 2D models (scheme B), discontinuous shales were implicitly modelled, by correlating shale properties (i.e. the average vertical distance between shales, the thickness, length and the NTG) from the scheme A models, and applying Begg and Kings' (1985) expression to determine the effective Kv:Kh ratio.

$$K_V = \frac{K_H(1-F_S)}{(1+s\frac{l}{2})^2}$$

equation 6.E

The third and final series of 2D models (scheme C) contained continuous shales. In these models, it was assumed that the extensive shales divided the reservoir into thinner layers with reduced thickness (H) (Figure 6.2). Assuming the sand between the shales was homogeneous, and the shales were distributed evenly throughout the reservoir. The thickness of a layer would be given by:

$$H = \frac{T - N_S t}{(N_S t + 1)}$$

equation 6.F

Therefore, in essence, simulations were conducted in stacked homogeneous models with thickness equal to the distance of separation between shales. Figure 6.C shows the effective flow path thickness in models of different NTG.

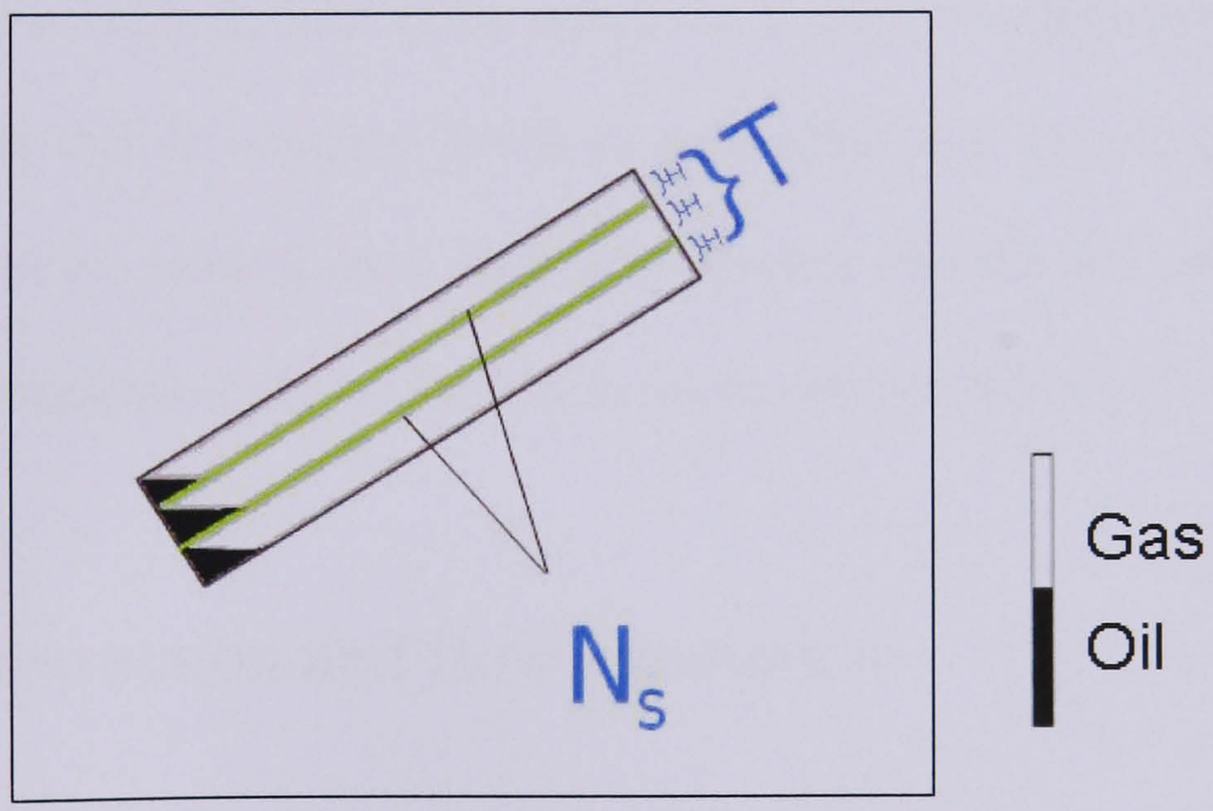


Figure 6.2. Extensive shales divide the reservoir into a number of thin layers.

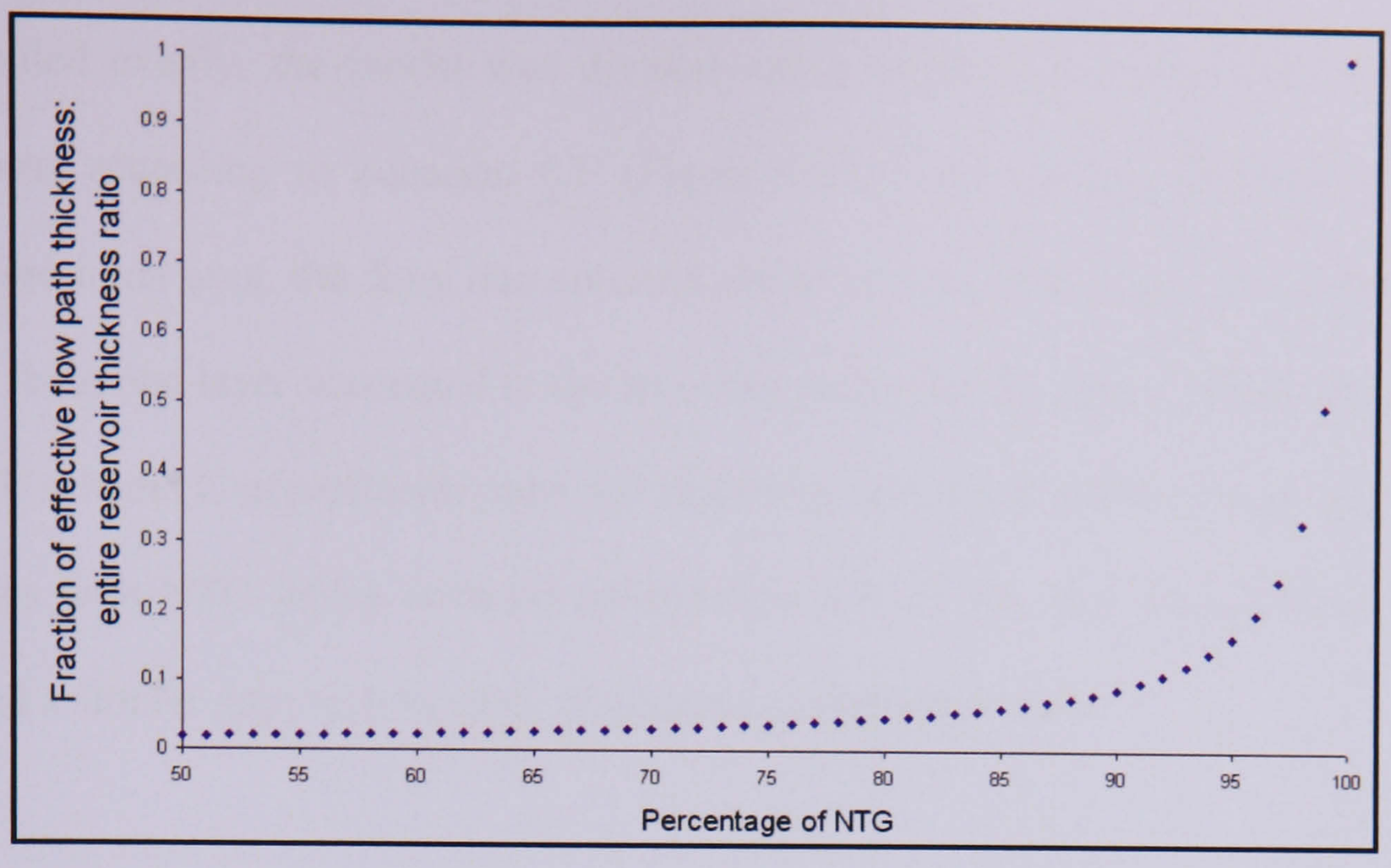


Figure 6.3. Variation of effective flow path thickness against percentage change of NTG. If the fraction of effective flow path: reservoir thickness ratio is 1 that means the reservoir thickness is equal to the effective flow path thickness.

Besides the heterogeneous models described above, two numerical simulations in homogeneous reservoirs with Kv:Kh ratio equal to 1 and 0 respectively were conducted. The purpose was to compare the cases with either the VE was perfectly achieved (Kv:Kh =1), or no vertical cross flow was possible (Kv:Kh =0). Hence the influence of different character of shales on displacement can be understood.

6.6 2D model construction and flow simulation

In order to perform the experiments described in section 6.5, gas-oil displacement with offtake rate c. 46.7% of Dietz's critical rate were conducted by numerical simulation in a range of dipping 2D reservoir models. With the offtake rate below Dietz's critical rate, the displacement was expected to be gravity force dominated. Each of these 2D models is 1000m long, 10m wide and the vertical thickness of each model is 100m. In scheme C, since the continuous shales were considered to be

distributed evenly, the model was divided into a number of layers with the same thickness according to equation 6.F (Figure 6.3). Since each layer had the same cross-sectional area, the flow rate entering each layer was the same, so the recovery factor from one layer was equal to the recovery factor for the whole model. Therefore, in each scheme C experiment, only one layer was simulated and the model thickness changes with NTG which is based on equation 6.F. de Riz and Muggeridge (1997) applied a similar approach to study displacements between shales.

Each grid cell is 10m long and wide and, given that the model thickness changes in scheme C (Figure 6.3) and the grid layer thickness was set to be 1/200 of the model's thickness, (i.e. for a model which has 100m on Z coordinate the grid cell thickness was 0.5m). Therefore all the models had 20,000 grid cells.

In Appendix 2, it is shown that a model with a grid cell thickness of 1/200 of the model thickness is capable of capturing any viscous fingers that could occur in a displacement. The details of these 2D models are summarised in Table 6.2.

Coordinate	Grid number	Model length /m	Grid block size/m
X	100	1000	10
Y	1	10	10
Z	200	100 (Thickness changes with scheme C models)	0.5 (Thickness changes with scheme C models)
	Total: 20000		

Table. 6.2. Information on reservoir model setup for the numerical simulations presented in this chapter.

Simplified fluid PVT description (incompressible fluids and dead oil), were applied to the numerical simulation. It was the same conditions that were used in Chapter 4.

A streamline simulator incorporating gravity effects (3DSL version 2.2) was used because to take the advantage of a shorter simulation time. The reliability of the streamline simulator is discussed in Appendix 6.

6.7 Results

6.7.1 On recovery at gas breakthrough in a reservoir model with NTG less than 100%

Figure 6.4 shows the cumulative oil recovery at breakthrough (CORB) at various NTG under various modelling schemes A-C as discussed earlier.

In scheme A, where shales were explicitly modelled in the reservoir, two results stood out. Firstly, it was found that the CORB reduced with decreasing NTG. For example, under scheme A (models with shale: reservoir length ratio equal to 0.01 of the reservoir length), the CORB decreased from c.67% at 99% NTG to c.22% at 60% NTG. A similar trend was found for all other models with various shale lengths.

Secondly, for model with the same NTG, the models with longer shales yielded a higher CORB. For example, comparing all the reservoir models with 90% NTG, CORB increased from c.64% to c.70% when the shale: reservoir length ratio increased from 0.01 to 0.8. In Figure 6.4, all the results from scheme A were represented by an average value from eight realisations. The standard deviation around the average value which represented the range of possible results from eight realisations was plotted.

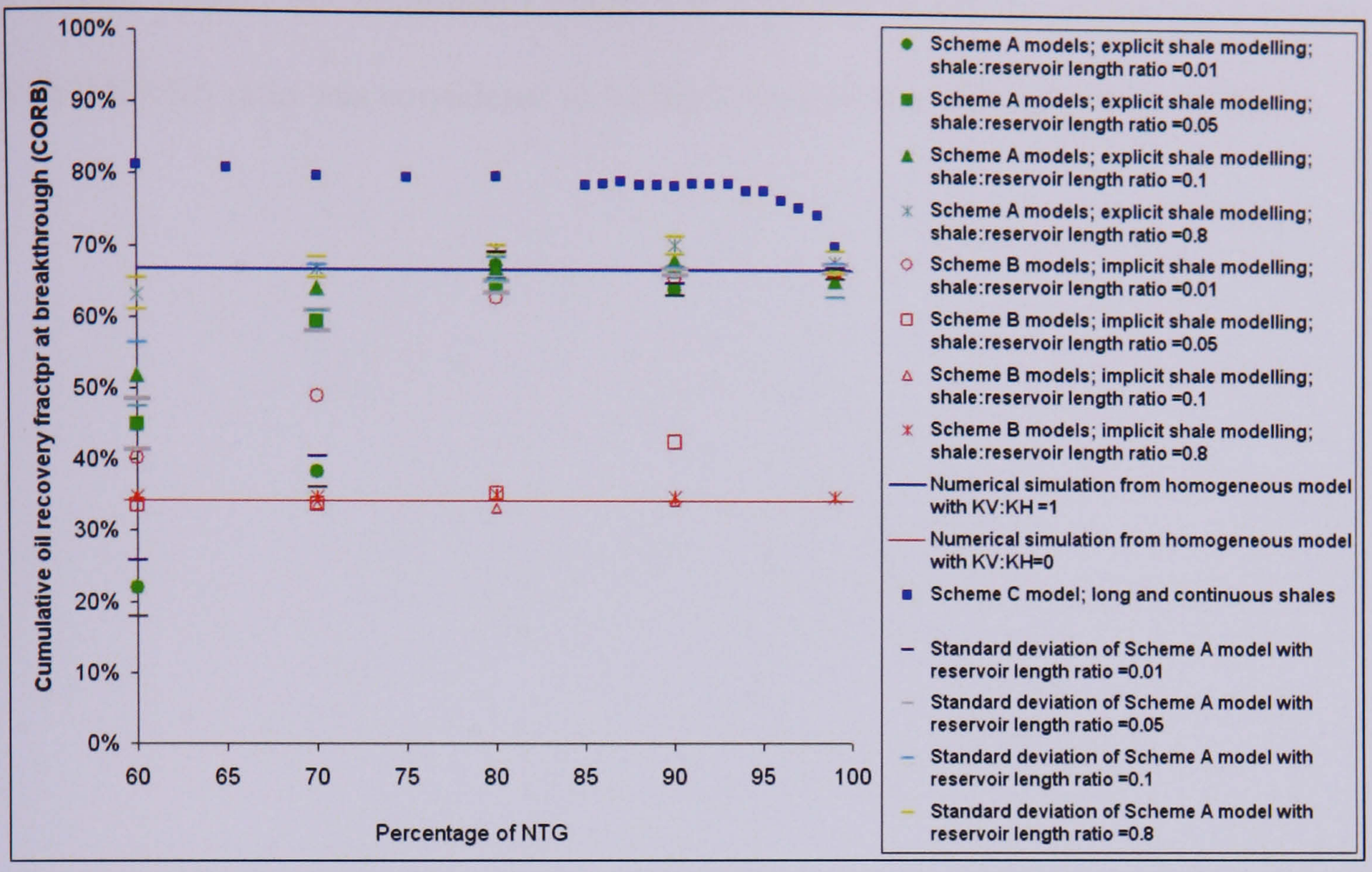


Figure 6.4. Cumulative oil recovery at breakthrough (CORB) under 46.7% Dietz's critical rate in various sand/shale 2D heterogeneous models with different modelling schemes. Three sets of numerical simulations were conducted to represent reservoirs containing shales of different continuity. The CORB values of 100% NTG reservoir model with Kv:Kh equal to 1 and 0 were also estimated.

In scheme B, where shale was implicitly represented by Kv:Kh ratio in the reservoir model, it was found that the CORB decreased with the decrease of NTG. This was similar to the results from scheme A. For example, under scheme B, models with shale: reservoir length ratio equal to 0.01, the CORB decreased from c.67% at 99% NTG to c.40% at 60% NTG. In scheme B, it was also found that, by comparing two reservoirs with the same NTG, the models representing shorter shale yielded a higher CORB. For example, in models with 90% NTG, the CORB reduced from c.66% to c.35% as shale: reservoir length ratio increased from 0.01 to 0.8. These results were the opposite to the results generated by corresponding models in scheme A. The decrease in CORB was due to the reduction in Kv:Kh ratio with increasing

shale length. It was found that under the assumption of 100% connected, the scheme B model yielded the minimum CORB. For a gravity stable displacement, a model with 0 Kv:Kh ratio was considered to be the lowest limit of the recovery estimation.

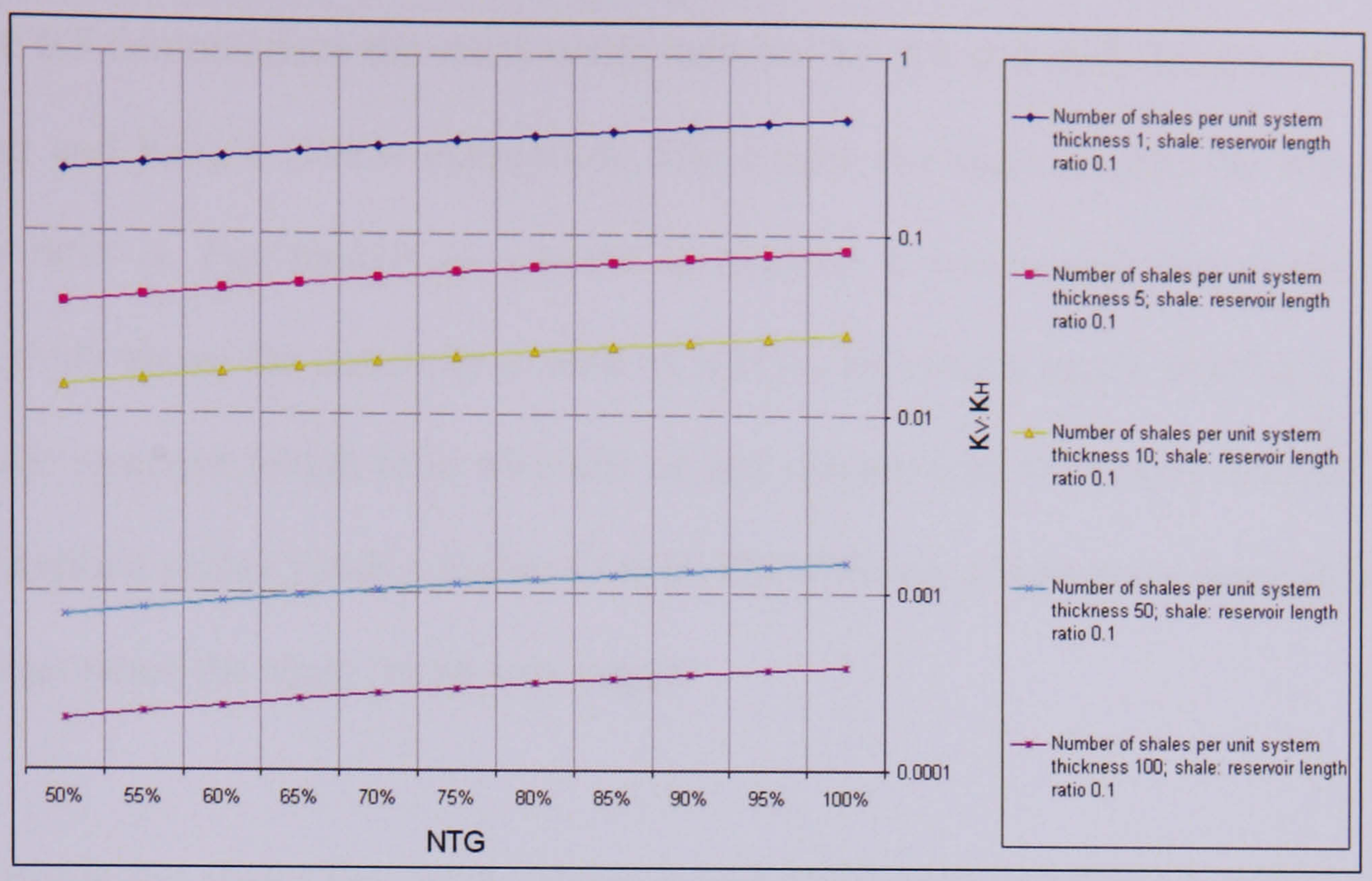


Figure 6.5A

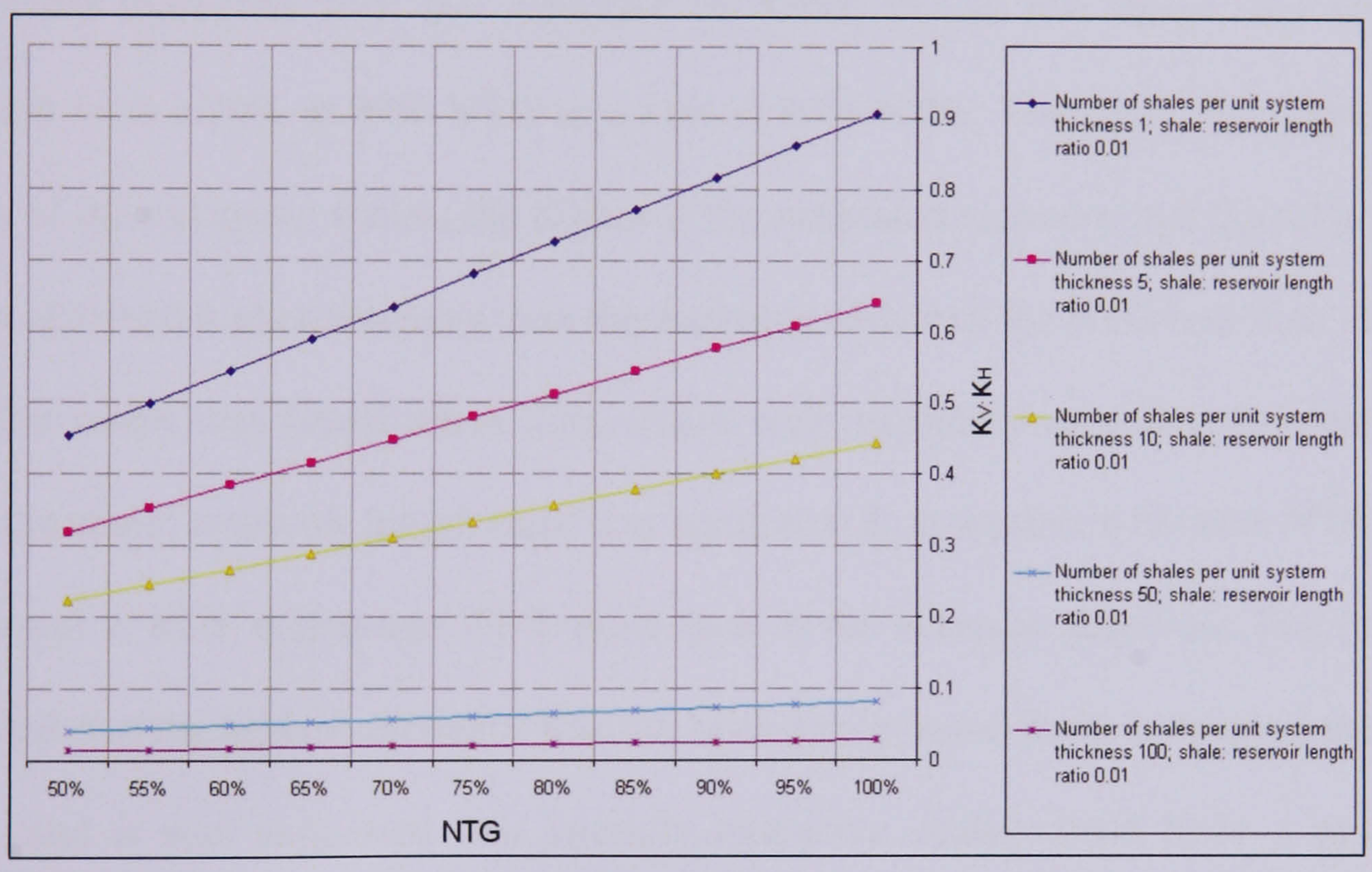


Figure 6.5B

Figure 6.5. Begg and King (1985) correlation of the Kv:Kh ratio with NTG assuming differ at shale length and density. The figure demonstrated two examples with different ratios of the shale length: (1) shale: reservoir length ratio equal to 0.1 which was plotted in a log scale **(A, top, plotted in log scale)**; and (2) shale: reservoir length ratio equal to 0.01 **(B, bottom)**. Increasing the number of shales present caused the Kv:Kh to reduce. Moreover, in models having the same shale density (NTG) the larger number of shales per unit reservoir thickness and longer shales resulted in lower Kv:Kh ratios.

Figure 6.5 demonstrates the relationship between Kv:Kh and shale length according to Begg and King's (1985) expression. The longer the shale length, the lower the Kv:Kh ratio is. For models in scheme B models, it was found that model with connectivity above the threshold (c.60% of NTG) , the results match scheme A when the shale: reservoir length ratio was 0.01 or less (Figure 6.4). However, a model with longer explicit shales yields a higher CORB. The difference between scheme A and B was larger when the shale length was larger.

By considering shales that were extensive and continuous (scheme C), it was found that CORB increased with the reduction of NTG. Figure 6.4 shows that CORB increased from c.70% at 99% NTG to c.81% at 65% NTG. Therefore, the higher the density of the extensive shales, the higher is the estimated recovery. All the scheme C models obtained higher recovery than the isotropic reservoir for NTG less than 100 %. A similar result was found when long shales were explicitly modelled (scheme A). When the shale: reservoir length ratio was equal to 0.8, in models with 80% NTG, the CORB was c. 69% which was 3.0% more than in the isotropic reservoir. The results suggested that the highest recovery was not necessarily found in an isotropic reservoir model, and it was suggested that laterally extensive shales could have a positive influence on recovery.

6.7.2 Oil recovery at gas breakthrough in 100% NTG reservoir model

Figure 6.4 shows the estimated value of the cumulative oil recovery at breakthrough (CORB) in a 100% NTG model which had Kv:Kh equal to 1 and 0 respectively. In an isotropic reservoir the estimated CORB is c.67%. On the other hand, in a 100% NTG model with Kv:Kh equal to 0, the CORB was estimated to be c.34%. Thus, by

changing the sand Kv:Kh ratio from 1 to 0, the CORB decreased by c.33%. This was because the displacement was out of VE as Kv:Kh ratio was 0 (R_L equal to 0) so the segregated flow model was no longer valid.

6.8 Discussion

6.8.1 Impact of shale continuity on recovery

6.8.1.1 System with discontinuous shales

Many researchers have demonstrated that discontinuous shales have a negative impact on gravity drainage and recovery (Haldorsen and Chang 1986; Richardson et al. 1987b; Ciammetti et al. 1995; Jackson and Muggeridge 2000). Discontinuous shales are commonly found in the Pereriv Suite, and they are considered vertical flow barriers because of their impermeable nature over production time-scales.

The influence of discontinuous shales depends on their length. If shales are short (e.g. shale: reservoir length equal to 0.01), their influence is commonly represented by a modified Kv:Kh ratio. An increase of the shale density or length causes the reduction of Kv:Kh because the vertical flow path becomes more tortuous. Figure 6.5 shows the relationship between Kv:Kh ratio and shale length and density. It was shown that the higher the shale density the lower the Kv:Kh ratio are. Similarly, lower Kv:Kh ratios were found with the increase of shale length.

Reducing the Kv:Kh ratio could cause a reduction in recovery for the mobility unstable displacement. Figure 6.6 demonstrates the relationship between the

cumulative oil recovery at gas breakthrough (CORB) and the Kv:Kh ratio in a 2D dipping model with 100% NTG. The results showed that recovery was more sensitive to the changes of Kv:Kh ratio when offtake rates were below Dietz's critical rate. This was expected as the displacement was gravity stable and VE was achieved if the Kv:Kh was high. However, when the offtake rate was larger than Dietz's critical rate, the gravity unstable displacement was less sensitive to the variation in Kv:Kh. Figure 6.6 demonstrates that if a displacement with 46.7% Dietz's critical rate and zero Kv:Kh, the CORB was approximately equal to the case with 187% of Dietz critical rate. The results demonstrate that when the displacement is not in VE (no vertical cross flow) it yields a similar value of CORB as a gravity unstable case. In the extreme case with zero Kv:Kh, the displacement behaviour is equivalent to a 1D (linear) Buckley-Leverett flow model because the displacement is perfectly out of VE. As there is no vertical segregation, the oil recovery only depends on viscosity ratio and relative permeability. This makes it possible to estimate the oil recovery analytically.

Figure 6.6 also demonstrates that the vertical cross flow had a larger influence on gravity stable displacement than gravity unstable displacement. This is because the gravity stable flow condition relies on the degree of VE. If the vertical cross flow was inhibited, the gravity stable displacement could not be achieved, even when the offtake rate was below the Dietz's critical rate. Hence, the geological anisotropy features which influence vertical cross flow yield a larger impact on gravity stable displacements.

In Chapter 5 it was observed that by increasing the offtake rate, the magnitude of the responses was reduced, although the rank order of the heterogeneities influence

remained the same (Figure 5.12). Figure 6.6 also gives the reason for the results in Chapter 5. It is understood that the geological features that influenced vertical cross flow are the most important factors affecting the oil recovery during gas-oil displacement.

It was observed that when 116.7% Dietz's critical rate was applied, the CORB was lower than the case with zero Kv:Kh. This is because when a displacement with offtake rate slightly higher than Dietz's critical rate, the gravity stable condition can not be achieved. In this case, a gas tongue developed at the top of the reservoir section. Thus the injected gas arrived rapidly at the production well, causing early breakthrough. In contrast if the displacement was dominated by viscous force (Kv:Kh equal to 0), no vertical segregation would occur and hence gas tongue would not be formed. Thus CORB in a case when Kv:Kh equal to zero is higher than the gravity unstable case.

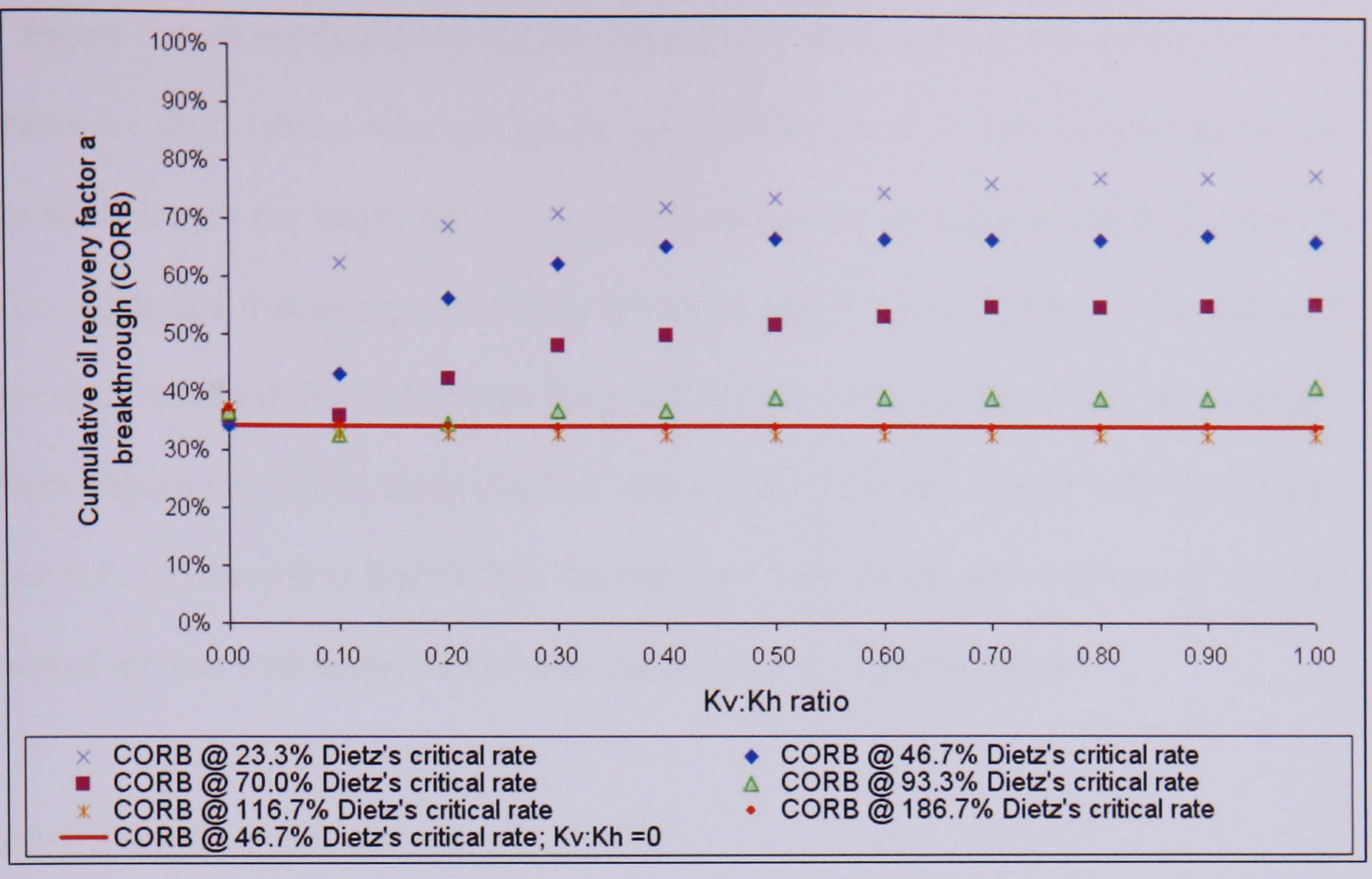


Figure 6.6. CORB as a function of Kv:Kh ratio of the homogeneous models. Realistic fluids description and six production rates were used (23.3%, 46.7%, 70.0%, 93.3%, 116.7% and 186.7% of the Dietz's critical rate were applied). It was observed that if the offtake rate was higher than Dietz's critical rate (186.7%) the CORB was equal to the case when displacement with offtake rate at 46.7% of the Dietz's critical rate in sandbody with Kv:Kh equal to 0. The result demonstrated that recovery was the same for any reason that prevents VE e.g. viscous dominated displacement or no vertical cross flow.

It is observed from Figure 6.4 that for the scheme A model with 60% NTG and sand: reservoir length ratio equal to 0.01, the resulting CORB below the case where sandbody with zero Kv:Kh. This is because the connectivity threshold for a 2D model is between c.50%-60% of its NTG (King 1990 and Hovadik and Larue 2007). Therefore, when a gravity stable displacement occurred in reservoir with no disconnected sandbodies, the lowest recovery was observed when the displacement was out of VE.

Figure 6.4 shows that using Kv:Kh to capture shale influence is only valid when shales are short (shale: reservoir length ratio is 0.01). It was observed that the longer the shale length the larger the discrepancy between the results for schemes A and B. This suggested that using a modified Kv:Kh to represent shale influence could yield incorrect results if the shales were long and that the error increases with shale length. From Figure 6.4 it was observed that when shale: reservoir length ratio was longer than 0.8; recovery was higher than the isotropic case. In the next section, an extreme case of models with continuous shales (scheme C) will be discussed.

6.8.1.2 System with continuous shales

Continuous shales sub-divide a reservoir into a number of layers that were equivalent to a stack of isolated reservoirs. Figure 6.3 correlated the relationship between variations in NTG and the thickness of the effective flow path when the reservoir was divided evenly by continuous shales with shale thickness 1/100 of the reservoir thickness (e.g. 1m shale thickness in sand reservoir of 100m thick). Recovery in 2D homogeneous models for segregated flow could be estimated by a graphical method based on Dietz analysis (Dake 1978) (Figure 6.7). Segregated flow assumed that VE was achieved. Figure 6.8 shows an analytical CORB estimation for gravity dominated displacement using a segregated flow model of different thickness under various rates. Such a phenomenon occurred purely because of the geometrical effect (Figure 5.11 and Figure 6.9). Therefore, for a given NTG, the presence of continuous shales improved recovery.

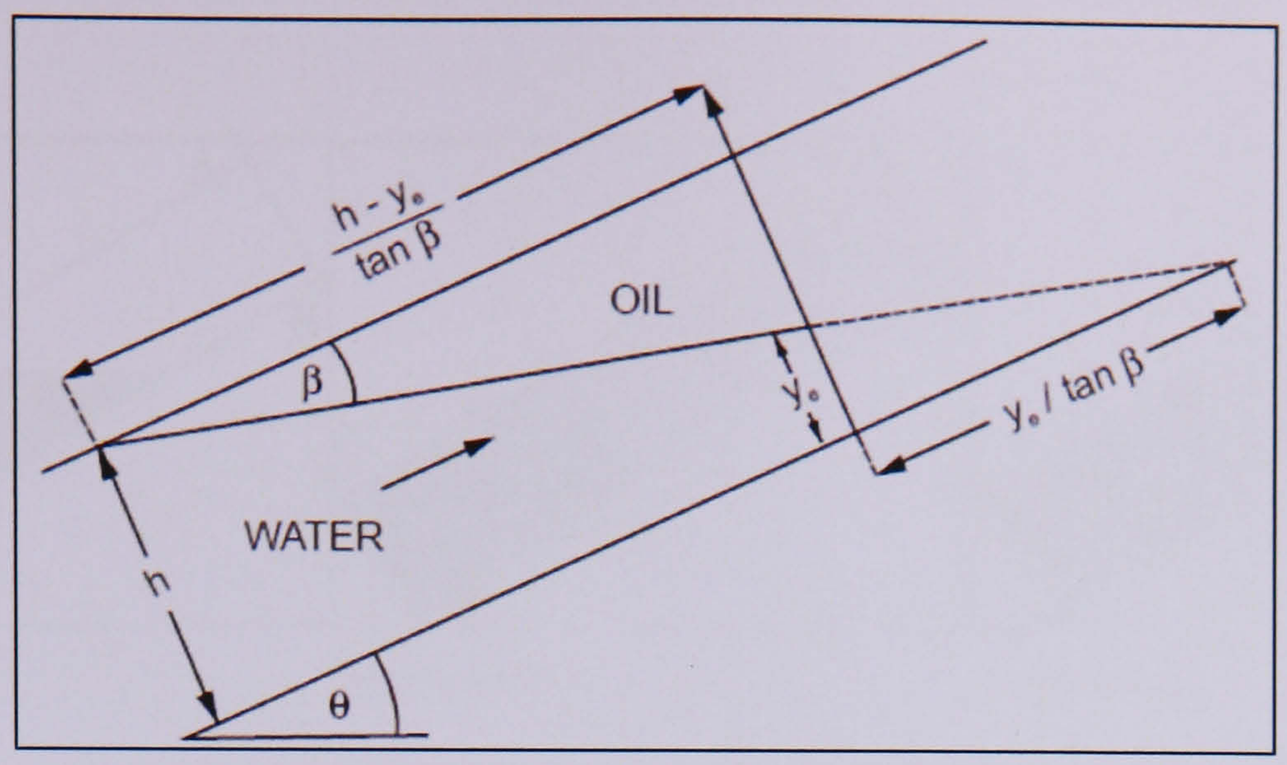


Figure 6.7. Example of analytical estimation of segregated displacement of oil by water (Dake 1978). It assumes that movable oil in the water-invaded zone was displaced. Simple trigonometry shows that recovery can be estimated by: oil recovery equal to $(1-\frac{(h-y_e)^2}{2hL\tan\beta})$. y_e is the water level height at different stages of displacement after breakthrough which corresponds to the fraction of water production. Therefore at breakthrough y_e is equal to 0. The equation was quoted from Dake 1978.

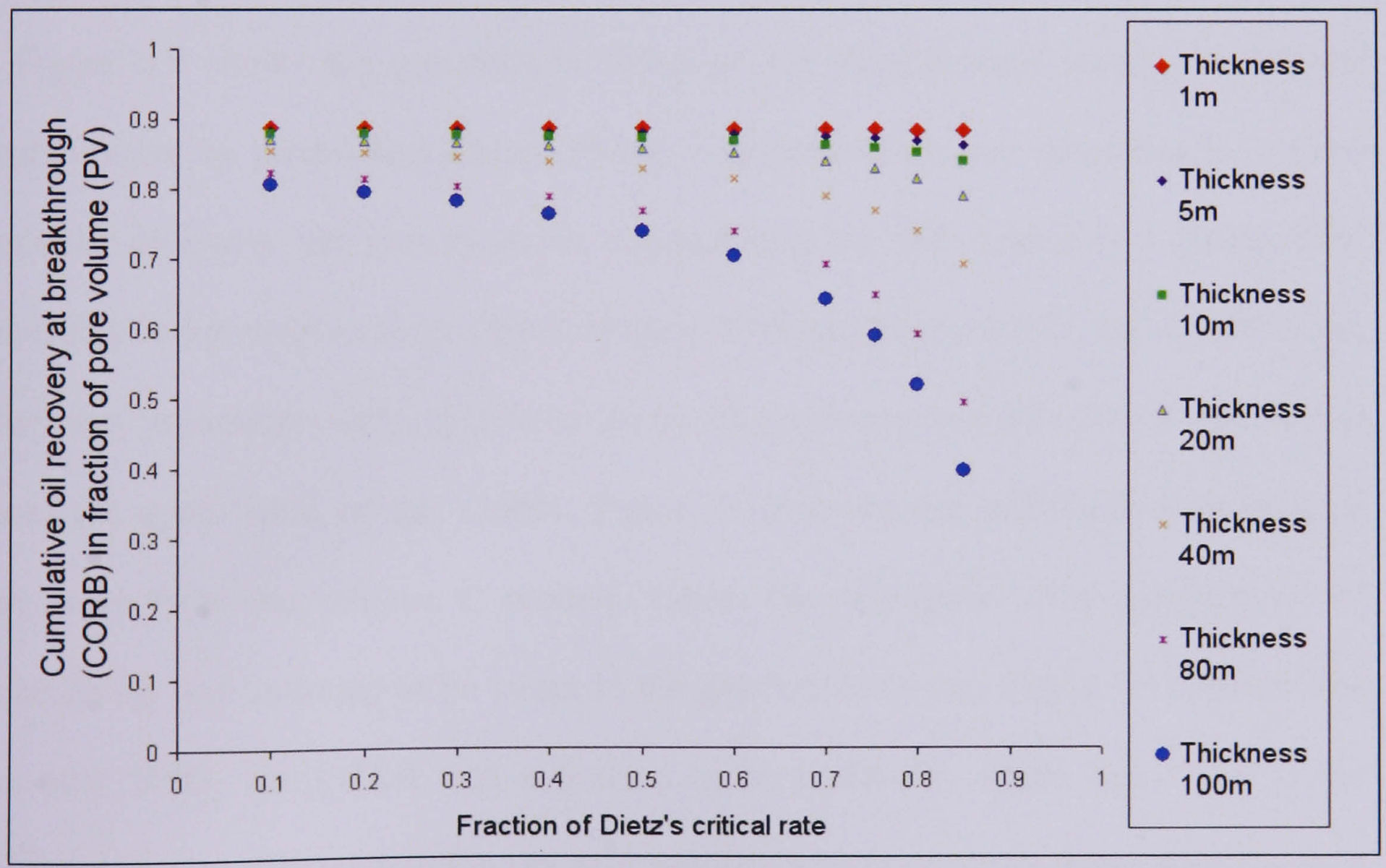


Figure 6.8. Analytical estimation of CORB under segregated flow model with different effective flow path thickness under various production rates. The figure demonstrate that for gravity dominated displacements, the recovery increases with a reduction of the reservoir thickness.

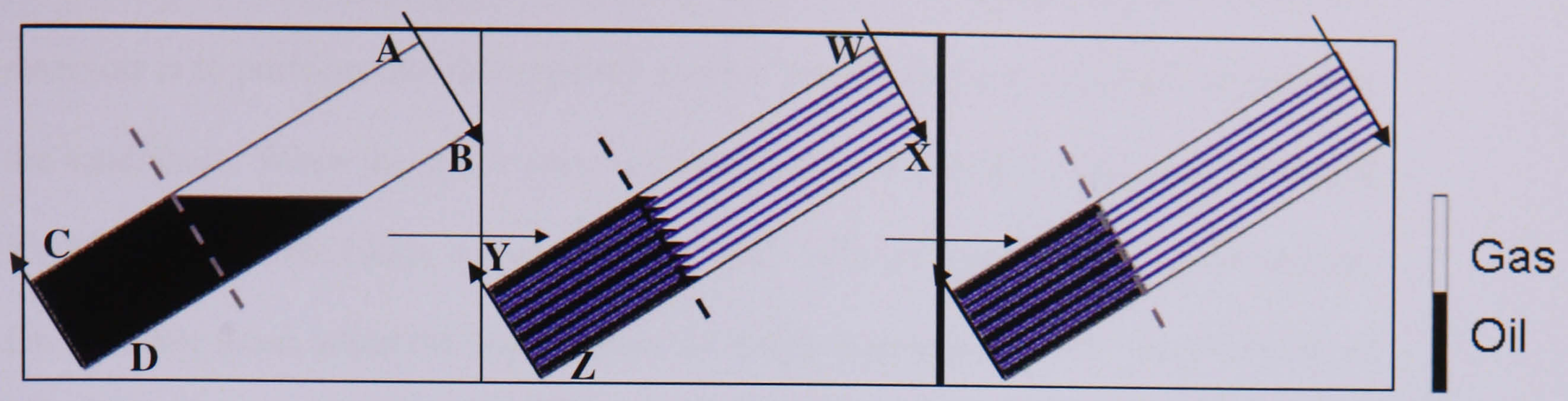


Figure 6.9A Figure 6.9B Figure 6.9C

Figure 6.9. (A-C) Impact on the displacement front when a reservoir was sub-divided into eight thin layers. When reservoir had no extensive impermeable shale the global Kv:Kh of the reservoir is equal to 1 **(A, left)**. Gas injected at point B could freely travel to point A or C. Whereas, in a case when laterally extensive impermeable shales were present **(B, middle)** gas injected at point X cannot travel to point W or Y, thus the global reservoir Kv:Kh was zero. However, the displacement in the reservoir was closer to a 'piston' like mobility stable displacement **(C, right)** instead of a Buckley-Leverett flow displacement which was out of vertical equilibrium, when Kv:Kh was considered to be zero or Buckley-Leverett flow.

Figure 6.9 shows the geometrical effect on the displacement shape of reservoir subdivision by continuous shales. When a reservoir was sub-divided into a large number of layers, the gravity stable displacement became similar to a 'piston-like' mobility stable displacement (M=1) (Figure 6.9B and Figure 6.9C), and therefore the recovery at breakthrough could be close to the maximum movable oil fraction, which was the upper limit of the CORB. Figure 6.10 shows the analytical estimation of recovery from the scheme C models. Under the segregated flow assumption, all mobile oil was assumed to be swept in the gas invaded zone. Figure 6.10 shows that at 60% NTG, the CORB was estimated to be c. 88.6%, which was close to the maximum movable oil fraction (88.8%) according to the relative permeability curves (Figure 3.2). Therefore, the upper boundary of recovery was estimated when a reservoir was characterised as being sub-divided into thin layers with thickness equivalent to the vertical distance between continuous shales.

From Figure 6.4 it is observed that the longer the shale length, the less likely the reservoir is to perform like the reservoir models which used a Kv:Kh ratio to estimate the sand/shale. When the shale: reservoir length ratio is c. 0.01 or less, the correlated Kv:Kh ratio is more likely to capture the shale's influence on reservoir performance. On the other hand, when the shale: reservoir length ratio equal to 0.8 with NTG above 80%, reservoir would behave similar to a case when it is divided into thinner layers by extensive shales. For cases in which the shale: reservoir length ratio is between 0.01 and 0.8, the reservoir shows mixed behaviour between the upper and lower boundaries. To predict recovery for such systems, reservoir models that explicitly capture shales must be constructed.

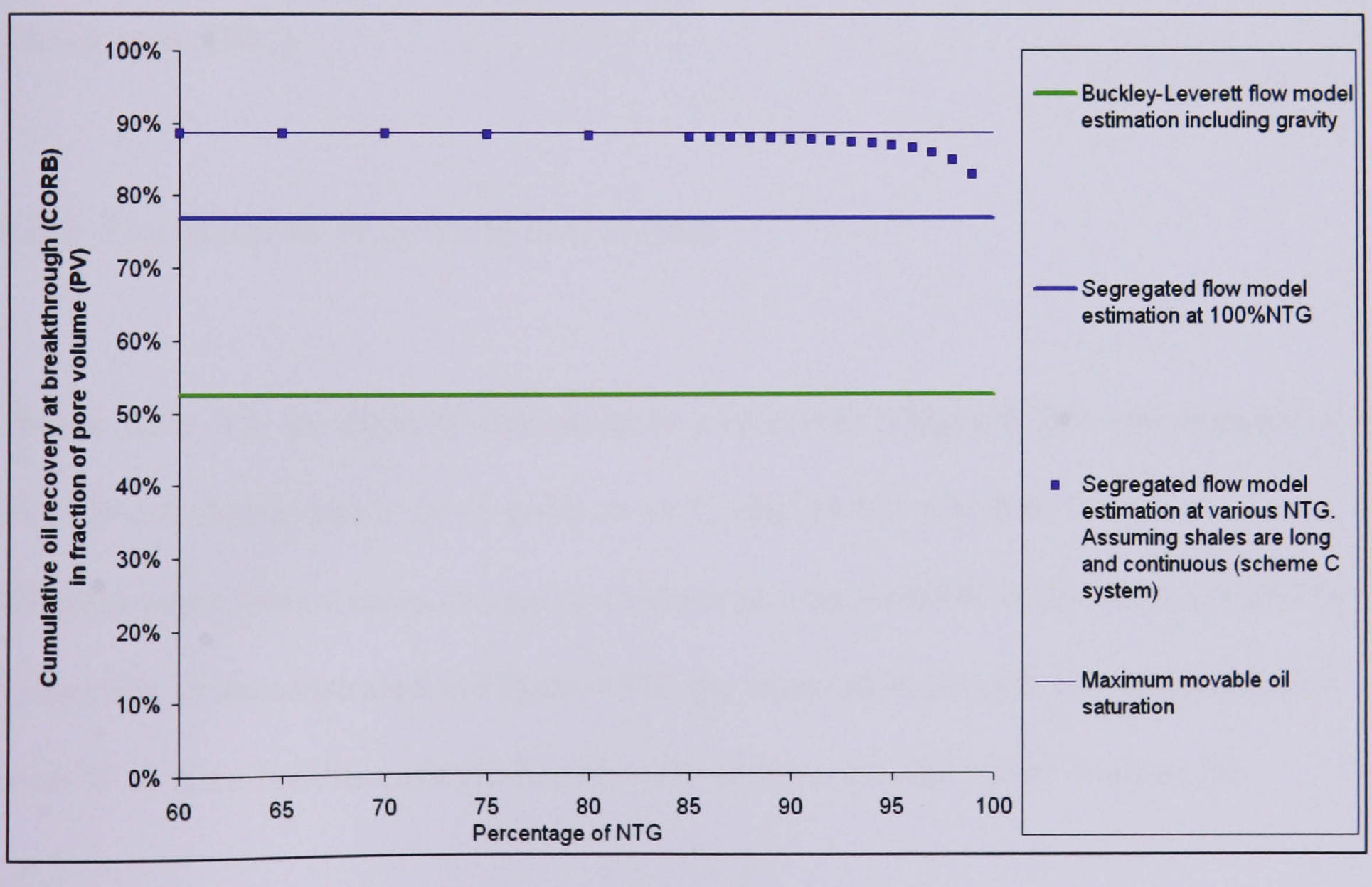


Figure 6.10. Estimation of cumulative oil recovery at breakthrough under 46.7% Dietz's critical rate in models with extensive shales and varying NTG.

Figure 6.10 demonstrates the analytical estimation of breakthrough time oil recovery for the two end-members under a mobility unstable displacement with offtake rate

below Dietz's critical rate. In order to indicate which end-member the recovery is closer to, one should firstly consider the vertical cross flow. If cross flow is limited (i.e. in an environment with high density of short and discontinuous shales) or the displacement is dominated by viscous force, the displacement should be described by the Buckley-Leverett flow model. If cross flow is significant, one should consider the displacement gravitational impact. For gravity stable displacement the variation of reservoir geometry (N_θ) has a large influence on recovery. If a reservoir contains continuous shales that are longer than the injector-producer inter-well spacing, the shale will effectively divide a reservoir into thinner layers. In the most extreme case, all movable oil can be recovered at breakthrough (Figure 6.10). On the other hand, if the displacement is gravity unstable, the influence of geometry becomes insignificant (Shook et al. 1992).

6.8.2. The problem of defining Kv:Kh ratio

When there was no impermeable shale in a reservoir (Figure 6.9A), gas injected at point B can freely move up to point A or C (the global effective Kv:Kh was one). Whereas when one or more extensive continuous impermeable shales were present in a reservoir as demonstrated in Figure 6.9B, gas injected at point X can never travel to point W or Y so for this case the Kv:Kh ratio of the reservoir is zero in this case.

The results demonstrated that by using the global Kv:Kh ratio for the whole reservoir (Figure 6.9 B,C) the recovery estimation could be misleading. For a case shown in Figure 6.9B the global Kv:Kh was zero, but vertical cross flow occurred in the sandbody between the shale, therefore the Kv:Kh between shales was one. Thus,

in the case where the reservoir was divided into a number of thinner layers by extensive shales, the displacement profile became similar to a mobility stable 'piston-like' displacement.

6.8.3. Limitations of the study

6.8.3.1 Impact of small scale geological features

The method developed by this study was demonstrated in a 2D dipping reservoir model. The investigation was conducted under simplified reservoir conditions. For example, it was assumed that sandbodies between shales were homogeneous which means the model omitted genetic-unit-scale and bed-form scale (c.1-0.1m Weber 1986) features. Previous research (e.g. Hartkamp-Bakker 1993; Ciammetti et al. 1995) demonstrated features like cross-bedding or lamination can influence displacement as these factors control small-scale sweep efficiency and capillary pressure.

6.8.3.2 On 2D net-to-gross

The recovery boundary estimation presented in this chapter is only valid in a high NTG system that lies above the connectivity threshold (60% NTG for a 2D system) predicted by percolation theory (King 1990; Hovadik and Larue 2007). Below 60% NTG, sandbodies were likely to be disconnected, and variations in sandbody connectivity would influence recovery. For example, in the case with short shales were explicitly modelled at 60% NTG it was found that the CORB obtained was below that of the Buckley-Leverett flow estimation (Figure 6.4). This effect arises because part of the sand was disconnected, resulting in lower recovery (Figure 6.4).

Moreover, the method was limited by considering all the layers that are sub-divided by continuous shales to have NTG above the connectivity threshold. In Chapter 4, it was demonstrated that if laterally extensive shales isolate a reservoir into high and low NTG layers, the absence of interlayer connectivity reduces the recovery of the whole reservoir. If there was free communication between the high and low NTG layers, the low NTG layers that were not directly connected to a well could still be swept via an adjacent high NTG layer. It was expected that in a 3D system the methodology would be valid for a wider range of NTG, considering the connectivity threshold of a 3D system is lower c. 30% -35% NTG (King 1990; Hovadik and Larue 2007).

6.8.3.3 Reliability of the streamline simulator

A streamline simulator was used to conduct the investigation because it has the advantage of a short simulation time. However, streamline simulation has limitations, as it did not recognise mass balance and therefore errors accumulate as simulation time increases (Batycky 1997). All the results presented here were evaluated at gas breakthrough in order to minimise this effect. Figure 6.11 shows that streamline simulation consistently under-estimates recovery compared with the analytical solution. It was hypothesised that this was because the streamline simulator did not honour the gravity force component acting against the bulk flow direction. Figure 6.11 showed that when gravity was neglected in simulations in a model with Kv:Kh equal to one, the result was similar to the Buckley-Leverett flow model estimate when gravity was not applied. On the other hand, when gravity was taken into account, the Buckley-Leverett flow model predicted a higher recovery at breakthrough compared to a simulation result from a model with zero Kv:Kh. Nevertheless, the purpose of

this investigation was to investigate the relative influence of shale length and Kv:Kh on displacement. Hence the use of streamlines was justified. All the simulations were carried out under the same simulation conditions so they were internally consistent. Finally, the boundary of the recovery estimation with shales of varying continuity was estimated by an analytical method and similar results were obtained. Therefore it was considered the upper and lower boundary estimated was reliable.

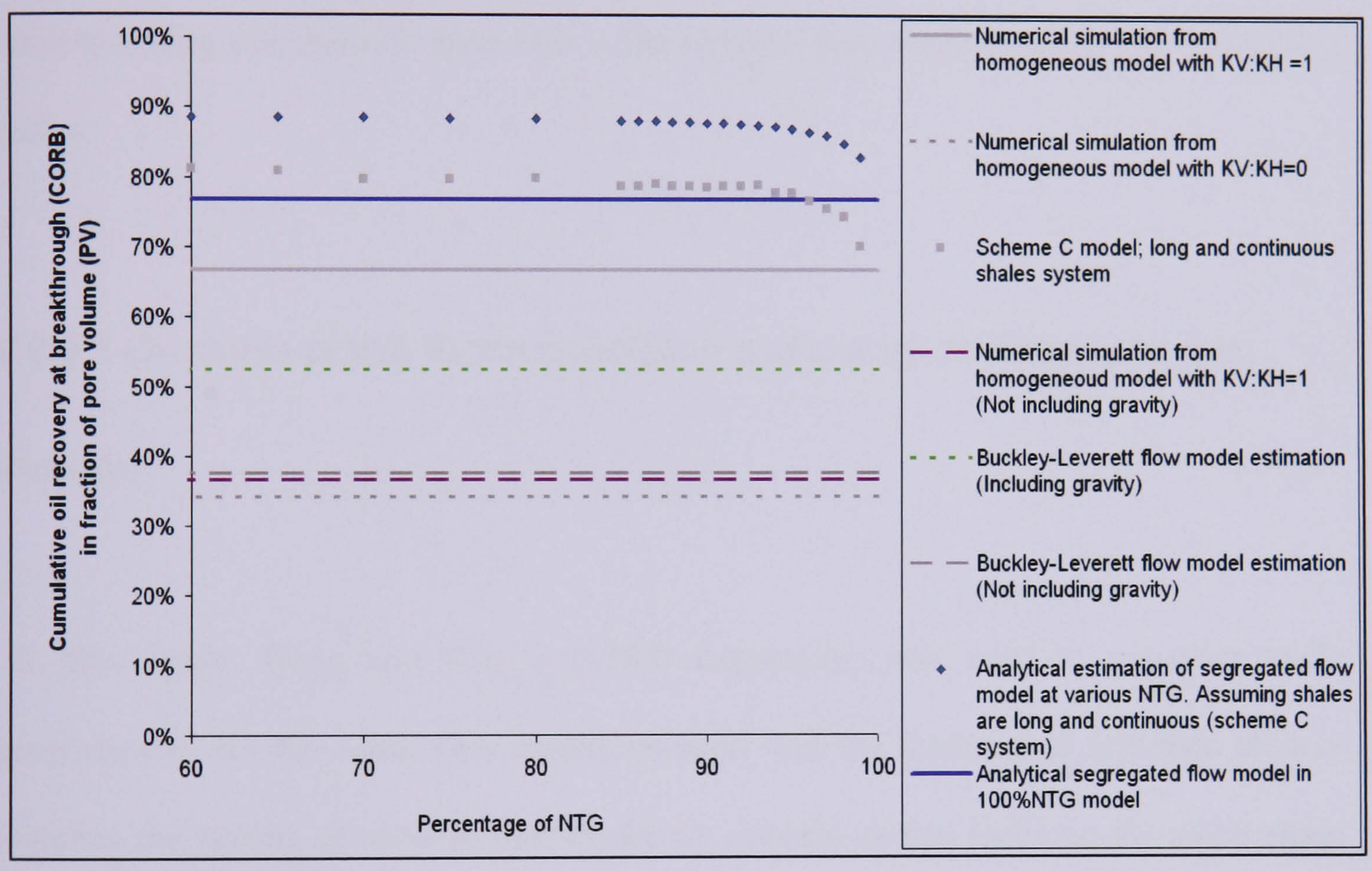


Figure 6.11. Estimation of cumulative oil recovery at breakthrough under 46.7% Dietz's critical rate in various analytical models. Analytical estimation of the gravity force dominated displacement recovery.

6.8.3.4 On grid refinement

It has been shown that a grid cell thickness of 1/200 of each model thickness was sufficient to capture any potential gas tongues that might occur in the displacement (Appendix 2). However, when shales are explicitly modelled, in some cases there

were only a few grid cells between shales, and therefore the grid resolution could be too low to capture the displacement accurately in those regions. To solve this problem would require tailor-made grid refinement i.e. explicitly increase the number of cells in regions between shales, or generate pseudo relative permeability curves to represent the shale effect. This problem could limit the reliability of the results for models containing long discontinuous shales. Nevertheless, under the assumption of no gravity drainage around shales, the boundaries of the recovery estimate and the corresponding conclusions were still valid because they were supported by analytical study.

6.8.3.5 On single-phase Kv:Kh correlation and gravity drainage after gas invasion

In this study, Begg and King's (1985) expression was used to correlate shale properties to Kv:Kh ratio. Our results showed that the correlation schemes closely matches the results of models that explicitly contain shales (scheme B) when shale lengths were short. However, such a correlation only considered single phase flow. Moreover, Richardson (1987) pointed out that the effect of discontinuous shales on reducing gravity drainage of oil from a region invaded by gas/water could be less important than predicted by single phase flow simulations. Such single phase Kv:Kh correlation could be inaccurate in the context of a two phase displacement and hence lead to inaccurate estimation of the oil recovery.

This study recognised that the increase of shale density and reduction of shale length would lower the Kv:Kh ratio, thus reducing the VE. Ypma (1983) also worked on a

gas-oil displacement mechanism in a 2D dipping reservoir. This author considered that recovery increased with the presence of shale because, during gas displacement, not all the oil was swept. The remaining oil in the gas-invaded zone then drained down and accumulated at the base of the reservoir or on the top surface of shales. Therefore, the saturation of oil was increased and oil tongues formed. The relative permeability of oil increased with the saturation of oil (i.e. the oil became more mobile). A pseudo relative permeability curve was generated to represent the presence of shales in the reservoir. Ypma (1983) concluded that if there are more shales in a reservoir, the recovery would be increased as the effective relative permeability of oil would be higher. However, the implications of this theory are not clear. For example, Ypma's (1983) paper did not explain how the proposed pseudo relative permeability curves correlated with variations in shale density (NTG) or shale length. Thus the theory did not explicitly explain cases where sandbodies were disconnected (high shale density) or shales were extensive enough to sub-divide a reservoir. These limitations of Ypma's (1983) theory prevented further assessment of its reliability.

6.9 Conclusion

This part of the project has estimated the upper and lower boundary of cumulative oil recovery at breakthrough in a 2D dipping heterogeneous reservoir under gravity dominated displacement.

The following is a summary of the findings in this section:

- If VE is achieved and shale lengths are sufficiently short (shale: reservoir length ratio equal to 0.01), the shale properties can be represented by a modified Kv:Kh ratio. However, if the reservoir has discontinuous shales: reservoir length ratio between 0.01 and 0.8, the recovery should be estimated by a model with shales explicitly represented.
- If VE is achieved and shales are continuous or shale lengths are sufficiently long (shale: reservoir length ratio grater than or equal to 0.8), the recovery can be estimated analytically by using a model with thickness equal to the distance between shales under the assumption that the intervening sands are homogeneous.
- For mobility unstable displacement, the maximum recovery can be found when the displacement is gravity stable, with extensive shales sub-dividing the reservoir into thin layers. The associated geometrical effect causes higher recovery than from an isotropic reservoir.
- For mobility unstable displacement, the minimum recovery is found when the displacement is gravity unstable. In this case the injected fluid can be segregated upward/downward (depending on its density relative to oil). However, as the displacement is also influenced by viscous force the injected

fluid cannot be stabilised and so a tongue is formed which causes early breakthrough (gravity unstable displacement).

- If the offtake rate of a displacement is higher than the Dietz's critical rate, maximum oil recovery can be found if the displacement is viscous force dominated (Buckley-Leverett flow model).

Chapter 7
Conclusion and recommendation

7.1 Overview

This research has covered the following four aspects:

1. A preliminary displacement study on water-oil and gas-oil displacement in the south flank and the north flank of the Azeri Field. The study estimated the recovery profile and the displacement stability of the different displacement mechanisms, based on the assumption of homogeneous rock properties.
2. An investigation of the impact of the reservoir-unit scale heterogeneities in fluvial deltaic environments on reservoir performance from gas and water flooding under a simplified fluid PVT description.
3. An investigation of the impact of the combination of genetic-unit and reservoir-unit scale heterogeneities that were found in fluvial deltaic environments on high NTG reservoir performance from gas flooding under both simplified and realistic fluid PVT descriptions.
4. An analytical estimate of the upper and lower boundary of cumulative oil recovery at breakthrough in a 2D heterogeneous reservoir under gravity stabilised mobility unstable displacement. The approach was to represent the effect of heterogeneities in terms of shales with different distribution and lengths.

7.2 Conclusions

7.2.1 Preliminary displacement study

Using a 'top-down' approach, the research started with an analysis of reservoir performance from the most simple reservoir model. The preliminary displacement stability analysis demonstrated the water flooding is mobility stable and under the current production rate, and the gas flooding was gravity stable. However, such analysis was based on the assumption of a homogeneous reservoir. The Dietz's stability analysis suggested that the current production rate was very close to the critical rate of unstable displacement. Therefore, the influence of geological heterogeneities may lead the displacement to become unstable. Preliminary analysis indicated that the more unstable the gas oil displacement, the lower the cumulative oil recovery is at breakthrough time. Thus, unstable displacement has a negative impact on recovery. Hence, a screening study on the influence of the reservoir-unit scale heterogeneity factors on reservoir performance was conducted and discussed in Chapter 4.

7.2.2 Screening study of reservoir-unit scale heterogeneities

At reservoir-unit scale, the investigation firstly demonstrated that the local variation in NTG within low NTG layers and the connectivity between low NTG layers and adjacent high NTG layers are the principal controls on oil recovery under both gas and water injection schemes. When net sand is present in low NTG layers, the overall recovery increased because it locally increased the STOIIP. However the overall sweep efficiency in low NTG layers was poor because of the low sandbody

connectivity in these layers. In regions that had net sand in the low NTG layer, sand presence was a positive influence on recovery if there was free communication between adjacent high and low NTG layers. This was because, if there was communication between the high and low NTG layers, some of the oil in the low NTG layer which were not connected directly to production wells could be swept from adjacent high NTG layers. Therefore the overall recovery improved. Thus total production of injected water and gas was then reduced.

In low NTG layers, recovery was mainly controlled by sandbody connectivity and sweep efficiency. Therefore, the variation of channel sinuosity and channel stacking were the two most important heterogeneities that influence recovery in the low NTG layer. Higher sinuosities result in higher connectivity between channel sandbodies and production wells. Additionally, sweep efficiency increased when channel sandbodies were stacked together to form multi-storey channel belts. In high NTG layers, geological heterogeneities only had a small impact on recovery when genetic-unit scale features are not considered.

7.2.3 Screening study of combined genetic-unit and reservoir-unit scale heterogeneities

A screening study of the influence of the combined genetic-unit and reservoir-unit scale heterogeneities on gas-oil displacement was conducted in a specific region of the reservoir with high NTG. The results showed that, in a high NTG layer, the heterogeneities that control the vertical equilibrium of the displacement had the largest influence on mobility unstable gas-oil displacement. Factors that reduced the

vertical equilibrium of the displacement had a negative impact on oil recovery. Therefore, factors such as the reduction of Kv:Kh ratio in channel-fill sandbodies or the presence of mud-clast lags at channel bases caused the reduction in oil recovery and a corresponding increased in gas production.

In the investigation both simplified and realistic fluid PVT descriptions were applied. It was found that a more realistic PVT description had a minor influence on the impact of the heterogeneities on reservoir performance. Using different fluid PVT descriptions the presence of extensive shales made a minor improvement on oil recovery. This was because if reservoir pressure dropped below bubble point, gas evolved from solution and the presence of the laterally extensive shale reduced the distance needed for gas to segregate. Hence the time for gas to be stabilized by the gravity was reduced.

In Chapter 5, a well control scheme was also applied to the screening study. When this was applied the reservoir behaviour was sensitive to different heterogeneities compared with the case with no well control. The results suggested that 'non-reservoir' factors such as well control schemes should also be taken into account for modelling purposes because human activity (well shut-in for pressure test) or equipment constraints (well shut-in because of GOR constraints) can interfere with how the reservoir responds to geological heterogeneities. This suggested that if 'non-reservoir' factors were introduced, various reservoir models should be built at various stages of production. This was because the reservoir conditions would be different after production wells re-open. This demonstrates that reservoir performance was sensitive to different heterogeneities after the 'non-reservoir' factors were introduced.

It was found that the rank order of the geological heterogeneities on gas flooding did not change between gravity stable and gravity unstable displacement. However with gravity unstable displacement, the reservoir performance was less sensitive to the influence of the geological heterogeneities. Gravity stable conditions rely on vertical equilibrium conditions. A displacement could not be stabilized by gravity if vertical equilibrium was not achieved. Hence, a gravity stable displacement was sensitive to factors that influence the vertical segregation, whereas such factors have less influence on a gravity unstable displacement. Therefore, the impact of heterogeneity on recovery reduced when the offtake rate increased.

7.2.4 Methodology for the rapid estimation of oil recovery

In the last part of the research a rapid methodology was developed to estimate the upper and lower boundary of oil recovery in a 2D heterogeneous reservoir under a gravity force dominated displacement. Heterogeneities that control the vertical equilibrium of the displacement had the largest influence on oil recovery in a reservoir with high NTG. By modelling geological character in terms of sand and shale, reservoir heterogeneities were represented as different continuities and lengths of shales.

In the case of a gravity force dominated displacement, the lowest oil recovery was found when the Kv:Kh ratio of the sandbodies is zero because vertical equilibrium cannot be achieved. This is the situation when shales were found to be short and discontinuous. On the other hand, the highest recovery was found when shales were continuous or extensive because continuous shales divided the reservoir into many

layers. This resulted in the reduction of effective fluid flow paths. Therefore, oil recovery increased because of the associated geometrical effect.

Both the upper and lower boundaries of oil recovery could be estimated by the analytical method. The lowest value of oil recovery occurs when vertical equilibrium could not be achieved, and it could be estimated by the classic Buckley-Leverett flow model. The highest value of oil recovery occurs when shales were considered to be continuous. By assuming sandbodies between shales were homogeneous and all the oil was swept in the gas/water invaded zone, the recovery could be estimated by geometrical estimation in all the layers bounded by continuous shales. In the most extreme case, if the reservoir was divided into a large number of layers, a 'piston-like' segregated displacement occurs (end-point mobility ratio equal to 1), which meant all the movable oil could be recovered at breakthrough.

7.3 Recommendations

The following are recommended for future investigation:

1. Extend the study on the influence of reservoir-unit scale heterogeneities on flow with a range of offtake rates in order to study the rank order and the magnitude of impact of the heterogeneities on reservoir performance under various states of stability.
2. It was found that reservoir-unit scale heterogeneity factors such as channel sinuosity and channel distribution have a significant influence on both water-oil and gas-oil displacement in low NTG environments (Chapter 4). It

would be beneficial if the investigation of the influence of the combined genetic-unit and reservoir-unit scale heterogeneity on both water-oil and gas-oil displacements in low NTG environments were to be extended.

3. In Chapter 5 it was found that the heterogeneity factors which have influence on the degree of vertical cross flow have the largest influence on mobility unstable (gas-oil) displacement. In order to test if the same heterogeneity factors have the same influence on mobility stable displacement it would be valuable to extend the investigation of the influence of the combined genetic-unit and reservoir-unit scale heterogeneity in high NTG environments on water-oil displacement.
4. Concerning the sand/shale reservoir model (Chapter 6): Further investigations of the recovery estimation methodology for gravity dominated displacement in reservoirs with shales character between the two extreme end-members would also be valuable.

References

Abdullaev, T., Falt, L.M., A.Akhundov, G.W.Graas, Kvamme, T., L.H.Flolo, K.Mehmandarov, A.A.Narimanov, T.S.Olsen, G.Seljeskog, O.Skontorp, T.Sultanzade, N.Tank, and E.Valieva, 1998, A reservoir model for the main Pliocene reservoirs of the Bahar Field in the Caspian Sea, Azerbaijan: Petroleum Geoscience, v. 4, p. 259-270.

Allen, J.R.L., 1983, Studies in fluviatile sedimentation: Bars Bar-complexes and sandstone sheets (low-sinuosity braided streams) in the brownstones (L. Devonian), Welsh borders: Elsevier Scientific Publishing Company, Amsterdam Sedimentary Geology, v. 33, p. 237-293.

Ambrose, W.A., Wang, F.P., Akhter, M.S., Skolnakom, J., Mendez, M., Alvarez, R., and Lagoven, S.A., 1997, Geologic Controls on Remaining Oil in Miolence Transgressive-Barrier, Coastal-Plain, and Mixed-Load Fluvial Systems in the Miocene Norte Area, Lake Maracaibo, Venezuela: SPE 38662; presented at SPE Annual Technical Conference and Exhibition, San Antonio; 5th - 8th October.

Anna, L.O., 2003, Groundwater flow associated with coal bed gas production, Ferron Sandstone, east-central Utah: International Journal of Coal Geology, v. 56, p. 69-95.

Baker, R.O., and Moore, R.G., 1996, Effect of reservoir heterogeneities on flow simulation requirements: SPE 35413; presented at Improved Oil Recovery Symposium, Tulsa; 21st April.

Ballin, P.R., Faria, R.T., Becker, M.R., Carrasco, B.N., and Teixeira, P.W., 1997, Reservoir studies in fluvial deposits: From outcrops to stochastic characterisation and flow simulation: SPE 39000; presented at 5th Latin American and Caribbean Petroleum Engineer Conference andExhibition, Rio de Janeiro; 30th Aug - 3rd Sept.

Barthel, R., 1991, The effect of large scale heterogeneities on the performance of water drive SPE 22697; presented at SPE Annual Technical Conference and Exhibition, Dallas; 6th - 9th Oct.

Batycky, R.P., 1997, A Three-Dimensional Two-Phase Field Scale Streamline Simulator: A Dissertation of Stanford University for Doctor of Philosophy.

Batycky, R.P., Blunt, M.J., and Thiele, M.R., 1996, A 3D field-scale streamline based reservoir simulator: SPE 36726; presented at SPE Annual Technical Conference and Exhibition, Denver; 6th - 9th Oct.

Begg, S.H., Carter, R.R., and Dranfield, P., 1987, Assigning effective values to simulator gridblock parameters for heterogeneous reservoirs: SPE 16754; presented at SPE Annual Technical Conference and Exhibition, Dallas; 27th - 30th Sept.

Begg, S.H., Chang, D.M., and Haldorsen, H.H., 1985, A simple statistical method for calculating the effective vertical permeability of a reservoir containing discontinuous shales: SPE 14271; presented at SPE Annual Technical Conference and Exhibition, Las Vegas; 22nd - 25th Sept.

Begg, S.H., Gustason, E.R., and Deacon, M.W., 1992, Characterisation of a fluvial-dominated delta:

zone 1 of the Prudhoe Bay Field: SPE 24698; presented at SPE Annual Technical Conference and Exhibition, Washington D.C. ; 4th - 7th Oct.

Begg, S.H., Kay, A., and Gustason, E.R., 1994, Characterization of a complex fluvial-deltaic reservoir for simulation: SPE 28398; presented at SPE Annual Technical Conference and Exhibition, New Orleans; 25th - 28th Sept.

Begg, S.H., and King, P.R., 1985, Modelling the effects of shales on reservoir performance: Calculation of effective vertical permeability: SPE 13529; presented at 1985 Reservoir Simulation Symposium, Dallas; 10th - 13th Oct.

Bhattacharya, J.P., 2006, Deltas: SEPM Special Publication, v. 84, p. 237-292.

Borner, D.L., Haldorsen, H.H., Harrison, P.F., Hopwood, A.P., and McDonald, C.J., 1988, Performance of vertical and horizontal wells in reservoirs containing discontinuous shales: Numerical studies of 2 North Sea Fields: SPE 17600; presented at SPE International Meeting on Petroleum Engineering, Tianjin; 1st - 4th Nov

Box, G.E.P., Hunter, W.G., and Hunter, J.S., 1978, Statistics for experiments (Chapter 6,10,12): Published by John Wiley and Sons. Inc; Wiley Series in Probability and Mathematical Statistics.

Brandsater, I., Wist, H.T., Nass, A., Lia, O., Arntzen, O.J., Ringrose, P.S., Martinius, A.W., and Lerdahl, T.R., 2001, Ranking of stochastic realisation of complex tidal reservoir using streamline simulation criteria: Pertuleum Geoscience, v. 7, p. 53-63.

Broekers, M.P., and Dorp, W.G.v., 1986, Miscible gas drive in unit 1 of the Statfjord reservoir: SPE 15876; presented at SPE European Petroleum Conference, London; 20th - 22nd Oct.

Buckley, S.E., and Leverett, M.C., 1942, Mechanism of fluid displacement in sands: Trans. AIME, v. 146, p. 107-116.

Burns, L.J., Richardson, J.G., and Kimber, R.N., 2002, Tertiary miscible gas injection in the Alwyn North Brent reservoirs: SPE 78349; presented at SPE European Petroleum Conference, Aberdeen; 29th - 31st Oct.

Buryakovsky, L.C., G; Aminzaden, F, 2003, Petroleum Geology of the South Caspian Basin: Gulf Professional Publishing.

C.Chu, 1990, Prediction of streamflood performance in heavy oil reservoirs using correlation developed by factional design method: SPE 20020; presented at 60th California Regional Meeting, Ventura; 4th - 6th April.

Cheong, Y.P., and Gupta, R., 2003, Experimental design in deterministic modelling: Assessing significant uncertainties: SPE 80537; presented at Asia Pacific Oil and Gas Conference and Exhibition, Jakarta; 9th - 11th Sept.

Chike, I., and Onyekonwu, M., 2005, Modelling channelized systems: A robust approach: SPE 98827; presented at SPE Annual Technical Conference and Exhibition, Abuja; 1st - 3rd Aug.

Chu, C., 1990, Prediction of streamflood performance in heavy oil reservoirs using correlation developed by factional design method: SPE 20020; presented at 60th California Regional

Meeting, Ventura; 4th - 6th April.

Ciammetti, G., Ringrose, P.S., Good, T.R., Lewis, J.M.L., and Sorbie, K.S., 1995, Waterflood recovery and fluid flow upscaling in a shallow marine and fluvial sandstone sequence: SPE 30783: presented at SPE Annual Technical Conference and Exhibition, Dallas; 22nd - 25th Oct.

Cubillos, H., Stright, D., and Navano, J.H., 2005, Successful peripheral miscible gas injection in RKF field , Berkine Basin, Algeria- field case history: SPE 94138; presented at SPE Europec/EAGE Annual Technical Conference and Exhibition, Madrid; 13th - 16th June.

Dake, L.P., 1978, Fundaments of reservoir engineering (Chapter 10 notes on Immiscible displacement): Printed by Elsevier Science B.V.

Damsleth, E., Hage, A., and Volden, R., 1991, Maximum information at minimum cost: A North Sea Field development study using experimental design: SPE 23139; presented at Offshore European Conference and Exhibition, Aberdeen; 3rd - 8th Sept.

Datta-Gupta, A., 2000, Streamline simulation: A technology update: SPE 65604; Distinguished Authir Series; Dec.

deRiz, L., and Muggeridge, A.H., 1997, Will vertical mixing improve oil recovery for gravity dominated flows in heterogeneous reservoirs?: SPE 37996; presented at SPE Reservoir Simulation Symposium; Dalas; 8th - 11th June.

Deutsch, C.V., and Tran, T.T., 2002, FLUVSIM: a program for object-based stochastic modelling of fluvial depositional systems.: Computers and Geosciences, v. 28, p. 525-535.

Deutsch, C.V., and Wang, L., 1996, Hierarchical object based geostatistical modelling of fluvial reservoirs: SPE 36514; presented at SPE Annual Technical Conference and Exhibition, Denver; Colorado; USA; 6th - 9th Oct.

Dietz, D.N., 1952, A theoretical approach of the problem of encroaching and by-passing edge water: Akad. van Wetenschappen. Amsterdam. Proc, v. 56-B.

Dyer, G.R., Ismanto, B., and Haas, M., 2000, New well architecture successfully optimises the development of fluvio-deltaic multi-layered gas field: SPE 64394; presented at Asia Pacific Oil and Gas Conference and Exhibition, Brisbane; 16th - 18th Oct.

Ekrann, S., 1992, An analysis of gravity segregated piston-like displacement in stratified reservoirs: SPE 18598; published in SPE Reservoir Engineering Journal June 28th

Fayers, F.J., and Muggerldge, A.H., 1990, Extensions to Dietz theory and behaviour of gravity tongue in slightly tilted reservoirs: SPE 18438; presented at Reservoir Simulation Symposium, Houston; 6th - 8th Feb.

Felletti, F., 2003, Statistical modelling and validation of correlation in turbidites: an example from the Tertiary Piedmont Basin, Castagnola, Northern Italy: Marine and Petroleum Geology.

Friedmann, F., Chawathe, A., and Larue, D.K., 2001, Assessing uncertainty in channelised reservoirs using experimental designs: SPE 71622; presented at SPE Annual Technical Conference and Exhibition, New Orleans; 30th Sept - 3rd Oct.

Galloway, W.E., 1975, Process Frame for Describing the Morphologic and Stratigraphic Evolution of

Deltaic Depositional Systems: Houston Geological Society, p. 86-98.

Geehan, G.W., Lawton, T.F., Sakurai, S., Klob, H., Cliffon, T.R., Inman, K.F., and Nitzberg, K.E., 1986, Geologic prediction of shale continuity Prudhoe Bay Field: Reservoir Characterisation, Academic Press; New York.

Gilman, J.R., Meng, H.Z., Uland, M.J., Dzurman, P.J., and Cosic, S., 2002, Statistical ranking of stochastic geomodels using streamline simulations: A field application: SPE 77374; presented at SPE Annual Technical Conference and Exhibition, San Antonio; 29th Sept - 2nd Oct.

Graaff, W.J.E.v.d., and Ealey, P.J., 1989, Geological modelling for simulation studies: The American Association of Petroleum Geologists Bulletin v. 73, p. 1436-1444.

Grammer, G.M., Harris, P.M., and Eberli, G.P., 2004, Integration of outcrop and modern analogs in reservoir modelling: Overview with examples from the Bahamas: AAPG Memoir, v. 80, p. 1-22.

Haajizadeh, M., and Begg, S.H., 1993, Sensitivity of oil recovery to grid size and reservoir description in fluvially dominated deltaic facies: SPE 26080; presented at the Western Regional Meeting, Anchorage; 26th - 28th May.

Haldorsen, H.H., 1986, Simulator parameter assignment and the problem of scale in reservoir engineering: Reservoir Characterisation, Academic Press; New York.

Haldorsen, H.H., and Chang, D.M., 1985, Notes on stochastic shales: From outcrop to simulation model: Reservoir Characterisation, Academic Press; New York, p. 445- 485.

Haldorsen, H.H., and Chang, D.M., 1986, Notes on stochastics shales: from outcrop to simulation model: Academic Press Inc.

Haldorsen, H.H., Chang, D.M., and Begg, S.H., 1987, Discontinuous vertical permeability barriers: a challenge to engineers and geologists: North Sea oil and gas reservoir, p. 127-151.

Haldorsen, H.H., and Damsleth, E., 1990, Stochastic Modelling: SPE 20321, JPT.

Haldorsen, H.H., and Lake, L.W., 1982, A new approach to shale management in field scale models: SPE 10976; presented at SPE Annual Technical Conference and Exhibition, New Orleans; 26th - 29th Sept.

Haldorsen, H.H., and McDonald, C.J., 1987, Stochastic modelling of underground reservoir facies (SMURF): SPE 16751; presented at SPE Annual Technical Conference and Exhibition, Dallas; 27th - 30th Sept.

Hand, J.L., Jr, A.L.M., and Yang, C.T., 1994, Geostatistical integration of geological petrophysical and outcrop data for evaluation of gravity drainage infill drilling at Prudhoe Bay: SPE 28396; presented at SPE Annual Technical Conference and Exhibition, New Orleans; 25th - 28th Sept.

Hartkamp-Bakker, C.A., 1993, Permeability heterogeneity in cross-bedded sandstones impact on water/oil displacement in fluvial reservoirs: Published by Krips repro meppel Postbus 1106 7940 KC Meppel; The Netherlands; PhD Thesis at Fault of Mining and Petroleum Engineering at the Delft University of Technology.

Hesthammer, J., Landro, M., and Fossen, H., 2001, Use and abuse of seismic data in reservoir characterisation: Marine and Petroleum Geology, v. 18, p. 635-655.

Hinds, D.J., Aliyeva, E., Allen, M.B., Davies, C.E., Kroonenberg, S.B., Simmons, M.D., and Vincent, S.J., 2004, Sedimentation in a discharge dominated fluvial-lacustrine system: the Neogene Productive Series of the South Caspian Basin, Azerbaijan: Marine and Petroleum Geology.

Hohn, M., E; McDowell, R,R; Matchen, D,L; Vargo, A,G, 1997, Heterogeneity of fluvial-deltaic reservoirs in the Appalachian Basin; a case study from the Lower Mississippian oil field in central West Virginia AAPG Bulletin, v. 81, p. 918-936.

Hovadik, J.M., and Larue, D.K., 2007, Static characterizations of reservoirs: refining the concepts of connectivity and continuity: Petroleum Geoscience, v. 13, p. 195-211.

Huang, W., DiDonato, G.., and Blunt, M.J., 2004, Comparison of streamline based and grid based dual porosity simulation: Journal of Petroleum Science and Engineering, v. 43, p. 129-137.

Hunedi, S., Danquigny, J., Morel, D., Maubeuge, F., and Guarrino, A., 2005, Applicability of enhanced oil recovery techniques on mature fields interest of gas injection: SPE 93368 presented at the 14th SPE Middle East Oil and Gas Show and Conference; Bahrain; 12th -15th March.

Idroho, E.A., Choudhary, M.K., and Datta-Gupta, A., 2000, Swept volume calculations and ranking of geostatistical reservoir models using streamline: SPE 62557; presented at the SPE/AAPG Western Regional Meeting, Long Beach; 19th - 23rd June.

Jackson, M.D., and Muggeridge, A.H., 2000, The effect of discontinuous shales on reservoir performance during immiscible flow: SPE 51919; presented at SPE Reservoir Simulation Symposium, Houston; 14th - 17th Feb.

Jackson, M.D., Yoshida, S., Johnson, H.D., Muggeridge, A.H., Nass, A., and Ringrose, P., 1999, Three dimensional reconstruction, flow simulation and upscaling of complex bedform scale sedimentary structures within tidal sandstone reservoir: Advanced Reservoir Characterisation for the 21st Century, Proceedings of GCS-SEPM Research Conference.

Jones, A., Doyle, J., and Jacobsen, T., 1992, A review of 'The effects of reservoir heterogeneities on recovery processes': BP/Statoil Alliance Project.

Jones, A., Doyle, J., Jacobsen, T., and Kjønsvik, D., 1995, Which sub-seismic heterogeneities influence waterflood performance? A case study of a low net to gross fluvial reservoir: De Hann, H.J.(e.d); New developments in improved oil recovery; Geological society special publication, p. 5-18.

Jones, A., and Jerauld, G., 2005, Azeri-Chirag-Gunashi Gas Displacement Behaviour: 1. Azeri-Gas Flood Pseudos Oct 2005; 2. Chirag GOR history match Dec 2004: BP exploration and production technology group internal report.

Jones, A., Verly, G.W., and Williams, J.K., 1994, What reservoir characterisation is required for predicting waterflood performance in a high net to gross fluvial environment?: North Sea oil and gas reservoir v. 3, p. 223-232.

King, P.R.., 1990, The connectivity and conductivity of overlapping sandbodies: North Sea oil and gas

reservoir; The Norwegian Institute of technology (Graham and Trotman). v. 2.

King, R.L., Stiles Jr, J.H., and Waggoner, J.M., 1970, A Reservoir Study of the Hawkins Woodbine Field: SPE 2972 American Institute of Mining, Metallurgical, and Petroleum Engineers, Inc.

Kjønsvik, D., Doyle, J., Jacobsen, T., and Jones, A., 1995, The effects of sedimentary heterogeneities on production from a shallow marine reservoir - What really matters?: SPE 28445; presented at European Petroleum Conference and Exhibition, London; 25th - 27th Oct.

Kleppe, J., 2004, Reservoir notes; 1. Mass balance equations; 2. Review of relative permeabilities and capillary; 3. Buckley-Leverett analysis; 4. Dietz's stability analysis: Reservoir Recovery Technique handout, Dept of Petroleum Engineering and Applied Geophysics; Norwegian University of science and Technology.

Knapp, R.M., and Yang, X., 1999, Identifying opportunities to increase oil recovery from fluvial dominated deltaic reservoirs in Oklahoma: SPE 52226; presented at SPE Mid-continent Operations Symposium, Oklahoma; 28th - 31th March.

Knox, P.R., and Barton, M.D., 1999, Predicting interwell heterogeneity in fluvial-deltaic reservoirs: Effects pf progressive architecture variation through a depositional cycle from outcrop and subsurface observations: AAPG Memoir, v. 71, p. 57-72.

Kortekaas, T.F.M., 1985, Water/oil displacement characteristics in cross bedded reservoir zones: SPE 12112; presented at SPE Annual Technical Conference and Exhibition, San Francisco; 5th - 8th Oct.

Kroonenberg, S.B., Alekseeuski, N.I., Aliyeva, E., Allen, M.B., Aybulatov, D.N., Baba-Zadeh, A., Badyvkova, E.N., Davies, C.E., Hinds, D.J., Hoogendoorn, R.M., Huseynou, D., Ibrahimov, B., Mamedov, P., Overeem, I., Rusakov, G.V., Suleymanava, S., Suitoch, A.A., and Vincent, S.J., 2005, Two deltas, two basins, one river, one sea: the modern Volga delta as an analogue of the Neogene Productive Series, South Caspian Basin: SEPM Special Publication, v. 83, p. 231-256.

Kroonenberg, S.B., Rusakov, G.V., and Suitoch, A.A., 1997, The wandering of the Volga delta: A response to rapid Caspian Sea-level change: Sedimentary Geology, v. 107, p. 189-209.

Kroonenberg, S.B.B., J.F; Hogendoorn, R.M; Overeem, I; Aliyeva, E; Huseynor, D; Badyukova, E.M; Suitoch, A.A; Hinds, D; Simmons, M.D, 2004, Sandstone deposition in Lacustrine Environments: Implications for exploration and reservoir development: AAPG Hedberg Conference

Larue, D.K., 2004. Outcrop and waterflood simulation modelling of the 100-foot channel complex, Texas and the Ainsa II channel complex, Spain: Analogs to multistory and multilateral channelized slope reservoirs: AAPG Memoir, v. 80, p. 337-364.

Larue, D.K., and Friedmann, F., 2005, The controversy concerning stratigraphic architecture of channelised reservoirs and recovery by waterflooding: Pertuleum Geoscience, v. 11, p. 131-146.

Larue, D.K., and Hovadik, J., 2006, Connectivity of channelised reservoirs: A modelling approach:

Petroleum Geoscience, v. 12, p. 291-308.

Lasseter, T.J., Waggoner, J.R., and Lake, L.W., 1986, Reservoir heterogeneities and their influence on ultimate recovery: Reservoir Characterisation, Academic Press; New York.

Lasseter, T.J.W., J.R; Lake, L.W, 1986, Reservoir heterogneeities and their influence on ultimate recovery: Reservoir Characterisation, Academic Press; New York.

Lerat, O., Doligez, B., Desaubliaux, G., Daniel, J.-M., Eschard, R., Garcia, F., Chauvin, H., Coureaud, B., Nussbaumer, C., and Rouvroy, P., 2002, Integration of Horizontal Wells in Reservoir Models: Input from an Outcrop Study: SPE 77627; presented at SPE Annual Technical Conference and Exhibition, San Antonio; 29th September - 2nd October.

LeRoux, J.P., 1992, Determining the channel sinuosity of ancient fluvial systems from paleocurrent data: Jorunal of Sedimentary Petrology, v. 62, p. 283-291.

Li, D., and Lake, L.W., 1995, Scaling fluid flow through heterogeneous permeable media: SPE 26648; SPE Advanced Technology Series v. 3.

Li, H., and White, C.D., 2003, Geostatistical models for shale in distributary channel point bars (Ferron Sandstone, Utah) from ground-penetrating radar data to 3-D dlow modelling: AAPG Bulletin, v. 87, p. 1851-1868.

Luo, J.M., S; Zhang, X; Yan, Shike; Wu , F, 2002, Reconstruction of the diagenesis of the fluvial-lacustrine- deltaic sandstones and its influence on the reservoir quality evolution- Evidence from Jurassic and Triassic sandstones, Yanchang Oil Field, Ordos Basin: Science in China (Earth Sciences), v. 45, p. 616-634.

Manceau, E., Mezghani, M., Zabalza-Mezghani, I., and Roggero, F., 2001, Combination of experimental design and joint modelling methods for quantifying the risk associated with deterministic and stochastic uncertainties- An intergrated test study.: SPE 71620; presented at SPE Annual Technical Conference and Exhibition, New Orleans; 30th Sept - 3rd Oct.

Matheron, G., Beucher, H., de Fouquet, C., Galli, A., Guerillot, D., and Ravenne, C., 1987, Conditional simulation of the geometry of fluvial-deltaic reservoirs: SPE 16753; presented at SPE Annual Technical Conference and Exhibition, Dallas; 27th - 30th Sept.

McLennan, J.A., and Deutsch, C.V., 2005, Ranking geostatistical realisation by measures of connectivity: SPE 98168; presented at SPE International Thermal Operations and Heavy Oil Symposium, Calgary; 1st - 3rd Nov.

Miall, A.D., 1985, Architectural-element analysis: A new method of facies analysis applied to fluvial deposits: Earth-Sci, v. 22, p. 261-308.

Miall, A.D.,1988, Architectural elements and bounding surface in fluvial deposits: anatomy of the Kayenta formation (lower Jurassic Southwest Colorado): Sediment. Geology, v. 55, p. 233-240.

Montgomery, D.C., 2005, Design and Analysis of Experiments: 6th Edition published by John Wiley and Sons, Inc.

Morton, A., Allen, M., Simmons, M., Spathopoulos, F., Still, J., Hinds, D., Ismail-Zadeh, A., and

S.Kroonenberg, 2003, Provenance patterns in a neotectonic basin: Pliocene and Quaternary Sediment supply to the South Caspian: Basin Research, v. 15, p. 321-337.

Narimanov, A., Akperov, N., and Abdullaev, T., 1998, The Barhar oil and gas-condensate field in the South Caspian Basin: Petroleum Geoscience, v. 4, p. 253-258.

Nikijuluw, R., Suwito, Z.A., and Arianto, M.A., 2005, Integrated reservoir assessment: A way to identify 'Overlooked' multilayered reservoirs: SPE 93198; presented at Asia Pacific Oil and Gas Conference and Exhibition, Jakarta; 5th - 7th April.

Olariu, C., and Bhattacharya, J.P., 2006, Terminal Distributary Channels and Delta Front Architecture of River-Dominated Delta Systems: Jorunal of Sedimentary Research, v. 76, p. 212-233.

Overeem, I., Kroonenberg, S.B., Veldkamp, A., Groenesteijn, K., Rusakov, G.V., and Suitoch, A.A., 2003, Small-scale stratigraphy in a large ramp delta: recent and Holocene Sedimentation in the Volga Delta, Caspian Sea: Sedimentary Geology, v. 159, p. 133-157.

Peake, W.T., Abadah, M., and Skander, L., 2005, Uncertainty assessment using experimental design Minagish Oolite reservoir: SPE 91820; presented at SPE reservoir simulation symposium, Houston; 31st Jan - 2nd Feb.

Prats, M., 1972, The influence of oriented arrays of thin impermeable shale lens or of highly conductive natural fractures on apparent permeability anisotropy: SPE 4163, JPT, Oct.

Prevost, M., Lepage, F., Durlofsky, L.J., and Mallet, J.-L., 2005, Unstructured 3D gridding and upscaling for coarse modelling of geometrically complex reservoirs: Pertuleum Geoscience, v. 11, p. 339-345.

Reading, H.G., and Collinsons, J.D., 1996, Clastic Coasts: BOOK.

Reynolds, A.D., Bowman, A., and Stirling, E., 2003, Sedimentology of the Productive Series: BP exploration and production technology group internal report; Implication for ACG (Azeri-Chirag-Gunashli).

Reynolds, A.D., and Riley, G., 2003, Outcrop Analogs for ACG: BP exploration and production technology group internal report; Implication for ACG (Azeri-Chirag-Gunashli).

Reynolds, A.D., Simmons, M.D., Bowman, M.B.J., Henton, J., Brayshaw, A.C., Ali-Zade, A.A., Guliyev, S.I., Suleymanova, S.F., Ataeva, E.Z., Mamedova, D.N., and Koshkarly, R.O., 1998, Imlications of outcrop geology for reservoirs in the Neogene Productive Series: Apsheron Peninsula, Azerbaijan: AAPG Bulletin, v. 82, p. 25-49.

Richardson, J.G., Harris, D.G., and Rossen, R.H., 1977, The effect of small, discontinuous shales on oil recovery: SPE 6700; presented at the SPE-AIME 52th Annual Fall Technical Conference and Exhibition, Denver; 9th - 12th Oct.

Richardson, J.G., Sangree, J.B., and Sneider, R.M., 1987a, Applications of geophysics to geologic models and to reservoir description: SPE 15784; Journal of Petroleum Technology.

Richardson, J.G., Sangree, J.B., and Sneider, R.M., 1987b, Permeability distributions in reservoirs: SPE 15785. JPT, Oct.

Richardson, J.G., Sangree, J.B., and Sneider, R.M., 1989, Deltas: SPE 15778; Journal of Petroleum

Technology

Ringrose, P.S., Nordahl, K., and Wen, R., 2005, Vertical permeability estimation in heterolithic tidal deltaic sandstones: Petroleum Geoscience, v. 11, p. 29-36.

Ringrose, P.S., Sorbie, K.S., Feghi, F.A., Pickup, G.E., and Jensen, J.L., 1993, Relevant reservoir characterisation: recovery process, geometry and scale: InSitu, v. 17, p. 55-82.

Sablok, R., and Aziz, K., 2005, Upscaling and discretization errors in reservoir simulation: SPE 93372: Presented in reservoir simulation symposium, Houston; 31st Jan- 2nd Feb.

Salhi, M.A., Rijen, M.v., Wei, L., Dijk, H., Alias, Z., Upadhya, A., and Lee, H., 2005, Structured uncertainty assessment for a mature field through the application of experimental design and response surface methods: SPE 93529; presented at SPE Middle East Oil and Gas Show and Conference, Bahrain; 12th - 15th March.

Schulte, A.M., Niko, H., and Swinkles, W., 1990, Analytical modelling of 2D flow in gravity stable secondary gas or water drives: SPE 20899; presented at Europec 90, The Hegue; 22nd - 24th Oct.

Schwab, A.M., Buchem, F.S.P.v., and Eberli, G.P., 2004, Integration of high-resolution outcrop and subsurface data to enhance interpretation of low-resolution seismic data in the Upper Devonian (Frasnian) carbonate system in Western Canada: AAPG Memoir, v. 80, p. 261-278.

Shmaryan, L.E., and Deutsch, C.V., 1999, Object based modelling of fluvial/deepwater reservoirs with fast data conditioning: methodology and case studies: SPE 56821; presented at SPE Annual Technical Conference and Exhibition, Houston; 3rd - 6th Sept.

Shook, M., Li, D., and Lake, L.W., 1992, Scaling immiscible flow through permeable media by inspectional analysis: InSitu, v. 4, p. 311-349.

Stalkup, F.I., and Ebanks, J., 1986, Permeability variation in a sandstone barrier island-tidal channel-tidal complex, Ferron Sandstone (Lower Cretaceous), Central Utah: SPE 15532; presented at SPE Annual Technical Conference and Exhibition, New Orleans; 5th - 8th Sept.

Sullivan, R.B., Hinson, D.L., and Hendrix, D.E., 2004, Benefits and Challenges Associated with CRA Injection Tubing in Corrosive Gas Wells: SPE 91692; presented at SPE Annual Technical Conference and Exhibition, Houston; 26th - 29th September.

Suro-Perez, V., P.Ballin, Aziz, K., and Journel, A.G., 1991, Modelling geological heterogeneities and its impact on flow simulation: SPE 22695; presented at SPE Annual Technical Conference and Exhibition, Dallas; 6th - 9th Sept.

Thiele, M.R., Rao, S.E., and Blunt, M.J., 1996, Quantifying uncertainty in reservoir performance using streamtubes: Mathematical Geology, v. 28.

Tyler, N., Barton, M.D., and Finley, R.J., 1991, Outcrop characterisation of flow unit and seal properties and geometries, Ferron sandstone, Utah: SPE 22670; presented at SPE Annual Technical Conference and Exhibition, Dallas; 6th - 9th Oct.

Urbanczky, C.H., and Wattenbarger, R.A., 1994, Optimization of well rates under gas coning conditions: SPE 21677, Advanced Technology Series, v. 2.

Vo, D.T., Witjaksana, R.S., Waryan, S., Dharmawan, A., and Harmawan, I., 2001, Reservoir management for ultra-thin oil column under gas-cap and water support: Attaka field examples: SPE 68675; presented at SPE Asia Pacific Oil and Gas Conference and Exhibition, Jakarta; 17th - 19th April.

Wach, G.D., Lolley, C.S., Mims, D.S., and Sellers, C.A., 2004, Well placement, cost reduction and increased production using reservoir models based on outcrop, core, well-log seismic data and modern analogs: Onshore and offshore Western Trinidad: AAPG Memoir, v. 80, p. 279-307.

Wang, P.M., and Shibli, S.A.R., 2001, Modelling a fluvial reservoir with multipoint statistics and principal components: Journal of Petroleum Science and Engineering, v. 31, p. 157-163.

Warren, J.E., and Skiba, F.F., 1963, Macroscopic dispersion: SPE 648; presented at SPE Annual Fall Meeting, New Orleans; 6th - 9th Oct.

Waryan, S., Vo, D.T., Stites, J., and Swanson, M., 2001, Integrated 3D geological data into fluid flow model improves reservoir management plan: Serang field case study: SPE 68646; presented at SPE Asia Pacific Oil and Gas Conference and Exhibition, Jakarta; 17th - 19th April.

Weber, J.K., 1982, Influence of common sedimentary structures on fluid flow in reservoir models: JPT March

Weber, J.K., 1986, How heterogeneity affects oil recovery: Reservoir Characterisation, Academic Press; New York, p. 487-544.

Weber, J.K., and van Geuns, L.C., 1990, Framework for constructing clastic reservoir simulation models: SPE 19582; presented at SPE Annual Technical Conference and Exhibition, San Antonio; 8th - 11th Oct.

Welge, H.J., 1952, A simplified method for computing oil recovery by gas or water drive: Trans, AIME, p. 91-98.

White, C.D., and Barton, M.D., 1997, Translating outcrop data to flow models with applications to the Ferron sandstone: SPE 38741; presented at SPE Annual Technical Conference and Exhibition, San Antonio; 5th - 8th Oct

White, C.D., and Royer, S.A., 2003, Experimental design as a framework for reservoir studies: SPE 79676; presented at SPE Reservoir Simulation Symposium, Houston; 3rd - 5th Feb.

Williams, G.J.J., Mansfield, M., MacDonald, D.G., and Bush, M.D., 2004, Top-Down reservoir modelling: SPE 89974; presented at SPE Annual Technical Conference and Exhibition, Houston; 26th - 29th Sept.

Yao, T., and Chopra, A., 2000, Integration of seismic attribute map into 3D facies modelling: Jorunal of Petroleum Science and Engineering, v. 27, p. 69-84.

Yortsos, Y.C., 1991, A theoretical analysis of vertical flow equilibrium: SPE 22612; presented at SPE Annual Technical Conference and Exhibition, Dallas; 6^{th}-9^{th} Oct

Yortsos, Y.C., 1992, Analytical studies for processes at vertical equilibrium: SPE 26022; presented at the 3^{rd} European Conference on the Mathematics of Oil Recovery, Delft, 17^{th}-19^{th} June.

Ypma, J.G.J., 1983, Analytical and numerical modelling of immiscible gravity-stable gas injection into

stratified reservoirs: SPE 12158; presented at SPE Annual Technical Conference and Exhibition, San Francisco; 5th - 8th Oct.

Appendix 1
Supplementary notes for preliminary displacement study

In order to simplify the preliminary displacement study in Chapter 3, a single value of sandbody porosity and permeability was applied for the preliminary displacement analysis in the Pereriv Suite.

The following expressions demonstrated that a Buckley-Leverett flow analysis from any layer within the Pereriv Suite can be applied to all the ensembles within the Pereriv Suite. All the parameters are summarized in Table A1.

Nomenclature	
L : length; F : force; t : time; m : mass; [=] means 'has units of'	
L	Reservoir length [=] L
H	Reservoir thickness [=] L
A	Cross-sectional area [=] L^2
W	Reservoir width [=] L
B_t	The time of breakthrough [=] t
NTG	Net to Gross [=] fraction
ϕ	Sandbody porosity [=] fraction
θ	Reservoir dipping angle [=] radians or degrees
g	Gravitational acceleration [=] L/t^2
k	Sandbody permeability [=] L^2
ρ_j	Density of phase j [=] m/L^3
μ_j	Viscosity of phase j [=] $(F\text{-}t/L^2)$
kr'_j	End-point relative permeability of phase j [=] fraction
q	Production rate for each Pereriv layer [=] L^3/t
S	Saturation [=] fraction
Q	Total production rate [=] L^3/t
Subscripts	
i	Denotes for parameter assigned between Pereriv A to E
$mean$	Mean value
o	Oil phase
f	Displacing fluid phase (i.e gas or water)
or	Residual oil
wc	Connate water

Table. A1 The summary of parameters that are used in the equations that are listed above.

Given that the proposed total production rate Q is 9%STOIIP of the whole Pereriv Suite.

$$Q = \frac{9\% \times H \times W \times L \times NTG_{mean} \times \phi \times (1 - S_{or} - S_{WC})}{year}$$

Set constant C:

$$C = {9\% \times W \times L \times \phi \times (1 - S_{or} - S_{WC})} \Big/ {year}$$

Therefore $Q = \frac{\sum_{i=A}^{E} (NTG_i \times H_i)}{H} \times H \times C$

Thus: $Q = \sum_{i=A}^{E} (NTG_i \times H_i) \times C$ equation A1.1

The production rate for each layer (q_i) is a fraction of Q which is proportional to k_iH_i of each layer (i) within the Pereriv Suite.

$$q_i = (\frac{k_i H_i}{\sum_{i=A}^{E} (k_i \times H_i)})Q$$

Given that permeability in each ensemble is:

$$k_i = k \times NTG_i$$ equation A1.2

Therefore the production rate for each layer can be written as:

$$q_i = (\frac{kNTG_i H_i}{\sum_{i=A}^{E} (k_i \times H_i)})Q$$ equation A1.3

The fractional flow equation of gas-oil displacement from up dip to down dip position:

$$f_i = \frac{1 - \frac{kk_{ro}A}{q\mu_o}(\rho_o - \rho_g)g\sin\theta}{1 + \frac{\mu_g k_{ro}}{k_{rg}\mu_o}}$$

The fractional flow equation of water-oil displacement from down dip to up dip position:

$$f_i = \frac{1 + \frac{kk_{ro}A}{q\mu_o}(\rho_o - \rho_w)g\sin\theta}{1 + \frac{\mu_g k_{ro}}{k_{rg}\mu_o}}$$

By setting $\Delta\rho = (\rho_o - \rho_f)$

The fractional flow of injected fluid from up dip to down dip position at layer i: f_i

$$f_i = \frac{1 - k_i k_{ro} WH_i / q_i (\Delta\rho g\sin\theta)}{(1 + \frac{\mu_f}{k_{rf}}\frac{k_{ro}}{\mu_o})}); \qquad \text{equation A1.4}$$

By substituting equation A1.3 in equation A1.4

$$f_i = \frac{1 - (k_i k_{ro} WH_i / (\frac{k_i H_i}{\sum_{i=A}^{E}(k_i \times H_i)})Q)(\Delta\rho g\sin\theta)}{(1 + \frac{\mu_f}{k_{rf}}\frac{k_{ro}}{\mu_o})})$$

Therefore $f_i = \frac{1 - (k_{ro}W / (\frac{1}{\sum_{i=A}^{E}(k_i \times H_i)})Q)(\Delta\rho g\sin\theta)}{(1 + \frac{\mu_f}{k_{rf}}\frac{k_{ro}}{\mu_o})})$ equation A1.5

All the parameters in equation A1.5 are universal for the whole Pereriv Suite. Therefore the same fraction flow curve can be used to conduct Buckley-Leverett flow analysis for the entire Pereriv Suite.

On the estimation of the time of breakthrough for a particular layer i (B_{ti})

$$Bt_i = W_{id}\left(\frac{PoreVolume_i}{q_i}\right)$$

$$Bt_i = W_{id}\left(\frac{W \times L \times \phi \times H_i \times NTG_i}{\left(\frac{kNTG_i H_i}{\sum_{i=A}^{E}(k_i \times H_i)}\right)Q}\right) \qquad \text{equation A1.6}$$

By substituting equation A1.3 into equation A1.6

$$Bt_i = W_{id}\left(\frac{W \times L \times \phi}{\left(\frac{k}{\sum_{i=A}^{E}(k_i \times H_i)}\right)Q}\right) \qquad \text{equation A1.7}$$

Since all the terms are constant equation A1.7 shows that when the production rate is proportional to the kH of each layer, the time of breakthrough for all the Pereriv Suite would be the same.

Finally, the dimensionless gravitational number G is also universal for all the layers.

$$G_i = \frac{k_i k'_{rf} A_i \Delta\rho g \sin\theta}{q_i \mu_f} \qquad \text{equation A1.8}$$

By substituting equation A1.3 into equation A1.8

$$G_i = \frac{k_i H_i W k'_{rf}\, \Delta\rho g \sin\theta}{\left(\frac{k_i H_i}{\sum_{i=A}^{E}(k_i \times H_i)}\right) Q \mu_f}$$

$$G = \frac{W k'_{rf}\, \Delta\rho g \sin\theta}{\left(\frac{1}{\sum_{i=A}^{E}(k_i \times H_i)}\right) Q \mu_f} \qquad \text{equation A1.9}$$

All the parameters in equation A1.9 are universal for all the Pereriv Suite layer. Therefore a single value of dimensionless number G can be applied to the whole Pereriv Suite.

Appendix 2
Test of the reliability of the grid cell resolution

Grid resolution is important for displacement simulation as it determines the reliability of the result. In the case when gravity force dominates displacement, grid resolution is especially important for simulation to capture gravity segregation (Ypma, 1983; Baker and Moore, 1996) that leads to inaccurate result. However, because of the computational power, it is only feasible to simulate a limit number of grid cells. Therefore, the balance between the reliable grid cell's resolution and the feasible number of grid cells is important.

Although grid cell's resolution might be enough to capture displacement in a homogeneous model, it is recognised that when heterogeneities are present in the same model, the flow path between the impermeable layers is much thinner than for the homogeneous model. Therefore, the reliability of the grid resolution should be determined from a heterogeneous model. A grid resolution analysis was conducted in one of the low NTG (Pereriv C) models which contain reservoir unit scale heterogeneity factors (e.g channels with 200m width and 6m thick). Both cumulative oil recovery and a cumulative gas production profile were obtained under a range of grid cell's thickness (Figure A2.1A and A2.1B).



Figure A2.1A

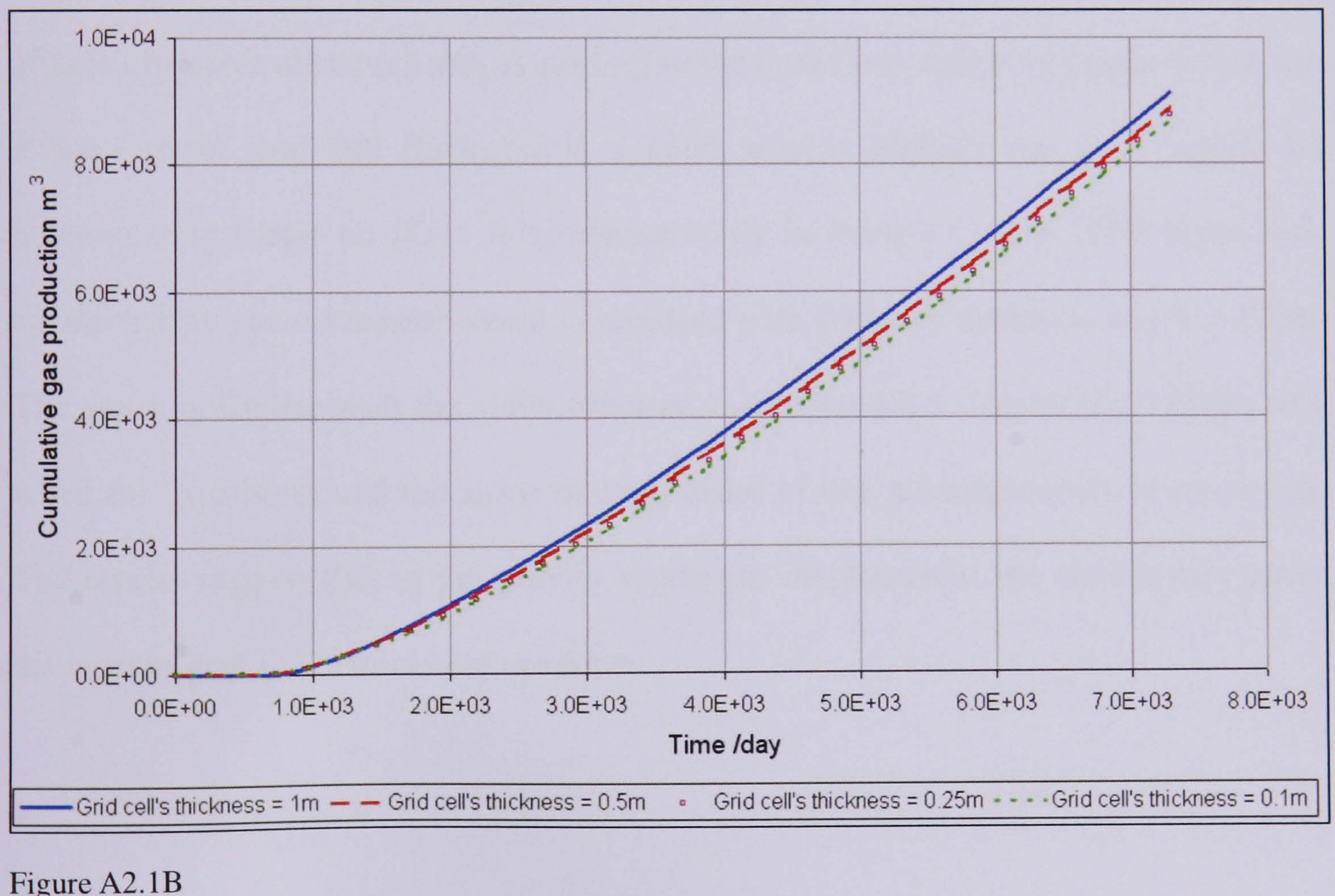


Figure A2.1B

Figure A2.1 (A-B). Shows the comparison of the oil recovery profile (A, top) with the gas production profile (B, bottom) in north flank Pereriv C models with varied grid cell thickness. The results show that the result converged when the grid cell is 0.5m.

The results show that the estimated values converge when the grid cell is 0.5m. When 1m thick grid cells were applied to the simulation models, the results of the cumulative oil recovery and the gas production has a few percentage differences from the converged results. Ideally, 0.1m thick grid cells should be applied to the simulation models. However, with the current grid cell thickness (1m) the north flank models at the 1st screening study contain approximately one million grid cells which is the limit of the streamline simulation. Therefore it is not feasible to reduce the grid size.

The main objective of this research is to identify the most significant factor that affects objective measurement. A grid refinement test was therefore conducted to test if the current grid cell thickness is a valid way to identify the most significant heterogeneity factor on flow. A screening study in Pereriv C (low NTG layer) was conducted by gas-oil displacement is repeated with grid cell thickness equal to 0.5m. The study is similar with the study reported in section 4.6.3. Figure A2.2 shows that when the grid is refined the same ranking order of key heterogeneities is recovered. The results suggest that in the gravity stable gas displacement the simulations under the current grid cell's thickness are robust.

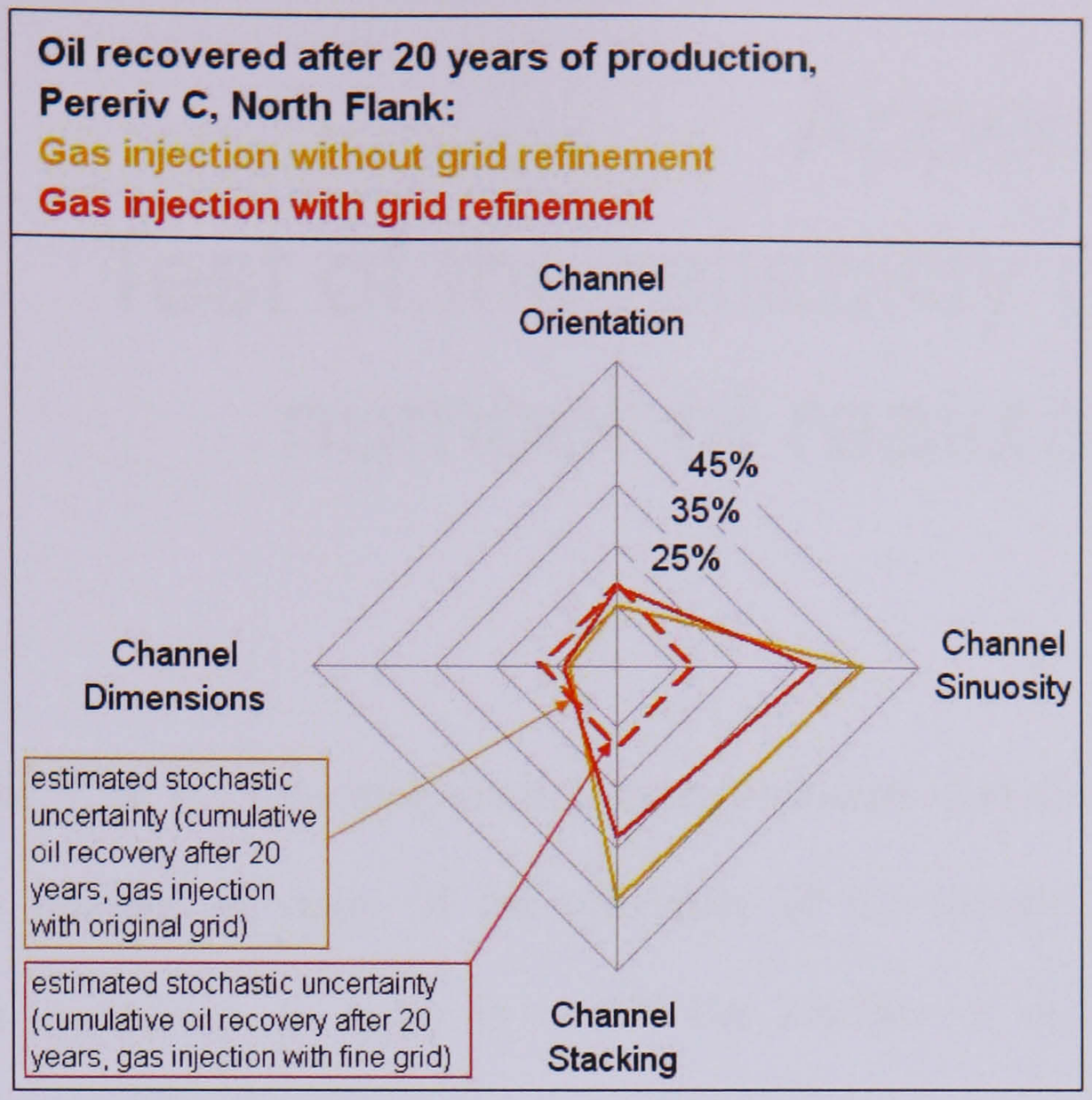


Figure A2.2. Shows the impact of different heterogeneities on flow in Pereriv C in the north flank. Absolute percentage change in total oil recovery after 20 years is plotted, in order to compare the current grid cell thickness (1m) and the grid refinement studies (grid cell thickness equal to 0.5m). Refining the grid does not change the relative impact of the different heterogeneities, suggesting the grid's resolution applied in this research are robust.

Appendix 3
Test of the reliability of the number of realizations

In Chapter 4 and 5, all the screening studies were conducted with three realizations of the reservoir models. A study of the reliability of the number of stochastic realizations was conducted, in order to test if the number of realizations were sufficient to capture reliable responses for the influence of the heterogeneities factors. Up to 15 stochastic realizations were applied in order to test whether the screening process can identify the factors which have the most significant impact on the objective measurement.

The test was conducted a screening study by using a single-phase TRACER simulation in high NTG layer (Pereriv B) to identify the most significant reservoir unit scale heterogeneity factor on the total oil recovery. Figure A3 shows the absolute response of the factors to the total oil recovery. The results suggest the magnitude of the response converge when there are more than 13 realizations of the reservoir models were generated. However, because of the time frame of this research project it is not feasible to apply such a high number of realizations to the screening studies. The result shows that the magnitude of the responses is different when the various numbers of realizations were used. However, the screening process can always identify the most significant factor for objective measurement when there are more

than three realizations. Therefore the results support that three realizations were reliable for the screening study.

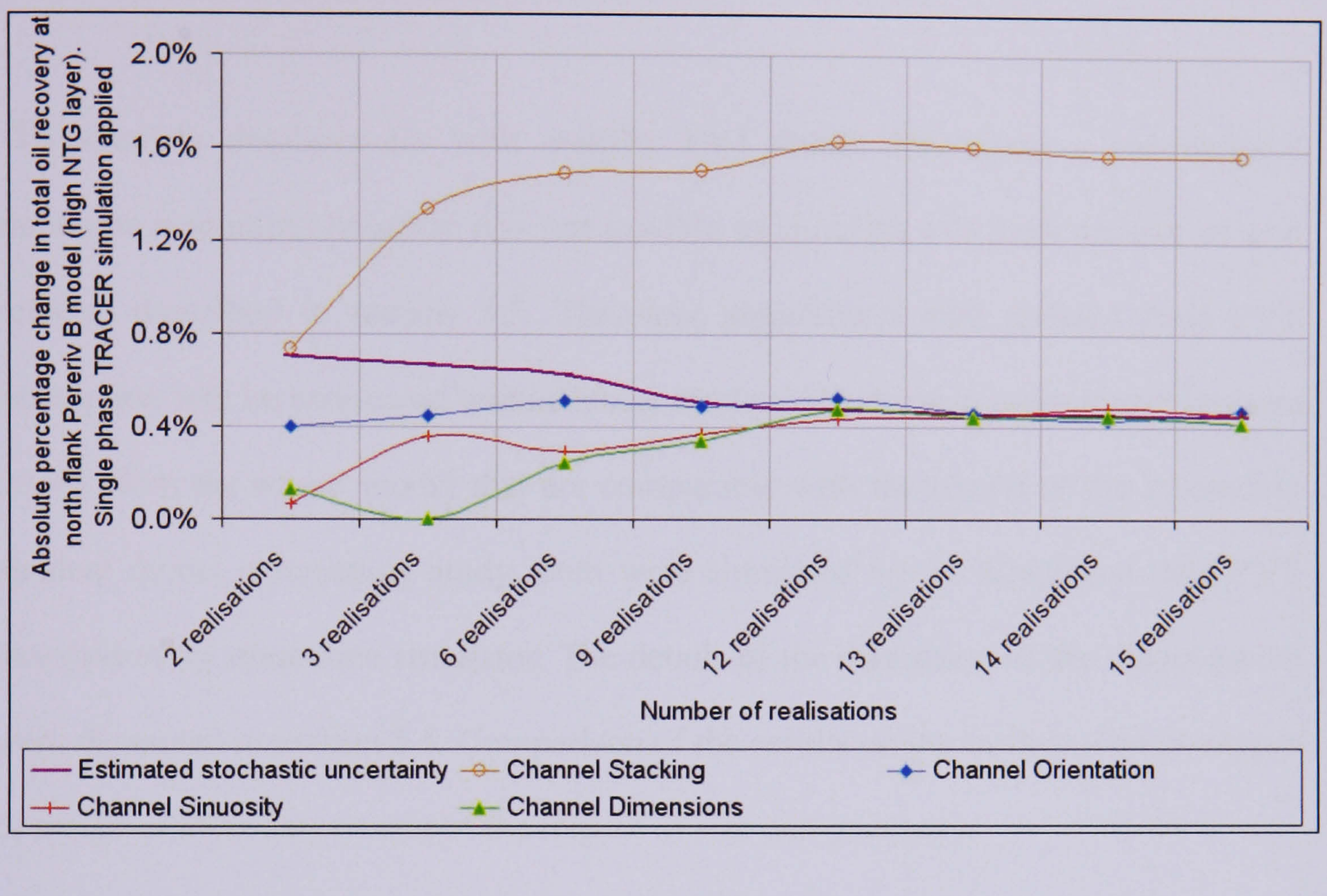


Figure A3. Shows the absolute percentage change of reservoir unit scale heterogeneity factors and stochastic noise in total oil recovery at north flank Pereriv B (high NTG layer). Single phase TRACER simulation was applied to conduct the test. Up to 15 realizations were applied to conduct the test; it is observed that the variation of the magnitude of the responses converge when 13 realizations were applied. However the screening process can always identify the most significant factors to the objective measure when more than 3 realizations were applied.

Appendix 4
Test of the variation of reservoir model size

To simulate displacement with realistic PVT fluids description a conventional simulator is required however it is not feasible to simulate with high number of grid cells as described in section 5.5. Therefore simulations with realistic fluid PVT description will be conducted within subset models. However in order to demonstrate results from the subset model that are comparable with the results of the symmetric element model a screening study, both were simulated by the simplified fluid PVT description by streamline simulator. The details of the dimension of the subset model were discussed in section 5.5. Comparison of the results on the models with two types of model enables assessment of the impact of size and geometry.

Since the model size is reduced, the displacement time for the sector has been recalculated to mimic the appropriate Dietz's flow rate in the original models. The calculation is described below:

Key:

V : volume of the reservoir model with the original geometry.

A : area of the reservoir model with the original geometry.

L : length of the reservoir model with original geometry.

Q : volumetric flow rate applied to the reservoir model with the original geometry.

t ': displacement time in reservoir model with the original geometry.

* denotes the parameter assigned for the sector models (e.g. t* : displacement time in sector models).

Principle is: $\frac{Volume\ of\ oil\ in\ place}{Volume\ of\ gas\ injected}$ at both models should be the same.

$$\frac{AL}{Qt} = \frac{Volume\ of\ oil\ in\ place}{Volume\ of\ gas\ injected}$$

t: time used for displacement; in the original model t = 20 years

$$\frac{AL}{Qt} = \frac{A^* L^*}{Q^* t^*}$$

$$\frac{A}{4} = A^* \quad ; \quad \frac{L}{2} = L^*$$

$\frac{Q}{A} = \frac{Q^*}{A^*}$ to keep Dietz's critical rate constant

Because A/Q=A*/Q*

L/t=L*/t* ; given L=2L* and Q*=Q/4

t*=t/2 and if t is equal to 20 years

Therefore t* =10 year

This shows that by using displacement time =10 year in the sector models it can mimic 20 years of gas injection at the original reservoir model setting. By careful setting of the ratio of injected fluid entry and exit from the two ends of the model, the simulated displacement of the subset model mimic that a local region in the reservoir (Figure 5.A). The comparison of the results for the two models sizes with simplified fluid PVT description, confirmed this.

A4.1 Results of the gas-oil displacement simulation in a high NTG layer with simplified fluids description; subset model

Figure A4.A1 shows the average percentage change in cumulative oil recovery and total gas production at the end of production period in symmetric model (Figure A4.A1) and subset model (Figure A4.A2). The mud-clast lags and Kv:Kh ratio are the two most significant factors. It is found that by increasing Kv:Kh ratio from 0.1 to 1, the total recovery factor increases by c.14.9 % in a symmetric element model and c. 14.3% in a subset model. The total gas production decreases by c.9.9% in a symmetric element model and c. 7.9% in a subset model.

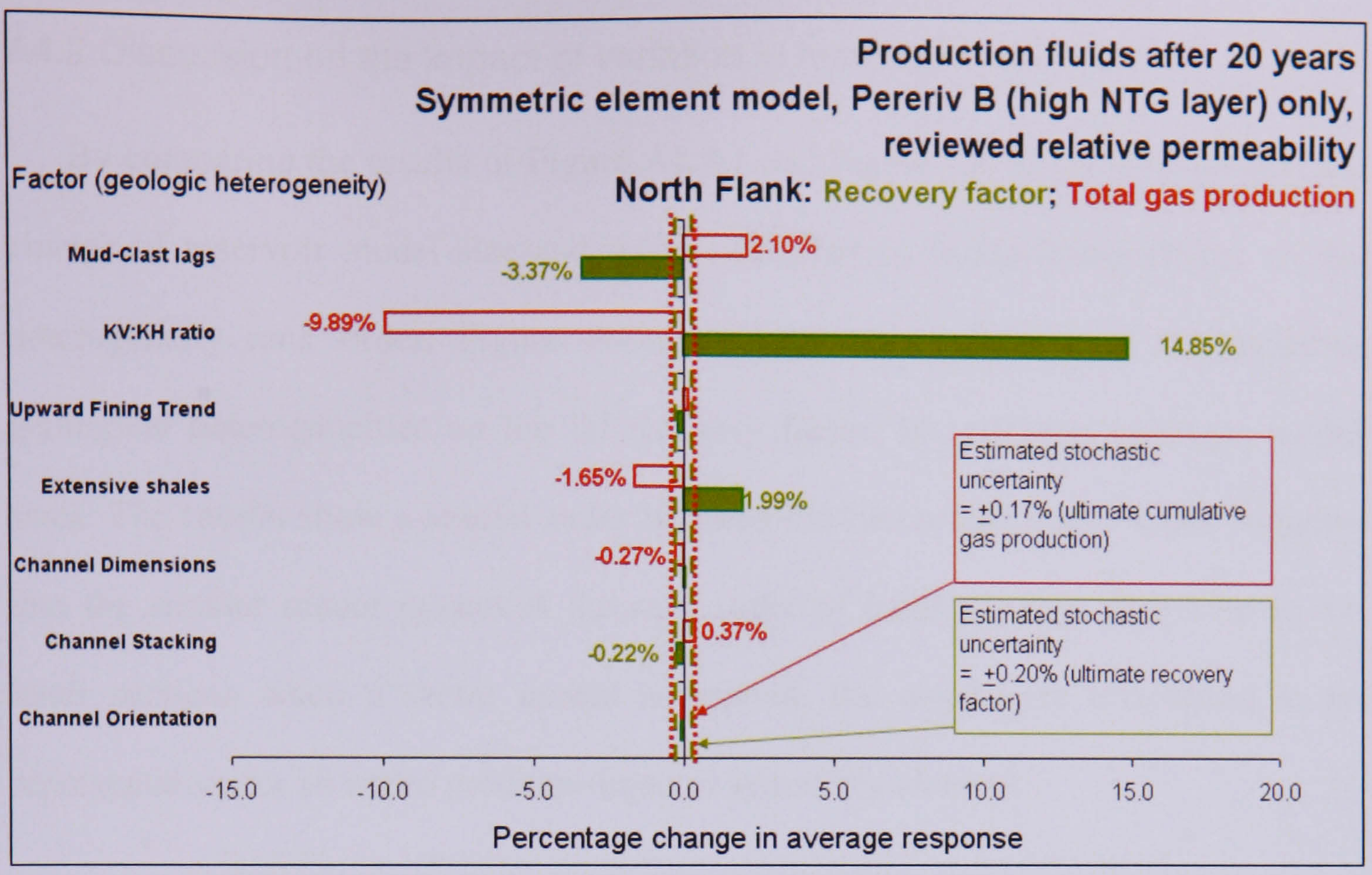


Figure A4.1A

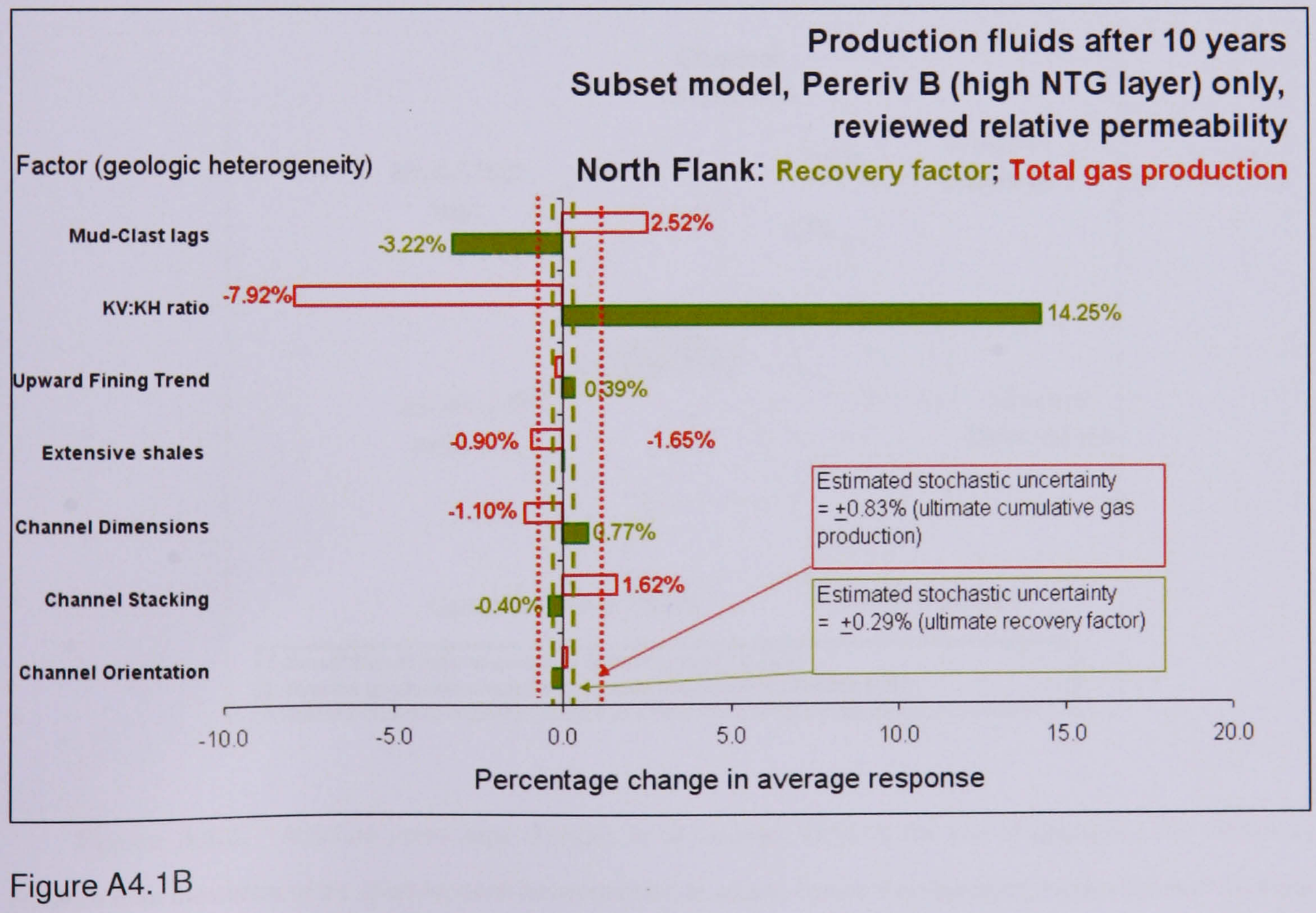


Figure A4.1B

Figure A4.1 (A-B). Average percentage change in recovery factor from reservoir models with different volume, observed when each factor in the sensitivity analysis is varied from setting 1 to setting 2 (Table 5.1). Result for symmetric element model is showed in **(A, top)** and subset reservoir models in **(B, bottom)**. If the bar lies to the right then the change is positive.

A4.2 Discussion on the impact of variation in reservoir model size

By comparing the results of Figure A4.A1 and Figure A4.A2) it is found that the change of reservoir model size and well setting has an insignificant impact on the heterogeneity rank order. Figure A4.B compares the influence of the different geological heterogeneities on the oil recovery factor, for different reservoir model sizes. The results show a similar order between the two model sizes, which suggests that the smaller model maintains the rank order of heterogeneity. Therefore in the latter sections when a sector model is applied, the results are considered to be representative for an entire producer-injector symmetry element.

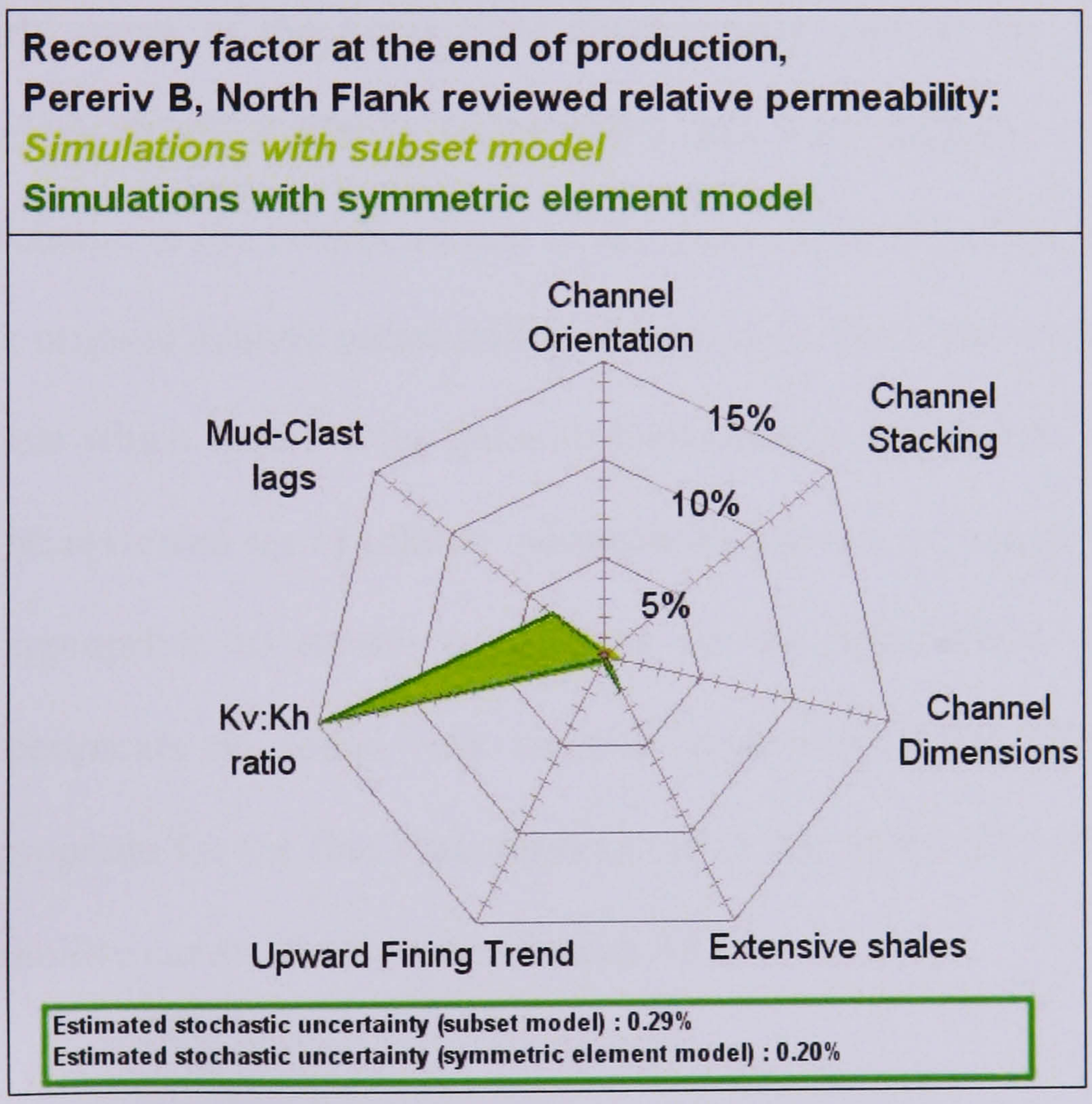


Figure A4.2. Absolute percentage changes in oil recovery factor at the end of production are plotted as distance from the centre of the chart for each heterogeneity, to enable comparison between the two different reservoir model sizes. The reduced model size does not change the relative impact of the different heterogeneities, suggesting that the subset reservoir models represent the symmetric element model setting.

Appendix 5
Test of the different gas-oil displacement relative permeability data

The original relative permeability curves that were used in Chapter 4 were obtained during the early stages of the Azeri Field development; refer to the general Azeri reservoir. A reviewed set of relative permeability data were obtained to describe the gas flooding scheme in the central section of the Azeri reservoir where gas injection is applied. The original relative permeability curve was designed for use in large scale full field models which describe the general displacement mechanism of the whole Azeri field. The reviewed set of relative permeability curves are representive gas/oil rock curves appropriate to central north flank of the Azeri Field. (A series of laboratory experiments on serval rock samples gave very similar curves). These curves are appropriate for the fine scale model used in this study. The different set of relative permeability curves are shown in Figure A5.1.

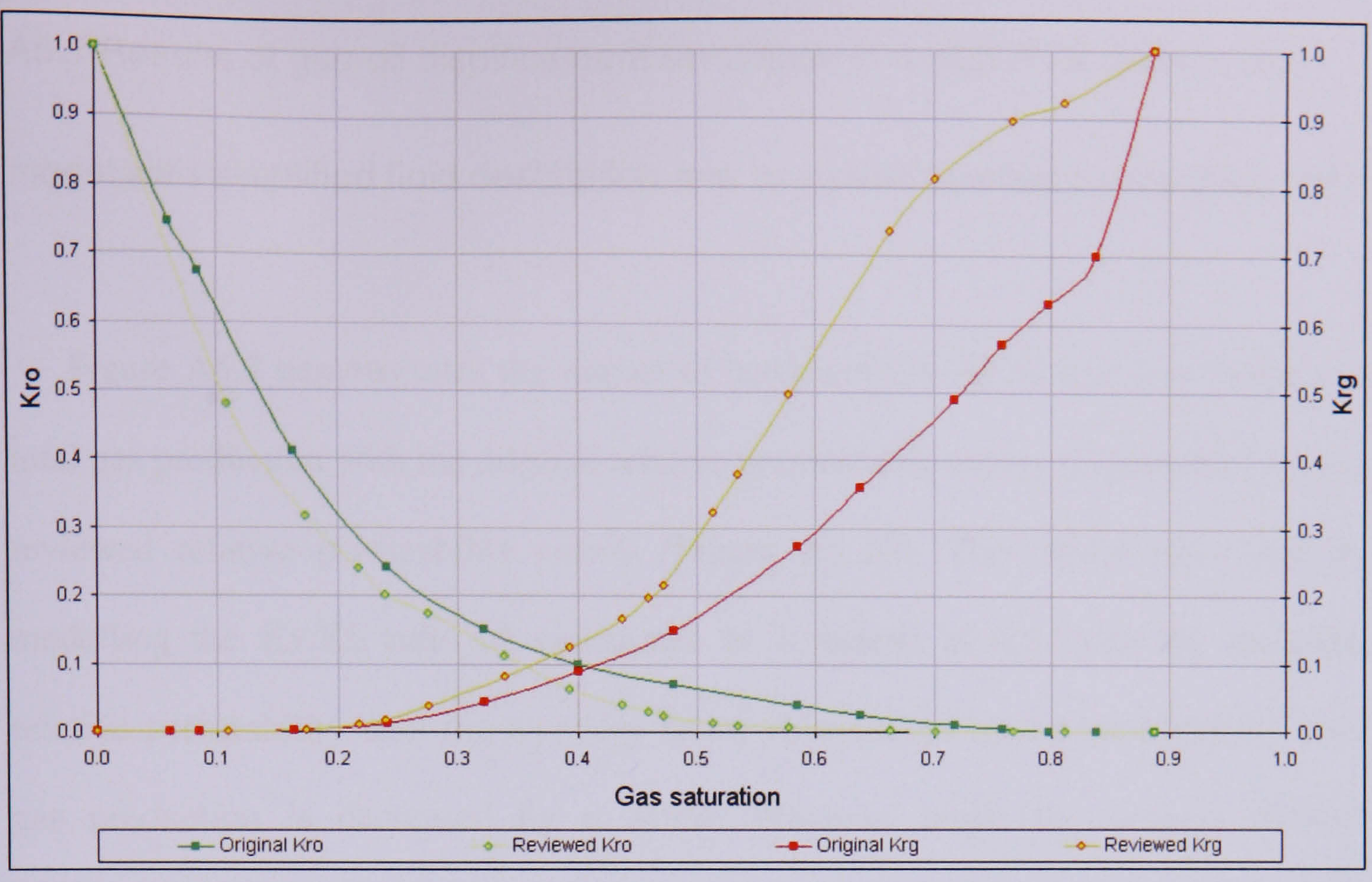


Figure A5.1. Representation of the original and reviewed Oil-Gas relative permeability measured in Azeri reservoir.

This reviewed data set is being used for the central Azeri Field displacement simulation. Having different relative permeability data to represent different locations within a reservoir is a common problem for a reservoir engineer, and relative permeability is a potentially control on reservoir performance. In order to study the impact of different relative permeability data on simulated flow behaviour, the two different sets of relative permeability are simulated in the sector models under simplified fluids description.

A5.1 Results of gas-oil displacement simulation in a high NTG layer sector model with simplified fluid description and re-viewed relative permeability data

Figure A5.2 demonstrates the impact of heterogeneity on oil recovery factor and total gas production with the original relative permeability curves (Figure A5.2A) and reviewed relative permeability curves (Figure A5.2B). The results show that by modelling the Kv:Kh ratio of sandstones as 1 instead of 0.1, with the reviewed relative permeability data the recovery factor is increased by c.14.9% and the total gas production is decreased by c. 9.9%. Whereas, under the original relative permeability, although the variation of Kv:Kh is also the heterogeneity factor has the highest rank but the recovery factor only increases by c. 4.9% and total gas production is only decreased by c.4.1%.

Mud-clast lags along channel base are the second most significant heterogeneity that influences reservoir performance. By including mud-clast lags at channel bases the recovery factors is decreased by c.3.4% and total gas production is increased by c. 2.1%. The results also demonstrate that the impact of varying the other heterogeneities are close to or below the level of stochastic uncertainty.

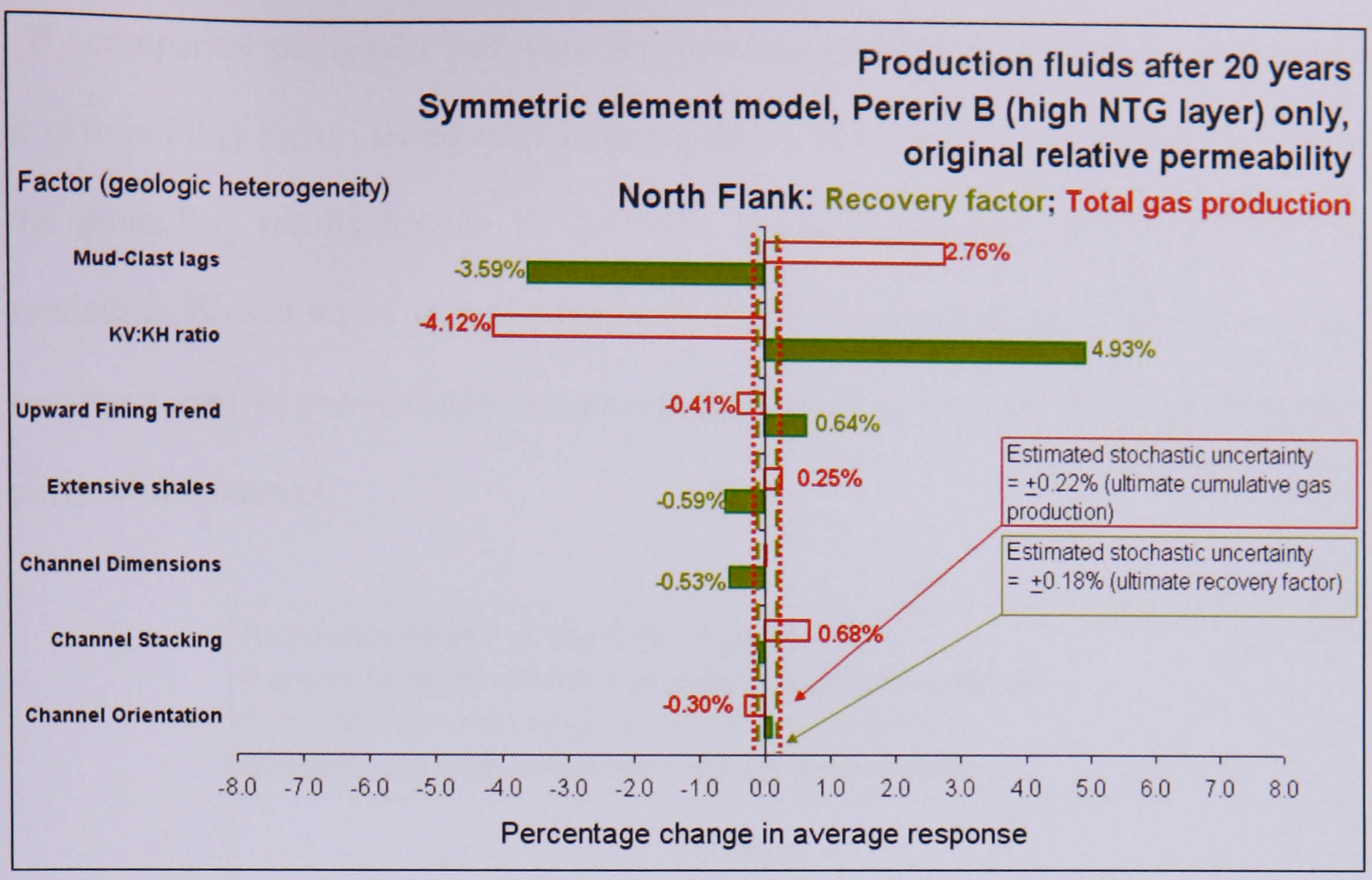


Figure A5.2A

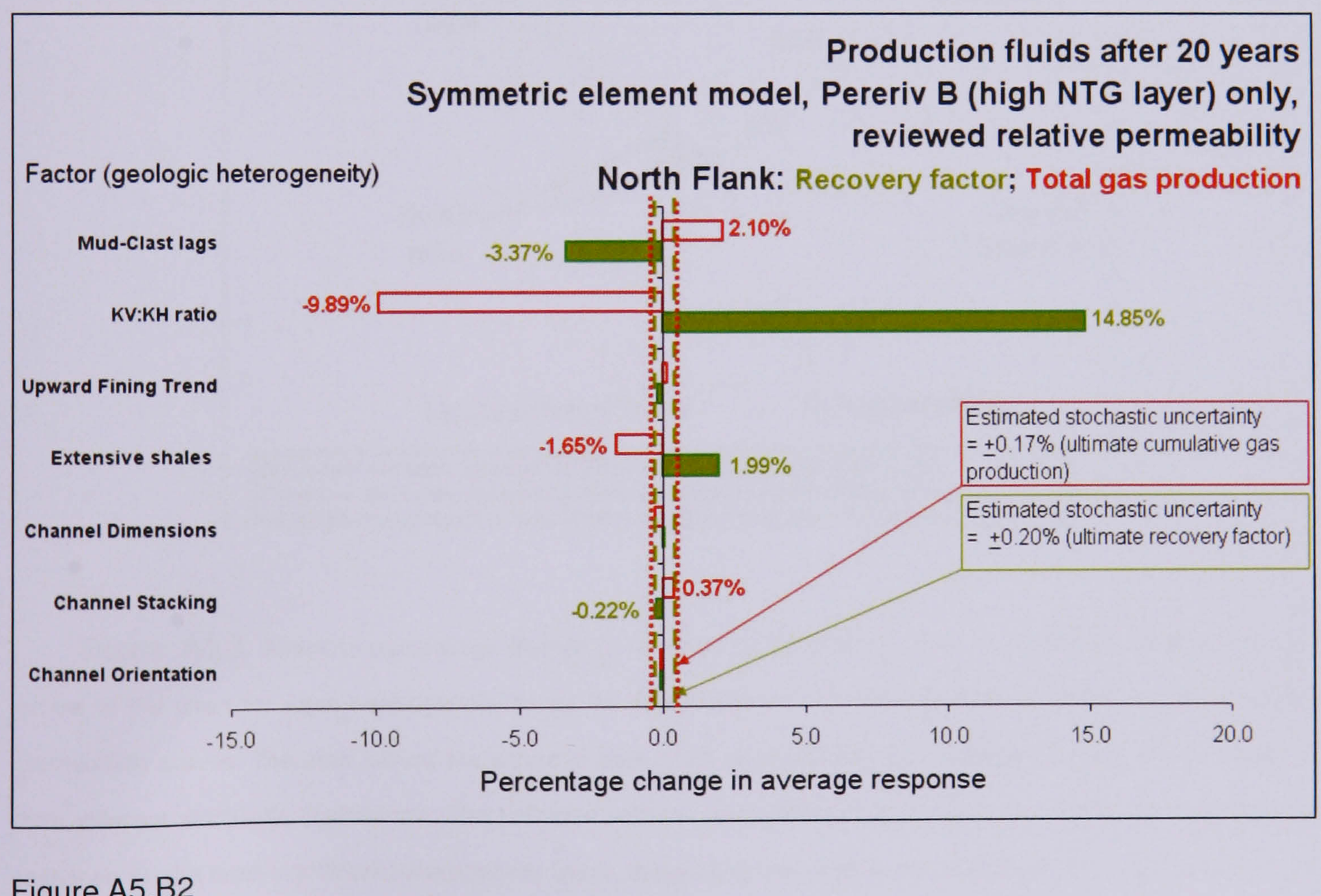


Figure A5.B2

Figure A5.2 (A-B). Average percentage change in recovery factor and total gas produced after 20 years in north flank symmetric element models of Pereriv B, observed when each factor in the sensitivity analysis is varied from setting 1 to setting 2 (Table 5A). The original relative permeability data are applied in **(A, top)** and reviewed relative permeability data are applied in **(B, bottom)**.

By comparing the results that were generated using different relative permeabilities, it is found that the reviewed relative permeability data produce a far storger effect on the modelling results for the Kv:Kh ratio. From Figure A5.3 it is found that by modelling Kv:Kh equal to 1 the recovery factor is increased by c. 14.9% with the reviewed relative permeability curves compared with c. 4.9% for the original relative permeability curves.

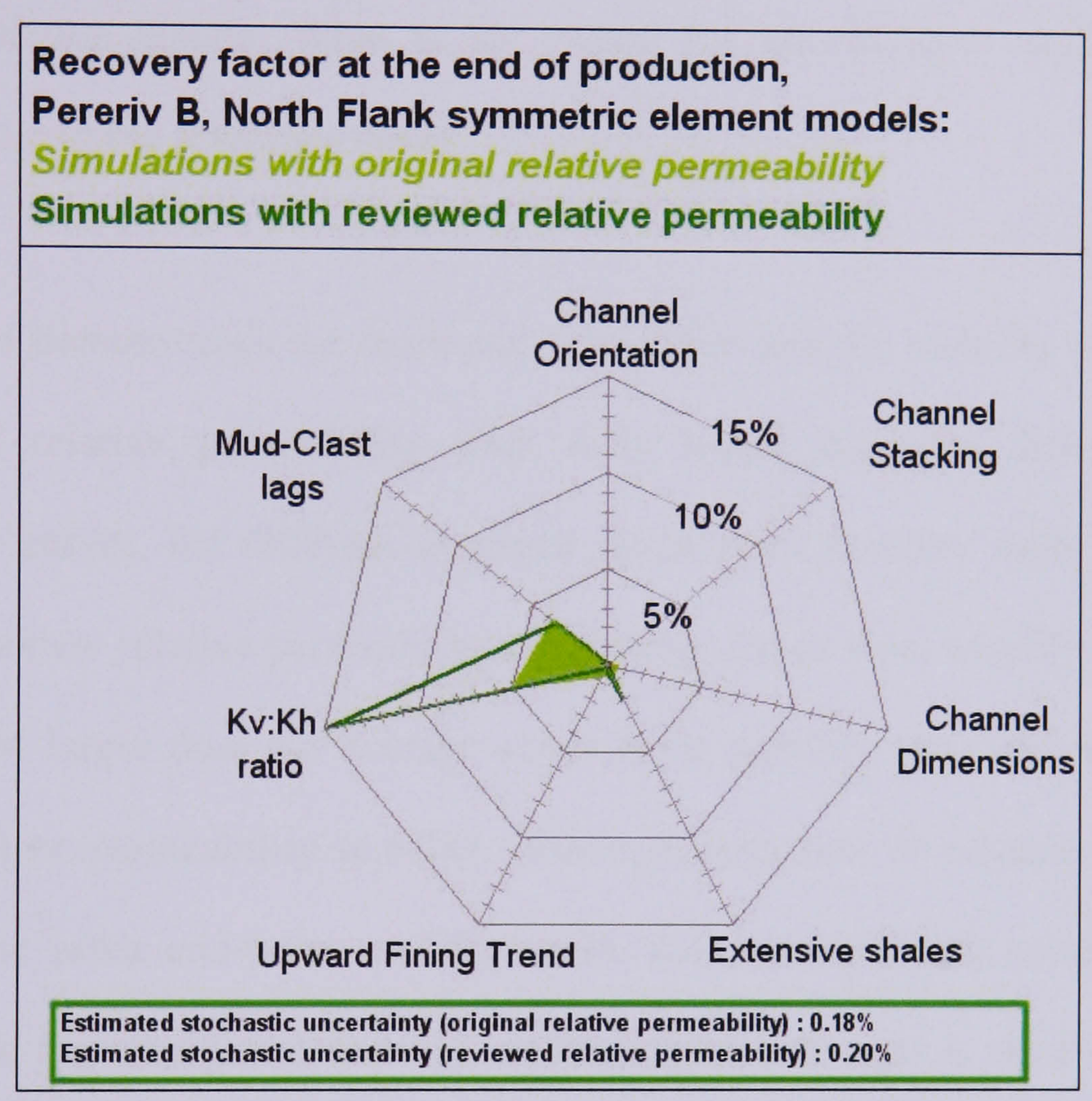


Figure A5.3. Absolute percentage change in recovery factor after 20 years is plotted as distance from the centre of the chart for each heterogeneity factor, to enable comparison between the two different gas-oil relative permeability curves. The area around the centre of each chart represents the absolute percentage change observed from different stochastic realizations. The reviewed relative permeability data included a much larger magnitude of response for the most significant heterogeneity factor, suggesting that relative permeability has a large impact on the displacement.

A5.2 Discussion on the impact of variation in relative permeability

In this chapter two different sets of gas-oil relative permeability curves are applied. Both sets of relative permeability data have the same end-point mobility ratio; therefore both yield identical results when Dietz's stability analysis is applied. Thus the results of the oil recovery prediction should be the same, but this is not confirmed by the simulation results. What is the reason for the different responses of the recovery factor in the screening study?

Figure A5.4 demonstrates the fractional flow curve and the mobility ratio for these two sets of relative permeability data. It is found the from different relative permeability curves, the different averaged shock front mobility ratio is found. By applies the review relative permeability the average shock front mobility ratio is 7.92 which is 1.64 larger than the average shock front mobility ratio obtained from the original relative permeability (c.6.28). Although both sets of relative permeability data have the same end-point mobility ratio, the reviewed data exhibits a higher mobility ratio for most gas saturations, which suggests that gas is more mobile when the gas saturation is not at its maximum value. Such an impact is not described by the Dietz's analysis; both sets of relative permeability have the same Dietz's critical rate. The results show that by using different sets of relative permeability data, the magnitude of the average response is different (Figure A5.3). By using the realistic set reviewed of relative permeabilities, it is found that the response to the variation of Kv:Kh ratio becomes a lot stronger (Figure A5.3). The difference in shock front mobility ratio is then hypothesized as the main reason for the different magnitude of re[illegible] on reservoir performance. This will be discussed further in the next section.

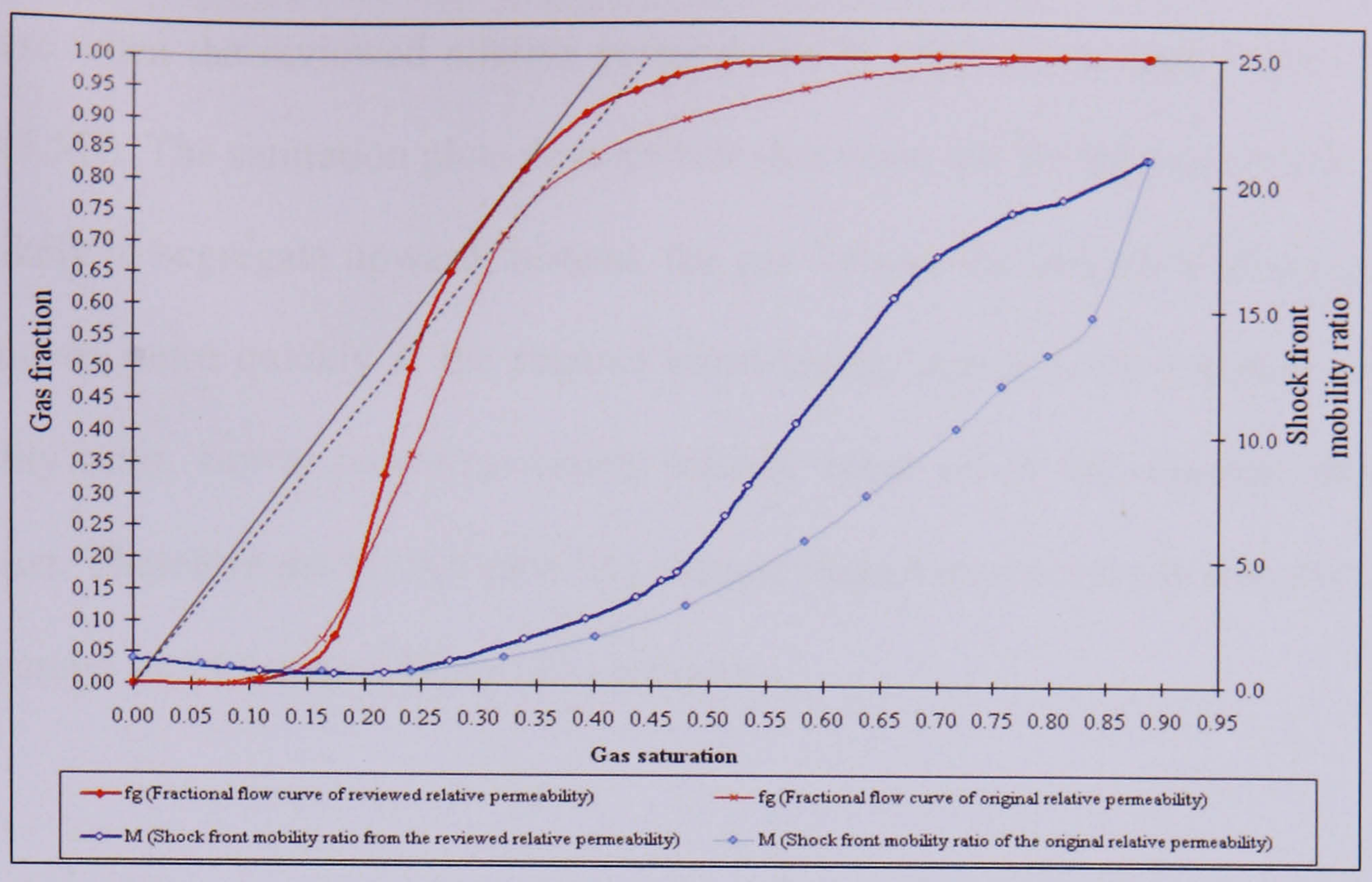
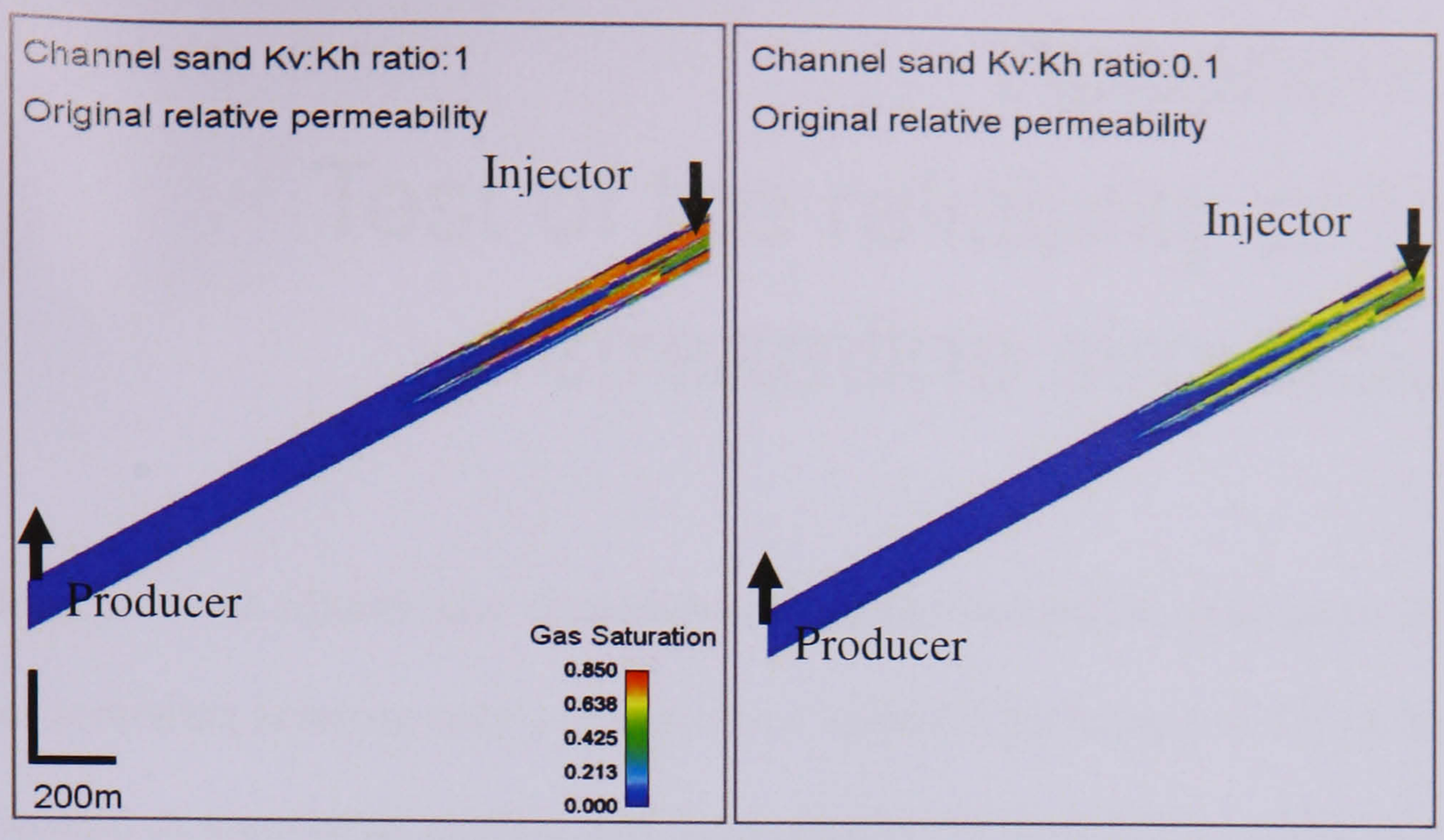


Figure A5.4. Fraction flow curves and shock front mobility ratio for different relative permeability data (Figure A5.1). The fractional flow curves include gravity. A tangent is drawn to the fractional flow curve from the initial water saturation. The tangent point indicates the saturation at breakthrough. The intercept of the tangent at f=1 indicated the average saturation behind the front up to the breakthrough time at the production well

Figures A5.5A to A5.5D show gas saturation in cross-section through models with different sand Kv:Kh after one year of production. The simulations were conducted with simplified fluid PVT description and both sets of relative permeability data were applied. Firstly by comparing both displacements with the same Kv:Kh ratio (Figure A5.5A and 5.5B) it is found that with the reviewed relative permeability data, there is lower gas saturation in the gas invaded zone, because gas is more mobile for the reviewed data. Secondly, by comparing displacements with the same relative permeability data (Figure A5.5C and A5.5D), it is found that when the Kv:Kh ratio is 0.1 the gas invades a greater area but the gas saturation within the invaded zone is lower compared with the case where Kv:Kh ratio is 1. Thus when Kv:Kh is equal to 1, the gas invaded zone has a relatively high gas saturation and gas is concentrated at the

top of the reservoir because of vertical equilibrium. This phenomenon is stronger in the case when the reviewed relative permeability is applied (compare Figure A5.5C and A5.5D). The saturation plots demonstrate that when the Kv:Kh ratio is low, gas is less likely to segregate upward; instead, the gas follows the bulk flow direction. The gas moves more quickly if the relative permeability curves yield a higher average mobility ratio. Lower recovery results because more oil is left unswept after gas invasion. Therefore the Kv:Kh ratio has a larger impact on recovery in the case where the average shock front mobility ratio is higher.



FigureA5.5A

Figure A5.5B

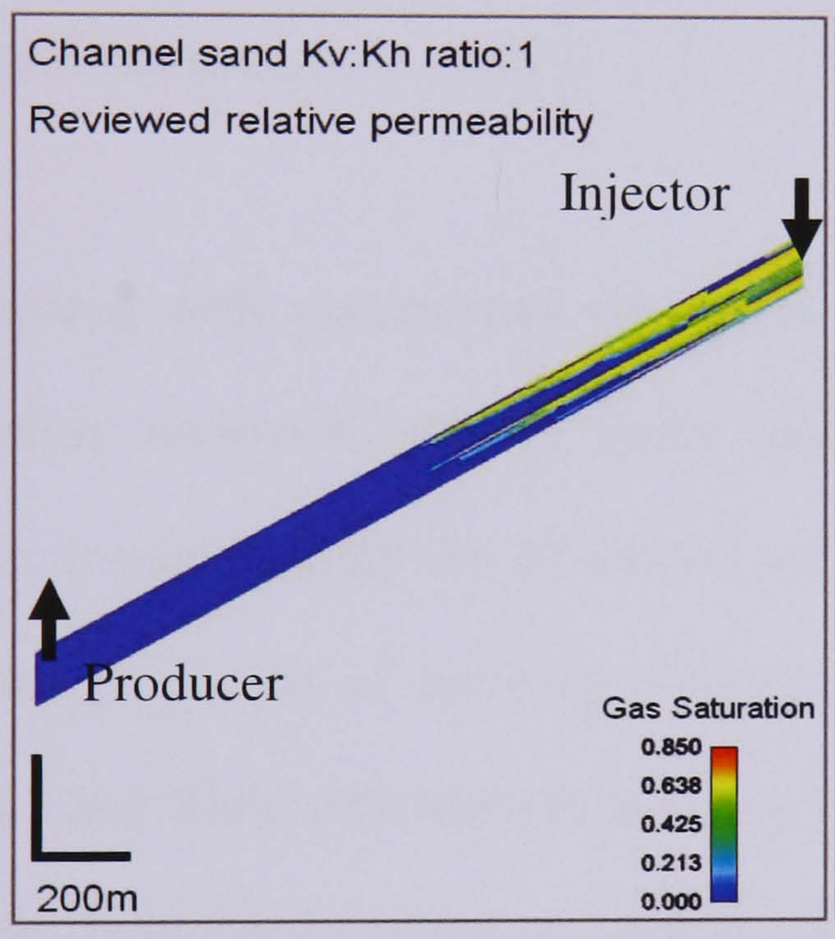


Figure A5.5C

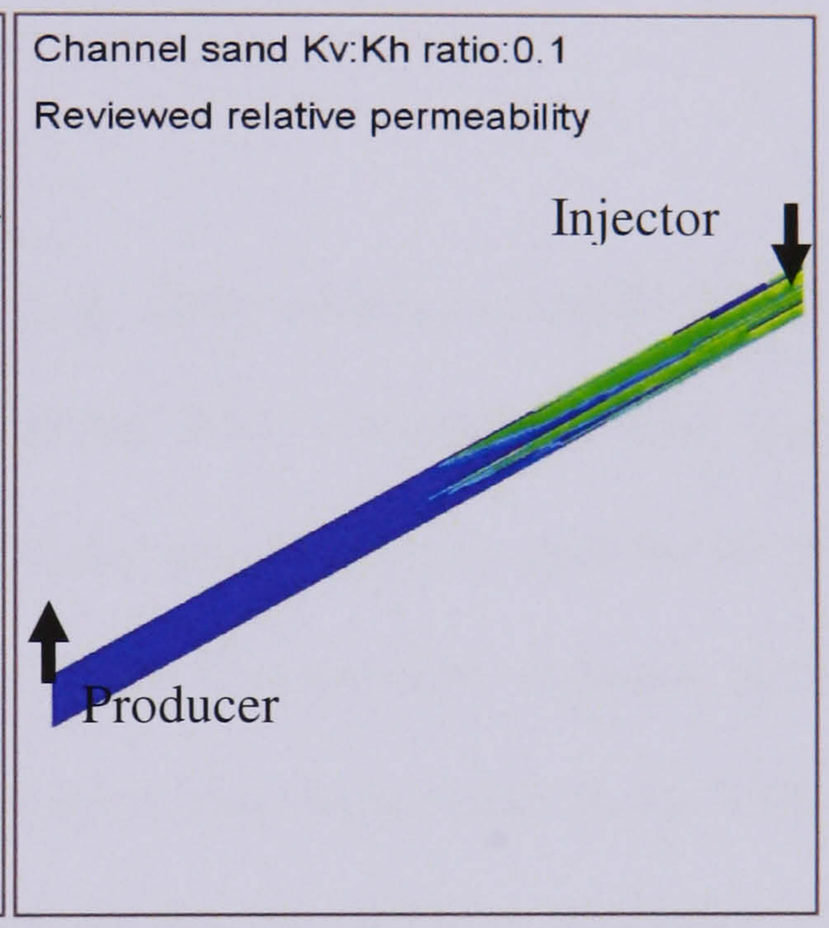


Figure A5.5D

Figure A5.5 (A-D). Vertical cross section view through the middle of a subset model of gas saturation after 1 year of displacement with the original relative permeability curves and the Kv:Kh of the channel sand equal to 1 **(A, top left)** and 0.1 **(B, top right)**. Compare with the case where reviewed relative permeability data are applied with the Kv:Kh of the channel sand equal to 1 **(C, bottom left)** and 0.1 **(D, bottom right)**. The producers and injector are labeled. The plots show that the gas saturation is higher in the invaded zone in models with sand Kv:Kh ratio equal to 1 (left) than 0.1 (right). The effect is more pronounced when the reviewed relative permeability data is applied.

Appendix 6
Test of the reliability of the streamline simulation

Many previous studies have demonstrated that the streamline simulator is a useful tool for screening heterogeneity's influence on reservoir performance. This is because it is capable of simulating models with large number of grid cells in order to capture detailed geological features (e.g. Thiele et al., 1996; Datta-Gupta, 2000; Idroho et al., 2000 and Gilman et al., 2002;).

Compared with commercial simulators (e.g. finite different simulators: Eclipse) streamline simulators operate under simplified PVT conditions. Some important physics is neglected by the streamline simulator and so it is not intended to produce rigorous prediction of recovery (Gilman 2002). Comparisons between streamline (3DSL) and finite different (Eclipse) simulation have been made under both water and gas flood displacement in order to compare the two different simulators (Figure A6.1 and A6.2). The water-oil and gas-oil relative permeability curves reported in Figure 3.2 were applied in this test.

In relation to water-oil displacement, Figure A6.1 shows the comparison of the oil recovery and the water production profile between Eclipse at IMPES mode and 3DSL. The test was conducted in 2D south flank homogeneous models. The result shows that the oil recovery and water production profile from the two different simulations are almost identical. That suggests that on water-oil displacement, the result

generated by the streamline simulator is as good as the finite difference simulator at the IMPES mode under simplified PVT conditions.

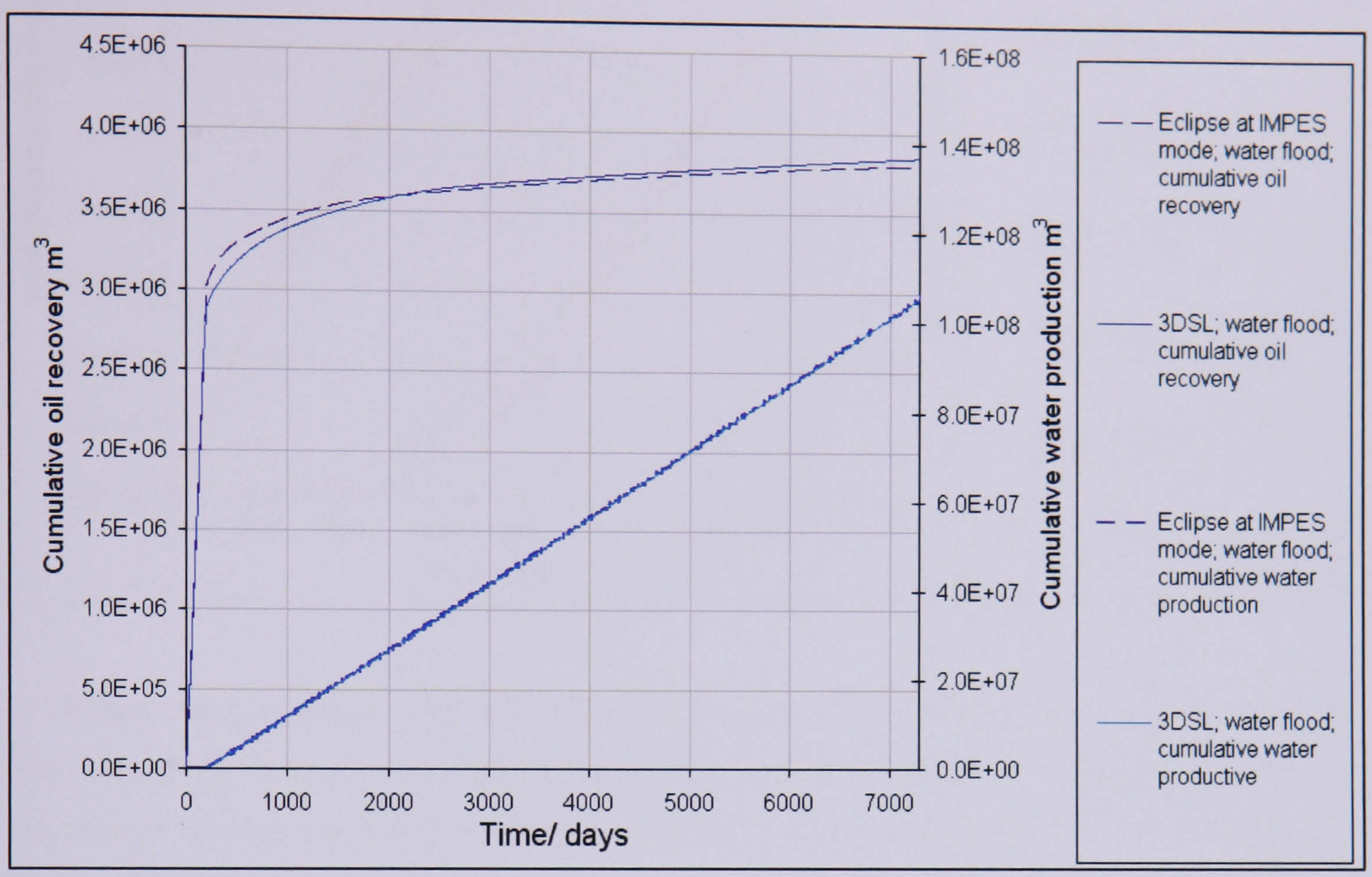


Figure. A6.1 Comparison of the 3DSL and Eclipse estimation on oil recovery profile and the water production profile under water-oil displacement in a 2D south flank homogeneous model. The result shows the estimation by 3DSL and E-Clipse on water oil displacement is almost identical.

On gas oil displacement, Figure A6.2 shows the comparison of the oil recovery and gas production profile between Eclipse at IMPES mode and 3DSL (streamline) simulation in 2D north flank homogeneous models., The gas flooding results, difference between the streamline and finite difference simulation are larger than water flooding. The results show that, regardless which timesteps is being used, under the streamline simulations, earlier breakthrough was estimated. Nevertheless, the ultimate recovery is the same for both the Eclipse and 3DSL's simulation.

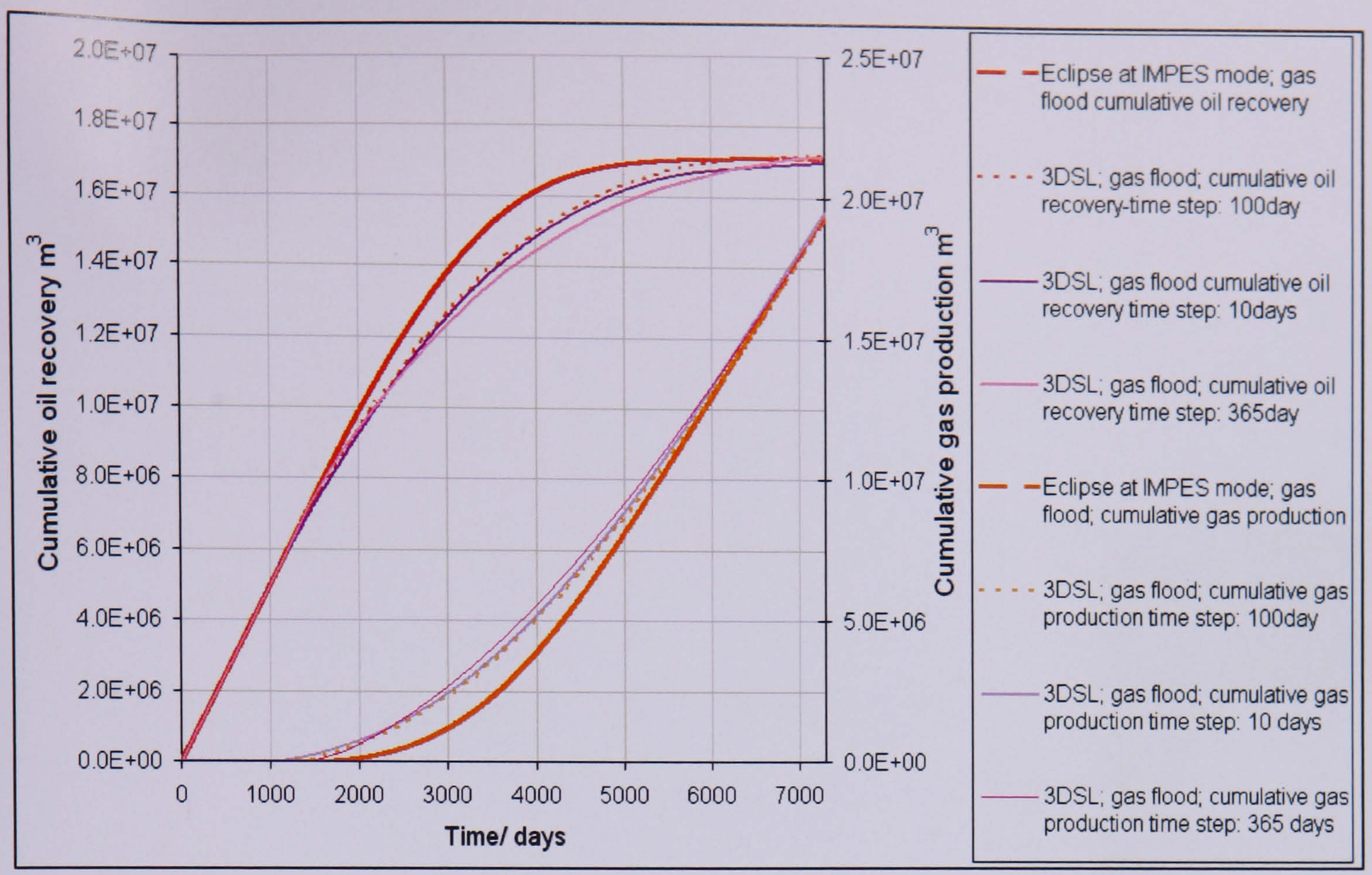


Figure. A6.2 Comparison of the 3DSL and Eclipse estimation on oil recovery profile and the gas production profile under gas-oil displacement in a 2D north flank homogeneous model. The total oil recovery and the total gas production are matched between 3DSL and Eclipse's estimation. Comparing the two simulations, in general, the streamline simulation (3DSL) estimated an earlier gas breakthrough time. The graph also shows that the results converged when 100 days timesteps (which were applied to all the gas flooding simulations in the research) applies on the streamline simulation.

Different time steps for 3DSL simulations were also tested. The results converge when 100 days timesteps are applied. Therefore, 100 days timesteps were applied in all the gas-oil displacement simulations in this research. Many previous studies also demonstrated that streamline simulation obtains similar results with the finite different simulation at IMPES model under simplified PVT conditions (e.g. Batycky et al., 1996 and Huang et al., 2004). In general, both previous research and the results of this study considered in this section also indicate that the results generated by streamline simulators are as good as the finite different simulator under simplified PVT conditions.

BIBL. LONDON UNIV.